Terms and Conditions of Use of Digitised Theses from Trinity College Library Dublin

Copyright statement

All material supplied by Trinity College Library is protected by copyright (under the Copyright and Related Rights Act, 2000 as amended) and other relevant Intellectual Property Rights. By accessing and using a Digitised Thesis from Trinity College Library you acknowledge that all Intellectual Property Rights in any Works supplied are the sole and exclusive property of the copyright and/or other IPR holder. Specific copyright holders may not be explicitly identified. Use of materials from other sources within a thesis should not be construed as a claim over them.

A non-exclusive, non-transferable licence is hereby granted to those using or reproducing, in whole or in part, the material for valid purposes, providing the copyright owners are acknowledged using the normal conventions. Where specific permission to use material is required, this is identified and such permission must be sought from the copyright holder or agency cited.

Liability statement

By using a Digitised Thesis, I accept that Trinity College Dublin bears no legal responsibility for the accuracy, legality or comprehensiveness of materials contained within the thesis, and that Trinity College Dublin accepts no liability for indirect, consequential, or incidental, damages or losses arising from use of the thesis for whatever reason. Information located in a thesis may be subject to specific use constraints, details of which may not be explicitly described. It is the responsibility of potential and actual users to be aware of such constraints and to abide by them. By making use of material from a digitised thesis, you accept these copyright and disclaimer provisions. Where it is brought to the attention of Trinity College Library that there may be a breach of copyright or other restraint, it is the policy to withdraw or take down access to a thesis while the issue is being resolved.

Access Agreement

By using a Digitised Thesis from Trinity College Library you are bound by the following Terms & Conditions. Please read them carefully.

I have read and I understand the following statement: All material supplied via a Digitised Thesis from Trinity College Library is protected by copyright and other intellectual property rights, and duplication or sale of all or part of any of a thesis is not permitted, except that material may be duplicated by you for your research use or for educational purposes in electronic or print form providing the copyright owners are acknowledged using the normal conventions. You must obtain permission for any other use. Electronic or print copies may not be offered, whether for sale or otherwise to anyone. This copy has been supplied on the understanding that it is copyright material and that no quotation from the thesis may be published without proper acknowledgement.

C-*ABL* IN HUMAN CANCER:
AN INVESTIGATION OF ITS ROLE IN APOPTOSIS
INHIBITION, DIFFERENTIATION AND ANGIOGENESIS.

A Thesis submitted for the degree of

Doctor of Philosophy

by

Jennifer M. Russell, B.Sc. (Hons).

Trinity College,

University of Dublin.

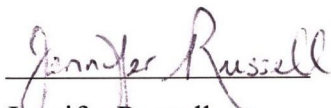September 2002

In loving memory of my Dad.

DECLARATION

I hereby certify that this thesis submitted for the degree of Doctor of Philosophy to the University of Dublin, has not previously been submitted for a degree or diploma to this or any other University. The work presented here is entirely my own, except where stated.

This thesis may be made available for consultation within the University library and may be photocopied or lent to other libraries for the purpose of consultation.

Jennifer Russell
September 2002

ABSTRACT

Research over the past number of decades has significantly advanced our understanding of the cell signalling effects that mediate a diverse array of cellular activities including cell proliferation, homeostasis and differentiation of both normal and cancer cells. Signal transduction within and between cells means that they can communicate important information and act upon it. Since signalling networks impinge on so many aspects of normal cellular function, it is not surprising that so many diseases have at least some basis in a signalling defect. Aberrant cell signalling has been implicated in the initiation, progression and metastasis of cancer. It is only recently that the molecular basis for these events has been studied, leading to the development of therapies that target one or more of the components of these series of events. Agents presently being evaluated as inhibitors of signal transduction include both natural and synthetic compounds, monoclonal antibodies and anti-sense oligonucleotides. Undoubtedly, a greater understanding of the precise role of individual proto-oncogenes and tumour suppressor genes in the development of human cancer will enable us to tailor more specific therapies.

The work described in this thesis concerns expression of the c-*abl* proto-oncogene in normal and tumour tissues. c-*abl* is located on chromosome 9, and encodes a non-receptor protein tyrosine kinase. Previously reported functions for c-Abl tyrosine kinase include inhibition of apoptosis and cellular differentiation. However the precise biological function of c-Abl remains unclear. In this study, it has been demonstrated that c-Abl is strongly expressed in certain tumour types including chondrosarcoma, liposarcoma and diffuse-type gastric adenocarcinoma. A relationship between Abl protein expression and tumour grade, level of apoptosis and cellular differentiation has been established. Strong Abl immunostaining is also observed in the neovasculature during enchondral ossification, in early placental villi and in tumour microvessels, particularly in myxoid liposarcoma and diffuse-type gastric carcinoma. These findings support a hitherto unreported role for c-Abl in angiogenesis.

The specificity of the results obtained by immunohistochemistry using the c-Abl/BCR-Abl antibody were confirmed at the molecular level using RT-PCR. RNA was

successfully extracted from a range of archival histological specimens. The levels of c-*abl* expression were monitored using real-time quantitative TaqMan® RT-PCR. The results obtained at the molecular level substantiated the differential expression of c-*abl* observed at the protein level. Further confirmation was attained by localising c-*abl* expression to individual cells using *in-situ* RT-PCR techniques.

The potential role for c-Abl in normal and neoplastic angiogenesis was evaluated *in vitro* using the HuVec (ECV-304) endothelial cell line. Convincing down-regulation of c-*abl* expression in response to oxidative stress and high doses of wortmannin has been confirmed using Real-Time TaqMan® RT-PCR. No change in c-*abl* expression is observed in response to either serum deprivation or heat shock. HuVec cells were cultured with varying concentrations of tumour cell media to determine the effect on c-*abl* expression in response to secreted metabolites from a number of tumour cell lines. Although extremely variable, upregulation of c-*abl* in the presence of leukaemic cell line media is observed while an opposing decrease in c-*abl* is observed in the presence of media from prostate, breast and lymphoma cell lines. While not conclusive, the results suggest that c-*abl* expression in endothelial cells is modulated in a tumour specific manner.

Overall, the results confirm that c-*abl* plays an important role in cell cycle regulation, apoptosis and differentiation. Regulation is exerted at both the level of transcription and translation. A novel function of c-*abl* during normal and tumour angiogenesis has been proposed. Understanding the precise role of c-*abl* in angiogenesis may provide an interesting avenue for testing Abl tyrosine kinase inhibitors as potential agents in pro-apoptotic and anti-angiogenic based treatments of disease.

ACKNOWLEDGEMENTS

To my dear friend and colleague, the late Dr. Frances Hogan. Your generosity, kindness and insatiable appetite for life were truly inspirational. And of course Jackie, who has kept me sane (almost) and shared the highs and lows of the past few years…..thanks for everything Professor!!!!!

Sincere thanks to all the DCU crew; particularly my own friends from undergrad years and those who shared their post-grad days with me. To all in the Vascular Biology Research centre for your companionship during the write-up days.

My heartfelt thanks to the two wise men, Fran and Damo, two wonderful friends who like a good pint of Bulmers believe that nothing should be added but time – eh lads, I think we've taken the biscuit!!!! Any more bright ideas on how to get rich quick???

True friends are hard to find. Yvonne and Fran - you have both been absolutely fantastic and have proved your worth in good times and bad. Yvonne, you are simply one in a million – thanks for everything 'Doc'!

Finally, to my family without whose support I would never have stuck at it so long. To Graham & Yvonne, Alison & Edward and Caroline (what's your job?) – thanks for putting up with me and my student ways for so many years…..what's the going rate for rent these days???

To my dear parents. Mam, your bavery, strength, loyalty and determination are beyond words, you helped us all through the darkest of days at the 'war office', and can never be thanked enough for all you've done. In the words of a very special person – 'Winston, you're brill!'

Dad, your encouragement, love and support, but above all your companionship down through the years meant the world to me. Undoubtedly the best friend I ever had, you were and always will be an inspiration to me – I wish you were here today to see this finally finished, I know you'd be 'chuffed'!!! This is for you D!

TABLE OF CONTENTS

LIST OF FIGURES

LIST OF TABLES

ABBREVIATIONS

ABI	Applied Biosystems Inc.
AGPC	Acid guanidium/thiocyanate/phenol chloroform
AI	Apoptotic Index
APES	3-aminopopyltriethoxy silane
ATCC	American Tissue Culture Collection
bp	Base pair
BSA	Bovine serum albumin
CCD	Charge-coupled device
cDNA	Complimentary DNA
CML	Chronic Myeloid Leukemia
CNS	Central Nervous System
CSA	Catalysed signal amplification
C_T	Threshold cycle
DAB	3,3' diaminobenzidine
DEPC	Diethylpyrocarbonate
Dig	Digoxigenin
DMF	Dimethylformamide
DNA	Deoxyribo Nucleic Acid
dNTPs	Deoxynucleotide triphosphates
DTT	Dithiothreitol
EB/AO	Ethidium Bromide/Acridine Orange
ECACC	European Collection of Animal Cell Cultures
EDTA	Ethylenediamine tetra acetic acid
EtBr	Ethidium bromide
FACS	Fluorescent Activated Cell Sorting
FAM	6-carboxy-fluoroscein
FCS	Fetal Calf Serum
FFPE	Formalin fixed paraffin embedded
GAPDH	Glyceraldehyde Pyruvate Dehydrogenase
GITC	Guanidium Isothiocyanate
GuSCN	Guanidium Thiocyanate
H&E	Haematoxylin and Eosin
H_2O_2	Hydrogen peroxide
HRP	Horseradish peroxidase
ICE	Interleukin-1β converting enzyme
IPTG	Isopropyl-β-D-thiogalactosidase
ISEL	*In situ* end labelling
ISH	*In situ* hybridisation
LAN	Linker-arm-modified nucleotide
LB	Luria-Bertani
MeOH	Methanol
$MgCl_2$	Magnesium Chloride

MI	Mitotic Index
Mn(OAc)$_2$	Manganese Acetate
mRNA	Messenger Ribonucleic Acid
NaCl	Sodium chloride
Na$_3$VO$_4$	Sodium orthovanadate
NBT	Nitroblue tetrazolium chloride
OD	Optical density
ODN	Oligonucleotides
PBS	Phosphate buffered saline
PCR	Polymerase chain reaction
PE	Perkin Elmer
POP 6™	Performance Optimised Polymer 6
PVDF	Poly vinylidene difluoride
RB	Retinoblastoma protein
RNAse	Ribonuclease
rpm	Revolutions per minute
ROX	6-carboxy-X-rhodamine
RT	Reverse transcription
S.N.A.P.	Simple Nucleic Acid Preparation
SDS	Sequence Detection System
Seq.	Sequencing
T$_A$	Annealing temperature
TAE	Tris acetate-EDTA
TAMRA	6-carboxy-tetramethyl-rhodamine
TBS	Tris buffered saline
TBST	Tris buffered saline + 0.1%v/v Tween 20
TdT	Terminal deoxynucleotidyl transferase
TE	Tris-EDTA
TET	Tetrachloro-6-carboxy-fluoroscein
T$_m$	Melting temperature
TSA	Tyramine signal amplification
TSR	Template Suppression Reagent
TUNEL	TdT-mediated dUTP nick end labelling
UPH$_2$O	Ultra pure water
UNG	Urasil-N-glycosylase

1. GENERAL INTRODUCTION

1.1 PROGRAMMED CELL DEATH (APOPTOSIS)

The selection process by which cells become destined for either cell death or survival must be carefully regulated if tissue homeostasis is to be maintained. It is a delicate balance of positive and negative signals derived from the interplay between many genes, some of which have been extensively characterised, others about which relatively little is known. Apoptosis refers to the genetically mediated process of cell death controlling the deletion of individual cells in normal and diseased tissues. Programmed cell death is an analogous process essential during embryonic growth and tissue/organ remodelling (Kerr *et al*, 1972; Abrams *et al*, 1993). Apoptosis is significant in a number of pathological diseases including cancer, AIDS (Sartorius *et al*, 2002) autoimmune diseases such as rheumatoid arthritis (Perlman *et al*, 2001) and inflammatory bowel disease and degenerate diseases of the CNS such as Alzheimer's disease and Parkinson's disease (Ameisen *et al*, 1991; Solary *et al*, 1996; Bamberger & Landreth, 2002). Apoptosis is characterised by a set of structural changes that are reproduced in cells of widely differing lineage (Kerr *et al*, 1972).

1.1.1 MORPHOLOGICAL FEATURES OF APOPTOSIS

Early apoptosis is characterised by the initial condensation of the chromatin into crescents along the nuclear envelope (Cohen, 1993). As condensation progresses, the nucleus collapses and ultimately splits into fragments (Figure 1.1). As the nucleus fragments, extensive cell surface protrusions develop and membrane bound apoptotic bodies of various size and composition are formed. In contrast to death by necrosis, there is no inflammatory response to cell death by apoptosis (Wyllie, 1992). Apoptotic bodies formed *in vivo* are rapidly phagocytosed by adjacent macrophages where the process of lysosomal degradation begins. This enables extensive cell deletion to occur with minimal tissue disruption.

The histologically visible part of apoptosis has a relatively short duration similar to that of cell division. In the initial stages, the apoptotic cell embedded in normal tissue, begins to lose contact with its neighbouring cells. By light and electron microscopy cell shrinkage can be observed without change in content of the intact

organelles. In the next stage, membrane ruffing and blebbing leads to cellular fragmentation. The rapidity with which the apoptotic bodies are engulfed by adjacent cells accounts for the relatively short time frame that they may be seen under a light microscope.

Apoptosis

1. Stimulation
Receptor mediated or non-receptor mediated

Genetic programming
Start "biological clock"

2. The Intracellular response
Signal transduction; activation of transcription factors; induction of apoptosis related genes; release of Ca⁺; depletion of ATP

3. Apoptosis
Cell dismantling; DNA degradation; expression of phagocyte recognition molecules

4. Phagocytosis

Failure of phagocyte recognition leads to secondary necrosis and release of intracellular contents

Persistence of inflammation

Figure 1.1 The morphological stages of apoptosis. This figure illustrates the 4 main stages of apoptotic cell death: stimulation, intracellular signalling, apoptosis and phagocytosis. In the absence of recognition of apoptotic bodies by neighbouring phagocytic cells, the apoptotic cell will eventually assume necrotic morphology, so called "secondary necrosis" (Afford & Randhawa, 2000).

1.1.2   APOPTOSIS AND TUMOUR GROWTH

Over recent years it has become increasingly accepted that the causes and consequences of spontaneous cell death are important parameters in neoplastic growth. Both apoptotic bodies and mitotic figures are sometimes numerous in rapid growing tumours: it is the balance between the two processes that determines the rate of enlargement (Kerr *et al*, 1972).

1.1.3   MECHANISMS OF APOPTOTIC CELL DEATH

A brief overview of the key factors influencing a common apoptotic pathway is described in Figure 1.2.

| Triggers | → | Modulators | → | Effectors | → | Cleavage Substrates | → | CELL DEATH |

DNA damage   p53   Cysteine Proteases   Protein fragmentation
Heat   bcl-2 family   DNA fragmentation
Ceramide   kinases
FAS/TNF   oncogenes
Growth factor   tumour suppressor genes
deprivation   cell cycle regulators
     Transcription factors
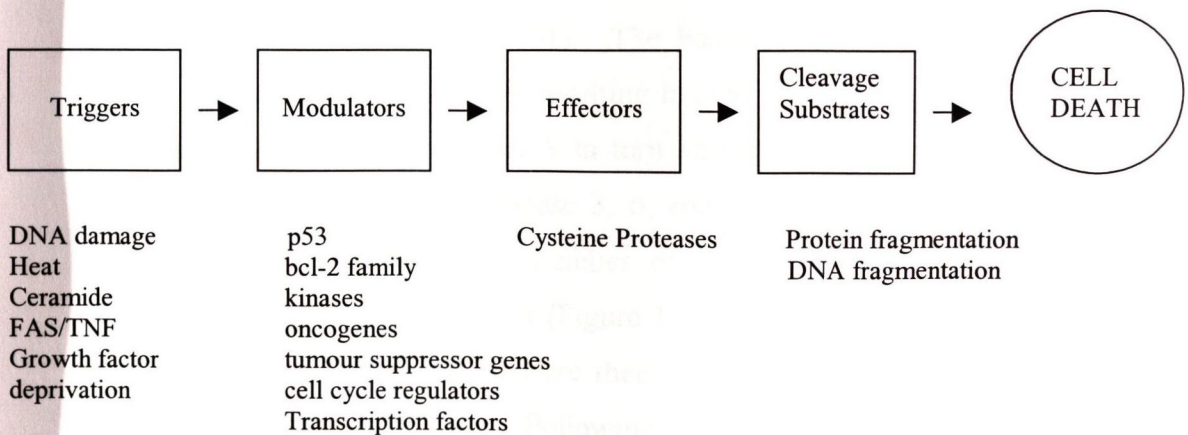
Figure 1.2   Events leading to cell death by apoptosis

A trigger is defined as a factor that induces the onset of apoptosis. Modulators are the multitude of pro- and anti-apoptotic influences that interact in the transduction of the signal and define the net outcome of the event (i.e. cell survival or cell death). If a cell embarks on the cascade of events leading to apoptosis, a group of ubiquitous molecules called 'effectors' will become activated. The ICE family of cysteine proteases (caspases) are currently the most extensively defined effectors of the apoptotic process (Rowan & Fisher, 1997; Mathiasen & Jaattela, 2002). The targets of effectors are cleavage substrates, many of which will lose function, but others will

gain novel activities (e.g. the nuclease responsible for the characteristic cleavage of DNA into its distinct DNA laddering pattern). There are two major pathways of apoptosis: the death receptor pathway and the mitochondrial pathway (Ashkenzai & Dixit, 1998; Gupta 2000; Gupta 2001).

1.1.4 DEATH RECEPTOR PATHWAYS

Death receptors belong to the tumour necrosis factor receptor (TNFR) gene superfamily, which comprise a similar cysteine-rich extracellular domain and a homologous cytoplasmic sequence called the death domain (DD). Among the most extensively characterised death receptors are Fas (CD95) and TNFRs. Fas plays a pivotal role in the development and functioning of the immune system (Ashkenzai & Dixit, 1998; Gupta, 2000). Briefly, binding of CD95 (Fas) to CD95L (Fas ligand) leads to clustering of Fas death domain, setting up a chain of events that culminates in apoptosis (reviewed in Gupta, 2001). The Fas-associated death domain (FADD) binds to cytoplasmic procaspase 8, resulting in autolytic cleavage into active caspase 8 (Figure 1.3). Activated caspase 8 in turn serves as an enzyme for activation of downstream effector caspase (caspase 3, 6, and 7) activation. The active effector caspases mediate cleavage of a number of cytoplasmic and nuclear substrates, resulting in cell death by apoptosis (Figure 1.3). In contrast, TNFRs do not exhibit enzymatic activity themselves and are therefore dependent on recruitment of other molecules for signal transduction. Following ligation of TNF with its receptor TNFR-I, the receptor death domain recruits an adaptor protein TRADD (TNFR-Associated Death Domain). TRADD subsequently recruits other adaptor molecules, initiating a signalling cascade that ultimately results in activation of the effector caspases.

1.1.5 MITOCHONDRIAL PATHWAYS

Mitochondria are considered to be key players in the control of stress-induced apoptosis (Kroemer et al, 1997; Zamzami et al, 1997 & 1998; Kroemer et al 1998; Desagher & Martinou, 2000). A number of stimuli including UV irradiation, reactive oxidative species and chemotherapeutic agents appear to mediate apoptosis in a death receptor independent manner via the mitochondrial pathway. The mitochondrion is composed of two well-defined compartments: the outer and inner membranes. The
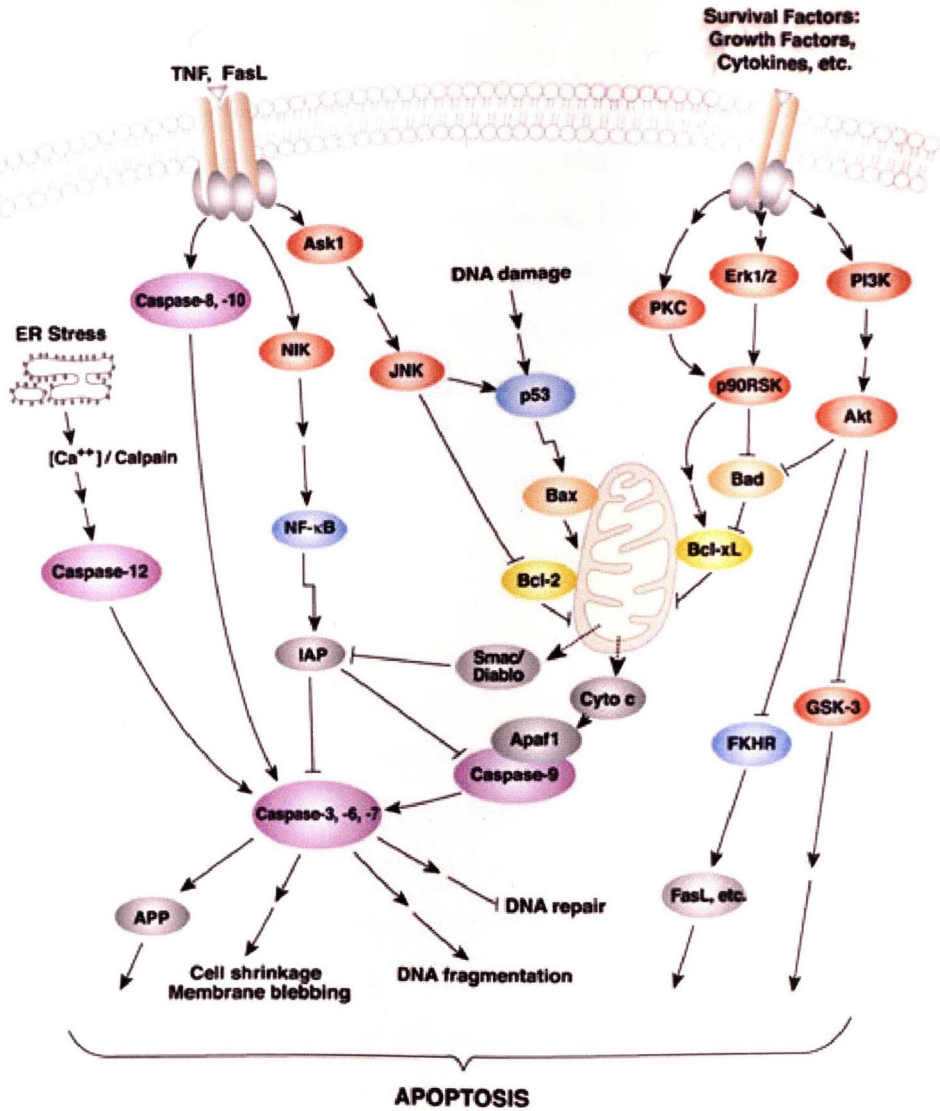
Figure 1.3 Regulation of apoptosis: Role of kinases, phosphatases and transcription factors. Taken from www.cellsignal.com.

majority of death signals that converge at the mitochondria are mediated through members of the Bcl-2 family such as Bid and Bad. Bcl-2 itself is located on the inner membrane and appears to play an important role in the maintenance of mitochondrial membrane potential (Susin *et al*; 1998). Opening of the permeability transition pores is a key event in apoptosis. The open pores result in the release of chemicals from the intermembrane space into the cytoplasm, among them cytochrome *c*, three different procaspases and Apaf1 (apoptosis inducing factor, Figure 1.3). The cytochrome *c* released in the cytosol binds Apaf1 and procaspase 9 (an initiator caspase) is recruited to form the apoptosome (Figure 1.3). The apoptosome-bound caspase 9 is then activated, which in turn activates caspase 3 resulting in cleavage of its substrates and apoptosis.

1.2   GENES AND CANCER

Everything in the cell is under genetic control, as all molecules in a cell are either themselves gene products or metabolites dependent on the actions of other gene products. The initiation of transcription in eukaryotes is an intricately defined and controlled process. Cancer may be defined as a progressive series of genetic events that occur in a clone of cells because of alterations in a limited number of specific genes: the oncogenes and the tumour suppressor genes. Activation or inactivation of as many as four or five different genes may be required for the development of a clinically recognisable cancer. Certain acquired genetic abnormalities may be necessary for the development of neoplasia, but few if any are solely causative.

As a generalisation, cancers may be regarded as diseases in which cellular signalling mechanisms have been disrupted so as to remove the growth and behaviour of the cell from normal constraints (Bartek *et al*, 1999). This could mean permanent activation of a receptor to produce growth-stimulatory signals whether or not its cytokine ligand is bound. Abnormal activity of a plasma-membrane bound tyrosine kinase could lead to over-stimulation of growth promoting pathways. Inappropriate expression of protein kinases (section 1.2.2) or phosphatases downstream of these initial signal transduction events could have similar effects.

Other stages in the multi-carcinogenic process could, as mentioned previously, include over-expression of a proto-oncogene – i.e. a gene that fulfills a normal role in untransformed cells but which can contribute to growth transformation when it functions aberrantly. An oncogene is any gene sequence contributing directly to neoplastic change. Most human cancers are generated when cellular genes (proto-oncogenes) change from a normal cellular gene to an oncogene by a variety of submicroscopic events including insertions, deletions, point mutations and translocations. The protein product of an oncogene is called an oncoprotein. In general, most oncogene products are either enzymes or regulatory components of transcription, translation or replication.

1.2.1 *SIGNAL TRANSDUCERS AS ONCOGENES*

Signal transduction at the cellular level refers to the movement of signals from outside the cell to inside the cell. The movement of signals can be simple, like that associated with receptor molecules of the acetylcholine class: receptors that constitute channels which, upon ligand interaction, allow signals to be passed in the form of small ion movement, either into or out of the cell. These ion movements result in changes in the electrical potential of the cells that, in turn, propagates the signal along the cell. More complex signal transduction involves the coupling of ligand-receptor interactions to many intracellular events. These events include phosphorylations by tyrosine kinases and/or serine/threonine kinases. Protein tyrosine kinases and proteins containing SH2 domains have been shown to play important roles in the transduction of mitogenic signals (reviewed in Ullrich & Schlessinger, 1990). Protein phosphorylations change enzyme activities and protein conformations. The eventual outcome is an alteration in cellular activity and changes in the program of genes expressed within the responding cells.

The binding of a growth factor to its receptor with tyrosine kinase activity induces receptor dimerization and conformational changes which enhance the kinase activity of the catalytic domain to its receptor. This results in tyrosine-specific auto-phosphorylation which creates binding sites on the receptor for effector molecules transducing the signal to the cell interior. Membrane-associated signal transducers with oncogenic potential are proteins with either (1) tyrosine kinase activity or (2)

GTPase activity (GTP binding proteins), recruited to the plasma membrane by an activated receptor.

1.2.2 PROTEIN PHOSPHORYLATION

Protein phosphorylation plays a pivotal role in regulating many cellular processes in eukaryotes. In particular, protein phosphorylation is a major effector of signal transduction pathways. Processes that are reversibly controlled by protein phosphorylation not only require a protein kinase but also a protein phosphatase. Target proteins are phosphorylated at specific sites by one or more protein kinase, and the phosphates are removed by specific phosphatases. In principle, the extent of phosphorylation at a particular site can be regulated by changing the activity of the cognate protein kinase or phosphatase, or both. The controlled, co-ordinated action of protein tyrosine phosphatases (PTPs) and kinases (PTKs) is a critical control mechanism for numerous physiological processes including growth, differentiation, metabolism, cell cycle regulation and apoptosis. The role of phosphatases and kinases in apoptosis is illustrated in Figure 1.3.

1.2.3 PROTEIN TYROSINE KINASES

The protein-tyrosine kinases constitute the largest functional group of oncogenes. The mammalian genome is estimated to encode between 100 and 200 tyrosine kinases (Hanks & Hunter, 1995). These enzymes phosphorylate tyrosine residues in specific protein substrates, as opposed to many other protein kinases which phosphorylate serines or threonines. PTKs are generally categorised as belonging to the receptor or the non-receptor family of PTKs by virtue of whether they possess or lack the receptor-like features of cellular ligand-binding and transmembrane domains. Many growth factors, differentiation factors and hormones mediate their effects via receptors with intrinsic tyrosine kinase activity.

1.2.4 RECEPTOR TYROSINE KINASES (RTKs)

The proteins encoding RTKs contain four major domains: (1) an extracellular ligand binding domain, (2) an intracellular tyrosine kinase domain, (3) an intracellular regulatory domain and (4) a transmembrane domain. The amino acid sequences of the tyrosine kinase domains of RTKs are highly conserved with those of cAMP-dependent protein kinase (PKA) within the ATP binding and substrate binding regions. Some RTKs have an insertion of non-kinase domain amino acids into the kinase domain termed the "kinase insert". RTK proteins are classified into families based upon structural features in their extracellular portions (as well as the presence or absence of a kinase insert) which include the cysteine rich domains, immunoglobulin-like domains, leucine-rich domains, Kringle domains, cadherin domains, fibronectin type III repeats, discoidin I-like domains, acidic domains, and EGF-like domains. Based upon the presence of these various extracellular domains the RTKs have been sub-divided into at least 14 different families (Table 1.1, reviewed in Ullrich & Schlessinger, 1990; Schlessinger & Ullrich, 1992)

Many receptors, other than those that are associated with cell surface receptors also have intrinsic tyrosine kinase activity. These receptors contain tyrosine residues, that upon phosphorylation, interact with other proteins of the signaling cascade. These other proteins contain a domain of amino acid sequences that are homologous to a domain first identified in the c-Src proto-oncogene. These domains are termed SH2 domains (Src homology domain 2). Another conserved protein-protein interaction domain identified in many signal transduction proteins is related to a third domain in c-Src identified as the SH3 domain.

The interactions of SH2 domain containing proteins with RTKs or receptor associated tyrosine kinases leads to tyrosine phosphorylation of the SH2 containing proteins. The result of the phosphorylation of SH2 containing proteins that have enzymatic activity is an alteration (either positively or negatively) in that activity. Several SH2 containing proteins that have intrinsic enzymatic activity include phospholipase C-γ (PLC-γ), the proto-oncogene c-Ras associated GTPase activating

Characteristics of the Common Classes of RTKs

Class	Examples	Structural Features of Class
I	EGF receptor, NEU/HER2, HER3	Cysteine-rich sequences
II	insulin receptor, IGF-1 receptor	cysteine-rich sequences; characterized by disulfide-linked heterotetramers
III	PDGF receptors, c-Kit	contain 5 immunoglobulin-like domains; contain the kinase insert
IV	FGF receptors	contain 3 immunoglobulin-like domains as well as the kinase insert; acidic domain
V	vascular endothelial cell growth factor (VEGF) receptor	contain 7 immunoglobulin-like domains as well as the kinase insert domain
VI	hepatocyte growth factor (HGF) and scatter factor (SC) receptors	heterodimeric like the class II receptors except that one of the two protein subunits is completely extracellular. The HGF receptor is a proto-oncogene that was originally identified as the Met oncogene
VII	neurotrophin receptor family (trkA, trkB, trkC) and NGF receptor	contain no or few cysteine-rich domains; NGFR has leucine rich domain

Table 1.1 Classification of Receptor Protein Tyrosine Kinases. Members are grouped according to the presence or absence of a kinase insert and based on the characteristic structural features in their extracellular portions.

protein (rasGAP), phosphatidylinositol-3-kinase (PI-3K), protein phosphatase-1C (PTP1C), as well as members of the Src family of tyrosine kinases (Cooper, 1999).

Receptor PTKs are activated by ligand binding to the extracellular region thus inducing receptor dimerization, trans-autophosphorylation and activation of PTK activity towards intracellular substrates (reviewed in Van der Geer *et al*, 1994). Receptor tyrosine kinases catalyse transfer of the γ phosphate of ATP to hyrdoxl groups of tyrosines on target proteins (Hunter, 2000).

1.2.5 *NON-RECEPTOR PROTEIN TYROSINE KINASES*

The cell surface receptors constitute only one group of protein tyrosine oncogenes: a second group of molecules encodes non-receptor protein tyrosine kinases. Non-receptor PTKs are cytoplasmic proteins that transduce extracellular signals to down-stream intermediates in pathways that regulate cellular growth, activation and differentiation. This group of proteins, in contrast to receptor PTKs, lacks extracellular or transmembrane domains. They are not therefore, integral membrane proteins but, in some cases, are peripherally associated with the plasma membrane via lipid which is covalently added after their translation (Kipreos & Wang, 1990; McWhirter *et al*, 1991).

Most of the proteins of both families of PTKs couple to cellular receptors that lack enzymatic activity themselves. There is considerable diversity of function amongst the PTK members, and although most are associated with receptors at or near the plasma membrane, a few tyrosine kinases are localised to the nucleus as well (Table 1.2). The non-receptor PTKs, like other signalling proteins, display a modular construction in which a series of discrete domains are joined together by linker sequences. The most important domains include a PTK catalytic domain (approximately 275 residues in length), an SH2 (Src homology) domain and an SH3 domain. Non-receptor PTKs can be further classified based on the criteria of amino acid similarity within the catalytic domain and the presence of common structural domains (Van der Geer *et al*, 1994; Hanks and Hunter, 1995). Table 1.2 summarises the non-receptor PTK families.

Family	Examples	Localisation	Function / Regulation
Abl	c-Abl, Arg	Cytoplasm, nucleus	c-Abl linked to cytoskeletal signalling and cell-cycle regulated transcriptional events. c-Abl activated by deletion of SH3 or BCR-mediated oligomerization, and by release from Rb in late G1
Src	c-Src, c-Yes, Blk,	Membrane associated	Roles in receptor PTK signalling and mitosis. Activity is negatively regulated by constitutive phosphorylation of a C-terminal tyrosine. Activated by receptor PTKs
Fes	c-Fes, Fer	Cytoplasm, nucleus	c-Fes in cytokine signalling, ? role in angiogenesis. Fer may signal through PTKs. c-Fes is activated by haematopoietic receptors, Fer by receptor PTKs
Syk	Syk, Zap70	Cytoplasm	Roles in cytokine receptor signalling. Activated by receptors such as BCR and TCR; Zap70 also depends on Lck for activation
Jak	Jak1, 2 & 3, Tyk2	Cytoplasm	Lead to activation of STAT transcription factors and MAP kinase activation. Activated by receptor PTKs and cytokine receptors.
Tec	Tek, Itk, Btk, Bmx	Cytoplasm	Btk is required for early B precursors to develop mature B cells.
Ack	Ack, Pyk1	*Cloned from hippocamus*	Binds to and inhibits the GTPase activity of Cdc42Hs
Fak	Fak, Cakβ	Fak: focal adhesions Pyk2: cell-cell contact	Lead to MAP kinase activation. Fak activated by plating onto fibronectin, role in integrin mediated signalling
Csk	Csk, Ctk	Cytoplasm	Csk negatively regulates Src family members by phosphorylation of a conserved C-terminal tyrosine, may be constitutively active.
Others	Rlk, Srm, Rak, Brk	----	Brk expressed exclusively in epithelial cells. Function of Srm still unknown.

Table 1.2 Classification and characterisation of Non-Receptor Protein Tyrosine Kinases.

Non-receptor PTK function depends on specific subcellular localisation which is dictated by intrinsic localisation signals (Table 1.2). Interestingly, the Fes and Abl PTK families partition between the cytoplasm and the nucleus. Shuttling between the two subcellular compartments may play a crucial role in the regulation of the biological activity of these kinases and may provide more information about their function *in vivo*. For the purpose of this study, the Abl family of non-receptor protein tyrosine kinases will be reviewed in greater detail.

1.3 ABL FAMILY

The two vertebrate members of this family are *c-abl* and c-*arg*. Both kinases are alternatively spliced to yield two proteins with distinct N-termini, one of which contains a N-terminal myristolation signal and one of which does not. Like the *src* subfamily of protein tyrosine kinases, the *abl* oncogene encodes a protein whose transforming potential is activated as a consequence of increased protein tyrosine kinase activity. The c-Abl tyrosine kinase is localised both in the cytoplasm, where it is weakly associated with actin filaments (McWhirter & Wang, 1993a), and in the nucleus where it is associated with chromatin (Van Etten *et al*, 1989).

1.3.1 STRUCTURE OF ABL PROTEIN

The Abl protein is discussed in detail in section 2.1.1. Briefly, c-Abl is characterised by its large C-terminal tail containing sites for nuclear transformation, DNA binding and F-actin binding (Figure 1.4). All three nuclear localisation signals (NLS), a nuclear export signal (NES) and a G-actin binding domain are also found at the C-tail region. The presence of G- and F-actin binding domains binding domains suggests a cytoplasmic function for c-Abl. However, the active transport of c-Abl in and out of the nucleus through its NLS and NES (Taagepera *et al*, 1998) suggests roles in both nuclear and cytoplasmic processes.

1.3.2 c-Abl TYROSINE KINASE

V	SH3	SH2	Tyrosine Kinase	Pro	NLS1	NLS2	NLS3	DNA	G-Actin, CTD-ID, F-Actin, NES

N-terminal Region
Intramolecular interactions
Binding to kinase regulators
Binding to substrates

C-terminal Region
Subcellular localisation due to
3 nuclear localisation signals (NLS) and
1 nuclear export signal (NES).
DNA binding domain
G-actin and F-actin binding domain
Binding to substrate (CTD-ID)

Figure 1.4   Functional domains of the c-Abl tyrosine kinase

Like c-Src, wild-type c-Abl protein does not transform fibroblasts or haematopoietic cells, even when over expressed (Van Etten *et al*, 1994), suggesting that Abl kinase activity is tightly regulated in cells. c-Abl is not phosphorylated in its inactive state.   Hyperphosphorylation during M phase (Kipreos & Wang, 1990) results in its dissociation from DNA at the end of the cell cycle, possibly regulating the gene expression program. Deletions and point mutations in the Abl SH3 domain that prevent binding of the proline rich SH3 ligands *in vitro* activate c-Abl kinase activity *in vivo* (Van Etten *et al*, 1999), resulting in phosphorylation of c-Abl and other proteins. Tyrosine phosphorylation of Abl is thought to reflect catalytic activity of Abl itself because ΔSH3 Abl bearing a kinase-inactivating mutation (K290R) is not phosphorylated at all (Barila *et al*, 1998).

A number of SH3 binding proteins have been identified including Abi-1 (Shi *et al*, 1995), Abi-2 (Dai & Pendergast, 1995), Aap1 (Zhu & Shore, 1996) and Atm (Baskaran *et al*, 1997). Abi-1 and Abi-2 interact simultaneously with the SH3 domain and a proline-rich motif at the C-terminal tail of c-Abl. Presumably, this interaction might sterically sequester the c-Abl kinase domain. Agami & Shaul, 1998, report remarkable activation of the c-Abl tyrosine kinase through the association of c-Abl with RFX1, a protein that binds the enhancers of several viruses and cell cycle

regulated genes. Notably, the RFX1 proline rich sequence is very similar to that of Abi-1. However, Abi-1 and RFX1 display opposite effects on c-Abl kinase activity, the former inhibits while the latter activates. Thus, the c-Abl SH3 domain may exert both positive and negative effects on its catalytic domain.

c-Abl is a Src-like tyrosine kinase with an unusual carboxy-terminal domain that contains nuclear localization signals and DNA-binding sites (Van Etten, 1999; Kharbanda *et al*, 1998). In accordance with its distribution to both the nucleus and the cytoplasm, immunoprecipitation data suggests that c-Abl binds DNA-PK, ATM, Rad51, Rb, p53, p73 and perhaps other proteins (Shaul, 2000). c-Abl activates protein kinase Cδ in response to ionising radiation (Yuan *et al*, 1998). The available biochemical and genetic evidence suggests that c-Abl is involved in multiple pathways activated by genotoxic and possibly oxidative stress (Fabbri *et al*, 1994; Kumar *et al*, 2001), regulated at several levels by protein-protein interaction and by phosphorylation.

1.3.3 *PHYSIOLOGICAL REGULATION OF C-ABL TYROSINE KINASE*

c-Abl is likely to be folded into an inactive conformation through intramolecular interactions between the SH3/SH2 and kinase domains similar to the structure of Src (Wang, 1993). An important question in the study of Abl function is to identify the physiological conditions under which Abl kinase becomes activated. Like other cytoplasmic tyrosine kinases, Abl is regulated by membrane bound receptors. Integrin-mediated adhesion to the extracellular matrix has been demonstrated to lead to the activation of c-Abl kinase activity and alters its subcellular localisation (Lewis *et al*, 1996). The nuclear c-Abl is also regulated during cell cycle progression and DNA damage. Interestingly, adhesion, cell cycle progression and DNA damage regulate Abl kinase through distinct biochemical mechanisms. Thus, c-Abl kinase is regulated by a hierarchy of multiple physiological signals.

1.3.4 ABL IN RESPONSE TO DNA DAMAGE

The cellular response to DNA damage can be split into three components: the recognition of injured DNA, a period of damage assessment (enforced by checkpoints), and the implementation of the appropriate response (DNA repair or cell death). Checkpoints have a critical role in the damage response system as they provide an opportunity to monitor the appropriateness of cell death over repair.

The nuclear c-Abl kinase activity can be regulated through DNA damage (Liu et al, 1996; Kharbanda et al, 1995b). Ionizing radiation (IR), cisplatin, mitomycin C, methylmethane sulfonate (MMS) and ara-C can all activate c-Abl, but UV irradiation cannot activate this tyrosine kinase (Liu et al, 1996; Kharbanda et al, 1995b). After DNA damage by ionizing radiation, c-Abl may be activated by phosphorylation through an ATM-dependent mechanism to enhance its kinase activity. The cycle arrest and apoptosis that are normally induced by ionizing radiation are prevented in cells that lack c-Abl or possess only a kinase-dead mutant.

Activation of c-Abl kinase by DNA damage is, however, cell cycle regulated. Only after nuclear c-Abl becomes active at G1/S phase can it then be further activated by MMS and IR (Liu et al, 1996). These observations suggest that the inhibitory effect of RB on the nuclear c-Abl kinase is dominant over the stimulatory effect of DNA damage. Only after the RB/c-Abl interaction is disrupted can c-Abl be further stimulated by DNA damage. Therefore, c-Abl kinase is expected to transduce DNA signal damage only after cells have committed to S phase. In other words, nuclear c-Abl only responds to DNA damage in proliferating cells, but not in resting cells.

1.3.5 FUNCTIONS OF C-ABL

The precise biological functions of c-Abl have not yet been fully clarified. The nuclear c-Abl is probably involved in the regulation of gene expression and the cytoplasmic c-Abl is likely to be involved in the transduction of adhesion signals. Biochemical and phosphorylation studies suggest a potential role for c-abl in cell cycle progression (Kipreos and Wang, 1990; Wong et al, 1995; Jena et al, 2002).

The shuttling of c-Abl between the two compartments may allow the cell to rapidly alter the subcellular locations of c-Abl to emphasise the nuclear or cytoplasmic function. Another possible reason for the continuous movement of c-Abl may be that Abl has the additional function of a carrier which can transport macromolecules between the two subcellular compartments. The nuclear and cytoplasmic functions of normal c-Abl are discussed in detail in sections 2.1.3 and 2.1.4 respectively.

1.3.6 *ONCOGENIC FUNCTION OF ACTIVATED ABL PROTEINS*

The first consistent chromosomal abnormality identified in a neoplasm was in chronic myeloid leukemia (CML), a haematological disorder bearing the characterisitic Philadelphia chromosome (Nowell and Hungerford, 1960). CML has an incidence of 1-2 cases per 100,000 people per annum, and accounts for approximately 15% of adult leukaemias (Faderl *et* al, 1999). Activation of the *abl* gene is implicated in CML in which a reciprocal translocation occurs between chromosomes 9 and 22 (Rowley, 1973; Bartram *et al*, 1983). This cytogenetic abnormality can be rapidly identified in a metaphase spread. Elucidation of the mechanism of *abl* activation by the Philadelphia translocation came both from analysis of translocation breakpoints and from studies of *abl* expression. The Philadelphia translocation on chromosome 9 occurs over a range of 50kb either upstream or downstream of *abl* exon 1A. On chromosome 22 however, most of the breakpoints occur within a region of 6kb, which is denoted as *bcr* (breakpoint cluster region). In effect, almost the entire open reading frame of c-*abl* on chromosome 9 is placed under the control of the *bcr* gene on chromosome 22. Transcription of the Philadelphia chromosome results in the fusion of *bcr* and *abl* coding regions by RNA splicing yielding a *bcr/abl* mRNA of approximately 8.5kb (Figure 1.5).
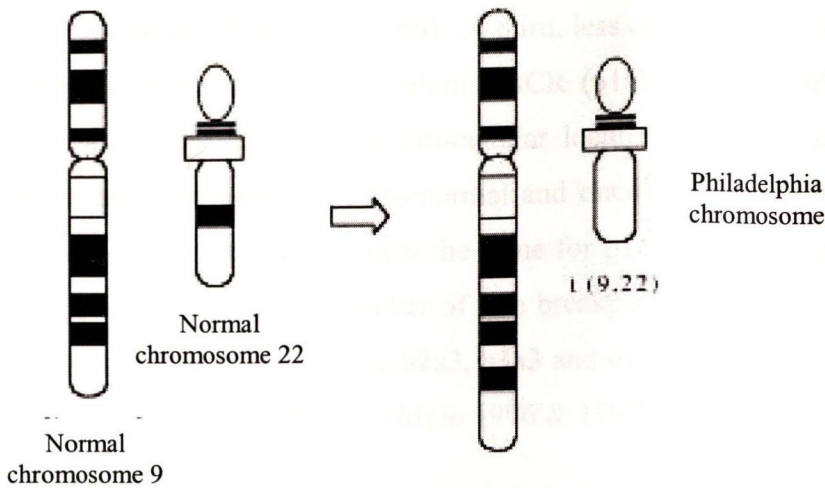
Figure 1.5 Philadelphia Chromosome t(9,22) characteristic of CML

The product of the translocated *bcr-abl* oncogene is a recombinant 210kDa protein in which the variable amino-terminal domain has been replaced by the corresponding domain of the *bcr* product (Adams, 1985). The BCR-ABL protein is found to have enhanced tyrosine kinase activity, similar to that of the viral oncogene protein. Following the formation of the BCR-ABL fusion protein, the serine/threonine kinase domain encoded by exon 1 of BCR activates the kinase domain of ABL in the BCR-ABL fusion protein (Muller *et al*, 1991) and overrides the negative regulatory activity of the SH3 domain (Fernandes *et al*, 1996). The p210Bcr-Abl contains 902 or 927 amino acids of Bcr fused to 2-11 of c-Abl (Shtivelman *et al*, 1985; Ben-Neriah *et al*, 1986). A 190kDa protein is produced in acute lymphocytic leukemia (ALL), in which the variable domain is replaced by the first 426 amino acids of Bcr. The fusion of c-*abl* to the breakpoint cluster region on chromosome 22 constitutively activates the tyrosine kinase activity of c-ABL (Konopka *et al*, 1984). Amplification of the c-*abl* gene has also been observed within the CML cell line, K562.

There are three principal forms of BCR/ABL (p190, p210 and p230 BCR/ABL) that are found in distinct forms of Ph-positive leukemias. The two major forms involve ABL exon2 and two different exons (exon 2 and 3) of the BCR gene. The transcripts, b2a2 and b3a2 respectively, encode for a p210 protein (Melo, 1996 & 1997). Another fusion gene leads to the formation of an e1a2 transcript which

encodes a p190 transcript (Pane *et al* 1996). A third, less common fusion gene is c3a2 [e19a2] which gives rise to a p230 protein. BCR (p160) and BCR/ABL proteins (p190 and p210) exhibit cytoplasmic sub-cellular localisation (Dhut *et al* 1988 & 1990). The levels of expression of the normal and oncogenic forms are equivalent indicating that the rate of transcription is the same for p160, p190 and p210 proteins (Dhut *et al*, 1990). In addition, a number of rare breakpoints have been identified in the BCR and ABL genes such as e6a2, b2a3, b3a3 and e1a3, the expression of which have been detected at the mRNA level (Melo 1996 & 1997).

The mechanism by which translocations activate *abl* appear to be fundamentally different from activation of *myc*: the *abl* translocations lead to formation of an altered protein whereas *myc* translocations result in abnormal expression of a normal gene product.

1.3.7   FUNCTIONS OF THE BCR-ABL ONCOPROTEIN

The *bcr-abl* fusion gene encodes a 210kDa protein product (Shtivelman *et al*, 1985) and exhibits enhanced tyrosine kinase activity (Konopka *et al*, 1984). Normal Abl is found primarily in the nucleus (Wetzler *et al*, 1993), however the oncogenic BCR-ABL protein localises to the cytoplasm of the cell (Dhut *et al*, 1990; Wetzler *et al*, 1993). A significant effect of BCR-ABL is a block on apoptosis (Bedi & Shakis, 1995; DiGiuseppe & Kastan, 1997). The expression of BCR-ABL tyrosine kinase has been implicated in the apoptotic resistance of CML cells (Cortez *et al*, 1995). The mechanism of CML growth advantage is likely to be a combination of increased proliferation and a failure to undergo programmed cell death to the same degree as normal cells. Decreasing the expression *in vivo* of a tretracycline-inducible Bcr-Abl1 gene in mice by tetracycline withdrawal leads to a rapid disappearance of leukaemic cells *in vivo*, mediated by increased apoptosis (Huettner *et al*, 2000).

BCR-ABL tyrosine kinase activity is also implicated in a number of cell signalling pathways including Ras (Goga *et al*, 1995), c-MYC (Sawyers *et al*, 1992) and also non-receptor tyrosine kinase pathways such as JNK (Sawyers *et al*, 1997). Ras plays a critical role in the transmission of mitogenic signals from receptor tyrosine kinases (Mulcahy *et al*, 1985, Wood *et al*, 1992). Ras involvement in the

signalling events during Abl-mediated transformation was first reported by Stacey *et al*, 1991. They demonstrated abrogation of transformation by v-Abl by anti-Ras antibody. BCR-ABL has been implicated in the Ras signalling pathway via its interaction with the cytoplasmic effector molecule GRB-2 (Pendergast *et al*, 1993). Other functions of BCR-ABL include activation of the p65 sub-unit of the transcription factor NF-κB (Hamdane *et al*, 1997) and the p-85 sub-unit of phosphoinositide-3 kinase (PI-3 kinase) in hemopoietic cells (Jain *et al*, 1996).

1.4   RATIONALE FOR THE STUDY OF C-ABL EXPRESSION

Although it has been sugsted that Abl is ubiquitously expressed, there is little data on tissues in which Abl is most strongly expressed. c-Abl kinase is activated in Philadelphia chromosome positive leukemias, raising the question of whether elevated Abl tyrosine activity may inhibit apoptosis and cause accumulation of leukemia cells in this way (Cotter, 1995). Previous work from our group has investigated c-*abl* expression in nomal tissues and in spontaneous tumours other than CML (O'Neill *et al*, 1997). Preliminary observations indicate that c-Abl is typically expressed in mature cells of certain adult tissues (hyaline cartilage, mucus cells, ciliated epithelium) and strongly expressed in a few specific tumour types (liposarcoma, chondrosarcoma). Furthermore, its distribution in fetal tissues and in the myxoid stroma and tumour microvessels of specific tumour types suggests possible additional roles in morphogenesis and angiogenesis.

This project aims to investigate the role of *abl* in apoptosis and the development of cancer. The shuttling of c-Abl between the nucleus and the cytoplasm is determined by a balance of nuclear import and export signals (Taagepera *et al*, 1998), and the dynamic equilibrium between the two processes may influence the precise biological functions of c-Abl *in vivo*. The ability to localise to the cytoplasm allows c-Abl access to numerous substrates through which it can exert its anti-apoptotic effects. Activation of c-*abl* through *bcr* results in a change in growth regulatory function from pro-apoptotic to anti-apoptotic. The regulatory roles of c-Abl in apoptosis through phosphorylation of different substrates and through binding of signalling molecules are still not clearly understood. A more comprehensive

understanding of the precise functions of abl *in vivo* may facilitate in future apoptosis-based approaches to the treatment of malignancy and other diseases.

1.5 SPECIFIC OBJECTIVES

This study proposes to determine the expression of the *abl* gene in fetal development and in selected human tumours. In particular, it will focus on those tumours which in preliminary work have shown strong Abl protein expression *i.e.* chondrosarcoma, liposarcoma, diffuse type gastric adenocarcinoma. The relationship, if any, between Abl expression and the degree of tumour cell differentiation and level of apoptosis will be examined. In addition, it is proposed to investigate more fully the role of c-*abl* in both normal and neoplastic angiogenesis.

Following from this, it is proposed to extend the observations of c-*abl* expression to the mRNA level. Recent advancements in quantitative RT-PCR and *in-situ* RT-PCR methodologies should enable a more accurate and informative evaluation of c-*abl* levels in tissue sections or, more specifically, within individual cells. Finally, we propose to investigate more fully the events leading to c-Abl upregulation in endothelial cells *in vitro*. A number of external stimuli will be investigated including heat shock, serum deprivation, reactive oxidative species (H_2O_2) and wortmannin. Ultimately, 3 main questions will be examined:

1. In what tissues is c-*abl* expressed and what role does Abl play in apoptosis, tumourigenesis and angiogenesis in non-haematopoietic tumours?

2. Is differential regulation observed at the protein and/or mRNA level?

3. Is c-*abl* mRNA in endothelial cells modulated in response to specific stress factors?

2.   ABL PROTEIN EXPRESSION IN NORMAL HUMAN TISSUES AND TUMOURS

2.1 INTRODUCTION

2.1.1 ISOFORMS OF C-ABL

The mammalian c-*abl* gene produces two proteins of 145kD that differ only at their N-terminus, due to alternative splicing of the first two exons (Ben-Neriah *et al*, 1986; Shtivelman *et al*, 1986). The isoforms are denoted type I and type IV c-Abl in mice and types Ia and Ib c-Abl in humans respectively. It has been proposed that the N-terminal variability may dictate the sub-cellular localisation of the two c-*abl* proteins: type I soluble and type IV membrane bound. Signals for nuclear localisation are primarily defined by C-terminal sequences where there is a nuclear translocation signal and a DNA binding domain (Kipreos *et al*, 1990). Also found within the C-terminal region of the molecule is the presence of an actin-binding domain (McWhirter *et al*, 1991), the signal for cytoplasmic localisation. The type IV c-*abl* isoform contains an N-terminal glycine, a possible site for myristylation which enables the protein to associate with the cell membrane.

Studies by Renshaw *et al*, 1988, investigated the relative abundance of the two major c-*abl* mRNAs (type I and type IV) in several mouse tissues and cell lines. They observed that the level of type IV c-*abl* mRNA is rather constant in a variety of cell types, whereas the level of type I mRNA is modulated (over a 10-fold range) in a tissue specific manner. The results have interesting implications for the functions of the two c-*abl* proteins. It is conceivable that as there are several isoforms of c-*abl*, with different promoters determining their expression, each c-*abl* isoform may have a specific biological function. Using an antisense approach, Daniel *et al,* 1996, demonstrated that type I c-*abl* is essential for cellular differentiation while type IV c-*abl* suppresses apoptosis.

2.1.2 SUBCELLULAR LOCALISATION OF C-ABL

Early efforts at understanding the role of c-Abl focused on where the protein resided in the cell, with the hope that the location would give important clues about its function. In addition, it would be important to determine whether the transition from the benign state to the fully malignant one may involve a change in subcellular residence. The subcellular localisation of c-Abl was first determined by Van Etten *et al*, 1989, by over-expressing the murine type IV protein in fibroblasts. Unexpectedly, it was found to be largely nuclear, however a significant fraction resides in the cytoplasm and is associated mostly with filamentous actin and the plasma membrane. This appears to be the endogenous Abl pattern in most cell types, although in some tissues such as primary hematopoietic cells and neurons, c-Abl is more cytoplasmic than nuclear (Wetzler *et al*, 1993; Koleske *et al*, 1998). Experiments aimed at over-expression of the non-myristolated type Ia/I form of c-abl are very difficult to perform and although its localisation is assumed to be similar to the myristolated form, this has not been demonstrated directly.

In quiescent and G_1 cells, nuclear c-Abl is kept in an inactive state by the retinoblastoma protein (Rb) that binds to the c-Abl tyrosine kinase domain and inhibits its activity (Welch & Wang, 1993 & 1995). Phosphorylation of Rb by cyclin-dependent kinases at the G_1/S boundary disrupts the Rb/c-Abl complex, leading to activation of the c-Abl tyrosine kinase. Activated nuclear c-Abl can phosphorylate the C-terminal repeated domain (CTD) of RNA polymerase II to modulate transcription (Baskaran *et al*, 1993 & 1996). Unlike nuclear c-Abl, the cytoplasmic pool of c-Abl is not regulated during cell cycle progression and is active in G_1 cells and during quiescence (Welch & Wang, 1995).

The observation that c-Abl is differentially phosphorylated in interphase versus mitotic cells also suggests that it may play a role in the regulation of cell proliferation. Kipreos *et al*, 1990, demonstrated that the c-Abl protein from metaphase arrested cells migrates with retarded mobility through an SDS-PAGE gel due to enhanced

phosphorylation. Analysis of the phosphotryptic peptides showed that three serine/threonine sites are phosphorylated in c-Abl during interphase and at least seven serine/threonine sites are phosphorylated as cells enter mitosis (Kipreos *et al*, 1990). All of the mitosis-specific phosphorylation sites are located in the COOH terminal. Mutant mice homozygous for a 3'-deletion of c-*abl* and expressing active c-Abl truncated at the COOH terminus have multiple defects at birth, suggesting that the COOH terminal is essential for biological function.

c-Abl has three nuclear localisation signals (NLSs), each comprising short basic sequences in the C-terminal domain (Figure 2.1). These three signals function differently in various cell types and exhibit overlapping and redundant functions in fibroblasts, such that the presence of any one of them is sufficient to localise Abl to the nucleus (Wen *et al*, 1996). The accumulation of c-Abl in the nucleus is balanced by the presence of a nuclear-export signal (NES) at the C-terminus of the protein (Figure 2.1) that mediates translocation of c-Abl to the cytoplasm in a pathway sensitive to leptomycin B (Taagepera *et al*, 1996). In the cytoplasm, the majority of over-expressed c-Abl is associated with the F-actin cytoskeleton. F-actin localisation requires the presence of a small C-terminal domain that overlaps with the NES (McWhirter *et al*, 1993; Van Etten *et al*, 1994). Daley *et al*, 1992, demonstrated that a portion of myristolated c-Abl is associated with the inner membrane, the myristol group essential for membrane localisation.

The presence of c-Abl in multiple cellular compartments suggests that the protein might move from one place to another within the cell, transducing signals in response to physiological stimuli. In 1996, Lewis demonstrated that c-Abl kinase activity is strictly dependent on integrin-mediated cell adhesion for activation in both cytoplasmic and nuclear compartments. When fibroblasts are trypsinized and replated onto fibronectin, there is a relocalisation of c-Abl from the nucleus to F-actin-rich focal adhesions, with a subsequent return to the nucleus within an hour, suggesting that nuclear-cytoplasmic shuttling of Abl occurs in response to integrin-induced signals.
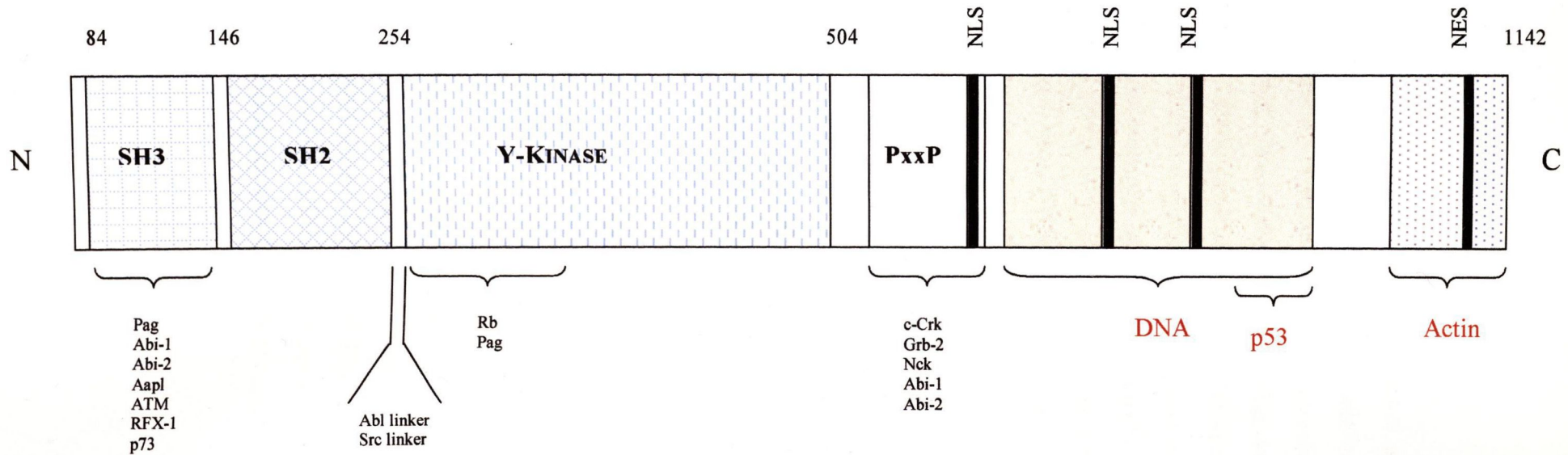
Figure 2.1 Structure of c-Abl. Schematic adapted from Shaul *et al*, 2000.

The PxxP region contains several PxxP motifs that may potentially interact with SH3 domains. All NLS and NES motifs are found at the C-tail region. SH3 region is approx. 50 aa in length and preferentially interacts with proline rich regions containing the PxxP motif. SH2 region is approx. 100 aa in length and interacts with tyosine phosphorylated residues. c-Abl is characterised by its long C-terminal tail.

2.1.3 NUCLEAR FUNCTIONS OF C-ABL

The precise biological functions of c-Abl are not fully understood but it is believed to play an important role in cell cycle regulation, signal transduction and inhibition of apoptosis. Several lines of evidence suggest a role for nuclear c-Abl in regulation of the cell cycle (Welch & Wang, 1995). As previously stated, a portion of the nuclear pool of c-Abl is found complexed to Rb in cells in G_1 phase of the cell cycle. Phosphorylation of Rb by cyclin-D-cdk4/6 kinases at the G_1/S boundary results in the release of c-Abl and activation of Abl kinase activity during S phase. Abl has also been shown to inhibit growth in G_1 phase (Wen *et al*, 1996; Sawyers, 1994). When over-expressed by transfection, c-Abl induces cell cycle arrest in G_1 with apoptosis of a significant fraction (Wen *et al*, 1996).

c-Abl has three tandemly repeated DNA binding domains which show homology to HMG proteins (Miao & Wang, 1996). The three DNA binding domains are roughly coincident with the three Abl nuclear localisation signals suggesting duplication of a functional unit. Although c-Abl was initially reported to have sequence-specific DNA binding activity, subsequent work has shown only a weak preference for AT-rich oligonucleotides. The disruption of DNA-protein interactions represents an important function of cdc-2 kinase during metaphase. Moreno *et al*, 1990, suggests that the general inhibition of protein-DNA interaction during mitosis serves the function of resetting the cellular gene expression programme at the end of each cell-cycle. This would probably involve disruption of initiation complexes assembled at the promoter.

Upon activation, c-Abl phosphorylates several nuclear substrates including DNA-PK (Kharbanda *et al*, 1995b), Rad51 (Yuan *et al*, 1998) and the p85 sub-unit of phosphatidylinositol-3 kinase (Yuan *et al*, 1997), negatively regulating their respective activities. Kharbanda *et al*, 1995a, also demostrated that c-Abl is involved in activation of stress-activated/*jun* N-terminal kinase (SAPK/JNK).

2.1.4 CYTOPLASMIC FUNCTIONS OF C-ABL

The function of c-Abl in the cytoplasm is very poorly understood in comparison with its nuclear counterpart. A number of constitutively active alleles of c-Abl have been created through mutational analysis. Mutations of the SH3 domain enhance c-Abl kinase activity, presumably by disrupting its interaction with regulatory proteins (Van Etten *et al*, 1989; Mayer & Baltimore, 1994). In contrast to growth arrest by nuclear c-Abl expression, the cytoplasmic c-Abl alleles cause transformation analogous to Bcr-Abl. It is the exclusion of *v*-abl and Bcr-Abl from the nucleus and the exclusive binding of Bcr-Abl to F-actin which indicates that cell transformation results from an activation of the cytoplasmic function of the Abl tyrosine kinase (Danial *et al*, 1998). Association of cytoplasmic c-Abl with the F-actin cytoskeleton is via the C-terminal F-actin binding domain.

2.1.5 ABL EXPRESSION IN HUMAN FETAL AND ADULT TISSUES AND TUMOURS

O'Neill *et al*, 1997, examined Abl expression in a wide range of normal and fetal human tissues and a variety of different tumour types. Abl immunoreactivity was similar to that previously reported for murine tissues (Renshaw *et al*, 1988) with ubiquitous expression in most human tissues. Intense Abl immunoreactivity was restricted to certain connective tissue cells such as adipocytes, chondrocytes and umbilical cord fibroblasts. In most of the cell types examined, Abl immunoreactivity was cytoplasmic. However mucous cells and chondrocytes often displayed nuclear staining. There was no Abl immunoreactivity of a number of normal cells and tissue types including tonsil, spleen, erythroid precursors, smooth, cardiac or skeletal muscle or blood vessels (O'Neill *et al*, 1997).

Fetal tissues showed a broadly similar staining pattern of Abl immunoreactivity. Developing white adipose tissue was moderately stained while strong staining was observed in chondrocytes. Most tumours showed weak Abl immunoreactivity, with intense staining in liposarcoma, chondrosarcoma and diffuse signet ring carcinoma of the

stomach. Tissues and structures that normally showed no Abl immunoreactivity were occasionally positive in the vicinity of Abl positive tumour cells.

The aim of this part of the study was to examine more fully the extent of Abl expression in normal and neoplastic chondrocytes, human placenta, liposarcoma, breast carcinoma and gastric carcinoma. Abl protein expression was assessed immuno-histochemically using a polyclonal antibody directed against the c-Abl/Bcr-Abl oncoprotein (Serotec, UK). The relationship between Abl expression and tumour grade, cellular differentiation and extent of apoptosis was also investigated.

2.2 MATERIALS & METHODS

All material used in this study was obtained, with consent, from the relevant Department of Histopathology as cited in the text.

2.2.1 FETAL CARTILAGE

Twenty-four blocks of fetal cartilage taken post-mortem were obtained from the files of the department of Histopathology, Rotunda Hospital, Dublin (courtesy of Dr. John Gillan). Specimens were taken to encompass gestational ages from 15 - 42wk. The material was well fixed and showed minimal autolysis.

2.2.2 CHONDROSARCOMA

Chondrosarcoma cases were obtained from the files of St. James's Hospital and Mater Misericordae, Dublin (courtesy of Prof. P.A. Dervan). Of the 20 cases diagnosed from 1989 to 1997, 16 cases were deemed suitably well preserved for this study following examination of their respective H&E sections.

Tumours were graded using standard criteria summarised by Bjornsson *et al*, 1998, as follows: grade 1 (n=6), grade 2 (n=5) and grade 3 (n=5, including one dedifferentiated chondrosarcoma). The sites of these tumours were: femur (n=4), rib (n=3), humerus (n=2), ilium (n=2), scapula (n=2), fibula (n=1) and site not recorded (n=2). For each case, one paraffin block was selected for Abl immunostaining and assessment of apoptosis and mitosis.

2.2.3 LIPOSARCOMA

Formalin-fixed paraffin-embedded material from 20 liposarcoma cases was obtained from the files of St. James's Hospital and Mater Misericordae, Dublin, and Brigham and Women's Hospital, Boston, MA (Dr. C.D.M. Fletcher). Tumours were

classified into the following sub-types: lipoma-like grade 1, myxoid grade 1, cellular myxoid grade 2 and round cell grade 3. The material under investigation had been embedded in paraffin for 1 to 44 years.

2.2.4 BREAST CARCINOMA

Twenty-three cases of breast carcinoma were obtained from the files of the department of Histopathology, St. James's Hospital, Dublin. Thirteen cases had been formalin fixed, paraffin embedded and 10 cases were snap frozen in liquid Nitrogen and stored at -70°C. The material under investigation included infiltrating lobular carcinoma, infiltrating ductal carcinoma and in-situ ductal carcinoma. For each case, sections were cut and mounted onto APES coated slides and stained immunohistochemically for the c-Abl/Bcr-Abl oncoprotein as outlined in section 2.2.7.4.

2.2.5 GASTRIC CARCINOMA

Eleven cases of formalin fixed paraffin embedded gastric carcinoma were obtained from St. James's Hospital and St. Vincent's University Hospital, Dublin. Of these, 6 were classified as diffuse type gastric adenocarcinoma and 5 as intestinal type adenocarcinoma.

2.2.6 PLACENTA AND UMBILICAL CORD

The material for this part of the study was kindly supplied by Dr. John Gillan, Pathology Department, Rotunda Hospital, Dublin. A total of 55 cases were investigated and these are sub-classified as follows:

4 cases	Normal villi
4 cases	Dysmature villi
4 cases	Fetal Artery Thrombosis (F.A.T.)
2 cases	Ectopic gestation

| 17 cases | Early placenta (6-17wk gestation) |
| 24 cases | Normal placenta (18-42wk gestation) |

All material was formalin fixed paraffin embedded and showed minimal autolysis.

2.2.7 IMMUNOHISTOCHEMISTRY

2.2.7.1   Anti c-Abl/Bcr-Abl antibody

The Abl oncoprotein was detected immunohistochemically using a sheep polyclonal antibody (Serotec, UK).   The antibody was raised against the synthetic heptadecapeptide:

Cys-Lys-Thr-Leu-Lys-Glu-Asp-Thr-Met-Glu-Val-Glu-Glu-Phe-Leu-Lys-Glu

derived from the *v*-abl amino acid sequence (Reddy *et al*, 1983).   The peptide was conjugated to keyhole limpet haemoxyanin via the N-terminal cysteine using m-maleimidobenzoic acid N-hydroxysuccinimide ester.   Purified IgG was prepared from whole serum by affinity chromatography.   The antibody does not differentiate between c-Abl and Bcr-Abl proteins or the different isoforms of c-Abl.

2.2.7.2   Stain optimisation

A range of dilutions of the primary antibody stock (1mg/ml) were prepared in Tris buffer, pH7.6 (1/10 to 1/400 dilution).   Serial sections from a number of tissue blocks were cut and stained immunohistochemically as outlined in section 2.2.7.4   Slides were evaluated to assess the optimum antibody dilution for determination of Abl immunoreactivity.   A ten-fold dilution of the primary antibody results in an unacceptable background staining, whereas 1/400 dilution results in specific but weak staining.   The optimum staining was achieved using a 1/200 dilution of the antibody demonstrating specific staining of the Abl oncoprotein with minimal background.

2.2.7.3 Controls

The primary antibody is either omitted for negative control, or preabsorbed (thus obliterating staining) with the immunising peptide against which it is directed. The immunising peptide (Serotec, UK) is supplied at a concentration of 1mg/ml. 13.3µl of peptide is incubated with 1ml primary antibody for 1hr at 37°C to achieve a 10-fold excess by weight (Handel *et al*, 1995). The volume is brought to 400ml with Tris buffer, pH7.4, prior to use. Using this control, the immunoreactivity is completely obliterated (Figure 2.3). For positive controls, sections of bone marrow containing immunoreactive mature myeloid cells are used.

2.2.7.4 Abl Immunoreactivity Assay

Sections of paraffin embedded tissue (4µm) are cut and mounted on 3-aminopropyltriethoxysilane (APES) coated slides and oven dried at 50°C overnight. Sections are deparaffinised in xylene (2 x 10min) and rehydrated through graded alcohols (100%v/v, 75%v/v, 50%v/v, 25%v/v, each for 10min). Endogenous peroxidase is quenched by incubating slides in 3%v/v H_2O_2 in MeOH for 30min. Non-specific binding sites are blocked with 0.1%w/v BSA for 30min at room temperature. Sections are incubated with sheep anti-c-Abl/Bcr-Abl oncoprotein antibody (polyclonal; Serotec, U.K; 1/200 dilution in Tris buffer, pH7.6) for 1hr at room temperature, followed by two 10min washes in Tris buffered saline (TBS). Approximately 50µl of biotinylated rabbit anti-sheep antibody (Serotec, U.K; 1/400 dilution in Tris buffer, pH7.6) is applied to each section for 30min and again slides are washed in two changes of TBS. This is followed by 30min incubation with peroxidase-conjugated streptavidin (Dakopatts, Denmark, 1/400 dilution in Tris buffer, pH7.6). The reaction product is visualised for 7min with 3,3' diaminobenzidine (DAB) and a haematoxylin counterstain. Sections are dehydrated through graded alcohols (over a period of 30min), clarified in xylene, mounted in DPX and coverslipped. Under these conditions, slides may be stored at room temperature, away from direct sunlight, for several years.

2.2.7.5   Assessment of staining

Abl immunoreactivity in the tissues under investigation is assessed using a simple three tiered system:

+   focal or weak staining

++   moderately intense staining

+++   intense staining

The data presented are the results of the slides being evaluated blind by two independent investigators. This is to ensure that an objective assessment of staining is achieved.

2.2.8   APOPTOSIS EVALUATION

2.2.8.1   Mayer's Haematoxylin & Eosin Stain (H&E)

Sections of paraffin embedded material (10μm) are cut and mounted onto glass microscopy slides. Mayer's Haematoxylin is freshly prepared as follows:

Haematoxylin	1g
Distilled water	1000ml
Potassium alum	25g
Sodium iodate	0.1g
Citric acid	0.5g
Chloral hydrate	25g

The haematoxylin, potassium alum and sodium iodate are dissolved in the distilled water by warming and stirring. The chloral hydrate and citric acid are added, the mixture is boiled for 5min and then cooled and filtered. The stain is ready for use immediately. Eosin Y is the most widely used stain in combination with an alum haematoxylin and is prepared as a 1%w/v solution in distilled water. A standard haematoxylin and eosin stain involves initially dewaxing sections in xylene and hydrating through graded alcohols to water. Mayers haematoxylin is applied for 8min and sections are washed in running tap water until 'blue' (5min). Sections are counterstained briefly in 1%w/v Eosin Y for approximately 40sec and washed in running tap water for a further 5min. Sections are dehydrated through graded alcohols, clarified in xylene and mounted in DPX.

2.2.8.2   Calculation of AI

H&E stained sections are assessed for apoptosis by light microscopy (Olympus BX40 microscope) according to the method of Staunton & Gaffney, 1995. Briefly, apoptotic cells/bodies are counted using the 40X objective lens with a calibrated eye-piece (1mm index 100 square grid, Graticules Ltd., Tonbridge, U.K.). The total number of tumour cells per field (as defined by the grid) is determined by counting tumour cells within the boundary of 20 or 50 grid squares (depending on cellularity and tumour cell distribution) and multiplying by 5 or 2 respectively. Ten fields are assessed for each case, avoiding areas of necrosis.

The apoptotic index (AI) is defined as the number of apoptotic cells expressed as a percentage of the total number of cells in 10 high powered fields (Potten, 1996).

2.2.8.3   *In Situ* End Labelling (ISEL) Apoptosis Detection Kit

An alternative method of apoptosis evaluation was assessed prior to commencement of this study (Gaffney *et al*, 1995). The ISEL technique exploits the ability of the enzyme TdT to incorporate digoxigenin labelled nucleotides into the DNA strand breaks characteristic of cells undergoing apoptosis (Alison, 1999; Carr & Talbot, 1997).

The optimised in situ end-labelling technique requires several modifications to the manufacturers (Oncor) protocol. Briefly, $4\mu m$ sections of formalin-fixed paraffin embedded material are cut and mounted on APES coated slides and dried overnight at $50^{\circ}C$. Sections are deparaffinised and hydrated as outlined in section 2.2.7.4. Endogenous peroxidase is quenched by placing slides in 3%v/v H_2O_2 in methanol (MeOH) for 10min at room temperature. Slides are quickly immersed in distilled water to remove alcohol and washed in phosphate buffered saline (PBS) for 5min. Permeabilisation of tissue sections is achieved by 15min digestion with Proteinase K

(20µg/ml) at 37°C in a humidified chamber. Slides are washed in two changes of dH₂O and PBS for 2min each. 75µl 1X equilibration buffer (supplied in kit) is applied directly onto each slide and left for 30min at room temperature. Enough working strength TdT enzyme solution to cover sections (30-50µl) is applied and slides placed in a 37°C humidified chamber for 1hr. Staining is achieved using anti-digoxigenin peroxidase and the chromagen substrate DAB as per guidelines. Finally, sections are counterstained with 1%w/v aqueous methyl green (2min).

The results obtained using this technique were variable and inconsistent when compared to those obtained from H&E stained sections. Consequently, all data relating to AI presented in this study are generated from H&E apoptotic counts and not from sections stained using the ISEL technique.

2.3 RESULTS

2.3.1 FETAL CARTILAGE

Abl staining in developing fetal chondrocytes was predominantly nuclear although cytoplasmic or cell membrane staining was found occasionally. Most epiphyseal reserve chondrocytes and proliferating immature chondrocytes in fetuses of all ages showed moderate to strong Abl staining. In contrast, hypertrophic chondrocytes about to undergo apoptosis during enchondral ossification showed minimal or no Abl staining (Figure 2.4).

There was intense Abl immunoreactivity of adjacent proliferating osteoblasts and invading metaphyseal blood vessels at sites of enchondral ossification. Apoptotic cells, although infrequent were visible at the growth plate from 16 weeks gestation. No difference in staining pattern was observed in fetuses of different gestational ages. Table 2.1 summarises the staining pattern observed in the different cell types.

Zone	Cell type	Abl staining	Staining Intensity
Bone shaft	Immature chondrocytes	Nuclear	70%
Proliferative Zone	Mature chondrocytes	Nuclear, cytoplasmic & membranous	70-80%
Growth plate	Hypertrophic chondrocytes	Absent	Minimal or absent
Growth plate	Osteoblasts	Nuclear	80%
Growth plate	Osteoblasts, proliferating endothelium	Nuclear & cytoplasmic	Striking staining of neovasculature

Table 2.1 Abl staining in normal fetal cartilage. Percentage staining is calculated by counting the total number cells and the number of stained cells in 10 fields as defined in section 2.2.8.2.

2.3.2 CHONDROSARCOMA

The Abl immunoreactivity observed in the chondrosarcoma cases studied, along with their respective apoptotic and mitotic indices, are summarised in Table 2.2.

Case	Tumour Grade	Abl Expression	AI (%)	MI (%)
1	G1	3+	0	0
2	G1	3+	0	0
3	G1	3+	0	0
4	G1	3+	0	0
5	G1	3+	0	0
6	G1	3+	0	0
7	G2	3+	0	0
8	G2	2+	0	0
9	G2	2+	0	0
10	G2	2+	0.6	0.2
11	G2	2+	1.9	0.6
12	G3	1+	0.8	0.3
13	G3	Neg	0.3	0.9
14	G3	Neg	2.8	0.8
15	G3	Neg	3.2	0.3
16	G3	Neg	1.2	0.5

Table 2.2   Abl immunoreactivity, Apoptotic and Mitotic Indices in chondrosarcoma.

In all 6 grade 1 chondrosarcomas, more than 70% of tumour cells showed intense (3+) nuclear Abl staining (Figure 2.5). Grade 2 chondrosarcomas showed moderate to intense nuclear c-Abl staining (3+ in one case and 2+ in the other 4 tumours). In grade 3 chondrosarcoma, Abl staining was minimal (1+) or absent (Figure 2.6). The

dedifferentiated chondrosarcoma show intense Abl immunoreactivity in the low grade component, but no staining in the high grade component (Figure 2.7).

Mean AI and MI (and ranges) for the 16 chondrosarcoma cases were 0.68% (0.3-2%) and 0.23% (0-0.9%) respectively. In all tumours except one, the number of mitoses was less than or equivalent to the number of apoptotic tumour cells. There were numerous apoptotic cells in the high grade component of dedifferentiated chondrosarcoma (Figure 2.7). There is a very significant linear correlation between the AI and MI ($p<0.0090$; $r=0.6294$).

2.3.3 LIPOSARCOMA

The extent of apoptosis in liposarcoma was assessed as outlined in section 2.2.8. Table 2.3 summarises the apoptotic indices, mean (and range), recorded in different grades of liposarcoma.

Subtype/Tumour Grade	AI Mean (and Range)
Lipoma-like and sclerosing, G1	0
Myxoid, G1	0
Cellular myxoid, G2	0.2% (0.1-0.6%)
Round cell, G3	1.0% (0.3-1.8%)

Table 2.3   Apoptotic Indices in liposaroma

The extent of apoptosis in liposarcoma is variable and is related to grade and the percentage of morphologically undifferentiated tumour cells. Although AI are generally low in liposarcoma, relatively small changes in AI represent significant changes in tumour cell kinetics.

Abl expression in liposarcoma was assessed in these cases using the immunohistochemical staining technique detailed in section 2.2.7.4 and 2.2.7.5, and the results summarised in Table 2.4. Abl angiogeneic vessel staining is most intense in myxoid liposarcoma in which a network of capillaries is prominantly observed.

Subtype/Tumour Grade	Apoptosis (AI)	Abl tumour cells	Abl angiogenic vessels
Lipoma like, G1	0	++	0
Sclerosing, G1	0	++	0
Myxoid, G1	0	+++	+++
Cellular myxoid, G2	0.2%	++	+/++
Round cell, G3	1.0%	0	0

Table 2.4 Abl expression in relation to liposarcoma subtype and grade, angiogenic vessel staining and apoptosis. Corresponding Figures 2.8 and 2.9.

2.3.4 BREAST CARCINOMA

Normal breast tissue demonstrates moderate Abl expression in myoepithelial cells, but no staining of epithelial cells (O' Neill *et al*, 1997). Abl immunostaining is quite variable in both the formalin fixed and fresh frozen breast tissue included in this study. Tumour cells are occasionally weakly to moderately positive (+/++), with staining predominatly nuclear although some cytoplasmic staining is also observed. Staining of tumour microvessels is weak and infrequent, although the vessels are often difficult to identify particularly in the frozen material. Interestingly, Abl expression in microvessels and capillaries is occasionally observed in an area in which tumour cells appear negative. Abl immunoreactivity in breast carcinoma is summarised in Table 2.5. Corresponding Figure 2.10 illustrates Abl immunoreactivity in tumour microvessels of breast carcinoma.

Subtype/Grade	Abl tumour cells	Abl angiogenic vessels
Infiltrating lobular carcinoma	+/++	+
Infiltrating ductal carcinoma	+/++	+
In-situ ductal carcinoma	+	+
Tubular carcinoma	++	++

Table 2.5 Abl expression in tumour cells and tumour microvessels of breast carcinoma.

2.3.5 GASTRIC CARCINOMA

Abl expression in gastric adenocarcinoma was assessed immunohistochemically as detailed in section 2.2.7.5. The results obtained are outlined in Table 2.6

Subtype/Grade	No. Cases	Abl tumour cells	Abl angiogenic vessels
Diffuse type	6	++	++
Intestinal type	5	+	+

Table 2.6 Abl expression in gastric adenocarcinoma. Moderate to intense Abl staining of tumour cells and tumour microvessels is observed in diffuse signet ring carcinoma of stomach. Weaker staining of tumour cells and vessels is observed in the intestinal type gastric adenocarcinoma. Corresponding Figure 2.11 illustrates Abl expression in diffuse type gastric adenocarcinoma.

There is no significant difference in the AI recorded for these two different type of gastric carcinoma (O'Neill *et al*, unpublished data).

2.3.6 PLACENTA

Very early placenta (6-7wks) shows strong nuclear Abl staining of fibroblast precusors, blood vessels and some connective tissues. Staining is also observed but to a weaker extent in placenta at 8-10wks. This is in contrast to the mature placenta in which there is no Abl staining of blood vessels or blood cells. There is faint staining (+) of surface trophoblast in mature placenta. Moderate staining (++) of the amnion and umbilicus is also observed in placenta of 38-42wks gestation.

Moderate to intense Abl staining is observed in the blood vessels of the villi of ectopic gestations, particularly in one earlier case (6-7wk old). There is weak staining (+) of the cytoplasm of endometrial glands but no staining of maternal blood vessels. Figure 2.12 shows moderate Abl protein expression in the developing umbilical cord fibroblasts of Wharton's jelly.
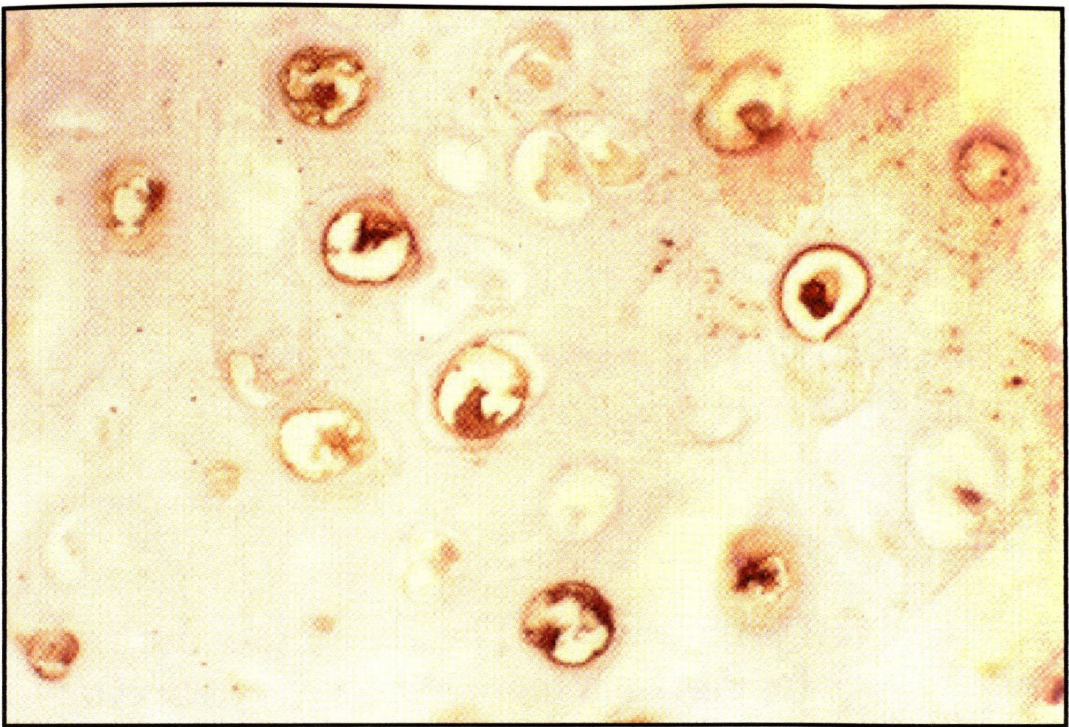
Figure 2.2 Abl immunostaining in normal chondrocytes. Intense nuclear Abl staining is observed in adult tracheal cartilage.
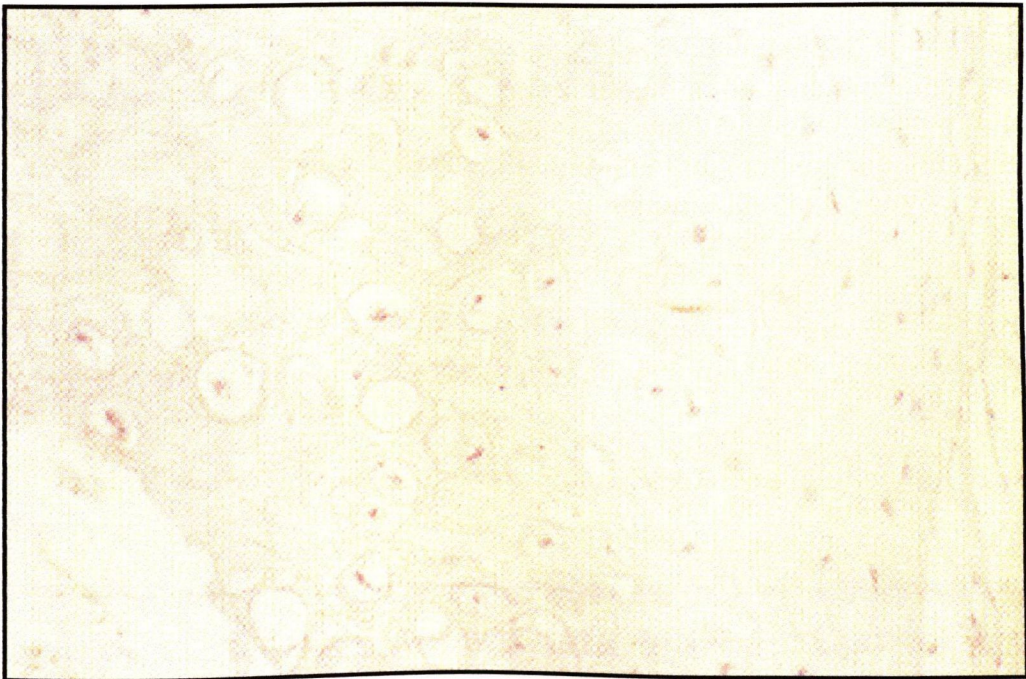
Figure 2.3 Abl immunostaining negative control. The primary antibody is preabsorbed with the immunizing peptide, completely obliterating staining.
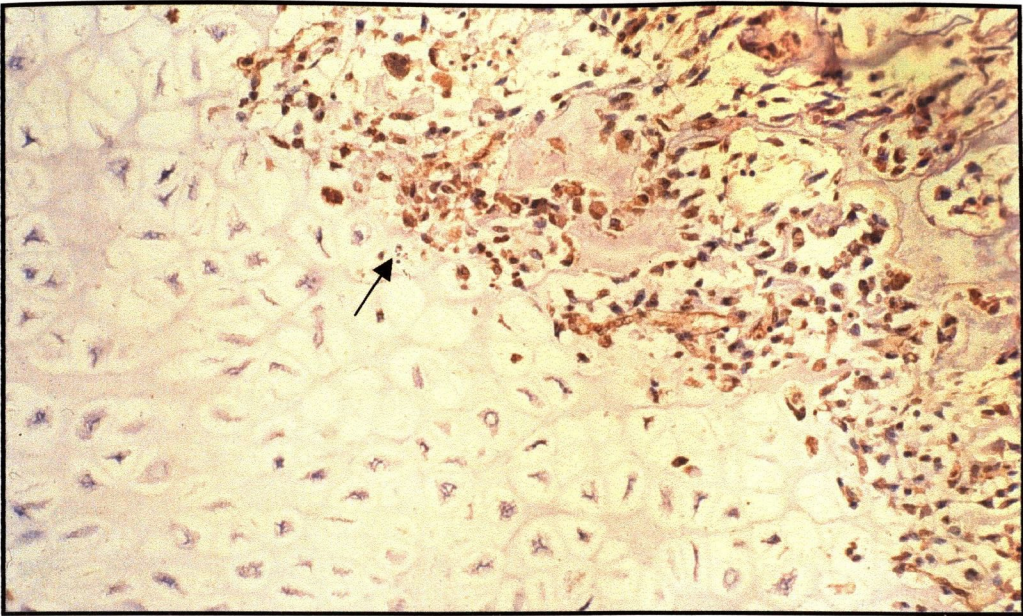
Figure 2.4   Abl expression in enchondral ossification of fetal rib.   Intense Abl immunoreactivity is observed in osteoblasts and proliferating blood vessels at the growth plate.   Adjacent hypertrophic chondrocytes show minimal or no staining, and one (indicated by arrow) has undergone apoptosis.
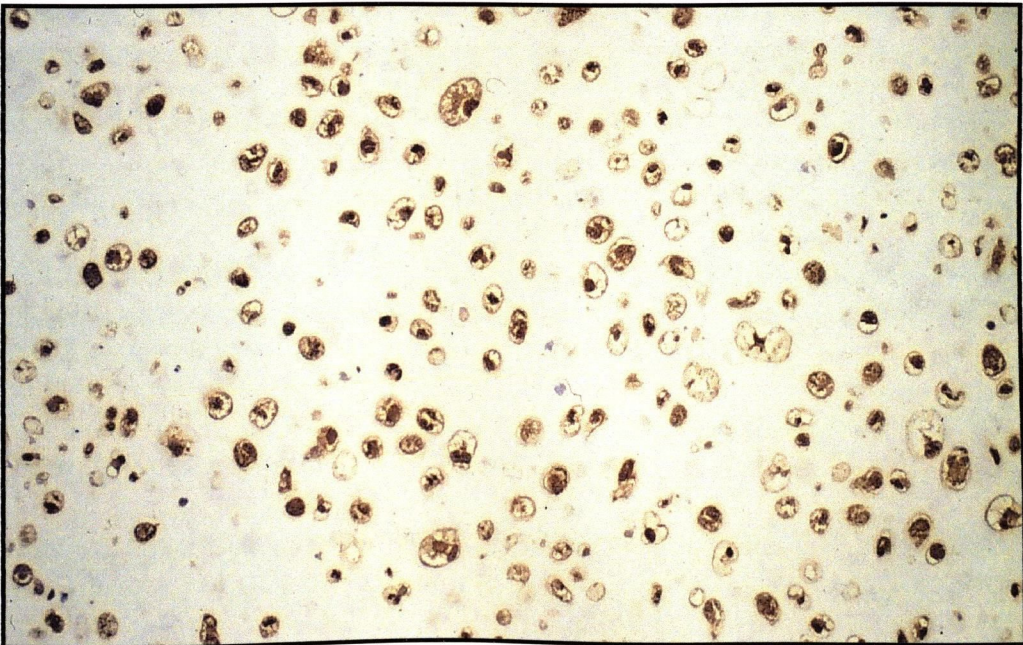
Figure 2.5   Abl expression in grade 2 chondrosarcoma.   The chondrocytes of Grade 2 chondrosarcoma show strong Abl expression.   Staining is predominantly nuclear, although some cytoplasmic and membranous staining is also observed.
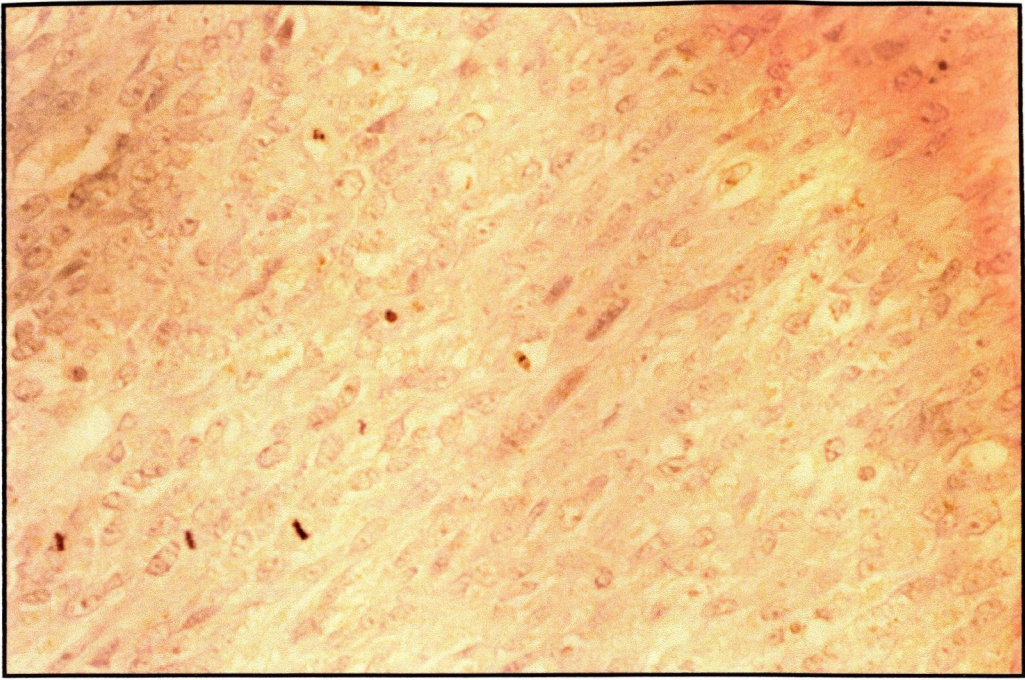
Figure 2.6   Abl expression in high grade chondrosarcoma. Abl immunoreactivity is minimal or absent in the poorly differentiated chondrocytes of Grade 3 chondrosarcoma.
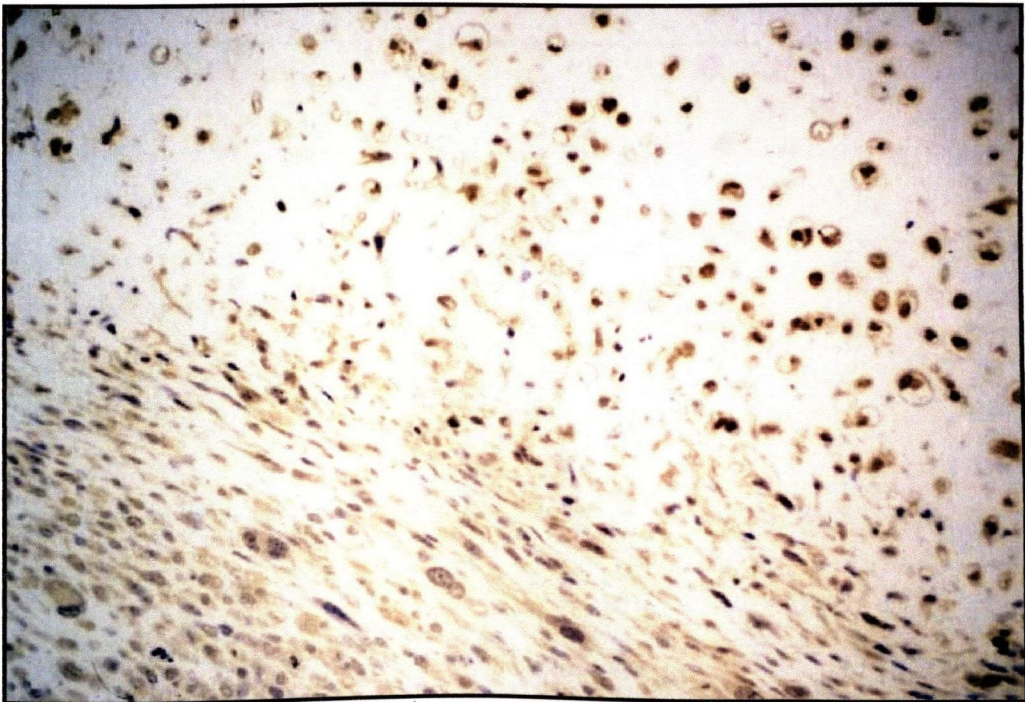
Figure 2.7   Abl expression in dedifferentiated chondrosarcoma. This figure contrasts the intensity of Abl immunostaining in the area of low grade tumour (strongly stained) and the adjacent area of dedifferentiation (weakly stained).
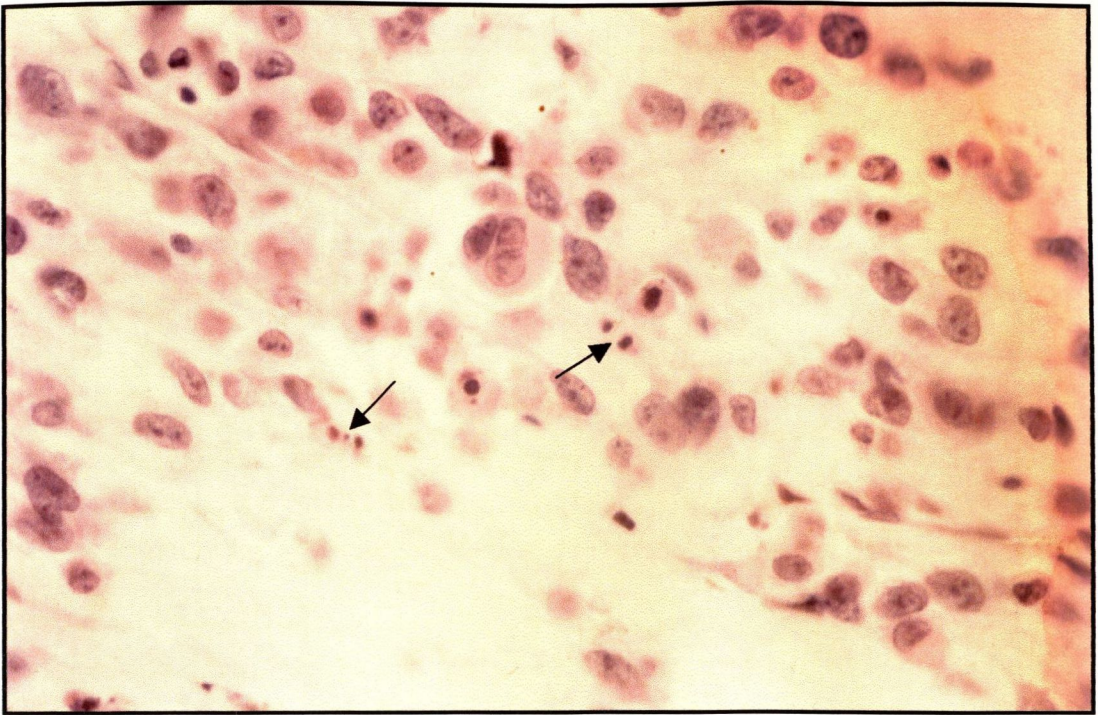
Figure 2.8   Apoptosis in high grade chondrosarcoma.   H&E stain of Grade 3 chondrosarcoma showing morphological evidence of apoptosis in poorly differentiated chondrocytes.
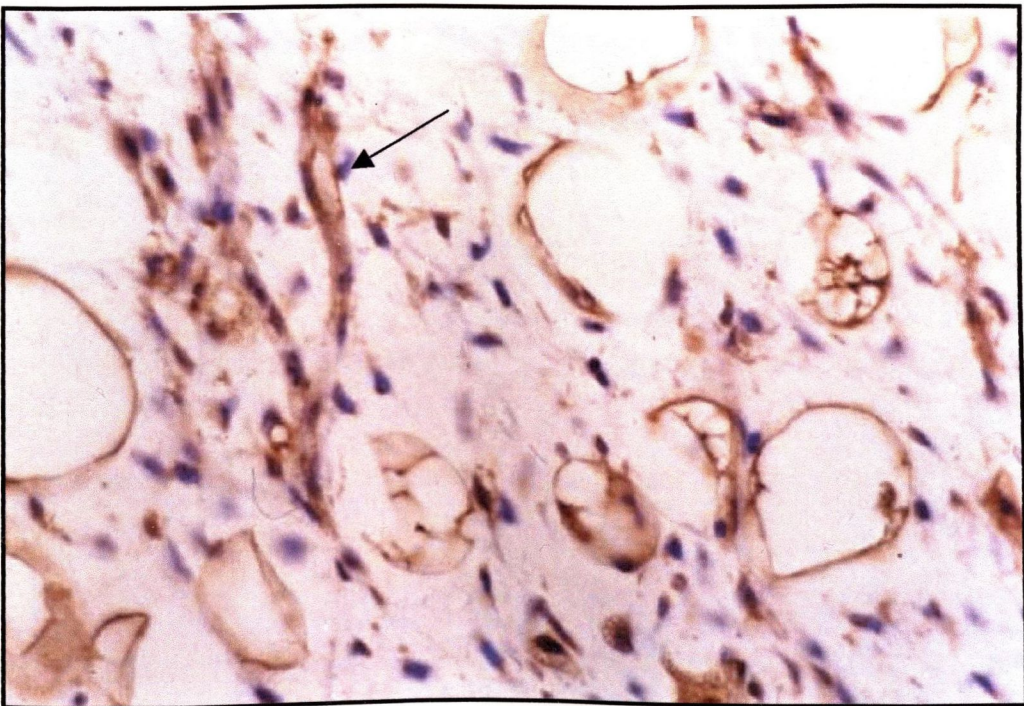
Figure 2.9   Abl expression in myxoid liposarcoma.   The arrow indicates the intense Abl immunostaining in the maturing tumour cells and neovasculature of myxoid liposarcoma.
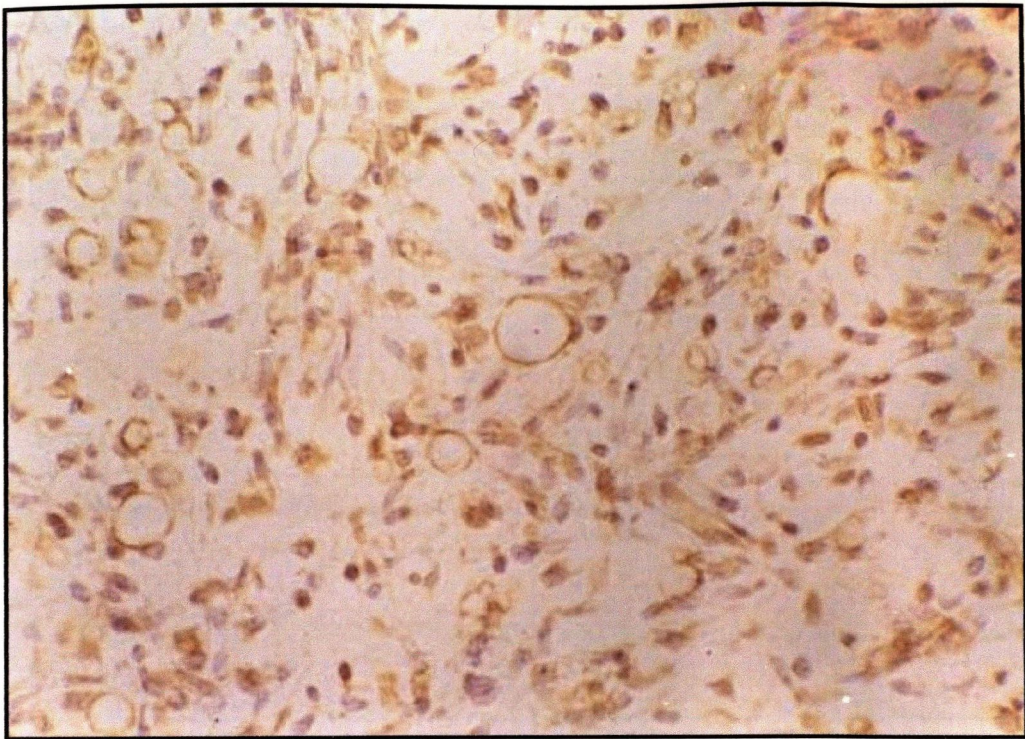
Figure 2.10   Abl expression in cellular myxoid liposarcoma.   Abl immunostaining is absent in undifferentiated cells and moderately strong in lipoblasts, adipocytes and blood vessels.
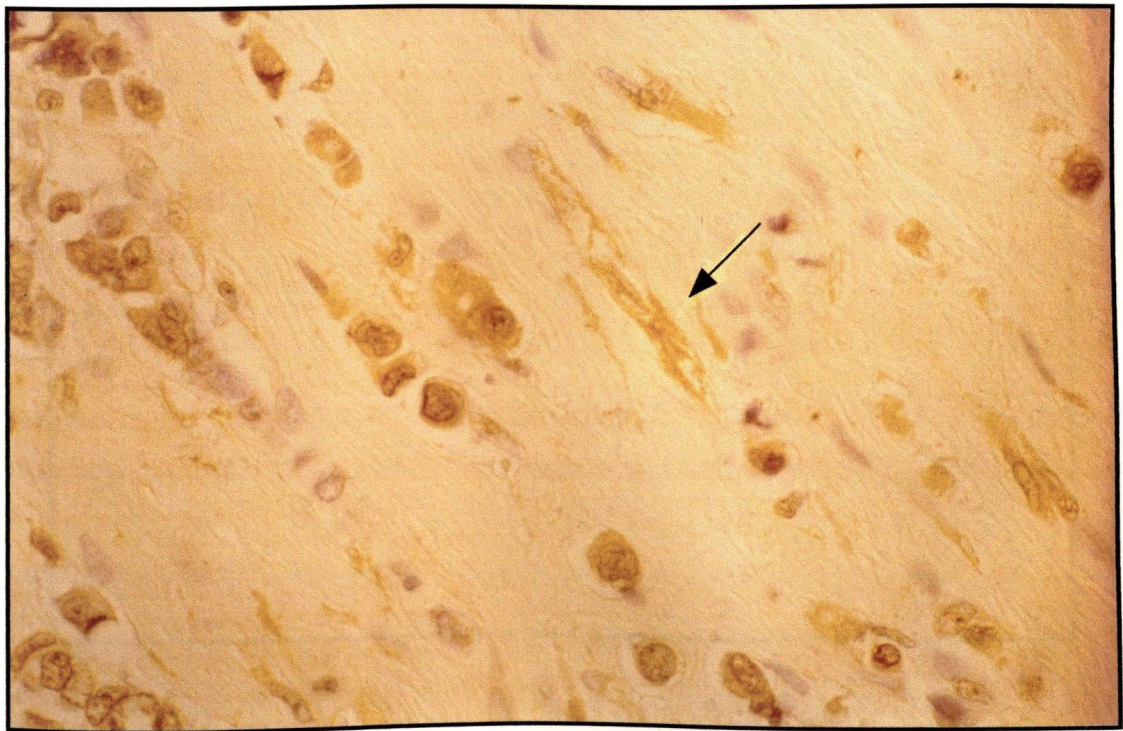
Figure 2.11   Abl expression in breast carcinoma. Variable Abl staining is observed in tumour cell nuclei and cytoplasm in breast carcinoma.   The arrow highlights moderate Abl immunoreactivity in angiogenic microvessels of breast carcinoma.
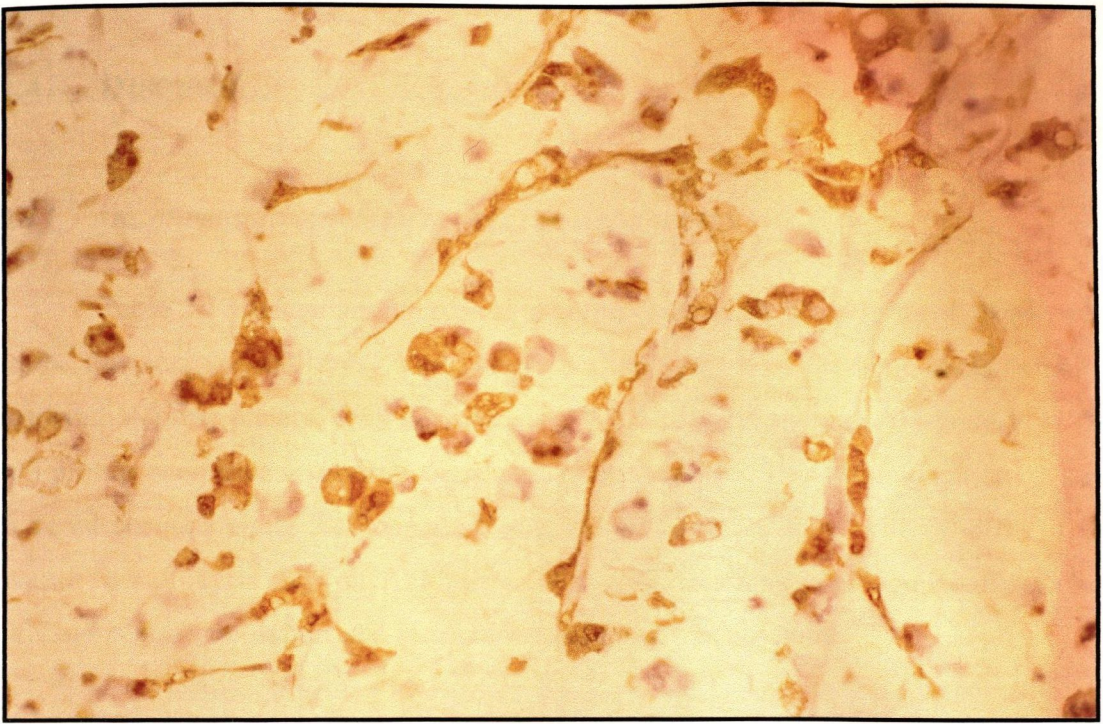
Figure 2.12   Abl expression in gastric carcinoma. Intense Abl expression in both tumour cells and microvessels in diffuse type signet ring carcinoma of stomach.
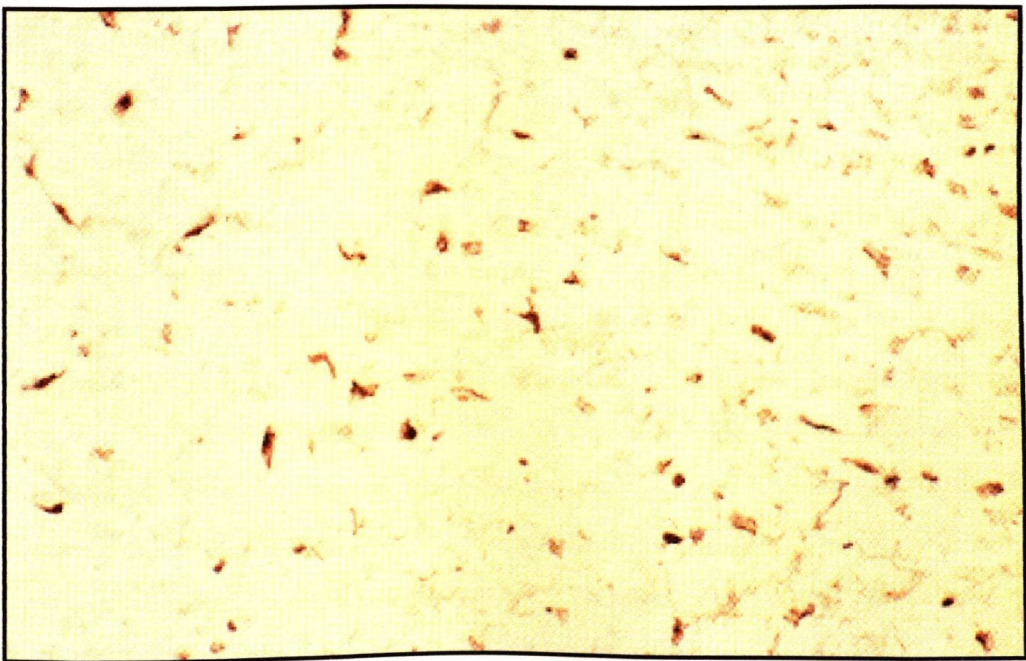
Figure 2.13   Abl immunostaining in umbilical cord. Umbilical cord fibroblasts of Wharton's jelly show variable Abl expression.

2.4 DISCUSSION

2.4.1 ABL EXPRESSION IN NORMAL FETAL CHONDROCYTES

Table 2.1 summarises the typical staining patterns observed in the various zones of the developing fetal limb. The immature chondrocytes of the bone shaft exhibit a scattered staining pattern, with approximately 70% of cells staining Abl positive. The Abl protein seen here is predominantly nuclear in location. This staining pattern is seen in serial sections along the bone shaft into the proliferative zone, with 70-80% of the mature chondrocytes showing Abl immunoreactivity. Staining is predominantly nuclear although some cytoplasmic and membranous staining was observed.

Figure 2.4 shows the typical staining pattern observed at the growth plate of fetal cartilage. The Abl oncoprotein is minimal or absent in those hypertrophic chondrocytes which are about to undergo apoptosis. Apoptotic cells, although infrequent, were visible at the growth plate from 16 weeks gestation. Therefore, the distribution of Abl staining is consistent with the developing chondrocytes progressive requirement for maturation, terminal differentiation and apoptosis. Striking Abl immunoreactivity was seen in the osteoblasts and their associated neovasculature at these sites of enchondral ossification. No differences in staining pattern were observed in fetuses of different gestational ages.

Enchondral ossification is the process whereby tissue that initially consists completely of cartilage is replaced by bone (Brighton, 1994). Opposing views of the fate of the hypertrophic chondrocyte have been put forward. Roach *et al*, 1995, describes the osteogenic differentiation of hypertrophic chondrocytes during enchondral ossification. Farnum *et al*, 1989, propose that all hypertrophic chondrocytes are terminal cells which degenerate and die by apoptosis. Our results suggest that Abl inhibits apoptosis in maturing chondrocytes but is lost in the hypertrophic chondrocytes about to undergo apoptosis. Although not conclusive, strong Abl expression in the proliferating osteoblasts and associated vasculature suggest a complementary survival role for Abl in the growth plate itself.

2.4.2 ABL EXPRESSION IN CHONDROSARCOMA

The well differentiated chondrocytes of grade 1 and grade 2 chondrosarcoma show intense staining for the Abl oncoprotein (Figure 2.5), with approx. 90% of cells positive. Nuclear, cytoplasmic and membranous staining are all clearly evident. Apoptosis is minimal or absent in these low grade tumours (Table 2.2).

In contrast, the poorly differentiated chondrocytes of high grade tumours (grade III and dedifferentiated chondrosarcoma) showed absence of or minimal and more diffuse Abl expression (Figure 2.6 and 2.7 respectively). Alongside this decrease in Abl expression is an increase in the extent of apoptosis (Figure 2.13) suggesting that a large reduction or absence of the Abl protein increases the susceptibility of tumour cells to apoptosis in grade 3 chondrosarcoma (Table 2.2).

The results provide further support for a previously described role for Abl inhibition of apoptosis: low grade tumours have intense Abl expression and minimal apoptosis and high grade tumours have weaker Abl expression and more conspicuous levels of apoptosis. It is likely however that the increased apoptosis and greater mitotic activity of high grade chondrosarcoma involves the participation of additional gene products and other factors associated with increased genomic instability (O'Donovan *et al*, 1999; Staunton & Gaffney, 1998). The contrast between Abl expression in well and poorly differentiated tumours is highlighted in tumours such as that shown in Figure 2.7. The differing intensities of Abl expression in the two components of dedifferentiated chondrosarcoma is quite marked.

There was a significant correlation between apoptotic and mitotic indices in chondrosarcoma ($p < 0.0114$ and $p < 0.0114$ respectively). The absence of mitoses observed in low grade chondrosarcoma has previously been documented (Bjornsson *et al*, 1998; Staunton & Gaffney, 1998). This may be related to the relatively more rapid completion of mitoses, and is a relationship that has been previously documented in other tumour types (Staunton & Gaffney, 1998).

The polyclonal antibody used is unable to distinguish between the different isoforms of Abl. However, it is interesting to note that the intense nuclear staining characterisitic of type I c-abl mRNA is found in the well differentiated grade I tumours. This is in keeping with the findings of McWhirter *et al*, 1991 and Franz *et al*, 1989, who each identify type I c-abl mRNA as the important isoform for cellular differentiation. The membrane-associated type IV isoform is demonstrated by these groups to be involved in inhibition of apoptosis. In this study, membrane staining is most evident in the low grade chondrosarcoma which had minimal or no apoptosis.

2.4.3   *ABL EXPRESSION IN LIPOSARCOMA*

The mature adipocytes and lipoblasts of the low grade liposarcoma, lipoma-like and sclerosing liposarcoma showed strong Abl immunoreactivity. Staining was predominantly membranous and cytoplasmic, and these tumours had minimal or no apoptosis (Table 2.3). The fibroblast-like preadipocytes of these tumours remained unstained.

In contrast, there was no staining of tumour cells or blood vessels in round cell liposarcoma in which apoptosis was conspicuous (Table 2.4). There was intense Abl expression in the plexiform blood vessels of myxoid liposarcoma (Figure 2.9). Intense Abl expression correlates with differentiation and lack of apoptosis or mitoses in liposarcoma. This would suggest cellular differentiation, anti-apoptotic and anti-proliferative functions of the Abl oncoprotein. Lack of Abl expression in round cell liposarcoma may partly explain its susceptibility to apoptosis and greater cell proliferation.

Of great interest is the apparent differential expression of Abl in the tumour microvessels of myxoid liposarcoma. Normal blood vessels do not express Abl. However, the selective Abl expression in physiological angiogenesis (early placental villi and the proliferating vessels during enchondral ossification) supports a possible previously undescribed role for Abl in angiogenesis.

2.4.4 ABL EXPRESSION IN BREAST CARCINOMA

The results demonstrate that Abl is weakly to moderately expressed in tumour cells of all grades of breast carcinoma investigated in this study, although weakest in the cases of In-situ ductal carcinoma. The staining is quite variable within the tissue sections. Abl immunostaining in the tumour cells is predominantly nuclear although cytoplasmic staining is also present. Figure 2.11 illustrates the staining of tumour cell nuclei in breast carcinoma. Abl immunoreactivity is also noted in some angiogenic microvessels (Table 2.5). Staining of vessels is weak (+, or ++ in tubular carcinoma) and often difficult to identify. Interestingly, tissues and structures that normally show no staining for Abl (e.g. breast lobular epithelium), occasionally showed Abl immunoreactivity in the vicinity of Abl positive tumour cells

2.4.5 ABL EXPRESSION IN GASTRIC CARCINOMA

A series of 11 cases of gastric carcinoma were stained for Abl, six diffuse type and five intestinal type. Intense Abl expression is observed in the diffuse signet ring carcinoma of the stomach, and weaker staining in the intestinal type (Table 2.6). Abl expression is variable in signet ring carcinoma, with tumour microvessel staining most prominent in less cellular, myxoid areas. Figure 2.12 clearly illustrates strong Abl expression in a vessel of diffuse type signet ring carcinoma. In normal gastric tissue, weak or focal Abl expression is observed in the gastric crypts while no Abl staining is observed in normal blood vessels. No significant difference is found between apoptotic indices in diffuse adenocarcinoma and intestinal-type gastric carcinoma, or between signet ring cell and undifferentitated areas in diffuse gastric adenocarcinoma (data not shown, O'Neill *et al*).

2.4.6 ABL IN PLACENTA

The placenta provides an excellent site for the study of normal angiogenesis. Vessels develop from the mesenchyme and develop to form a network of capillaries. The most intense Abl immunoreactivity is observed in the early placenta (6-7wks). Strong nuclear staining of c-Abl is observed in the developing endothelium, and moderate

staining of some connective tissues is also noted. A similar staining pattern, but less intense is observed in early placentas older than 8wks. Particularly strong Abl protein expression was observed in the vessels of one early ectopic pregnancy.

In the later normal placenta cases (28-42wks), umbilical cord fibroblasts of Wharton's jelly show variable moderate to intense Abl staining (Figure 2.13). Similar immunoreactivity is observed in umbilical cord blood vessels, the amnion and chorion. Surface trophoblasts are weakly positive for c-Abl, but there is no staining in maternal blood vessels.

2.5   CONCLUSIONS

We have demonstrated differential Abl expression in a variety of normal tissue and tumour types. Intense Abl expression in differentiating chondrocytes, growth plates, adipose cells and the umbilical cord strongly suggest hitherto undescribed functions for Abl in the differentiation and survival of specific connective tissue. Loss of Abl expression in hypertrophic chondrocytes at the growth plate coincides with Abl expression in proliferating osteoblasts and formation of new blood vessels. Abl therefore appears to be an important factor in the events leading to enchondral ossification.

Abl expression was moderate to intense in low grade liposarcomas and chondrosarcomas, both of which were shown to have negligible apoptosis (Staunton & Gaffney, 1995) and low proliferative indices (Hasegawa et al, 1995; Remmelink et al, 1994). Abl expression correlated with the degree of differentiation and levels of apoptosis in the tumour groups investigated in this study. It is important to note however that expression of a single apoptosis-modulating gene product does not always correlate with net apoptosis (O'Neill et al, 1996; Tormanen et al, 1995) and hence the interaction of c-abl with other oncogenes/tumour suppressor genes must be considered.

Another significant finding in this study is the expression of Abl protein in the microvessels in liposarcoma, breast carcinoma and diffuse type signet ring carcinoma of

the stomach. We have also demonstrated moderate Abl staining in the neovasculature during enchondral ossification, in fibroblast precursors and vessels in early placental villi and in umbilical cord blood vessels. As previously stated, Abl protein expression is not usually seen in normal adult blood vessels. This raises the possibility that Abl, like many other oncogene products, might be either directly or indirectly angiogenic. In order to validate the significance of the immunohistochemical observations, it was decided to investigate more fully the role of c-*abl* at the mRNA level.

3. RNA EXTRACTION AND ANALYSIS FROM FORMALIN-FIXED PARAFFIN EMBEDDED TISSUES

3.1   INTRODUCTION

Many diseases result from the inadequate or inappropriate spatial expression of specific genes. Consequently, an understanding of the exact site and level of expression of the gene(s) involved is often important in elucidating the molecular basis of disease. Analysis of specific cells or tissues over time courses of growth or differentiation can give valuable information about tissue and temporal specificity of RNA expression. Gene expression can be analysed at either the protein or mRNA level, however measurement of the amount of a protein present gives no indication of its rate of synthesis. In Chapter 2, differential expression of the Abl protein was observed by immunohistochemistry during enchondral ossification, tumour cell differentiation and apoptosis and in angiogenesis. Evaluating the amount of mRNA coding for a specific protein is assumed to reflect more accurately the rate at which the cell is making that protein.

Regulation of gene activity pertains to all the steps involved in protein synthesis and protein function. In eukaryotic cells, there are four primary levels of control of gene activity (Figure 3.1):

1. **Transcriptional control:** There are a number of mechanisms that serve to control which genes are transcribed and/or the rate at which transcription occurs
2. **Post-transcriptional control:** Differential processing of mRNA and also the speed at which mRNA leaves the nucleus can affect the amount of gene expression finally realised.
3. **Translational control:** The life expectancy of mRNA can vary, as can its ability to bind ribosomes. It is also possible that some mRNA may need additional changes before they are translated at all.
4. **Post-translation control:** Even after translation has occurred, the polypeptide product may have to undergo additional changes before it is biologically functional.
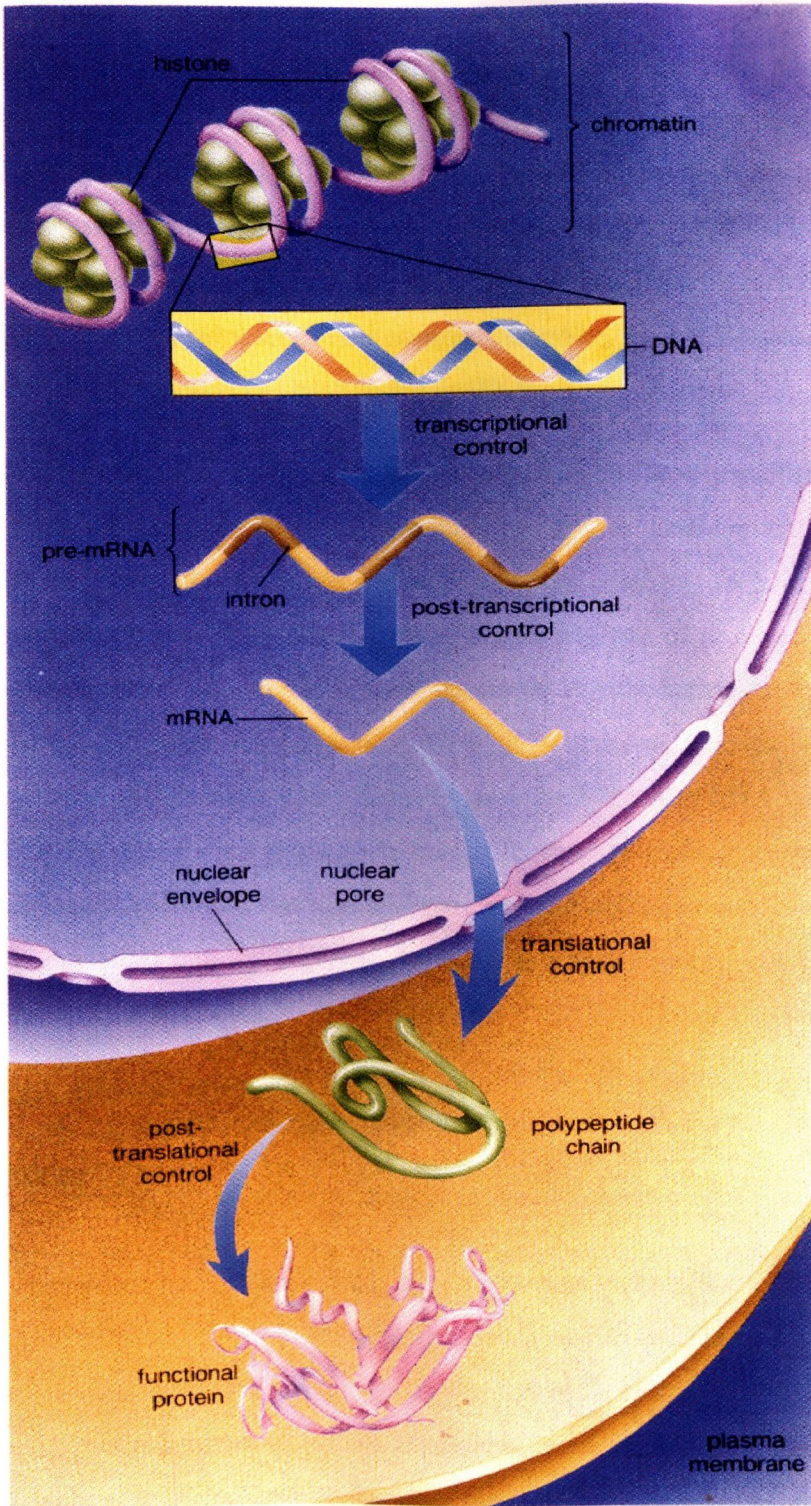
Figure 3.1   Levels at which control of gene expression occurs in eukaryotic cells. Transcriptional and post-transcriptional control occur in the nucleus, translation and post-translational control occur in the cytoplasm (Mader, 1990).

Gene transcription is the dominant control point in the production of any protein and is carefully regulated through the combined activities of a number of highly specialised nuclear proteins. RNA, like DNA is comprised of a long chain of individual nucleotide bases. As its name implies however, RNA contains a ribose sugar group rather than the deoxyribose group found in DNA. RNA is usually single stranded and is synthesised from DNA in a complementary manner. In addition, RNA contains the base uracil (U) instead of the thymine (T) base found in DNA.

The ability to perform molecular analysis on formalin-fixed paraffin embedded material has many applications in both investigative studies and clinical diagnoses. Applying RT-PCR (reverse transcription polymerase chain reaction) techniques to such material provides the most useful means of retrospective analysis of nucleic acids which may be partially degraded due to the effects of tissue devitalization, processing and paraffin embedding. However, RNA detection by PCR in archival material is faced with a number of technical difficulties. The relatively short half-life of mRNA can lead to a higher level of RNA degradation prior to fixation. Tissues processed for pathological analyses are subject to hydration, fixation and paraffin embedding in conditions that are not RNAse (ribonuclease) free. In addition, formalin is a cross-linking agent which can introduce 'nicks' into nucleic acids.

3.1.1 EFFECT OF FIXATION ON THE AMPLIFICATION OF NUCLEIC ACIDS FROM ARCHIVAL MATERIAL

A study published by Ben-Ezra *et al*, 1991, investigated the effect of fixation type and time on amplification of RNA from paraffin embedded tissues. They confirmed the results of other investigators (Goelz *et* al, 1985; Warford *et* al, 1988; Bramwell & Burns, 1988; Greer *et al*, 1990) demonstrating the deterioration of PCR signal obtained from formalin fixed tissues with increasing fixation time. The results also showed that ethanol-based neutral-pH fixatives are less damaging to nucleic acids than formalin based fixatives, which is in keeping with the findings of other groups (Greer *et al*, 1991, Jackson *et al*, 1990; Rogers *et al*, 1990). Ethanol, because of its lack of cross binding, is also an excellent fixative for immunohistochemistry (Battifora & Kopinski, 1986).

Extreme difficulty is encountered in trying to extract RNA from Zenker's, Bouins or B-5 fixed samples (Ben-Ezra *et al*, 1991).

The age of the tissue specimen must also be taken into consideration for investigators proposing a study on archival material. Shibata *et al*, 1988, successfully amplified DNA from archival paraffin embedded material which was 40 years old. Goelz *et al*, 1985, reported that the size of DNA fragments amplifiable from four to six year old samples is often significantly smaller than those from samples less than two years of age. Assuming however that paraffin blocks are stored in a reasonably controlled environment, it seems likely that little further degradation occurs after formalin fixation and embedding due to inactivation of nucleases during processing.

Tissues for histopathology based examination are usually preserved in a fixative aimed at preservation of morphology. Although RNA is extensively damaged during histological processing, small intact fragments survive that can function as templates for RT-PCR. Unfortunately, several factors such as the time interval between tissue resection and processing and the quality and duration of formalin fixation may vary greatly from specimen to specimen.

3.1.2   *HANDLING OF RNA SAMPLES*

Ribonucleases (RNAses) are very stable and active enzymes that generally do not require any cofactors to function. RNA in sample material is subject to degradation by such intracellular enzymes until it is flash frozen, processed or disrupted and homogenised in the presence of RNAse-inhibiting or denaturing agents. It is imperative therefore that samples are stored at $-70^{\circ}C$ or are processed as soon as they are harvested. Since RNAses are difficult to inactivate and only minute amounts are sufficient to destroy RNA, plasticware and glassware must first be treated to eliminate possible RNAse contamination. Solutions and glassware should first be treated with 0.1%v/v DEPC (diethylpyrocarbonate). DEPC is a strong but not absolute inhibitor of RNAses, which acts by covalent modification of RNAses. Residual DEPC must be removed by

heating solutions to $100^{\circ}C$ as trace amounts of DEPC will modify purine residues in RNA by carboxymethylation. Carboxymethylated RNA is translated with very low efficiency in cell free systems.

3.1.3 QUANTITATION OF TOTAL RNA

The concentration and purity of RNA can be determined by measuring the absorbance at 260nm (A_{260}) and 280nm (A_{280}) in a spectrophotometer. An absorbance reading of 1 unit at 260nm corresponds to $40\mu g$ of RNA per ml (valid for measurements in water only). The ratio between the readings taken at 260nm and 280nm (A_{260}/A_{280}) provides an estimation of the purity of RNA. This ratio is however influenced by pH.

Agarose gel electrophoresis and ethidium bromide staining can verify the integrity and size distribution of total RNA purified. The ribosomal bands should appear as sharp bands, although this is not always true of the more degraded RNA extracted from archival material. It is also important to note that no currently available purification method can guarantee that RNA is completely free of DNA, even when the DNA is not visible on an agarose gel.

3.1.4 CONTROL GENES IN REVERSE TRANSCRIPTASE-POLYMERASE CHAIN REACTION ASSAYS

Determining the presence of 'amplifiable' RNA is an essential control step in any RT-PCR experiment. Until quite recently, amplification of the β-actin gene was the most widely used approach to determining the quantity of intact RNA in a given sample. However, the human genome has at least 19 processed β-actin pseudogenes (Leavitt *et al*, 1984), which can result in amplicons from genomic DNA having similar size to those generated from cDNA. In addition β-actin is a highly expressed gene and yields strong amplification signals even in the presence of very small template amounts. This may lead to misinterpretation of PCR assays if the gene under investigation is expressed at a markedly lower level. Consequently, alternative housekeeping genes for RNA analysis have been sought.

Throughout the literature, numerous genes have been cited for use as housekeeping genes for the purpose of quantitative RT-PCR experiments. Finke *et al*, 1993 demonstrated the porphobilinogen deaminase (PBGD) gene to be a suitable candidate housekeeping gene for RNA analysis from formalin-fixed, paraffin-embedded tissues by RT-PCR. PBGD is a cytosolic enzyme involved in the heme biosynthesis pathway and is expressed ubiquitously in a tissue-specific manner. Despite much evidence that Abl expression in tissues changes in response to such cellular events as differentiation and apoptosis (O'Neill *et al*, 1997; O'Donovan *et al*, 1999) and during tumour angiogenesis (Russell *et al*, 1998b,c), some investigators continue to use c-*abl* as a reference gene for RT-PCR analyses (Mannhalter *et al*, 2000).

In choosing a suitable control gene for RT-PCR analysis, the following points should be considered: (1) suitable genes should have no pseudogenes in the human genome and should be ubiquitously expressed at a level which does not differ greatly from that of the gene under investigation (2) RT-PCR products from control genes should be mRNA/cDNA specific. This may be achieved using primer combinations which will yield PCR products of different size from cDNA and genomic DNA templates. Alternatively, primers should span exonic boundaries such that only cDNA and not contaminating genomic material can be amplified.

Glyceraldehyde-3-phosphate dehydrogenase is widely used as a housekeeping gene for quantitative RT-PCR assays. The suitability of GAPDH, along with Human PKG and β-2-microglobulin as a control gene is evaluated and discussed in section 6.3.1. Briefly, however, it is demonstrated that GAPDH is a suitable house-keeping gene in the evaluation of c-*abl* mRNA from formalin fixed, paraffin embedded tissue.

3.1.5 QUANTITATIVE PCR STRATEGIES

To date several procedures have been proposed for the accurate detection and measurement of PCR products. The most common method employed is gel electrophoresis and ethidium bromide staining of the bands. Agarose or acrylamide gels

can be used, the latter giving better resolution of bands differing by only a few bases. The use of radioactively labelled dNTP's or oligonucleotides can provide a more sensitive procedure than ethidium bromide staining. After electrophoresis, the labelled bands can be visualised by autoradiography and/or scanning densitometry.

3.1.5.1   Competitive PCR

Competitive PCR represents a reliable approach to nucleic acid quantitation and is based on the addition of a competitor target (RNA or DNA) to the PCR reaction. The competitor template should have the same primer recognition sites and amplify as efficiently as the target template. During the annealing step of PCR, the nucleic acid target and competitor target compete for the primers. After PCR the two amplicons are separated by conventional agarose gel electrophoresis and the ratio between the two species is evaluated. By comparing the signal generated by the target template to that of known concentrations of the competitor, accurate quantitation can be achieved. Since the initial amount of competitor is known, the amount of target DNA is estimated according to the T:C ratio, where:

T = amount of amplification product from the target
C = amount of amplification product from the competitor

When the T:C ratio equals 1, the initial concentration of target DNA corresponds to the amount of competitor DNA (Figure 3.2). An ideal competitor for quantitative PCR should be:

1. amplified with the same primers as the target DNA
2. distinguishable from target DNA (e.g. different size, different restriction fragment pattern etc.)
3. purified and obtained at a known concentration

Amount of Competitor (copy number)

10^5 $\quad$ 10^6 $\quad$ 10^7 $\quad$ 10^8

T:C	10	3.2	1	0.32
Log (T:C)	1	0.5	0	-0.5
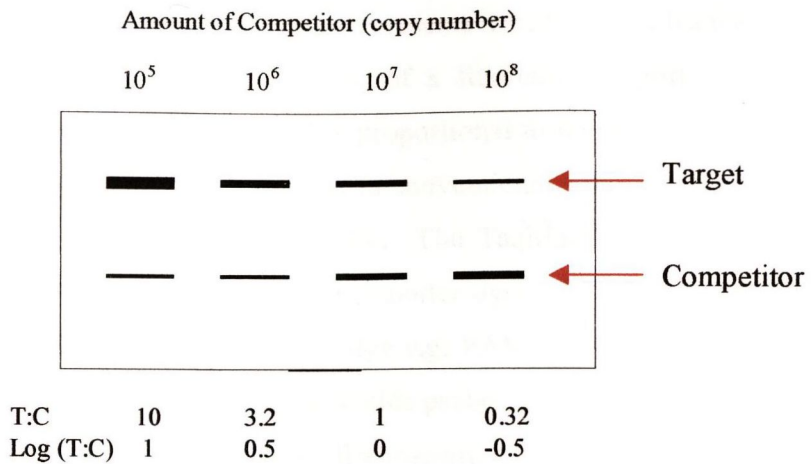
Figure 3.2 Competitve PCR. Samples are analysed by agarose gel electrophoresis and the amount of competitor required to give a ratio of 1 is determined. In this example, the amount of target DNA corresponds to 10^7 copies of competitor.

It is important to recognise that the use of DNA competitors for RNA quantitation may be erroneous due to the large variability of reverse transcription efficiency. Competitors may be used as either internal or external standards (Hoof *et al*, 1991; Sestini *et al*, 1996). In the latter case the competitor is amplified independently to the sample and used to generate a standard curve. This strategy does not therefore take into account the variability of PCR between one tube and the next. The most accurate protocol appears to be the use of the competitor as an internal standard in which a known amount of the competitor is added to each assay tube.

3.1.5.2 Fluorescence based Quantitative PCR

In 1991, Holland *et al* described a novel procedure for the detection of a specific nucleic acid sequence based on the use of a fluorogenic probe. The probe is designed to hybridise within the target sequence and generate a signal proportional to the amount of original starting template. The TaqMan® 5' Exonuclease Assay System from PE Biosystems described below provides an innovative procedure for DNA and RNA quantitation.

3.1.5.3   Principles of TaqMan® 5' Exonuclease Assays

The development of 5' nuclease assays represents a significant advance in nucleic acid quantitation. In such assays, the release of a fluorescent reporter dye from a hybridisation probe in real time during PCR is proportional to the accumulation of PCR product. TaqMan® PCR uses a primer pair (as in conventional solution phase PCR) and an internal oligoprobe, called a TaqMan® probe. The TaqMan® probe consists of an oligonucleotide 20-30 bases in length with a 5' reporter dye, a 3' quencher dye and a 3' blocking phosphate. The fluorescent reporter dye e.g. FAM (6-carboxy-fluoroscein), is covalently linked to the 5' end of the oligonucleotide probe. TET (tetrachloro-6-carboxy-fluoroscein) and HEX (hexachloro-6-carboxy-fluoroscein) can also be used as fluorescent reporter dyes in this system. Each of these dyes is quenched by TAMRA (6-carboxy-tetramethyl-rhodamine) that is attached by a LAN (linker-arm-modified nucleotide) to the 3' end of the probe. The 3' blocking phosphate groups prevents probe elongation during the extension step.

When the probe is intact (linearised), the proximity of the reporter dye to the quencher dye results in direct suppression of the fluorescence of the reporter dye by Forster-type energy transfer. During PCR, if the target of interest is present, the probe will specifically anneal between the forward and reverse primer. Due to the nucleolytic activity of the AmpliTaq® DNA Polymerase, the probe is cleaved between the reporter and quencher sequence only if the probe is hybridised to its target. The release of the fluorescent reporter only occurs if target specific amplification occurs, obviating the need to confirm the amplicon following amplification. The absence of post-amplification manipulation is a significant factor in reducing the possibility of cross-contamination of samples. Another feature of the TaqMan® assay aimed to prevent sample carry over is the use of uracil-*N*-glycosylase (UNG) before amplification. The incorporation of dUTP instead of dTTP into the PCR amplicon allows specific degradation of possible PCR product contaminants prior to amplification. The first denaturation step (heating to 95°C) serves to inactivate the UNG before the specific PCR product is generated.

Schematic of TaqMan® PCR
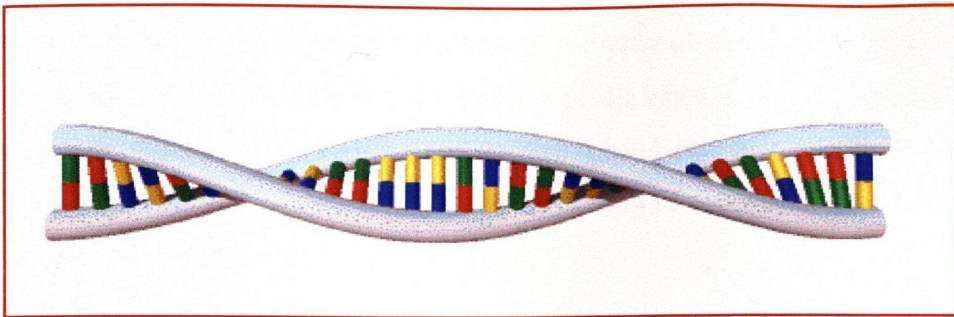
1. Double Stranded DNA Template
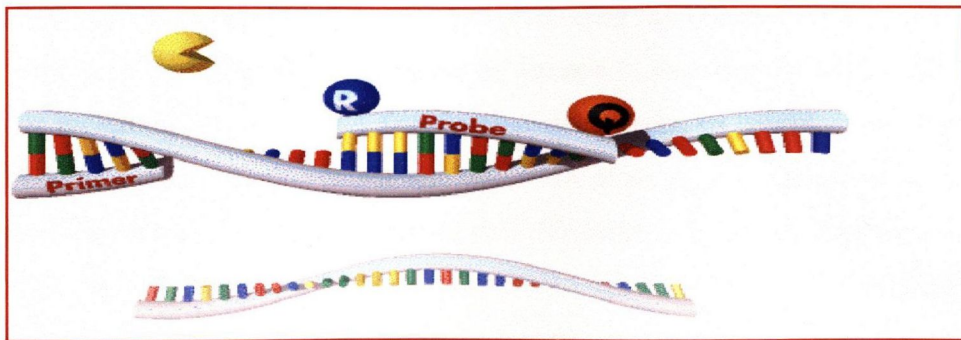
2. Annealing of TaqMan® probe with reporter (R) and quencher (Q) moieties

3. Primer extension and probe cleavage due to 5' exonuclease activity of Taq polymerase, resulting in release of reporter (R) from quencher (Q) molecule.

Figure 3.3 Principles of TaqMan® PCR (adapted from PE Biosytems Manual)

The target specific oligonucleotide probe used in such assays is advantageous for 3 reasons: (1) generation of reporter fluorescence is only observed if amplification of the target specific sequence occurs, (2) the release of the reporter dye is dependent on the starting copy number of the target template thus giving rise to a quantitative assay (3) sensitivities as low as 1-5 viral copies in 10^6 mammalian sequences have been detected (Kennedy *et al*, 1998).

3.1.5.4   Probe Design - Primer Express™

TaqMan® primer and probe sets can be designed using the Primer Express Software™, PE Biosystems. The DNA/cDNA sequence of interest is imported in any of a number of formats including MS Word and Simple Text documents, or downloaded directly from GenBank or alternative gene databases. For RNA analyses it is important to ensure that the exonic boundaries are clearly marked as it desirable to select primer/probe sets which will span exons. Using this strategy, only cDNA corresponding to spliced mRNA and not contaminating genomic DNA can be successfully amplified.

The optimum design parameters are set as default, the following being the most crucial factors in successfully designing TaqMan® Probe and primers.

Primer T_m 58-60°C

20-80% GC (opt. 50%)

Length 9-40 bases

< 2°C difference in T_m of the two primers

Maximum of 2 G/C at the 3' end of forward primer

Probe T_m 10°C higher than primer T_m

20-80% GC (opt. 50%)

Length 9-40 bases

No G on the 5' end

< 4 contiguous G's

Must not have more G's than C's

Amplicon   50-150bp in length

3'end of forward primer as close to probe as possible without overlapping

The Primer Express Software will identify all TaqMan[®] primer and probes in the area defined by the user and assign a penalty score to each set based on how closely they comply with the above mentioned criteria.

3.1.5.5   ABI PRISM[®] 7200 Sequence Detection System

The 7200 SDS[®] Assay is based on end-point determinations of the fluorescence emitted during a PCR reaction. Basically, the TaqMan[®] reactions are performed in 96 well plates on an Applied Biosystems 9600 thermal cycler and the plate then transferred to the ABI PRISM[®] 7200 SDS instrument where fluorescence in each well is recorded. The difference in fluorescence recorded in a sample well (R_n^+) compared with that of a no template control (R_n^-) is referred to the ΔR_n value (Figure 3.4).
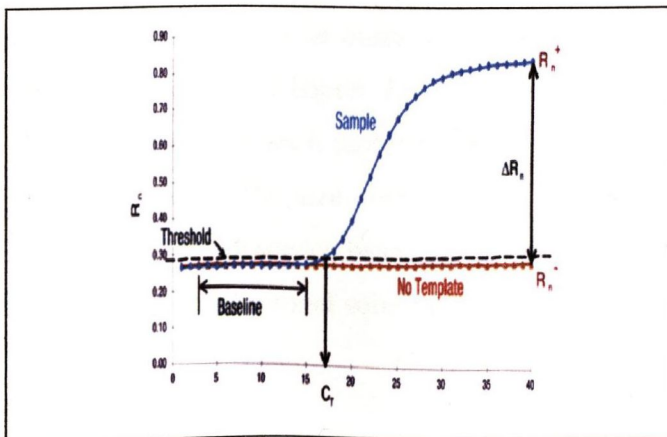
Figure 3.4 Model of sigmoidal amplification plot characterisitic of a PCR. The early cycles of PCR show no accumulation of fluorescence signal, and this defines the baseline

or threshold level. The amplification plot is known as the ΔR_n – the plot of the change in fluorescence signal $(R_n^+ - R_n^-)$ versus cycle number of the amplification plot.

The following equation expresses the relationship of these terms:

$$\Delta R_n = (R_n^+) - (R_n^-)$$

where: $R_n^+ = \dfrac{\text{Emission Intensity of Reporter}}{\text{Emission Intensity of Passive Reference}}$ PCR with template

$R_n^- = \dfrac{\text{Emission Intenisity of Reporter}}{\text{Emission Intensity of Passsive Reference}}$ PCR without template or baseline value

RNA samples are co-amplified for the gene of interest (i.e. c-*abl*) and a suitable house–keeping gene (i.e. GAPDH). ΔR_n values are calculated for both the target gene and the house-keeping gene and a realtive ratio calculated for each sample $(\Delta R_{n\ c\text{-abl}} / \Delta R_{n\ \text{GAPDH}})$. The relative ratio enables comparions of c-*abl* expression between samples.

The aim of this part of the study is to investigate c-*abl* mRNA expression in a variety of formalin fixed paraffin embedded tissues in order to substantiate the observations made in relation to Abl protein expression (Chapter 2). Extreme difficulties in successfully extracting and amplifiying RNA from such material have been widely reported (section 3.1.1). We hypothesise that the smaller size amplicon of TaqMan® RT-PCR combined with the enhanced sensitivity of fluorescence based assay systems will permit analysis of mRNA expression levels where convenitonal solution phase PCR may fail.

3.2   MATERIALS AND METHODS

3.2.1   MATERIAL

A variety of tumour types were investigated by immunohistochemistry for Abl protein expression in Chapter 2. The same sample material is used in this part of the study which examines c-*abl* mRNA expression using RT-PCR and TaqMan® 7200 technology (section 3.1.5.5). RNA extraction and amplification techniques are first optimised on RNA extracted from two different cell lines: HL60 and K562, both of which are leukaemic cell lines known to express c-*abl*. Both cell lines are obtained from the ECACC.

3.2.2   RNA EXTRACTION FROM CELL LINES

High quality total RNA is extracted from cell lines using the RNeasy Mini Kits (Qiagen Ltd.). The RNeasy procedure combines the selective binding properties of a silica-gel-based membrane with the speed of microspin technology. Stringent lysis of biological samples with Guanidium Isothiocyanate (GITC) immediately inactivates RNases for isolation of intact RNA. The technique employed enriches for mRNA and prevents RT-PCR mispriming by excluding RNAs below 200 bases unlike acid-phenol procedures.

Cells grown in monolayer in cell culture dishes may be lysed directly in the culture vessel using up to 700μl of lysis buffer. Cells grown in suspension should be pelleted by centrifugation at 330g for 5min. After centrifugation, supernatant is aspirated and up to 700μl of lysis buffer is added. Cells are disrupted using the QIAshredder columns which are designed for rapid homogenisation of cell lysates without cross-contamination. The QIAshredder unit consists of a unique biopolymer shredding system in a microcentrifuge spin column format. Lysates from up to 3×10^7 cells can be processed in a QIAshredder unit. Briefly, a QIAshredder column is placed into a 2ml microcentrifuge tube. The cell lysate is transferred to the column by pipetting or

decanting and centrifuged for 2min in a bench-top microcentrifuge at 14,000g. The spin column is then discarded.

350µl of the homogenised lysate is added to an equal volume of 70%v/v ethanol and mixed well by pipetting. Lysates should not be centrifuged at this point. The 700µl sample is applied to an RNeasy mini spin column sitting in a 2ml collection tube and centrifuged for 15sec at 8,000g. Flow-through is discarded and the collection tube can be re-used. Buffer RW1 (700µl) is pipetted onto the RNeasy column and centrifuged for 15sec at 8,000g to wash. Both flow-through and collection tube should be discarded. The RNeasy column is transferred into a new 2ml collection tube. Buffer RPE (500µl) is pipetted onto the column and centrifuged for 15sec at 8,000g to wash. The Buffer RPE wash is repeated, this time centrifuging for 2min to dry the RNeasy membrane. The RNeasy column is transferred to a new 1.5ml collection tube and 30µl of RNase-free water pipetted onto the RNeasy membrane. The column should be centrifuged for 1min at 8,000g to elute the RNA. Total RNA may be stored at –20°C or –70°C in water.

3.2.3 RNA EXTRACTION FROM PARAFFIN EMBEDDED MATERIAL

As mentioned in section 3.1.1, RNA extraction from formalin-fixed paraffin embedded material is hampered by high levels of RNA degradation both prior to and during fixation. A number of protocols for RNA extraction were assessed for both yield and quality of RNA attainable.

3.2.4 PROTOCOLS FOR RNA EXTRACTION FROM FFPE MATERIAL

3.2.4.1 AGPC (acid guanidium/thiocyanate/phenol chloroform extraction)

Guanidium thiocyanate (GuSCN) has been shown to be a powerful tool in the purification and detection of both DNA and RNA because of it's potential to lyse cells combined with it's potential to inactivate nucleases (Chomiczynski & Sacchi, 1987). The fundamental aim of a phenol extraction is the deproteinization

of an aqueous solution containing the desired nucleic acids. The phenol reagent is mixed with the samples under conditions which favour the dissociation of proteins from nucleic acids. Centrifugation of the mixture yields two distinct phases: a lower organic layer containing the protein and the upper aqueous layer containing the intact nucleic acids. An important consideration for such extractions is pH. At pH5-6 DNA is selectively retained in the organic phase leaving RNA in the aqueous phase. An added advantage of using low pH during RNA isolation from biological samples is the reduced level of activity of many nucleases under these conditions. Several variations of the phenol chloroform extraction technique were assessed in combination with each of the methods of tissue homogenisation outlined in section 3.2.5. A major disadvantage of this technique is the toxicity of the individual reagents.

3.2.4.2 TRIzol™ Reagent (Total RNA Isolation Reagent), Life Technologies

TRIzol reagent is a ready-to-use reagent for the isolation of total RNA from cells and tissues. The reagent, a mono-phasic solution of phenol and guanidine isothiocyante, is an improvement of the single-step RNA isolation method of Chomiczynski & Sacchi, 1987. During tissue homogenisation the TRIzol reagent maintains the integrity of the RNA while disrupting cells and dissolving cell components. Addition of chloroform followed by centrifugation will cause separation of the organic and aqueous phases. RNA remains exclusively in the aqueous phase and may be recovered using a simple isopropyl alcohol precipitation. The simplicity of this techniques allows simultaneous processing of a large number of samples in approximately one hour.

3.2.4.3 RNeasy Mini Kit, Qiagen

The principles of the RNeasy mini kit are described in section 3.2.2. Briefly, biological samples are first lysed and homogenised (3.2.5) in the presence of a highly denaturing guanidium isothiocyanate containing buffer which immediately inactivates RNases to ensure isolation of intact RNA. A specialised high salt buffer system then allows up to 100μg of RNA longer than 200 bases to bind to

the RNeasy silica gel membrane. Ethanol is added to promote binding and all contaminants are efficiently washed from the column. The high quality RNA bound to the column is eluted in nuclease free water.

3.2.4.4 Gentra PureScript™ RNA isolation kit, Flowgen

Gentra PureScript™ RNA isolation kits allow purification of RNA from cells, tissues and body fluids. The kits employ a proprietary modified salt precipitation procedure combined with highly effective inhibitors of RNase activity. Isolated RNA is precipitated in the presence of 100%v/v isopropanol. A detailed explanation of the different stages of this protocol is given in section 3.2.6. Central to the success of any of the RNA extraction techniques is adequate tissue homogenisation to permit reagent access to the RNA. A number of methods of tissue homogenisation were evaluated in conjunction with the above-mentioned RNA extraction techniques.

3.2.5 *METHODS OF TISSUE HOMOGENISATION*

3.2.5.1 Homogeniser

Most tissues can be quickly and thoroughly homogenised with rotor-stator homogenisers. Because the rotor turns at very high speed, the tissue is rapidly reduced in size due to a combination of turbulence and mechanical shearing. The process is quite fast, and depending on the toughness of the tissue sample, desired results are obtainable in less than one minute. However, the probe of the homogeniser must be removed between each sample, carefully cleaned in 0.1%v/v DEPC water, and subsequently autoclaved to inactivate residual DEPC. As a result only one sample can be processed at a time with a long interval between samples.

3.2.5.2 Narrow-bore syringe

This method of tissue disruption was employed in conjunction with the AGPC method of RNA extraction. Tissue sections are deparaffinised and rehydrated

through graded alcohols as previously described. The guanidium solution is added to the pellet and the tissue is sheared by repeatedly drawing the tissue through a sterile narrow bore (18-20 gauge) syringe and expelling the homogenate back into the eppendorf. While this method is effective in homogenising the tissue, it can be difficult to perform as the syringe can become blocked with tissue. Expelling the contents under pressure to clear the syringe often results in splashing of the guanidium and therefore this method of homogenisation and was not deemed suitable for routine use.

3.2.5.3 Pestle & Mortar

Pestle and mortars are first treated with DEPC to eliminate any possible RNase contamination. The deparaffinised tissue pellet is placed in the mortar with the appropriate volume of lysis buffer. Initial attempts to grind the tissue at room temperature led to the generation of heat due to friction, which was detrimental to the RNA in the sample. Subsequent efforts involved placing liquid Nitrogen in the mortar dish prior to addition of the tissue pellet. The tissue is then homogenised under liquid Nitrogen and the homegenate is transferred back into an eppendorf tube. Much of the sample is however lost in this transfer step. In addition, this procedure results in very poor sample throughput due to the fact that the pestle and mortar must be DEPC treated and autoclaved between each sample.

3.2.5.4 Tube pestles

The most effective, reproducible and user friendly method of tissue homogenisation involves use of tube pellet mixers (Treff Lab), which are disposable pestles specifically designed to fit into 1.5ml eppendorf tubes. Once again the tissue is deparaffinised and rehydrated through graded alcohols. The appropriate volume of lysis buffer is added to the tissue pellet and the eppendorf is then immersed in liquid Nitrogen until the tissue/buffer is snap frozen. The tube pestles are then used to grind the tissue and the homogenate can then be used in the subsequent extraction procedure.

3.2.6 MODIFIED PROTOCOL FOR RNA EXTRACTION FROM FFPE MATERIAL

The protocol for RNA extraction contains a number of changes to that recommended by the manufacturer (Flowgen Pure*Script*, Gentra Systems Inc.). Sections (2x10μm) are cut and placed in a sterile 1.5ml eppendorf. Xylene (500μl) is added and tubes incubated for 5min at room temperature with occasional mixing. The tissue is pelleted by centrifugation at 13,000g for 3min and the supernatant is discarded. The xylene wash is repeated three times to ensure tissue is completely de-paraffinised. Following this, samples are dehydrated by addition of 500μl of 100%v/v ethanol to each tube. Tubes are incubated for 5min at room temperature before pelleting tissue by centrifuging at 13,000g and discarding ethanol.

Tissue disruption is achieved by first adding 300μl of cell lysis solution to the de-paraffinised tissue homogenate. The tube is immersed in liquid Nitrogen until contents are snap frozen and the pellet is homogenised using a sterile tube pestle by grinding. Proteinase K (20μg) is added to each tube and samples incubated overnight, with constant rotation at 50°C. The digests are cooled to room temperature and 100μl protein/DNA precipitation solution is added. The tubes are inverted 10 times and placed on ice for 5min. Tubes are centrifuged at 13,000g for 15min to give a tight pellet that contains the DNA and proteins.

The RNA-containing supernatant is carefully decanted into a clean sterile eppendorf tube containing 300μl 100%v/v Isopropanol. At this point, 1μl glycogen (20μg/μl), which acts as a carrier, is added to aid precipitation of the smaller fragments of RNA. The RNA is pelleted by centrifugation at 13,000g for 15min. The supernatant is carefully removed and the pellet washed twice in 70%v/v ethanol before being allowed to air dry for 15min. Finally, 25μl of RNA hydration solution is added and samples are allowed to rehydrate for at least 30min on ice. RNA samples should be stored at −70 to −80°C and vortexed vigorously for 5sec before use.

3.2.7   CDNA SYNTHESIS

The procedure used for cDNA synthesis using MuLV (Murine Leukaemia Virus) is only slightly modified compared to that recommended by the supplier. In a final volume of 20µl, the reaction mixture contains 0.5mM of each deoxyribonuclease triphosphate (dNTP), 2.5 units of MuLV Reverse Transcriptase, 1 unit RNAsin and 1 µl random hexamers (2.5µM). The reactions are heated at $25^{o}C$ for 10min and $45^{o}C$ for 1hr, and the reaction was stopped by heating to $95^{o}C$ for 5min. cDNA is stored at $-20^{o}C$ until used for PCR.

3.2.8   SOLUTION PHASE RT-PCR – ABL (A+C) ASSAY

To ensure that the product of the double stranded amplification corresponds to mRNA, the primers are designed to span a long intron beyond the amplification possible with the PCR. Figure 3.5 outlines the approach taken in designing primers for RT-PCR experiments using the c-*abl* cDNA sequence.

8pmol of oligonucleotide primers corresponding to *abl* cDNA positions 450-474bp of exon 2 ($^{5'}$ttc agc ggc cag tag cat ctg act t$^{3'}$) and 621-650bp of exon 3 ($^{5'}$tgt gat tat agc cta aga ccc gga gct ttt$^{3'}$) are added to 2µl of RNA and expanded to a 25µl reaction with 1x EZ Buffer, 2.5mM each dNTP, 2.5U EZrTtH and $Mn(OAc)_2$ to a final concentration of 1mM.

The reverse transcription step consists of heating the tubes to $58^{o}C$ for 45 minutes. Following an initial denaturation step of 1min at $94^{o}C$, each of the 40 amplification cycles consists of denaturation at $94^{o}C$ for 45sec, primer annealing at $55^{o}C$ for 45sec and extension at $72^{o}C$ for 1min. The resulting amplicon is 201bp in length.

3.2.8.1   *c-abl* **7200 TaqMan® Assay Design**

Section 3.1.5.4 outlines the design of TaqMan® primer and probe sets using Primer Express® Software, PE Biosystems. Using the optimum design parameters as default, a suitable primer and probe set were selected for the *c-abl* TaqMan® Assay (Figure 3.5). Once again, primers were designed to span exonic junctions to ensure that products generated resulted from amplification of cDNA and not genomic DNA. The optimal amplicon size for TaqMan® assays is between 50-150bp. The selected oligonucleotides are as follows:

Forward Primer: exon 8 (1755-1787 bases)

         $5'$gcc cag aga agg tct atg aac tca$^{3'}$

Reverse Primer: exon 9 (1846-1872 bases)

         $5'$gag ata ctg gat tcc tgg aac att gt$^{3'}$

TaqMan® Probe: exon 9 (1802-1823 bases)

         $5'$ccc tct gac cgg ccc tcc ttt g$^{3'}$

         5' label = FAM

         3' label = TAMRA

Amplicon length: 120bp

3.2.8.2   **7200 TaqMan® Assay – Primer Titration Curve**

A primer titration curve is performed on all new TaqMan® primer and probe sets to determine the optimal concentration of primers for that assay. A standard master mix is prepared as outlined in Table 3.1.

EXON 2   atgttg gagatctgcc tgaagctggt gggctgcaaa tccaagaagg ggctgtcctc
      421 gtcctccagc tgttatctgg aagaagccct tcagcggcca gtagcatctg actttgagcc
      481 tcagggtctg agtgaagccg ctcgttggaa ctccaaggaa aaccttctcg ctggacccag
      541 tgaaaatgac cccaaccttt tcgttgcact gtatgatttt gtggccagtg gagataacac
      601 tctaagcata actaaag

EXON 3   gtg aaaagctccg ggtcttaggc tataatcaca atggggaatg
      661 gtgtgaagcc caaaccaaaa atggccaagg ctgggtccca agcaactaca tcacgccagt
      721 caacagtctg gagaaacact cctggtacca tgggcctgtg tcccgcaatg ccgctgagta
      781 tccgctgagc agcgggatca atggcagctt cttggtgcgt gagagtgaga gcagtcctag
      841 ccagaggtcc atctcgctga gatacgaagg gagggtgtac cattacagga tcaacactgc
      901 ttctgatggc aag

EXON 4   ctctacg tctcctccga gagccgcttc aacaccctgg ccgagttggt
      961 tcatcatcat tcaacggtgg ccgacgggct catcaccacg ctccattatc cagccccaaa
    1021 gcgcaacaag cccactgtct atggtgtgtc ccccaactac gacaagtggg agatggaacg
    1081 cacggacatc accatgaagc acaagctggg cgggggccag tacgggggagg tgtacgaggg
    1141 cgtgtggaag aaatacagcc tgacggtggc cgtgaagacc ttgaag

EXON 5   gagg acaccatgga
    1201 ggtggaaagg ttcttgaaag aagctgcagt catgaaagag atcaaacacc ctaacctagt
    1261 gcagctcctt g

EXON 6   gggtctgca cccgggagcc cccgttctat atcatcactg agttcatgac
    1321 ctacgggaac ctcctggact acctgaggga gtgcaaccgg caggaggtga acgccgtggt
    1381 gctgctgtac atggccactc agatctcgtc agccatggag tacctagaga agaaaaactt
    1441 catccacag

EXON 7   a gatcttgctg cccgaaactg cctggtaggg gagaaccact tggtgaaggt
    1501 agctgatttt ggcctgagca ggttgatgac aggggacacc tacacagccc atgctggagc
    1561 caagttcccc atcaaatgga ctgcacccga gagcctggcc tacaacaagt tctccatcaa
    1621 gtccgacgtc tggg

EXON 8   catttg gagtattgct ttgggaaatt gctacctatg gcatgtcccc
    1681 ttaccoggga attgaccgtt cccaggtgta tgagctgcta gagaaggact acggcatgaa
    1741 gcgcccagaa ggctgcccag agaaggtcta tgaactcatg cgagcat

EXON 9   gtt ggcagtggaa
    1801 tccctctgac cggccctcct ttgctgaaat ccaccaagcc tttgaaacaa tgttccagga
    1861 atccagtatc tcagacg

EXON 10   aag tggaaaagga gctggggaaa caaggcgtcc gtggggctgt
    1921 gactaccttg ctgcaggccc cagagctgcc caccaagacg aggacctcca ggagagctgc
    1981 agagcacaga gacaccactg acgtgcctga gatgcctcac tccaagggcc agggagagag
    2041 cg

Abl (A+C) Primers
Abl TaqMan Probe
Abl TaqMan Primers

Figure 3.5   Strategy for primer design in RT-PCR experiments. The c-*abl* exon boundaries are clearly marked. In both the conventional solution phase RT-PCR assay (Abl A+C primers) and the c-*abl* TaqMan® assay, forward and reverse primers are located in different exons.

Reagent	Concentration (per reaction)
Glycerol	6µl
Buffer A	1X
MgCl$_2$	5mM
DATP	400µM
DGTP	400µM
DUTP	400µM
DCTP	400µM
AmpliTaq® Gold	1.25 Units
UNG	0.25 Units

Table 3.1 Mastermix for TaqMan® PCR. Final reaction volume is 25µl. Glycerol is obtained from BDH chemicals, all other reaction components are obtained from PE Applied Biosystems.

Every combination of each primer concentration (50, 300 and 900nM) is tested to establish the optimal primer concentration for TaqMan® PCR. A negative control is also set up at the 300nM forward, 300nM reverse primer concentration. Thermal cycling is performed under the following conditions:

94°C x 2min (UNG inactivation)

94°C x 15sec ⎤
60°C x 1min ⎦ 40 Cycles

The fluorescent signal generated in each tube is measured using the ABI Prism® 7200 Sequence Detection Plate Reader (PE Biosystems). Figures 3.10 and 3.11 illustrates the results obtained. Optimal amplification is achieved using 300nM of each primer, consequently all subsequent assays are performed at this concentration.

3.2.8.3   c-*abl* 7200 TaqMan® Assay

The 5' exonuclease based c-*abl* RT-PCR is performed using a PE Biosystems 9600 96-well thermal cycler in the presence of 0.1μmol/L of the c-*abl* specific probe. The probe is labelled with FAM at the 5' end and TAMRA at the 3' end. A fluorescent dye 6-carboxy-X-rhodamine (ROX) is included in the TaqMan® buffer as an internal reference. PCR is carried out in 25μl reactions containing 1X TaqMan® buffer, 5mM MgCl$_2$, 400μM each of dUTP, dATP, dGTP and dCTP, 300nM of each primer, 0.25U of AmpErase® urasil-N-glycoylase (UNG) and 1.25U of AmpliTaq® Gold.

The reaction mix is first heated to 50°C to activate the UNG, followed by a denaturation step of 95°C for 10min. The DNA is then subjected to 40 cycles of a two-step PCR. Each cycle consists of a 15sec denaturation at 95°C and a 1min combined annealing/extension step at 60°C. The ABI Prism® 7200 Sequence Detection System is then used to measure the amount of fluorescence generated during PCR.

3.2.8.4   GAPDH 7200 TaqMan® Assay

The control gene TaqMan® Assay is performed using the PE Biosystems GAPDH Human Control Reagents kit (P/N 402869) according to the manufacturers protocol. Reactions are performed in a final volume of 25μl. Thermal cycling is performed under the same conditions described for the c-*abl* TaqMan® assay (section 3.2.8.3) *i.e.* 40 cycles of 95°C for 15sec and 60°C for 60sec. Signal generated is detected using the ABI Prism® 7200 Sequence Detection System.

3.2.9 AGAROSE GEL ELECTROPHORESIS

PCR products are visualised using agarose gel electrophoresis and ethidium bromide staining. A 2%w/v agarose solution in 1X TAE buffer is heated until the agarose has completely dissolved. The solution is allowed to cool, but before the gel solidifies ethidium bromide is added to a final concentration of 5μg/L. Horizontal slab gels are

poured in the Horizon 95 gel rig (Life Technologies) and allowed to set. Samples are electrophoresed until the dye front has travelled towards the end of the gel. Bands are visualised under UV light and recorded using the ImageStore gel documentation system.

3.2.10 STATISTICAL ANALYSIS OF 7200 SDS® DATA

The *standard deviation from the mean* is used widely in statistics to indicate the degree of dispersion of parametric data. It takes into account the deviation of every value from the mean and is found as follows:

(a) The mean, $\overline{x}$, of the set of n values, is first calculated.

(b) The deviation of each of these n values from the mean is calculated and the results squared, i.e. $(x_1-\overline{x})^2$; $(x_2-\overline{x})^2$ ....$(x_n-\overline{x})^2$.

(c) The average of these results is then found and the result is called the **variance** of the set of observations.

(d) The square root of the variance gives the standard deviation, denoted by the Greek letter 'sigma':

$$\text{Standard deviation} = \sigma$$

Data generated using the ABI Prism® 7200 End-point SDS is assessed for statistical significance using standard deviation measurements. If ΔR_n is **less** than $\pm 2\sigma$, the result is **not** considered to be statistically significant. If ΔR_n is **greater** than $\pm 2\sigma$, the result is considered to be **statistically significant**.

(K.A.Stroud in "Engineering Mathematics", Third Edition, Macmillan Publishing, 1992. Programme 27 'Statistics'; page 805-845).

3.3 RESULTS

3.3.1 SOLUTION PHASE RT-PCR OPTIMISATION

RNA was extracted from the HL6O cell line using the RNeasy mini kit, Qiagen, as outlined in section 3.2.2. The amplicon generated using the Abl A+C primer pair is 220 bases in length. Primer titration curves and Manganese acetate curves were performed (data not shown) to establish optimal conditions for the RT-PCR reaction. Following thermal cycling, 5µl of each PCR product is applied to a 1.5%w/v agarose gel and electrophoresed and the bands visualised by staining with ethidium bromide. Figure 3.6 shows the Abl (A+C) amplicon generated under optimal conditions outlined in section 3.2.8.

1.	100bp DNA ladder
2.	2µl ffpe gastric RNA
3.	1µl HL60 RNA
4.	1.5µl HL60 RNA
5.	2.0µl HL60 RNA
6.	Neg. Control

Figure 3.6 Abl (A+C) RT-PCR assay - template titration curve

3.3.2 C-ABL EXPRESSION IN FORMALIN FIXED PARAFFIN EMBEDDED MATERIAL

Section 3.2.4 outlines the many RNA extraction protocols and methods of tissue homogenisation tested in an attempt to obtain amplifiable RNA from archival material. Figure 3.7 illustrates the typical 'smearing pattern' observed on amplifying

RNA from paraffin embedded material. All homogenates are incubated with 20µg Proteinase K overnight at 50°C. RNA from samples extracted using the Flowgen kits is precipitated in Isopropanol using glycogen as a carrier (section 3.2.6). This smearing is in contrast to the sharp, discrete band obtained from HL60 RNA. The absence of any amplification from the RNA extracted from colon (lane 4) may be due to the fact that the tissue homogenates tend to block the Qiagen spin columns.

1.	100bp ladder
2.	Neg. Control
3.	HL60 RNA – Qiagen
4.	Colon RNA – Qiagen
5.	Gastric RNA – Flowgen
6.	Breast RNA – Flowgen
7.	Lymph Node RNA – Flowgen
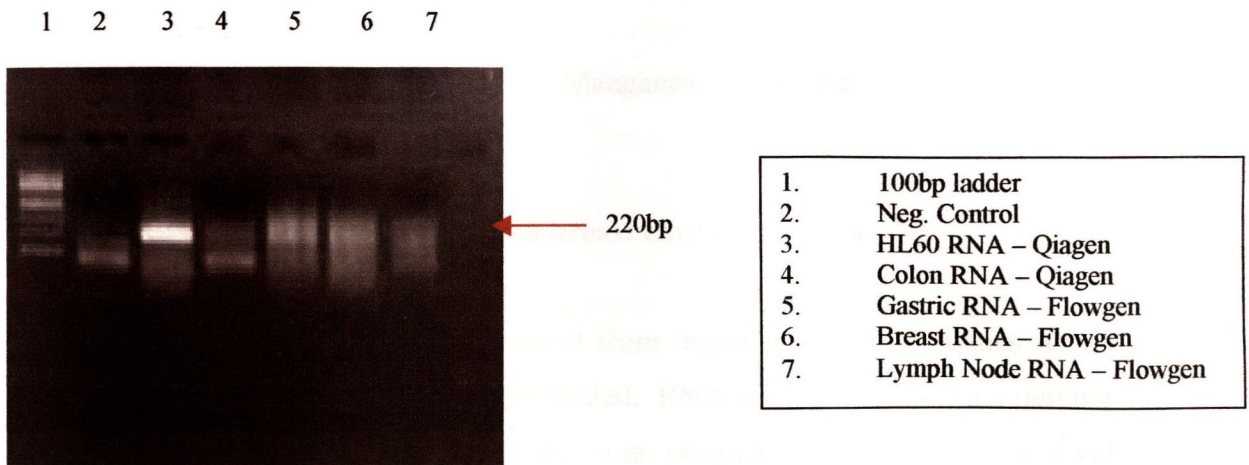
Figure 3.7   Abl (A+C) RT-PCR assay – using RNA from ffpe material as template

3.3.2.1   Manganese acetate curve

Initial optimisation of the Abl (A+C) RT-PCR assay used HL60 RNA as template. Due to the fact that RNA extracted from the archival material is at much lower concentrations and is considerably more degraded, a manganese acetate curve was repeated using RNA from a paraffin embedded gastric carcinoma. Figure 3.8 demonstrates that amplification is not achieved at any of the manganese acetate concentrations tested.

1.	100bp ladder
2.	Neg. control
3.	HL60 RNA – 1.0mM Mn(OAc)$_2$
4.	ffpe RNA – 0.6mM Mn(OAc)$_2$
5.	ffpe RNA – 0.8mM Mn(OAc)$_2$
6.	ffpe RNA – 1.0mM Mn(OAc)$_2$
7.	ffpe RNA – 1.2mM Mn(OAc)$_2$
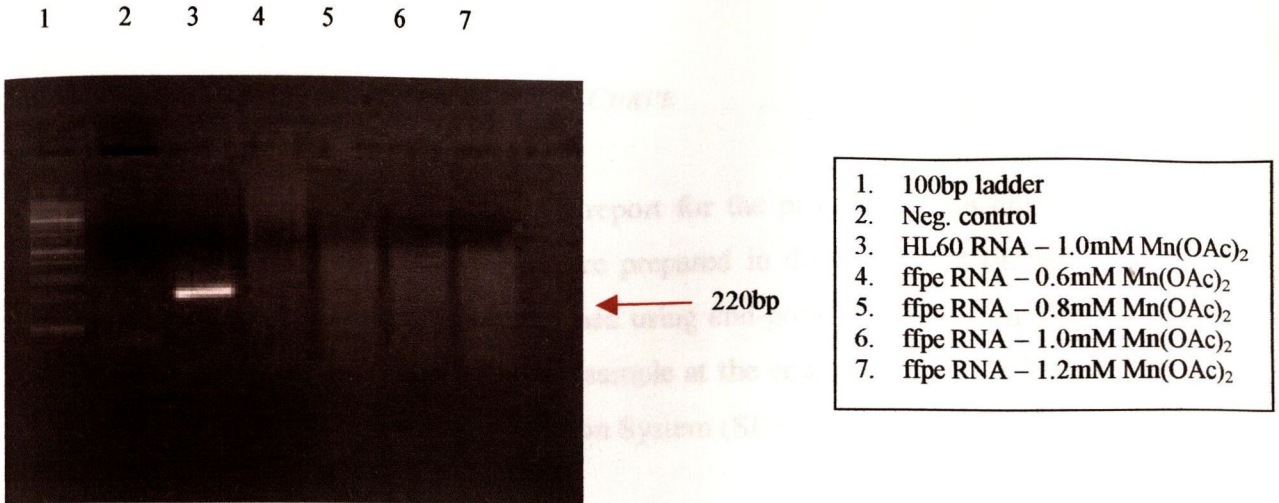
Figure 3.8   Abl (A+C) RT-PCR assay – Manganese acetate curve on ffpe material

3.3.2.2   c-*abl* expression in frozen breast carcinoma cases

Amplifiable RNA is more readily extracted from frozen tissues than tissues which have been formalin fixed and paraffin embedded. RNA was extracted from a number of frozen breast carcinoma cases using the same protocol as that used for archival material (section 3.2.6). Figure 3.9 is typical of the results obtained following RT-PCR.

1.	100bp ladder
2.	Neg. control
3.	Br1 RNA – frozen
4.	Br2 RNA – frozen
5.	Br3 RNA – frozen
6.	Br4 RNA – frozen
7.	HL60 RNA
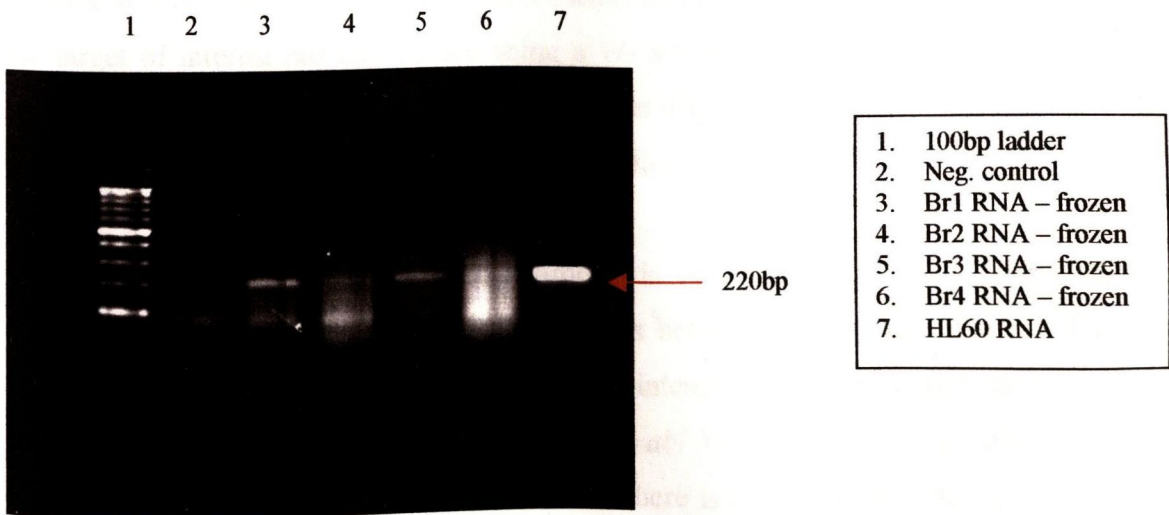
Figure 3.9 Abl (A+C) RT-PCR assay – c-*abl* expression in a series of frozen breast carcinoma cases

3.3.3   C-ABL TAQMAN® 7200 ASSAY PRIMER CURVE

Figure 3.10 shows the experimental report for the primer titration curve as described in section 3.2.8.1. All samples are prepared in duplicate, and the assay performed in triplicate. The assay is performed using end-point determination. This involves measuring the fluorescence of each sample at the end of the TaqMan® PCR using the ABI Prism® 7200 Sequence Detection System (SDS).

The SDS® software records and analyses the data and generates an Experimental Report for the assay as shown in Figure 3.10. The first column gives the **well** position of each sample within the plate. The second column gives information on the sample **type**, i.e. whether it is a negative control (NTC), a standard (STD) of known concentration of starting template or a sample of unknown (UNKN) concentration of starting template. Samples are named according to the concentrations of forward and reverse primer used in the reaction. For example, well A5 on the experimental report (Figure 3.10) contains a **sample name** 50/300 which indicates that the sample was is amplified using 50nM forward primer and 300nM reverse primer. If replicates of the same sample are performed, this is noted in the fourth column (**replicate**). In this particular assay, the **PCR** column is not applicable. In some subsequent assays however, this column will denote whether amplification of the target of interest has taken place using a +/- scoring system (Figure 3.10). The relative fluorescent (**Rn**) value for each sample is displayed, along with the standard deviation (**St. Dev.**) and **mean** for each set of replicates.

The raw spectra for each of the samples is shown in Figure 3.11. The 7200 Sequence Detection System® captures emissions between 500nm and 650nm. The raw spectra represents a plot of the fluorescent intensity (Y-axis) of each sample at each wavelength within this range (X-axis). The *abl* TaqMan® probe is labelled with FAM and has an emission maxima at 515nm. There is a significant difference in the fluorescent intensity of the samples at 515nm compared to that of the NTC's (Spectrum A1 & A2).

Sample Information

Well	Type	Sample Name	Replicate	PCR	Rn	Std. Dev.	Mean
A1	NTC	A1	a	No Amp	11.88	0.21	11.73
A2	NTC	A2	a	No Amp	11.58	0.21	11.73
A3	UNKN	50/50	b	No Amp	26.41	0.60	26.83
A4	UNKN	50/50	b	No Amp	27.25	0.60	26.83
A5	UNKN	50/300	c	No Amp	25.32	0.40	25.60
A6	UNKN	50/300	c	No Amp	25.88	0.40	25.60
A7	UNKN	50/900	d	No Amp	27.25	0.10	27.18
A8	UNKN	50/900	d	No Amp	27.11	0.10	27.18
A9	UNKN	300/50	e	No Amp	27.05	0.30	27.26
A10	UNKN	300/50	e	No Amp	27.48	0.30	27.26
A11	UNKN	300/300	f	No Amp	27.68	0.07	27.73
A12	UNKN	300/300	f	No Amp	27.78	0.07	27.73
B1	UNKN	300/900	g	No Amp	27.74	1.25	26.85
B2	UNKN	300/900	g	No Amp	25.97	1.25	26.85
B3	UNKN	900/50	h	No Amp	28.22	0.43	27.91
B4	UNKN	900/50	h	No Amp	27.61	0.43	27.91
B5	UNKN	900/300	i	No Amp	28.77	0.31	28.99
B6	UNKN	900/300	i	No Amp	29.22	0.31	28.99
B7	UNKN	900/900	j	No Amp	27.79	0.65	27.33
B8	UNKN	900/900	j	No Amp	26.87	0.65	27.33

Figure 3.10 c-*abl* TaqMan® Assay – Primer titration curve Experimental Report. Corresponding Figure 3.11 illustrates the raw spectra observed for each sample and no template controls.
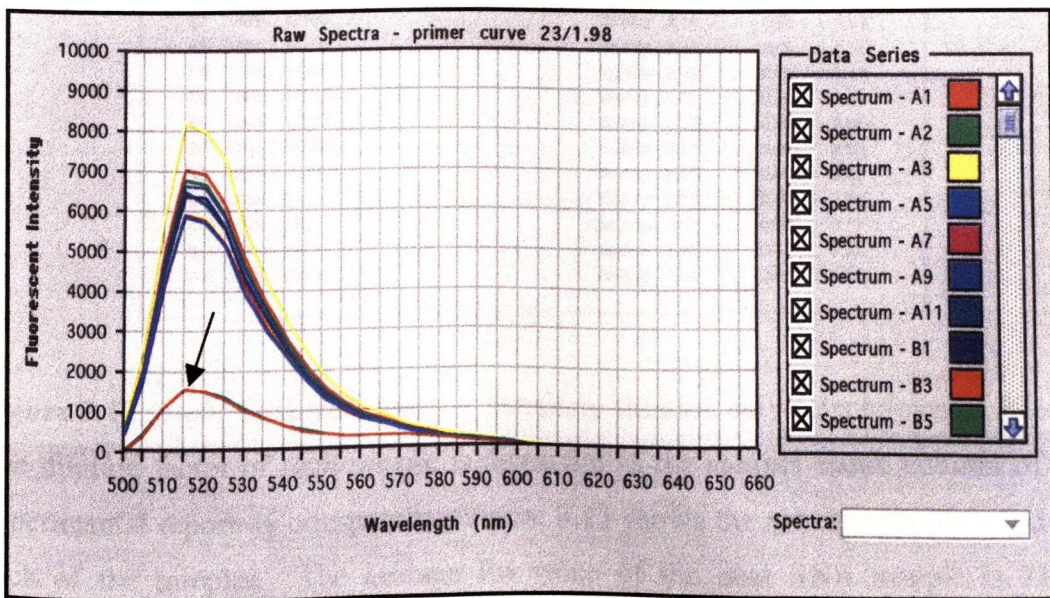
Figure 3.11 c-*abl* TaqMan® Assay – Primer titration curve Raw Spectra. Arrow indicates the emission spectra for the Negative control samples (NTCs).

3.3.4 C-ABL TAQMAN® ASSAY TEMPLATE TITRATION

A template titration curve was performed using serial dilutions of RNA from formalin fixed paraffin embedded gastric carcinoma tissue. The results demonstrate that quantities of RNA present in extractions from paraffin embedded tissue sections is such that no further dilutions of template are necessary. Figure 3.12 illustrates the Experimental report generated performing c-*abl* TaqMan® RT-PCR on serial dilutions of the extracted RNA.

PE Applied Biosystems   Sequence Detection Systems 1.6

File Name: template titration   Plate Type: 7200 Single Reporter⊡
User: Jenny
Date: Fri, Oct 1, 1999
Comments:

Sample Information

Well	Type	Sample Name	Replicate	PCR	Rn	Std. Dev.	Mean
A1	NTC	A1		No Amp	8.21	0.00	8.21
A2	NTC	A2		No Amp	8.40	0.00	8.40
A3	NTC	A3		No Amp	8.28	0.00	8.28
A4	NTC	A4		No Amp	8.21	0.00	8.21
A5	UNKN	neat		No Amp	21.40	0.00	21.40
A6	UNKN	neat		No Amp	20.97	0.00	20.97
A7	UNKN	neat		No Amp	21.33	0.00	21.33
A8	UNKN	neat		No Amp	21.28	0.00	21.28
A9	UNKN	1/10		No Amp	8.32	0.00	8.32
A10	UNKN	1/10		No Amp	8.40	0.00	8.40
A11	UNKN	1/10		No Amp	8.54	0.00	8.54
A12	UNKN	1/10		No Amp	8.65	0.00	8.65
B1	UNKN	1/100		No Amp	8.17	0.00	8.17
B2	UNKN	1/100		No Amp	8.14	0.00	8.14
B3	UNKN	1/100		No Amp	8.32	0.00	8.32
B4	UNKN	1/100		No Amp	8.40	0.00	8.40
B5	UNKN	1/1000		No Amp	8.08	0.00	8.08
B6	UNKN	1/1000		No Amp	8.06	0.00	8.06
B7	UNKN	1/1000		No Amp	8.53	0.00	8.53
B8	UNKN	1/1000		No Amp	8.43	0.00	8.43
B9	UNKN	B9		No Amp	7.93	0.00	7.93
B10	UNKN	B10		No Amp	8.07	0.00	8.07
B11	UNKN	B11		No Amp	7.89	0.00	7.89
B12	UNKN	B12		No Amp	7.79	0.00	7.79

Figure 3.12 c-*abl* TaqMan® Assay – Template titration curve Experimental Report. The dilution factor of each sample is displayed in the **sample name** column of the experimental report. Corresponding Figure 3.13 shows the raw spectra observed for each of the samples. The average Rn value of the neat RNA sample is 21.25 compared to an Rn value of between 8.06 and 8.65 for all other dilutions and the 'no template controls' (NTCs).
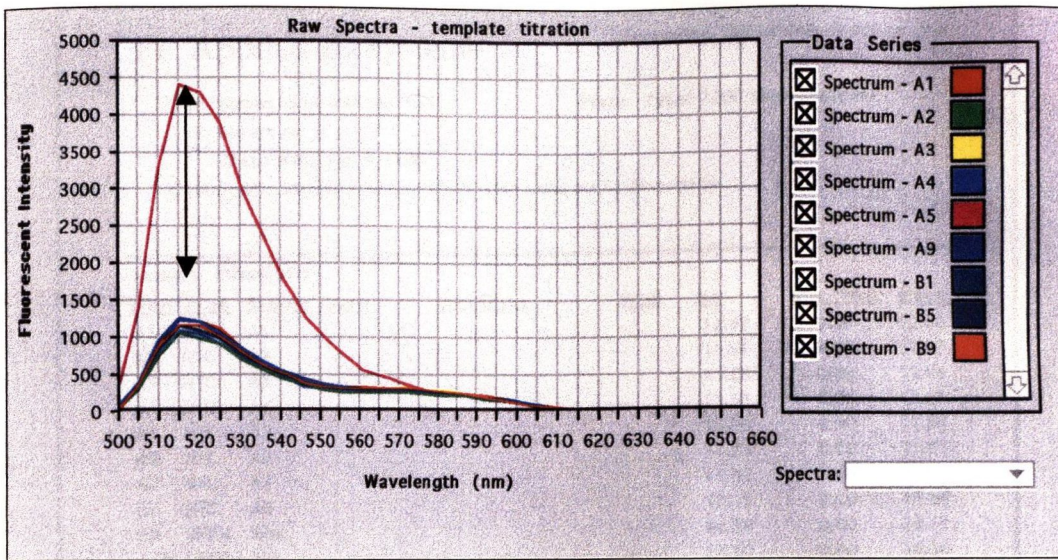
Figure 3.13 c-*abl* TaqMan® Assay – Template titration curve Raw Spectra. This figure illustrates the emission spectra generated for a series of RNA samples as shown in corresponding Figure 3.12. The arrow indicates the difference in fluorescent intensity observed between the sample containing neat RNA (pink spectrum) from paraffin embedded gastric tissue and those in which the RNA had been diluted.

3.3.5   c-abl TAQMAN® ASSAY STANDARD CURVE

The 7200 SDS end-point TaqMan® RT-PCR assay used in this study employs a two-step RT-PCR methodology. Extracted RNA is initially reverse transcribed using MuLV Reverse Transcriptase. In a separate reaction then, the generated cDNA is amplified using Taq® polymerase. It is important to verify that the assay is linear with respect to the reverse transcription step and subsequently to the TaqMan® PCR step. The linear range of the assay is established by constructing a standard curve of RNA concentration versus fluorescent intensity (end-point measurement using the 7200 Sequence Detection System). Each concentration of RNA is assayed in triplicate and representative results are shown in the Experimental Report (Figure 3.14). The data is accompanied by the corresponding raw spectra as shown in Figure 3.15.

PE Applied Biosystems

Sequence Detection Systems 1.6

File Name: HL60 RNA Std Curve
User: Jennifer
Date: Mon, Aug 9, 1999
Comments: Standard Curve of HL60 cDNA using abl TaqMan Assay

Plate Type: 7200 Single Reporter

Sample Information

Well	Type	Sample Name	Replicate	PCR	Rn	Std. Dev.	Mean
A1	NTC	A1		-	12.62	0.00	12.62
A2	NTC	A2		-	11.67	0.00	11.67
A3	NTC	A3		-	11.84	0.00	11.84
A4	NTC	A4		-	11.61	0.00	11.61
A5	NTC	A5		-	11.94	0.00	11.94
A6	NTC	A6		-	11.25	0.00	11.25
A7	NTC	A7		-	11.92	0.00	11.92
A8	NTC	A8		-	12.19	0.00	12.19
A9	UNKN	Neat		+	28.39	0.00	28.39
A10	UNKN	1/2		+	26.80	0.00	26.80
A11	UNKN	1/4		+	26.52	0.00	26.52
A12	UNKN	1/8		+	27.22	0.00	27.22
B1	UNKN	1/16		+	25.35	0.00	25.35
B2	UNKN	1/32		+	24.99	0.00	24.99
B3	UNKN	1/64		+	23.56	0.00	23.56
B4	UNKN	1/128		+	22.02	0.00	22.02
B5	UNKN	Negative		-	11.81	0.00	11.81

Figure 3.14 c-*abl* TaqMan® Assay – Standard Curve Experimental Report. This report shows the Rn values generated from series of HL60 RNA samples. The dilution factor of the RNA is given in the **sample name** column. The corresponding RNA concentration (ng/µl) is given in corresponding Table 3.2.
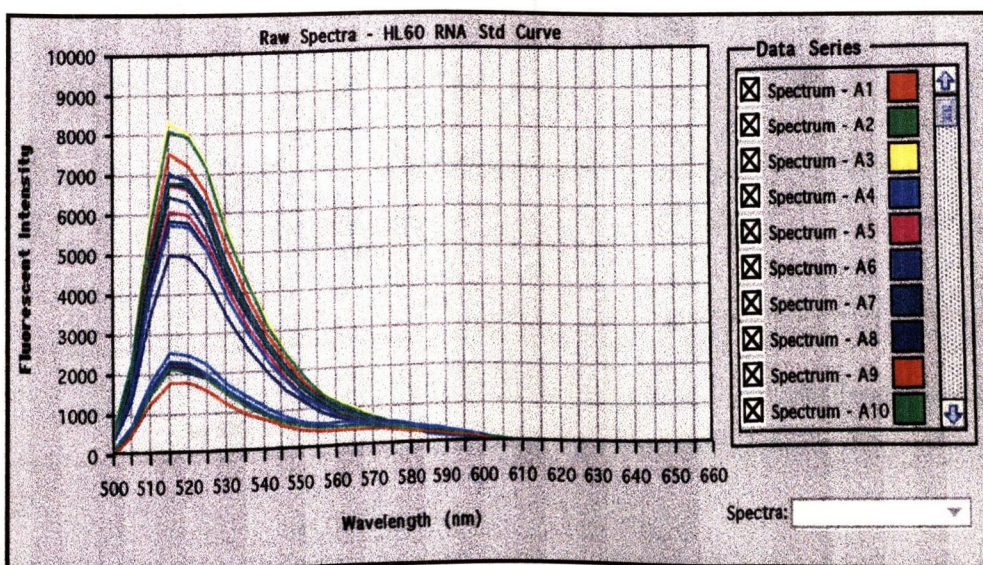
Figure 3.15 c-*abl* TaqMan Assay – Standard Curve Raw Spectra. This figure show the spread of fluorescent emission intensities observed at a maxima of 515nm

corresponding to the Rn values illustrated in the corresponding experimental report (Figure 3.14)

The results obtained are summarised in Table 3.2. From this data, a plot of RNA concentration and log RNA concentration versus Rn value can be prepared (Figure 3.16 & 3.17 respectively).

RNA Conc. (ng/ul)	log RNA Conc.	Rn Value (Next Day)
112	2.04921802	28.5
56	1.74818803	27.43
28	1.44715803	26.52
14	1.14612804	26.05
7	0.84509804	25.41
3.5	0.54406804	24.91
1.75	0.24303805	23.88
0.875	-0.0579919	22.58

Table 3.2 Summary of results obtained for TaqMan Standard Curve
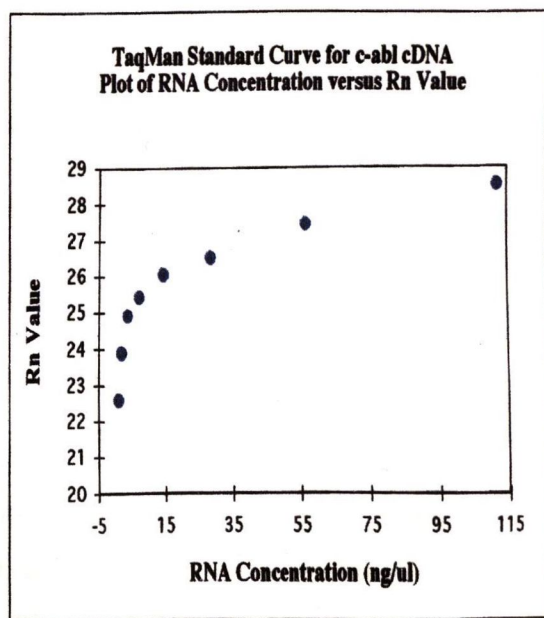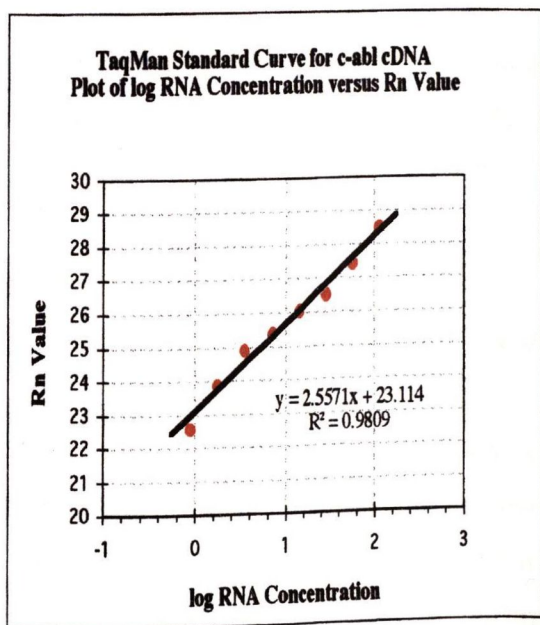
Figure 3.16 Plot of log RNA conc. Versus Rn Value   **Figure 3.17** Plot of RNA conc. Versus Rn Value

3.3.6   c-abl TAQMAN® ASSAY ON FFPE MATERIAL

RNA previously extracted from a variety of formalin fixed paraffin embedded tissues was assayed for c-*abl* using TaqMan® PCR using appropriate controls. The number of cases from which it was possible to reproducibly amplify c-*abl* mRNA by TaqMan® RT-PCR is summarised in Table 3.3

Tissue type	Fixation	No. of cases investigated	No. of cases amplified for c-*abl*
Chondrosarcoma	ffpe	20	5
Liposarcoma	ffpe	15	2
Gastric carcinoma	ffpe	11	9
Breast carcinoma	frozen	15	15

Table 3.3 Effect of tissue type and fixation on RNA extraction. All extractions were performed in triplicate and subsequently analysed in triplicate using the c-*abl* TaqMan® assay described in section 3.2.8.3.

3.3.7 c-abl TAQMAN® ASSAY – STUDY OF A SERIES OF GASTRIC CARCINOMA

Table 3.3 indicates that amplifiable RNA is extracted more efficiently from gastric tissue than any of the other ffpe materials investigated in this study. The experimental report (Figure 3.18) shows c-*abl* expression as measured using the c-*abl* TaqMan® assay described previously. In order to normalise the results for variations in starting quantity of RNA, a GAPDH assay is performed in parallel (as outlined in section 3.2.8.4) and the resultant experimental report shown in Figure 3.19.

PE Applied Biosystems   Sequence Detection Systems 1.6

File Name: Abl New   Plate Type: 7200 Single Reporter
      User: Jenny
      Date: Mon, Oct 4, 1999
Comments: Abl expression in a series of Gastric carcinoma cases using TaqMan RT-PCR

Sample Information

Well	Type	Sample Name	Replicate	PCR	Rn	Std. Dev.	Mean
A1	NTC	A1		-	12.48	0.00	12.48
A2	NTC	A2		-	12.55	0.00	12.55
A3	NTC	A3		-	12.16	0.00	12.16
C1	UNKN	HL60		+	26.99	0.00	26.99
C2	UNKN	HL60		+	29.49	0.00	29.49
C3	UNKN	Gastric 1		+	13.83	0.00	13.83
C4	UNKN	Gastric 2		+	13.81	0.00	13.81
C5	UNKN	Gastric 3		+	13.59	0.00	13.59
C6	UNKN	Gastric 4		+	13.64	0.00	13.64
C7	UNKN	Gastric 5		-	13.21	0.00	13.21
C8	UNKN	Gastric 6		+	14.27	0.00	14.27
C9	UNKN	Gastric 7		+	14.70	0.00	14.70
C10	UNKN	Gastric 8		+	13.96	0.00	13.96
C11	UNKN	Gastric 9		-	13.21	0.00	13.21
C12	UNKN	Gastric 10		+	13.97	0.00	13.97
D1	UNKN	Gastric 11		+	14.17	0.00	14.17
D5	NTC	D5		-	12.58	0.00	12.58
D6	NTC	D6		-	12.28	0.00	12.28

Figure 3.18 c-*abl* TaqMan® Assay in a series of gastric carcinoma cases. Experimental report shows the Rn values obtained following c-*abl* amplification of RNA from 11 gastric carcinoma cases by TaqMan® RT-PCR

PE Applied Biosystems   Sequence Detection Systems 1.6

File Name: Gpadh new   Plate Type: 7200 Single Reporter
      User: Jenny
      Date: Mon, Oct 4, 1999
Comments:

Sample Information

Well	Type	Sample Name	Replicate	PCR	Rn	Std. Dev.	Mean
E1	NTC	E1		-	0.88	0.00	0.88
E2	NTC	E2		-	0.85	0.00	0.85
E3	NTC	E3		-	0.85	0.00	0.85
E4	NTC	E4		-	0.85	0.00	0.85
E5	NTC	E5		-	0.83	0.00	0.83
G1	UNKN	HL60		+	7.25	0.00	7.25
G2	UNKN	HL60		+	7.69	0.00	7.69
G3	UNKN	Gastric 1		+	1.21	0.00	1.21
G4	UNKN	Gastric 2		+	0.95	0.00	0.95
G5	UNKN	Gastric 3		+	1.16	0.00	1.16
G6	UNKN	Gastric 4		-	0.90	0.00	0.90
G7	UNKN	Gastric 5		-	0.83	0.00	0.83
G8	UNKN	Gastric 6		+	1.04	0.00	1.04
G9	UNKN	Gastric 7		+	1.05	0.00	1.05
G10	UNKN	Gastric 8		+	1.06	0.00	1.06
G11	UNKN	Gastric 9		+	1.35	0.00	1.35
G12	UNKN	Gastric 10		+	1.13	0.00	1.13
H1	UNKN	Gastric 11		-	0.94	0.00	0.94

Figure 3.19 GAPDH TaqMan® Assay in a series of gastric carcinoma cases. Experimental report shows the Rn values obtained following GAPDH amplification of RNA from 11 gastric carcinoma cases by TaqMan® RT-PCR

The results are summarised in Table 3.4 along with the relative ratio of GAPDH:abl for each sample.

Case	Abl (ΔRn)	GAPDH (ΔRn)	Ratio
Gastric 1	13.83	1.21	11.43
Gastric 2	13.81	0.95	14.54
Gastric 3	13.59	1.16	11.72
Gastric 4	13.64	Neg	N/A
Gastric 5	Neg	Neg	N/A
Gastric 6	14.27	1.04	13.72
Gastric 7	14.70	1.05	14.00
Gastric 8	13.96	1.06	13.17
Gastric 9	Neg	1.35	N/A
Gastric 10	13.97	1.13	12.35
Gastric 11	14.17	Neg	N/A

Table 3.4 Normalised results for c-*abl* expression in gastric carcinoma by TaqMan® RT-PCR. **Neg** indicates that a negative result was obtained and as such no amplification of the target gene was achieved. Where no amplification of either GAPDH or c-*abl* was recorded, it is not possible to calculate a relative ratio value (N/A).

3.4 DISCUSSION

3.4.1 RNA ANALYSIS

Thus far, differential expression of the abl gene has been assessed at the protein level using immunohistochemistry. It would be of interest to determine whether the apparent upregulation of *abl* expression, for example, in tumour microvessels of myxoid liposarcoma, is at the level of transcription (mRNA) or translation (protein). mRNA extraction from formalin fixed paraffin embedded material proved to be extremely difficult and very much tumour type dependent. Conventional SP RT-PCR was the initial method of choice for examining gene expression at the mRNA level. Primer pairs were designed to amplify a fragment of 220 bases in length (section 3.2.7). An exhaustive amount of optimisation went into every stage of RNA extraction and amplification in an attempt to achieve good, reproducible and informative PCR results. However it appears that the RNA extracted from archival material is degraded to such an extent that it is difficult to amplify fragments of this length. This is supported by the fact that some of the RNA extracted could not be amplified for c-*abl* by SP RT-PCR but could be subsequently amplified for c-*abl* using TaqMan RT-PCR (in which amplicon lengths are only approximately 120 bases).

Throughout the course of this study a number of RNA extraction protocols were assessed (3.2.4). The Qiagen RNeasy mini kit is the method of choice for extracting RNA from cell lines. Cells are first homogenised using the QIAshredder columns, Qiagen, which consist of a biopolymer shredding system in a microcentrifuge spin column format. Using this protocol (3.2.2), very high yields of good quality RNA can be obtained. In addition, the RNeasy spin columns facilitate multiple, simultaneous processing of samples in less than 30 minutes. This is considerably faster and less tedious than many existing techniques such as alcohol precipitation or CsCl gradient ultracentrifugation. In addition, it does not involve the use of toxic chemicals such as phenol and/or chloroform (Boom *et al*, 1990; Coates *et al*, 1991).

The QIAshredder columns and RNeasy mini kits are not however suitable for RNA extraction from tissues (either frozen or paraffin embedded). Both are column based techniques and the tissue homogenates tend to remain on top of the column resin, unable to pass through even during centrifugation. In addition, the RNeasy mini kits enrich for mRNA and prevent mispriming events by excluding RNAs below 200bp in length. Given the template degradation and consequent smaller fragment size which is characteristic of formalin fixed paraffin embedded tissues, it is unlikely that the RNeasy mini-kits are suitable for RNA extraction from such tissues. Once again, exhaustive optimisation of a number of RNA extraction procedures (section 3.2.4) was performed in order to maximise the quantity and quality of extractable RNA from formalin-fixed paraffin embedded tissues. Ultimately, the Flowgen Gentra Pure*Scripts* RNA isolation kit (3.2.6) was proven to be the most effective method for RNA isolation from tissues. Adequate tissue homogenisation is pivotal to the success of this technique – the methods of tissue homogenisation are discussed elsewhere (3.2.5). The manufacturers guidelines suggest digesting tissue homogenates with Proteinase K for 1 hour, however in our hands an overnight digestion significantly increased RNA yields. As mentioned previously, the RNA fragments attainable from archival material are quite small and may be difficult to precipitate. Therefore glycogen, which acts as a carrier molecule, is added to the Isopropanol to aid in the precipitation of the smaller fragments. The protocol which reproducibly gave the best RNA yields from tissues is outlined in section 3.2.6. It is important to note that RNA yields were so low that they could not be measured using UV spectrophotmetry (section 3.1.3) or by simply visualing on an ethidium bromide stained agarose gel (section 3.2.9). The only way to determine if RNA had been successfully extracted was to subject all RNAs to solution phase RT-PCR and look for amplification, if any, of PCR products.

3.4.2 *SOLUTION PHASE RT-PCR*

The Abl (A+C) RT-PCR assay was designed as outlined in section 3.2.8 for the amplification of a 220bp fragment of the c-*abl* mRNA. Despite extensive optimisation it is not possible to reproducibly amplify the RNA extracted from formalin-fixed paraffin

embedded tissues by solution phase RT-PCR. Every RNA sample was assayed using the Abl (A+C) RT-PCR assay and PCR products visualised by agarose gel electrophoresis. Invariably, the degraded template resulted in either reaction failure or a smeared, undefined band on the agarose gel (Figure 3.7). This is in contrast to the discrete bands observed when amplifiying RNA from cell lines (Figure 3.6) and selected frozen breast cancer cases (Figure 3.9). It may therefore be concluded that conventional solution phase RT-PCR is not suitable for determining levels of c-*abl* mRNA expression from formalin fixed tissues. The most significant factor resulting in the failure of this technique is believed to be amplicon size. The solution phase assay is designed to amplify a fragment of c-*abl* mRNA 220bp in length, and it is likely that the RNA extracted from formalin fixed tissues is degraded to such an extent that fragments of this size are not present. The previously described Abl TaqMan$^®$ assay (section 3.2.8.3) is designed detect an amplicon which is 120bp in length (Figure 3.5). It was expected that TaqMan$^®$ RT-PCR may allow amplification of RNA extractions whose fragments proved to small to amplify and detect by conventional SP-PCR and agaraose gel electrophoresis.

3.4.3 TAQMAN$^®$ RT-PCR ANALYSIS

3.4.3.1   TaqMan$^®$ Primer Curve

In order to optimise the TaqMan$^®$ End-Point RT-PCR assay, a primer titration curve was performed using the *abl* TaqMan$^®$ primer and probe set as outlined in section 3.2.8.1. It is evident from the experimental report (Figure 3.12) that the efficiency of the TaqMan$^®$ assay is not greatly affected by varying the concentration of either of the primers, suggesting a robust assay has been designed. The data is accompanied by the raw spectra for each concentration combination (Figure 3.13). The Rn values range from 25.32-29.22, with the smallest standard deviation between duplicates observed when 300nm of each primer is used. The mean Rn value at this primer concentration is 27.73, superseded only slightly by of the reactions containing 900nM of forward primer. Consequently it was decided that the optimum primer concentration for use in the *abl*

TaqMan® assay is 300nM of both forward and reverse primer. This provides a balanced PCR, with maximum Rn values and minimum standard deviation between replicates.

3.4.3.2 TaqMan® Template Curve

As with any PCR assay, optimisation of template concentration is central to the efficiency of the reaction. RNA extracted from formalin fixed paraffin embedded gastric carcinoma was reverse transcribed as previously described (section 3.2.7). A 'template titration curve' was performed using 2µl of each dilution of the cDNA (neat, 1/10, 1/100, 1/1000) and the assay conditions as outlined in section 3.3.4. The experimental report (Figure 3.12) outlines the Rn values obtained at each dilution – showing that a positive reading (at the 99.7% confidence limit) is only observed in samples containing the undiluted cDNA as template. Consequently all future assays use 2µl of neat cDNA unless otherwise stated.

3.4.3.3 TaqMan® Standard Curve

It is important to establish the relationship which exists between the amount of RNA present in a sample and the fluorescent intensity observed for that sample in a TaqMan® assay. Such analyses comprise a two step process: firstly, the reverse transcription of RNA to cDNA and secondly, the exponential amplification of the cDNA in the presence of Taq polymerase and the specific TaqMan® probe. The aim of this experiment is to establish if the reverse transcription step is in fact linear with respect to starting concentration of RNA and also to determine the linear range of the *abl* TaqMan® assay.

Serial dilutions of HL60 RNA were performed (range: 112mM – 875µM) and each sample was then reverse transcribed as in section 3.2.7. 2µl of cDNA from each reaction was then used in a subsequent TaqMan® assay using the *abl* primer and probe set. The experimental report for the assay is shown in Figure 3.14. Wells A1-A8 are no template controls (NTC's), wells A9-B4 are varying concentrations of HL60 RNA. The

sample Rn values recorded are analysed using the 99.7% confidence interval. Figure 3.15 shows the raw spectra for each of the above mentioned wells – there is a significant difference in the emission intensity of the samples compared to that of the NTC's. Table 3.2 summarises the Rn values obtained for each concentration of RNA. From this data a plot of log RNA concentration versus Rn value was prepared (Figure 3.16), giving a correlation co-efficient of 0.9809. The results clearly suggest that a linear relationship exists between the starting quantity of RNA and the fluorescent intensity recorded within the concentration range examined.

3.4.4 EFFECT OF TISSUE TYPE ON RNA YIELDS

TaqMan[®] SDS technology was applied to the RNA samples which had previously proved impossible to detect by RT-PCR and agarose gel electrophoresis. Table 3.3 summarises the types of tumours studied and the number of cases from which RNA was successfully amplified by TaqMan[®] RT-PCR followed by 7200 End-Point detection. Clearly extreme difficulty was encountered with the cases of chondrosarcoma where RNA was amplified in only 25% of cases (5/20). There are a number of features of this tumour group which may account for such a poor success rate. Firstly, there is a very high nuclease content in the stroma of chondrosarcoma so much of the RNA may have been degraded prior to fixation. Secondly, many of the chondrosarcoma cases studied had undergone acid decalcification as part of their processing that would have undoubtedly had a detrimental effect on the RNA. This group of samples highlights an important factor for consideration when performing a retrospective study on archival material – while every precaution may be taken during the extraction step to preserve the integrity of the RNA, much of the degradation may have occurred prior to fixation over which the researcher has no control.

Poor success rates were also associated with the cases of liposarcoma studied (2/15). The mature adipocytes of the low grade liposarcoma are quite large and as such the number cells per section is considerably less than in other grades of liposarcoma (e.g. round cell) and in other tissue types. This also has the effect of limiting the amount of

RNA available for extraction. The RNA extraction protocol was much more efficient when applied to a series of formalin fixed paraffin embedded gastric carcinoma.

3.4.5   c-abl EXPRESSION IN GASTRIC CARCINOMA CASES USING TAQMAN® 7200 RT-PCR

Eleven cases of gastric carcinoma were selected for study on the basis of strong Abl expression as demonstrated by immunohistochemistry (unpublished data, O'Neill *et al*). RNA was extracted and reversed transcribed as previously described. *abl* expression was assessed using the TaqMan® assay at the 99.7% confidence interval. The experimental report (Figure 3.18) demonstrates that c-*abl* expression is detected in 9 of the 11 cases under investigation. RNA from the same extractions is also assayed for GAPDH using the appropriate assay conditions (Figure 3.19). On this occasion, positive Rn values are obtained in 8 of the 11 cases.

Table 3.4 is a summary of the results obtained in this experiment. Clearly, in the absence of GAPDH readings, a number of samples cannot be normalised and as such no meaningful interpretation can be assigned to the *abl* expression data for each sample. The importance of normalisation with a house-keeping gene is highlighted in sample 2, which despite having a relatively low *abl* expression (Rn 13.81), has the highest ratio index value (14.54). There are insufficient cases of gastric carcinoma in this study to establish any pattern in *abl* expression with respect to tumour grade, differentiation and extent of apoptosis.

It is interesting to consider why GAPDH did not amplify in a number of samples from which c-*abl* was successfully amplified. The primers and probe for the Abl TaqMan® Assay were designed using Primer Express® software according to the guidelines outlined in section 3.1.5.4. One of the most critical factors in the design of such oligonucleotides is amplicon size, which should ideally be between 50-150bp. Consequently we designed the c-*abl* assay to generate and amplicon of 120bp in length. The GAPDH primers and probe set were obtained from PE Biosystems in the form of the

TaqMan® GAPDH Human Control Reagents kit (P/N 402869). On consultation with PE Biosystems it was discovered that the control kit results in the generation of a GAPDH fragment 227bp in length, whereas the c-*abl* primer pair results in an amplicon of 120bp. We have previously discussed the problems encountered when trying to amplify a 220bp fragment using conventional RT-PCR (section 3.4.2) and this would explain why some samples showed amplification of c-*abl* but not GAPDH.

3.5 CONCLUSION

In summary, it may be concluded that RNA can be extracted from archival gastric carcinoma material with greater efficiency than RNA from cases of chondrosarcoma and liposarcoma. The results obtained from the various tissues examined indicate that the success of RNA extraction is at least partly tumour type and micro-architecture dependent. Unfortunately, due to the relatively small numbers of chondrosarcoma and liposarcoma cases from which RNA was successfully extracted and amplified, it is not possible at this stage to correlate expression of c-*abl* mRNA with that of the Abl protein as observed by immunohistochemistry. During the course of this study however, advancements in technology led to the development of a new generation of sequence detection instuments (ABI PRISM® 7700 SDS technology, PE Biosystems). This technology monitors fluorescent signal generation in Real-Time, permitting a more sensitive, accurate and quantitaive determination of mRNA levels. End-Point 7200 TaqMan® assays enabled us to detect c-*abl* mRNA in a number of archival tissue specimens. It did not however allow us to assign any quantitative significance to the results obtained. We hypothesised that Real-Time TaqMan® RT-PCR would enable quantification of c-*abl* message in the samples under investigation.

4. *C-ABL* EXPRESSION IN FORMALIN-FIXED PARAFFIN EMBEDDED TISSUES BY REAL-TIME TAQMAN® RT-PCR

4.1   INTRODUCTION

Chapter 3 clearly demonstrates that RNA can be succesfully extracted and amplified from formalin-fixed paraffin embedded material.   Unfortunately, extreme difficulties are encountered in trying to interpret the results from both soultion phase RT-PCR assays and TaqMan® 7200 end point determinations.   The 7200 SDS® measures the total amount of fluorescence generated after 40 cycles of PCR.   At this stage, however the samples are no longer in the exponential phase of amplification.   In order to accurately quantitate the levels of c-*abl* mRNA in the sample material, careful consideration must be given to the fundamental criteria of quantitative RT-PCR assays.

4.1.1   QUANTITATIVE PCR

The term quantitative PCR refers to any PCR technique which allows a reliable measurement of a specific nucleic acid target in a biological sample.   Many experiments often only require a semi-quantitative estimate of genetic material rather than an absolute determination of copy number.   Relative quantitation is quite a common procedure used to compare differences in nucleic acid targets among different samples.   This may be achieved by assaying a reference gene such as GAPDH separately or together with the unknown target and thus evaluating the level of expression as a simple ratio.   Alternatively a calibration sample may be used, which allows the evaluation of a biological effect in terms of percent variation in comparison to a basal condition.   This is the approach used most frequently for *in vitro* studies in which it is expected that changes in gene expression will be induced by some experimental conditions.

Absolute quantitative PCR determines the exact number of copies of nucleic acid target in a sample.   This can only be performed using a reference material with specific properties.   It should be as close as possible in size and chemical structure to the target, allowing an amplification efficiency comparable to the target.   In addition, its' concentration should be accurately quantitated.

4.1.1.1 Factors affecting the quantitative power of PCR

Optimisation of the amplification process is one of the key factors in attaining a quantitative assay. It is important to minimise non-specific hybridisation events that often happen in the early cycles and can lead to erroneous results. To this end 'hot-start PCR' is now widely used. This procedure involves omitting addition of one of the reaction components (usually Taq$^{®}$ polymerase) until the sample tubes have been heated to the permissive temperature.

The linear range of amplification is another crucial factor for consideration in the development of quantitative PCR assays. Theoretically, if the amplification proceeds with 100% efficiency, the amount of amplicons is doubling at each cycle. However in most PCR assays the overall efficiency may be as low as 70-80% during the exponential phase of the reaction (Wang *et al*, 1996). This increase in the amount of amplicon remains exponential for only a limited number of cycles before a 'plateau' is reached (Figure 4.1).
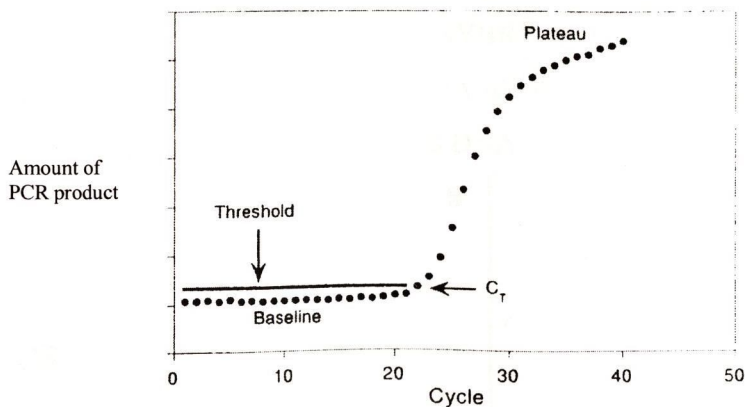
Figure 4.1 Sigmoidal amplification plot characteristic of the polymerase chain reaction

The plateau phenomenon arises from limiting factors including substrate saturation of the enzyme, incomplete product strand separation and exhaustion of reaction components. In the plateau phase of a PCR reaction, the amount of product formed is no longer

proportional to the amount of starting material. It is therefore imperative that any quantitative strategy clearly identifies the window in which the amplification is at constant efficiency and in an exponential phase (a major limitation of the 7200 TaqMan® End-Point Assay, Chapter 3).

4.1.1.2 Double stranded DNA Binding Dyes

The analysis of PCR kinetics was pioneered by Higuchi *et al*, 1992, by constructing a system that detects PCR products as they accumulate. A number of different chemistries have been employed in real-time quantitation of DNA. Small dyes that bind to double-stranded DNA can be sub-divided into two classes: intercalators and minor groove binders (Nielsen, 1991). Higuchi *et al*, 1992, used the intercalator ethidium bromide for their real-time detection of PCR products. A widely used example of a minor groove binding dye is Hoeschst 33258, whose fluorescence increases over 100 fold when bound to double-stranded DNA (Searle and Embrey, 1990). The two fundamental criteria for any DNA binding dye are increased intensity of fluorescence when bound to double stranded DNA, and no effect on the efficiency of the PCR reaction. One chemistry which has recently been developed as a DNA binding dye is the SYBR® Green I dye by PE Biosystems. The precise mode of action of SYBR® Green I remains unclear and it is yet unclassified as either an intercalator or a DNA binding agent. However, it is certain that SYBR® Green binds only to double-stranded DNA, without inhibiting PCR.
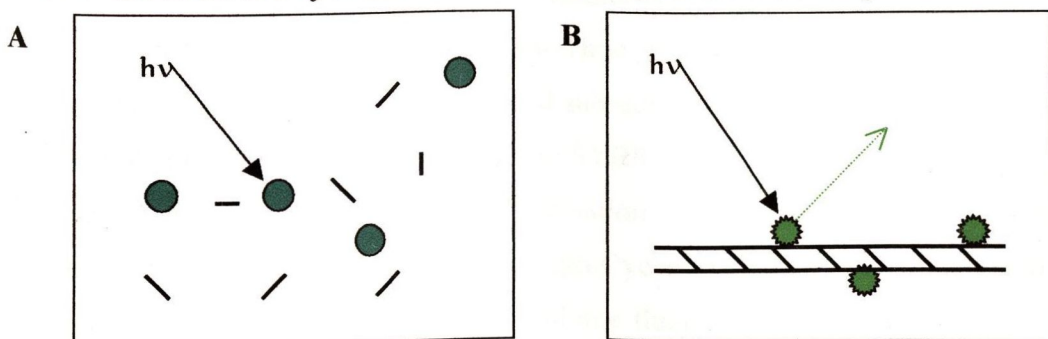
Figure 4.2 SYBR® Green I binding to double stranded DNA. The SYBR® Green dye is unable to bind to single stranded DNA (Panel A). When bound to double-stranded to DNA, a 100-fold increase in fluorescence intensity is observed (B).

The ability of DNA binding dyes to bind to any double stranded DNA molecule is both a major advantage and a major pitfall of these techniques. The generic DNA binding dyes can be used to detect any amplified product, regardless of sequence, providing a universal, versatile and relatively inexpensive assay. It is no longer necessary to purchase specific oligonucleotide probes for every newly designed PCR assay. However, the fact that SYBR green and other DNA binding dyes are not specific increases the risk of false positives and inaccuracies in the data generated. This is particularly problematic if the PCR results in the formation of any primer dimers or non-specific PCR product. It is not possible to differentiate between the fluorescence generated from specific amplification of the target sequence and that arising from any mis-priming event which would normally be detected as a spurious band on an electrophoretic gel.

In addition, multiple dyes bind to a single amplified molecule, which increases the sensitivity for detection amplification products. Consequently, if the amplification efficiencies are the same, amplification of a longer product will generate more signal than a shorter one. This is in contrast to the use of fluorogenic probes in which a single fluorophore is released for each molecule synthesised, regardless of length.

4.1.1.3 LightCycler® System Instrument, Roche Molecular Biochemicals

The LightCycler® from Roche Molecular Biochemicals is a system for qualitative and quantitative PCR, permitting Real-Time monitoring of PCR reactions. The LightCycler® is capable of monitoring and subsequently evaluating PCR products formed using either (a) DNA binding dyes such as SYBR Green I or (b) fluorophores coupled to sequence specific oligonucleotide hybridisation probed that only bind certain PCR products (e.g. LightCycler – Red 640, LightCycler – Red 705 and Fluorescein). The optical unit of the LightCycler, a micro-volume fluorimeter, can measure fluorescence in three separate channels simultaneously. In the LightCycler system, PCR temperature cycling is achieved using circulating air as opposed to a conventional thermal block. The specificity and sensitivity of SYBR Green I detection can be monitored by performing a melting curve analysis after the amplification reaction. The advantages of real-time

detection over end-point determinations have been discussed previously (section 4.1.1). However, the LightCycler is also capable of providing sequence confirmation of the amplified product through melting curve analysis. Combining amplification with melting curve analysis can enhance specificity and sensitivity of amplification reactions. Each dsDNA product has its own specific melting temperature (T_m), which is defined as the temperature at which 50% of the DNA becomes single stranded and 50% remains double stranded. By performing a melting curve analysis after the run, the identity of the PCR product can be confirmed by confirming its T_m with the T_m of a positive control (Figure 4.3). This technology allows easy differentiation of specific primer PCR product from non-specific products such as primer-dimers, without the need for DNA sequencing.
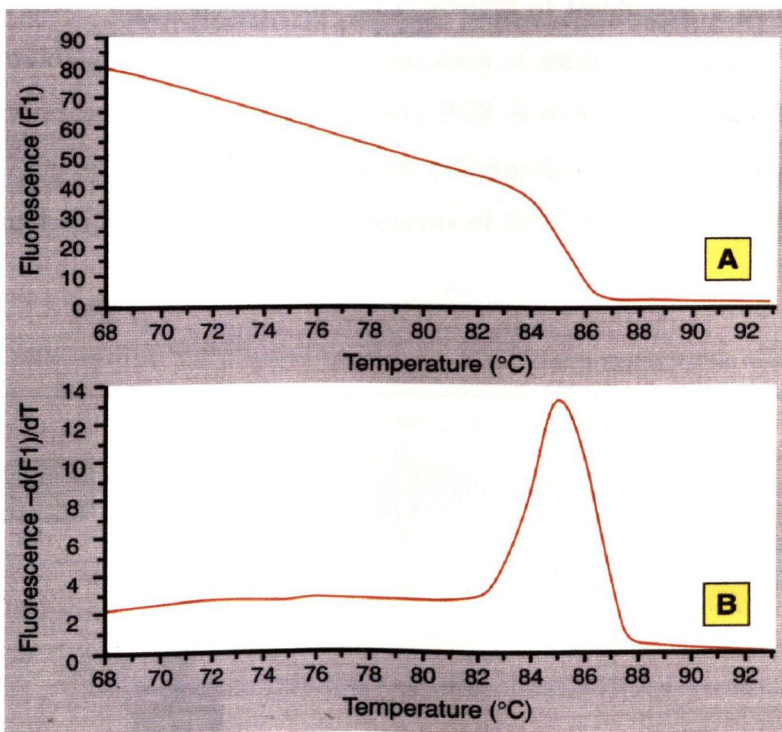
Figure 4.3 Sample melting curve of a 100bp β-actin PCR fragment on the LightCycler System. After PCR, products are slowly heated from 55 to 95°C, and the fluorescence measured at 0.2°C intervals. In Panel A, a sharp drop in fluorescence is noted as the product is denatured. The melting temperature is easily visualised by taking the first derivative (-dF/dT) of the melting curve (Panel B), resulting in a fragment specific T_m peak.

4.1.2 TAQMAN® REAL-TIME ASSAYS

The principles of TaqMan® PCR have been discussed previouly (section 3.1.5.3). Briefly, PCR is performed in the presence of a TaqMan® probe, consisting of an oligonucleotide 20-30 bases in length with a 5' reporter dye, a 3' quencher dye and a 3' blocking phosphate. During PCR, if the target of interest is present, the probe will specifically anneal between the forward and reverse primer. Due to the nucleolytic activity of the AmpliTaq DNA Polymerase, the probe is cleaved between the reporter and quencher sequence resulting in the emission of a fluorescence signal. Earlier work presented in this thesis utilised the 7200 SDS®, which measured the amount of fluorescence generated at the end of the thermal cylcling process. However, a new generation of SDS® instruments enable measurement of fluorescence generated in real-time, thus providing a more accurate determination of starting template. In this type of assay, the fluorescent signal generated during PCR is monitored in real-time using the ABI Prism® 7700 Sequence Detection System (PE Applied Biosystems, Foster City, CA, USA). Figure 4.4 illustrates the key components of the 7700 SDS fluorescent detection system.
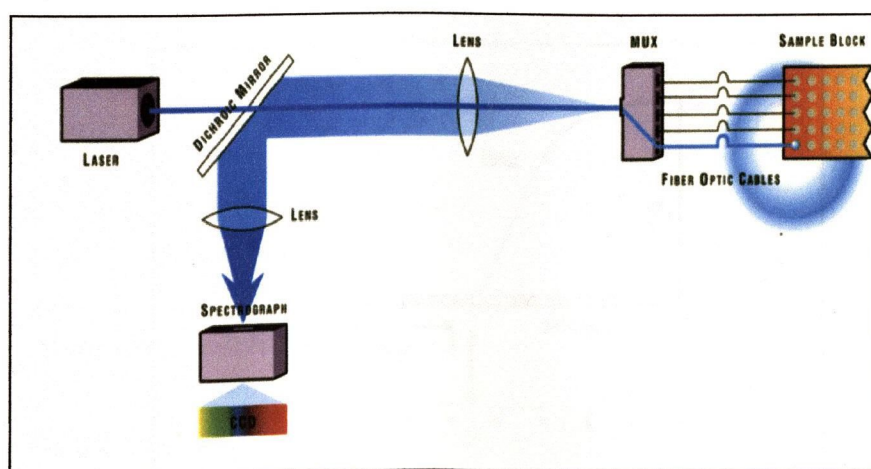
Figure 4.4 Components of ABI PRISM® 7700 Sequence Detection System

During PCR the multiplexer directs an argon ion laser through fibre optic cables which are positioned directly above each position of a 96-well plate causing excitation of electrons in the fluorescein reporter molecules. The emissions between 500nm and 660nm are captured through fibre optic cables and focused by a dichroic mirror into a spectrograph. The light is separated according to wavelength by the CCD camera and the data analysed by the software's algorithms. The 7700 technology permits complete data collection from all wells approximately once every 7 seconds.

During the PCR reaction, the emission intensities of both the reporter and quencher dyes are evaluated. The intensity of the latter remaining relatively constant during PCR and as such is used to normalise variations in reporter emission intensities. The software calculates a value termed Δ**Rn** (or Δ**RQ**) using the following equation: Δ**Rn** = **(Rn^{+}) – (Rn^{-})**, where Rn^{+} is the emission intensity of the reporter/ emission intensity of the quencher at any given time in a reaction tube, and Rn^{-} is the emission intensity of the reporter/ emission intensity of the quencher prior to amplification in that same reaction tube.

A TaqMan$^{®}$ amplification plot displays the typical sigmoidal shape amplification plot characterisitic of any PCR (Figure 4.5).
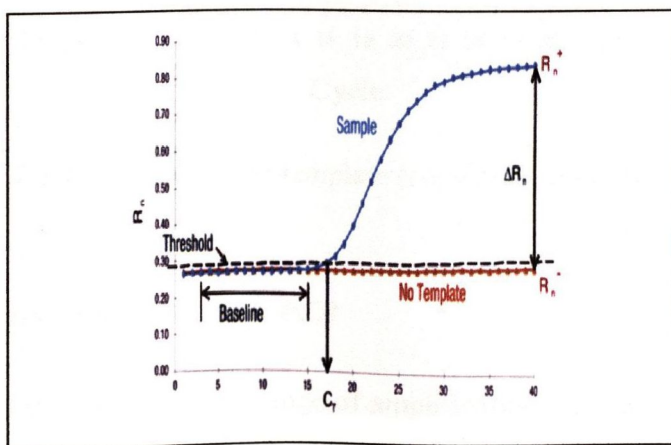
Figure 4.5 Typical amplification curve observed in a TaqMan$^{®}$ PCR assay. The threshold Cycle (C_T) represents the point at which fluorescent intensity rises above the threshold level.

In the initial cycles, insufficient reporter is cleaved to elevate the emission intensity above baseline. After a certain number of amplification cycles (C_T) probe cleavage is such that reporter emission intensity rises above the baseline – this is referred to as the threshold cycle. C_T is dependent on the starting template copy number, the efficiency of amplification and the cleavage of the TaqMan® probe. An inverse relationship is observed between the amount of template present and the threshold cycle for that reaction – this is expected because reactions with fewer starting copies of the target molecule require greater amplification cycles to generate a detectable signal. Consequently C_T can be used as a quantitative measurement of the input target number.
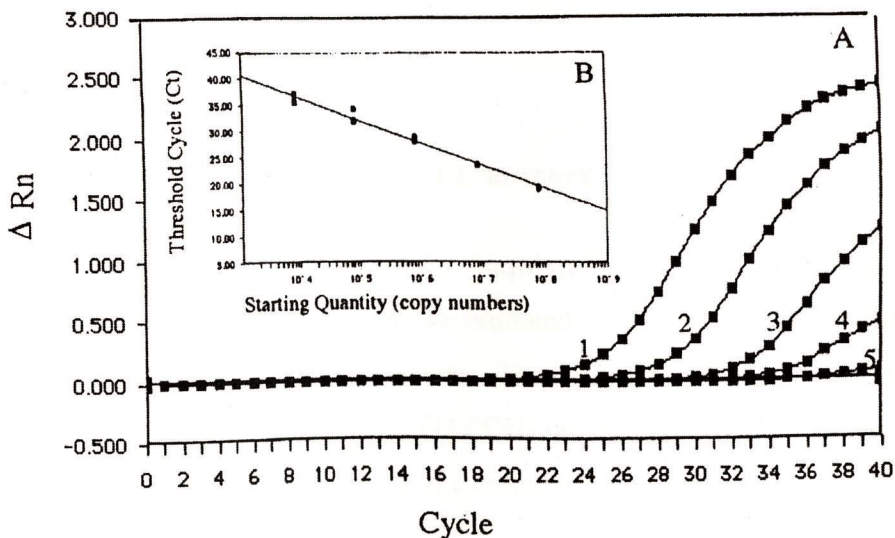
Figure 4.6 Plot of Starting quantity of template (copy number) versus threshold cycle (C_T).

4.1.3 STANDARDS FOR QUANTITATIVE PCR

In order to evaluate the linear range of amplification, standard samples of known concentration and similar composition to the test samples are also analysed. Standards may be either external or internal. In the case of external samples, the standards are amplified in separate PCR tubes and the data used to generate a standard curve from which sample concentration may be extrapolated. Alternatively, a co-amplification of the reference standard and the target sequence may be performed. In this case, any variations

in amplification efficiency can be compensated for through normalisation with the internal standard. A prerequisite for this type of analysis is that the amplification of the standard must not compromise that of the target or vice versa. In addition, both targets should amplify with the same efficiency.

It is important to note that DNA standards are not always appropriate for the quantitation of RNA targets as they do not take into account variations in the reverse transcription step. Therefore it is preferable to use known concentrations of RNA or cRNA (copy RNA) as standards in such assay systems. cRNA may be generated through cloning the cDNA fragment of interest into an appropriate vector containing a transcription site.

4.1.4 RELATIVE QUANTITATION OF GENE EXPRESSION

Relative quantitation of gene expression by TaqMan $^®$ RT-PCR is achieved using the Comparative Ct method according to the recommended guidelines in User Bulletin #2: ABI Prism$^®$ 7700 Sequence Detection System. The expression level of the target gene is normalised to a house-keeping gene (e.g. GAPDH), and compared to that of a calibrator or reference sample. The equation used in the comparative Ct method is

$$2^{-\Delta\Delta Ct}$$

where ΔCt is the difference between the target gene Ct and the reference gene Ct,

$\Delta\Delta Ct$ is the difference between the sample ΔCt and the calibrator or reference ΔCt

(See Appendix 1 for deriviation of the Comparative Ct formula).

We hypothesise that TaqMan® Real-Time RT-PCR will enable us to evaluate c-*abl* expression levels in mRNA extracted from fromalin-fixed, paraffin embedded material. A newly designed GAPDH primer and probe set (80bp amplicon, Section 4.2.3) should ensure that basal RNA levels can be detected even in those samples which could not be detected using the larger GAPDH fragment and 7200 end-point determinations. Measurement of Ct instead of Rn values will provide a much more accurate assessment of mRNA levels. The Comparative Ct method of Index calculations will also facilitate accurate interpretation of the data obtained and allow a direct comparaison to be made between c-*abl* mRNA levels in different grade tumours.

4.2   MATERIALS & METHODS

4.2.1   CDNA SYNTHESIS

RNA is extracted from formalin fixed paraffin embedded tissues (see section 3.2.1) using the Gentra Pure*Script*™ method described in section 3.2.6.   Reverse transcriptions are performed in duplicate using the MuLV reverse transcriptase enzyme.   In a final volume of 20μl, the reaction mixture contains 9μl paraffin-extracted RNA, 0.5mM each dNTP, 2.5U MuLV, 1.0U RNAsin, 125nM random hexamers and dH_20 as required.   The reactions are heated at 25°C for 10min, held at 45°C for 1hr and the reactions stopped at 95°C for 5min.   cDNA is stored at –20°C until ready for use.

4.2.2   c-abl REAL-TIME 7700 SDS TAQMAN® ASSAY

All variables of this assay were previously optimised as described in section 3.2.8.3. Table 4.1 outlines the composition of each reaction using the c-abl TaqMan® primer and probe set (section 3.2.8.1)

Component	Concentration/Volume
c-*abl* Forward Primer	300nM
c-*abl* Reverse Primer	300nM
c-*abl* TaqMan® Probe	100nM
cDNA	2μl
dNTPs (A,G,C,U)	400μM each
AmpliTaq Gold	1.25U
$MgCl_2$	5mM
PE TaqMan® Buffer	1X
Urasil-*N*-Glycosylase	0.25U
dH_2O	As required
Final Volume	25μl

Table 4.1 Composition of c-*abl* TaqMan® Assay reactions

The optimal thermal cycling conditions for this assay were found to be an initial hold at 50°C for 2min followed by 10min at 95°C. 45 cycles of 95°C for 15sec and 60°C for 1min are then performed.

4.2.3 GAPDH REAL-TIME 7700 SDS TAQMAN® ASSAY

The need to create an alternative GAPDH primer and probe set which will give rise to an amplicon of the desired length for TaqMan® PCR (less than 150bp) has already been discussed (section 3.4.5). GAPDH primers and TaqMan® probe were designed using Primer Express Software, PE Biosystems as outlined in section 3.1.5.4. The resultant primer/probe set is outlined in Table 4.2.

Oligonucleotide	Sequence	Amplicon Size, bp
GAPDH Forward Primer	$^{5'}$TGTTCCAATATGATTCCACCCA$^{3'}$	
GAPDH Reverse Primer	$^{5'}$TTGATGACAAGCTTCCCGTTC$^{3'}$	
GAPDH TaqMan® Probe	$^{5'}$TTCCATGGCACCGTCAAGGCTG$^{3'}$	80bp

Table 4.2 Sequences of the primer and probe set used for GAPDH amplification, as designed using Primer Express® Software.

The optimal composition of each reaction using the GAPDH TaqMan® primer and probe set is shown in Table 4.3.

Component	Concentration/Volume
GAPDH Forward Primer	300nM
GAPDH Reverse Primer	300nM
GAPDH TaqMan® Probe	100nM
cDNA	2µl
dNTPs (A,G,C,U)	400µM each
AmpliTaq Gold	1.25U
MgCl$_2$	5mM
PE TaqMan® Buffer	1X
Urasil-N-Glycosylase	0.25U
dH$_2$O	As required
Final Volume	25µl

Table 4.3 Composition of GAPDH TaqMan® Assay reactions

The optimal thermal cycling conditions for this assay were found to be an initial hold at 50°C for 2min followed by 10min at 95°C. 45 cycles of 95°C for 15sec and 60°C for 1min are then performed.

Relative quantitation of gene expression is performed using the comparative C_t method as defined previously (section 4.1.4).

4.2.4 POST-PCR MANIPULATION

In order to verify that the amplicon generated during PCR is precisely that for which the primer set was designed, post PCR products are sequenced using the ABI PRISM® 310 Genetic Analyzer. Initially, products are visualised by agarose gel electrophoresis. The bands are cut from the gel and the DNA isolated using GenElute™ Agarose Spin columns according to the manfacturers protocol. The purified DNA fragment is cloned into a plasmid cloning vector using the Invitrogen TopoTA™ Cloning kit as described in the accompanying User Manual. The cloned

fragment is removed from the plasmid by restriction digest with the restriction endonuclease Eco R1 (Boehringer Mannheim, Inc.) and is then ready for sequencing.

4.2.5 *ABI PRISM 310 GENETIC ANALYSER*

4.2.5.1 Sample Preparation using Big Dye (BD) Chemistry

The following is a brief outline of the protocol for DNA sequencing (using M13 and M-13 primers supplied in ABI Prism® Big Dye™ Terminator v3.0 Cycle Sequencing kit, P/N 4390236, PE Biosystems).

Sequencing Reaction:

Primer	5pmol
DNA template	200-500ng DNA
Seq. MasterMix:	8µl
Water	as required
Total Vol.	20µl

Thermocycling conditions:

$96^{o}C$ x 10sec
$50^{o}C$ x 5sec
$60^{o}C$ x 4min

for 25 cycles

Unincorporated dyes may be removed using a simple isopropanol precipitation step or using DyeEx Spin columns.

4.2.5.2 DyeEx Spin Columns

Qiagen DyeEx Spin kits are designed for fast and easy removal of unincorporated dye terminators directly from sequencing reactions. The recommended protocol is as follows:

1. The spin column is gently vortexed to resuspend the resin
2. The cap of the column should be loosened one quarter turn to avoid a vacuum inside the spin column
3. The bottom closure of the spin column is snapped off and the column placed in a 2ml collection tube

4. A centrifugation step at 3000 rpm for 3min is then performed

5. The spin column is then carefully transferred into a clean eppendorf. The 20μl sequencing reaction is then slowly applied to the gel bed

6. Again, the column is centrifuged for 3min at 3000rpm

7. After centrifugation, the spin column is removed from the eppendorf. The eluate contains the purified DNA

8. Samples are dried in a vacuum centrifuge and resuspended in TSR (Template Suppression Reagent)

9. Samples are denatured by heating for 2min at 95°C and chilled immediately on ice to prevent reannealing

4.2.5.3   ABI Prism 310 sequencing

Sequencing was performed on the ABI Prism® 310 Genetic Analyser, PE Biosystems as outlined in User Manual Bulletin 4317588 (PE Biosystems, March 1997). As PCR products to be sequenced were less than 600bp in length, the short read green capillary (47cm x 50μm, P/N 402839) was used. Before use, a matrix file had to be created for the dye set in use to account for spectral overlap and individual dye retardation within the capillary. dRhodamine Matrix Standards were purchased from PE Biosystems (P/N 403047). Refer to User Bulletin *Dye Terminator Sequencing using Performance Optimised Polymer 6 and the 1.0ml Syringe* (PE Biosystems, March 1997) for details on how to generate a matrix file.

4.2.6   Laser Capture Microdissection

Individual cells were selected and removed from tissues sections using the PixCell II™ Laser Capture Microdissection System, Acturus Engineering Inc. Standard protocols for preparation of cell smears and tissue sections are followed using standard microscopy slides. The sample is visualised through the video monitor and the CapSure™ caps placed over the cell(s) of interest. Pulsing the low power infrared laser (25mW, 1.5mS) allows the cells within the laser beam to adhere to the transfer film. The cap is then lifted with the desired cell(s) attached to the transfer

film while the surrounding tissue remains in tact. The cap is placed directly onto a standard microcentifuge tube containing the extraction buffer. The cellular DNA, RNA or protein are ready for molecular analysis. The accompanying PixCell II™ Image Archiving Workstation permits accurate monitoring and documentation of cell transfers.

4.3 RESULTS

The terms below are used throughout this results section and may be defined as follows:

Rn: Relative ratio of target gene to housekeeping gene. A simple ratio based on threshold cycles of both target and housekeeping PCR reactions, normalised against a passive internal reference (section 3.1.5.5). An inverse relationship exist between Rn values and starting concentration of target template.

Ct value: Threshold cycle. This value represents the cycle at which the fluorescence emission intensity of a sample rises above the baseline. Ct is dependent on the starting template copy number, the efficiency of amplification and cleavage of the TaqMan® probe. An inverse relationship is observed between the amount of template present and the threshold cycle for that reaction (section 4.1.2)

ΔCt: Delta Ct value. This figure represents the difference between the threshold cycle observed for the target gene and that observed for the reference gene.

ΔΔCt: Delta, delta Ct value. ΔΔCt is the difference between the sample ΔCt and the calibrator or reference ΔCt. A direct relationship exists here; the greater the ΔΔCt, the greater the difference in target gene expression between the sample and the calibrator or reference sample.

Index: The Index value enables a direct comparison of samples to be made. The index value is calculated from the ΔΔCt value, as described in section 4.1.4. In all cases, expression of the target gene in the calibrator or reference sample obtains an index value of 1, and the expression of the target gene in all other samples is expressed relative to this. The equation is linear, such that an index value of 10, for example, represents a 10-fold difference in target gene expression between test and control samples.

4.3.1 c-abl EXPRESSION IN CHONDROSARCOMA BY 7700 SDS® TECHNOLOGY

RNA was extracted from 14 cases of chondrosarcoma and reversed transcribed as outlined previously (section 3.2.6 and 3.2.7). c-abl and GAPDH expression were quantitated simultaneously using the previously optimised TaqMan® 7700 SDS assays (section 4.2.2 and 4.2.3). Average Ct values were recorded and Index values calculated using the comparative Ct method as described in section 4.1.4. Amplification plots for GAPDH and c-abl are shown (Figure 4.7 and 4.8 respectively). Table 4.4 summarises the Relative Ratio (Rn) and Delta Ct (ΔCt) value for each case analysed.

Case	Histology Grade	Ave. c-abl Ct	Ave. GAPDH Ct	Rn Value	Δ Ct Value
1	Grade 1, dedifferentiated	30.46	38.13	0.80	-7.67
2	Grade 1, myxoid	31.29	36.61	0.85	-5.33
3	Grade 1	30.77	34.43	0.89	-3.66
4	Grade 1	31.52	33.02	0.95	-1.50
5	Grade 1	33.21	33.29	1.00	-0.07
6	Grade 2	31.63	36.91	0.86	-5.28
7	Grade 2	29.82	33.34	0.89	-3.53
8	Grade 2	32.14	35.51	0.91	-3.37
9	Grade 2	27.47	29.72	0.92	-2.25
10	Grade 3	30.86	31.39	0.98	-0.52
11	Grade 3	30.95	30.31	1.02	0.64
12	Grade 3	32.10	30.85	1.04	1.25
13	Grade 3, cellular	29.75	25.28	1.18	4.47
14	Grade 3, undifferentiated	33.29	28.63	1.16	4.67

Table 4.4 TaqMan® analysis of c-abl expression in chondrosarcoma with resultant average Ct values for GAPDH and c-abl, ΔCt and Rn values. Corresponding Figure 4.7 and 4.8 illustrates amplification plots for GAPDH and c-abl in chondrosarcoma respectively. An inverse relationship exists between Rn and expression levels, i.e. a higher Rn value is indicative of lower c-abl expression.

Index values are assigned to the different grades of tumour using the compartive Ct equation as described in section 4.1.4. The average ΔCt value is calculated for each grade of tumour. $\Delta\Delta$Ct values are then calculated using Grade 1 (average ΔCt) values as the reference value. From this the Index of each grade chondrosarcoma can be calculated. Table 4.5 summarises the results.

Chondrosarcoma	Ave. ΔCt	$\Delta\Delta$Ct	Index
Grade 1	-3.646	0	1.00
Grade 2	-3.6075	0.0385	0.97
Grade 3	2.102	5.748	0.02

Table 4.5 Normalisation of c-*abl* expression in chondrosarcoma using the comparative Ct method. Grade 1 chondrosarcoma is assigned an index value of 1 and is used as the reference population in calculating indices for the other populations (i.e. Grade 2 and Grade 3 chondrosarcoma). Average ΔCt value for Grade 1 tumours is shown to be -3.646, with a standard deviation of 3.017. Based on $\pm$2 standard deviations, the ΔCt of case 13 and 14 (Table 4.4) are deemed to be statistically significant.
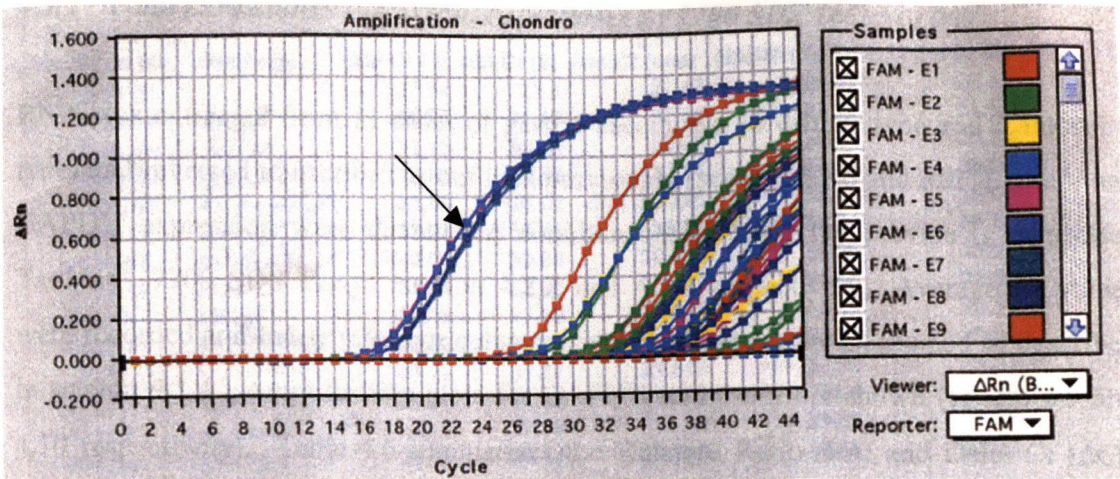
Figure 4.7 TaqMan® amplification plot for GAPDH expression in a series of formalin fixed paraffin embedded chondrosarcoma cases. The arrow points to amplification curves of four HL60 cell line control RNA samples. Remaining amplification plots correspond to samples 1-14 (in triplicate), average Ct values for each sample recorded in Table 4.4.
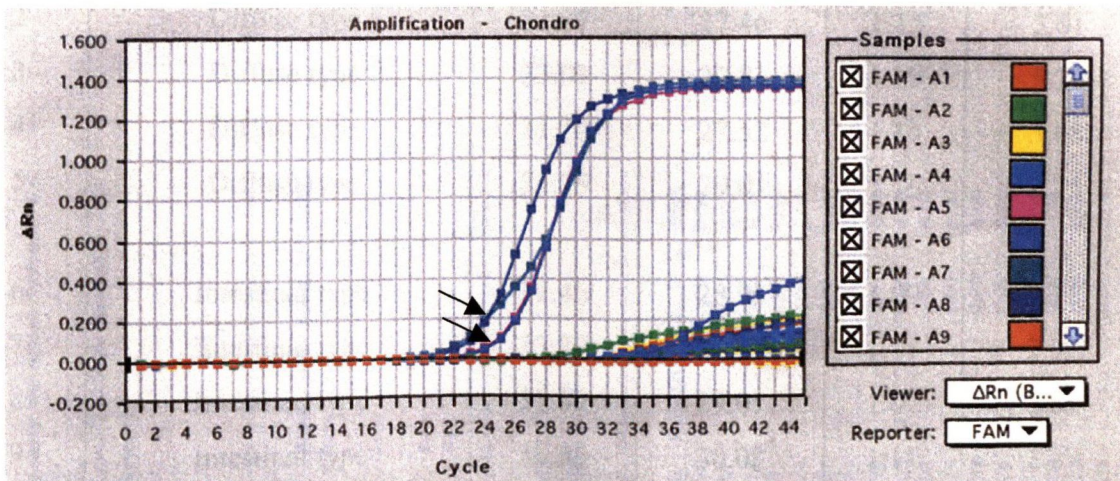
Figure 4.8 TaqMan® amplification plot for c-*abl* expression in a series of formalin fixed paraffin embedded chondrosarcoma cases. Again, the arrows point to amplification curves of four HL60 cell line control RNA samples. Remaining amplification plots correspond to samples 1-14 (in triplicate), average Ct values for each sample recorded in Table 4.4. Due to the high levels of c-*abl* expression in the four control RNAs, the amplification plots appear scaled down in this illustration. In addition, the very low levels of c-*abl* mRNA in the paraffin embedded tissues results in a less steep amplification curve compared to the cell line mRNA extracts.

4.3.2   c-abl EXPRESSION IN GASTRIC CARCINOMA BY 7700 SDS TECHNOLOGY

RNA was extracted from 11 cases of gastric carcinoma (6 diffuse type and 5 intestinal type) and reversed transcribed as outlined previously (section 3.2.6 and 3.2.7). c-*abl* and GAPDH expression were quantitated simultaneously using the previously optimised TaqMan® 7700 SDS assays (section 4.2.2 and 4.2.3 respectively). Average Ct values were recorded and Index values calculated using the comparative Ct method as described in section 4.1.4. Amplification plots for GAPDH and c-*abl* are shown (Figure 4.9 and 4.10 respectively).   Table 4.6 summarises the Relative Ratio (Rn) and Delta Ct (ΔCt) value for each case analysed.

Case	Histology Grade	Ave. c-*abl* Ct	Ave. GAPDH Ct	Rn Value	Δ Ct Value
1	Diffuse type	33.18	28.17	1.18	5.01
2	Diffuse type	31.07	27.46	1.15	3.61
3	Diffuse type	33.01	27.81	1.19	5.20
4	Diffuse type	31.20	27.52	1.15	3.68
5	Diffuse type	31.26	29.01	1.10	2.25
6	Intestinal type	31.46	28.95	1.09	2.11
7	Intestinal type	33.29	30.37	1.11	2.92
8	Intestinal type	31.89	29.01	1.07	2.88
9	Intestinal type	33.35	30.08	1.11	3.27
10	Intestinal type	30.08	32.84	0.93	-2.76
11	Intestinal type	**neg**	**neg**	-	-

Table 4.6 TaqMan® analysis of c-abl expression in gastric carcinoma with resultant average Ct values for GAPDH and c-*abl*, ΔCt and Rn values. Insufficient RNA (**neg**) was extracted from case 11 to detect either c-*abl* or GAPDH mRNA   Corresponding Figures 4.9 and 4.10 illustrate TaqMan® amplification plots for GAPDH and c-*abl* in gastric carcinoma.

Index values are assigned to the tumour cases using the compartive Ct equation as described in section 4.1.4. The average ΔCt value is calculated for each case and ΔΔCt values are then calculated using case 1 as the reference value. From this the Index of each type of gastric carcinoma can be calculated. Table 4.7 summarises the results.

Case	Histology Grade Adenocarcinoma	Δ Ct Value	ΔΔ Ct Value	Index
1	Diffuse type	5.01	0	1.00
2	Diffuse type	3.61	1.40	0.38
3	Diffuse type	5.20	-1.19	1.14
4	Diffuse type	3.68	1.33	0.40
5	Diffuse type	2.25	2.76	0.15
6	Intestinal type	2.11	2.90	0.13
7	Intestinal type	2.92	2.09	0.23
8	Intestinal type	2.88	2.23	0.21
9	Intestinal type	3.27	1.74	0.30
10	Intestinal type	-2.76	7.77	0.005
11	Intestinal type	-	-	-

Table 4.7 Normalisation of c-*abl* expression in gastric carcinoma using the comparative Ct method. Average index value for diffuse type gastric carcinoma is 0.614 (Std. Dev 0.43) compared with an average index value of 0.17 (Std. Dev. 0.11) for intestinal type.
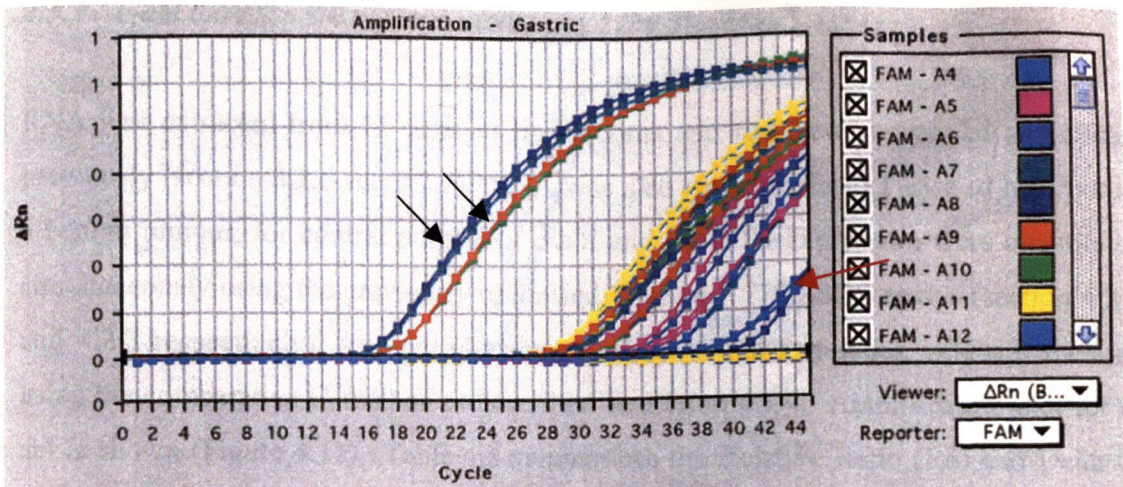
Figure 4.9 TaqMan® amplification plot for GAPDH expression in a series of formalin fixed paraffin embedded gastric carcinoma cases. The black arrows point to amplification curves of four HL60 cell line control RNA samples. Remaining amplification plots correspond to gastric carcinoma cases 1-11 (in triplicate). The average Ct values for each sample recorded in Table 4.6. The red arrow points to the amplification plots for sample 3, which with an average Ct value of 40 is deemed to be a negative result.
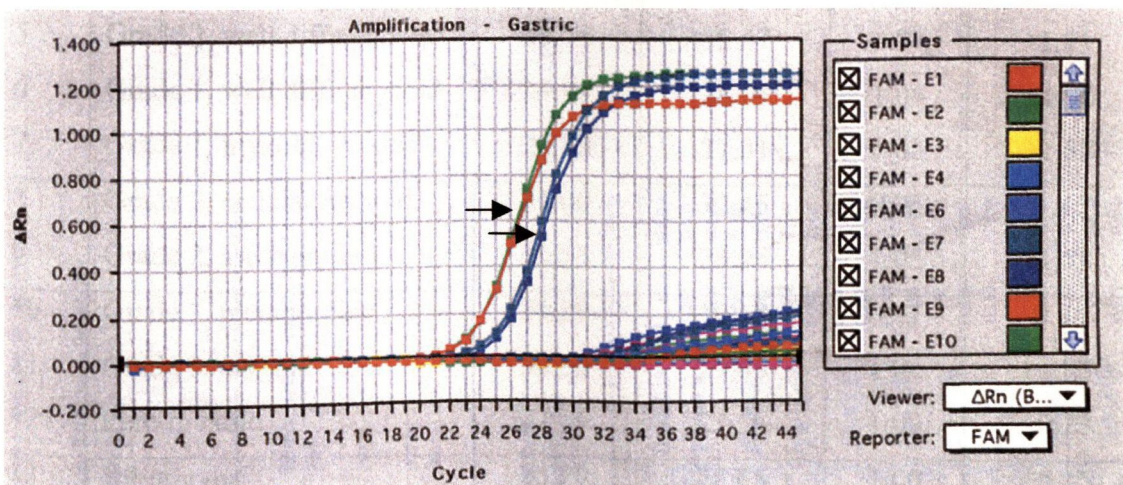
Figure 4.10 TaqMan amplification plot for c-*abl* expression in a series of formalin fixed paraffin embedded gastric carcinoma cases. The black arrows point to amplification curves of four HL60 cell line control RNA samples. Remaining amplification plots correspond to gastric carcinoma cases 1-11 (in triplicate). The average Ct values for each sample recorded in Table 4.6. Again, the scale of the sample amplification plots is minimised due to the high c-*abl* levels in the HL60 cell line RNA.

4.3.3   c-abl EXPRESSION IN LIPOSARCOMA BY 7700 TAQMAN® ASSAY

RNA was extracted from 12 cases of liposarcoma and reversed transcribed as outlined previously (section 3.2.6 and 3.2.7). RNA was also extracted from 1 case of hibernoma, a benign tumour, for control purposes. c-abl and GAPDH expression were quantitated simultaneously using the previously optimised TaqMan® 7700 SDS assays (section 4.2.2 and 4.2.3 respectively). Average C_t values were recorded and Index values calculated using the comparative C_t method as described in section 4.1.4. Amplification plot for c-abl is shown (Figure 4.11). Table 4.8 summarises the Relative Ratio (Rn) and Delta C_t (ΔC_t) value for each case analysed.

Case	Histology Grade	Ave. c-abl Ct	Ave. GAPDH Ct	Rn Value	Δ Ct Value
1	Grade 1, well differentiated	30.11	32.41	0.92	-1.30
2	Grade 1, well differentiated	30.46	33.68	0.90	-3.33
3	Grade 1, well differentiated	31.79	30.08	1.05	+1.71
4	Grade 1, well differentiated	32.33	31.93	1.02	+0.40
5	Grade 1, well differentiated	29.76	32.47	0.91	-2.71
6	Grade 1, well diff., myxoid	29.94	28.04	1.06	+1.90
7	Grade 1, myxoid, vessels	28.89	27.31	1.05	+1.58
8	Grade 2, cellular myxoid	31.00	32.45	0.95	-1.45
9	Grade 2, areas grade 3	30.56	28.98	1.05	+1.58
10	Grade 3, pleomorphic	29.89	30.65	0.97	-0.76
11	Grade 3, myxoid	30.50	29.65	1.02	+0.85
12	Pure myxoid	27.79	27.56	1.00	+0.23
13	Hibernoma	25.20	25.05	1.00	+0.15

Table 4.8   TaqMan® analysis of c-abl expression in liposarcoma with resultant average Ct values for GAPDH and c-abl, ΔCt and Rn values. Corresponding Figure 4.11 illustrates amplification plots for c-abl in liposarcoma.

Index values are assigned to the different grades of liposarcoma using the comparative Ct equation as described in section 4.1.4. The average ΔCt value is calculated for each grade of tumour. ΔΔCt values are then calculated using Grade 1 (average ΔCt) values as the reference value. From this the Index of each grade liposarcoma can be calculated. Table 4.9 summarises the results.

Liposarcoma	Ave. ΔCt	ΔΔCt	Index
Grade 1	-0.23	0	1.00
Grade 2	+0.065	+0.295	0.82
Grade 3	+0.106	+0.129	0.91
Hibernoma	+0.150	+0.380	0.78

Table 4.9 Normalisation of c-*abl* expression in liposarcoma using the comparative Ct method. Grade 1 liposarcoma is assigned an index value of 1 and is used as the reference population in calculating indices for the other populations (i.e. Grade 2 and Grade 3 liposarcoma). Average ΔCt value for Grade 1 tumours is shown to be −0.23, with a standard deviation of 2.168. Based on ±2 standard deviations, the changes in c-*abl* expression indices calculated in Table 4.9 are not deemed to be statistically significant.
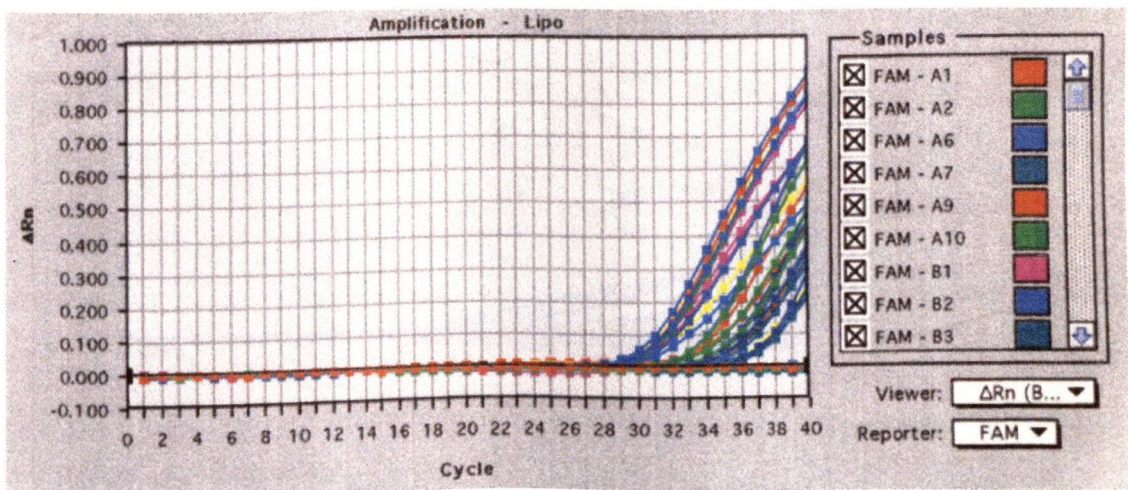
Figure 4.11 TaqMan® amplification plots for c-*abl* expression in formalin fixed paraffin embedded liposarcoma. All samples were assayed in triplicate Average Ct values were calculated using the accompanying SDS® software and are shown in Table 4.8.

4.3.4   ABI PRISM® 310 SEQUENCING OF PCR PRODUCTS

To confirm the sequence of the PCR generated amplicons, PCR products were cloned using the TOPO TA™ cloning kit, Invitrogen Inc.   DNA sequencing is performed using Big Dye terminator chemistry and the ABI PRISM® 310 Genetic Analyser (section 4.2.5).   Each plasmid is sequenced bidirectionally and in triplicate.   The sequence generated from one of the plasmids containing the 'c-*abl* TaqMan insert' is shown in Figure 4.12.   The sequence is then aligned to the known sequence as obtained from the GenBank database to verify the origin of the sequence.

4.3.5   LASER CAPTURE MICRODISSECTION

Individual cells from selected formalin-fixed paraffin embedded tissue sections were micro-dissected using the PixCell™ Laser Capture Microdissection System, Acturus Engineering Inc. (section 4.2.6).   RNA was extracted (section 3.2.6) and amplified for both c-*abl* and GAPDH using TaqMan® RT-PCR (sections 4.2.2 and 4.2.3 respectively). However, there was insufficient mRNA in the extracts to accurately quantify using Real-Time Quantitative RT-PCR.
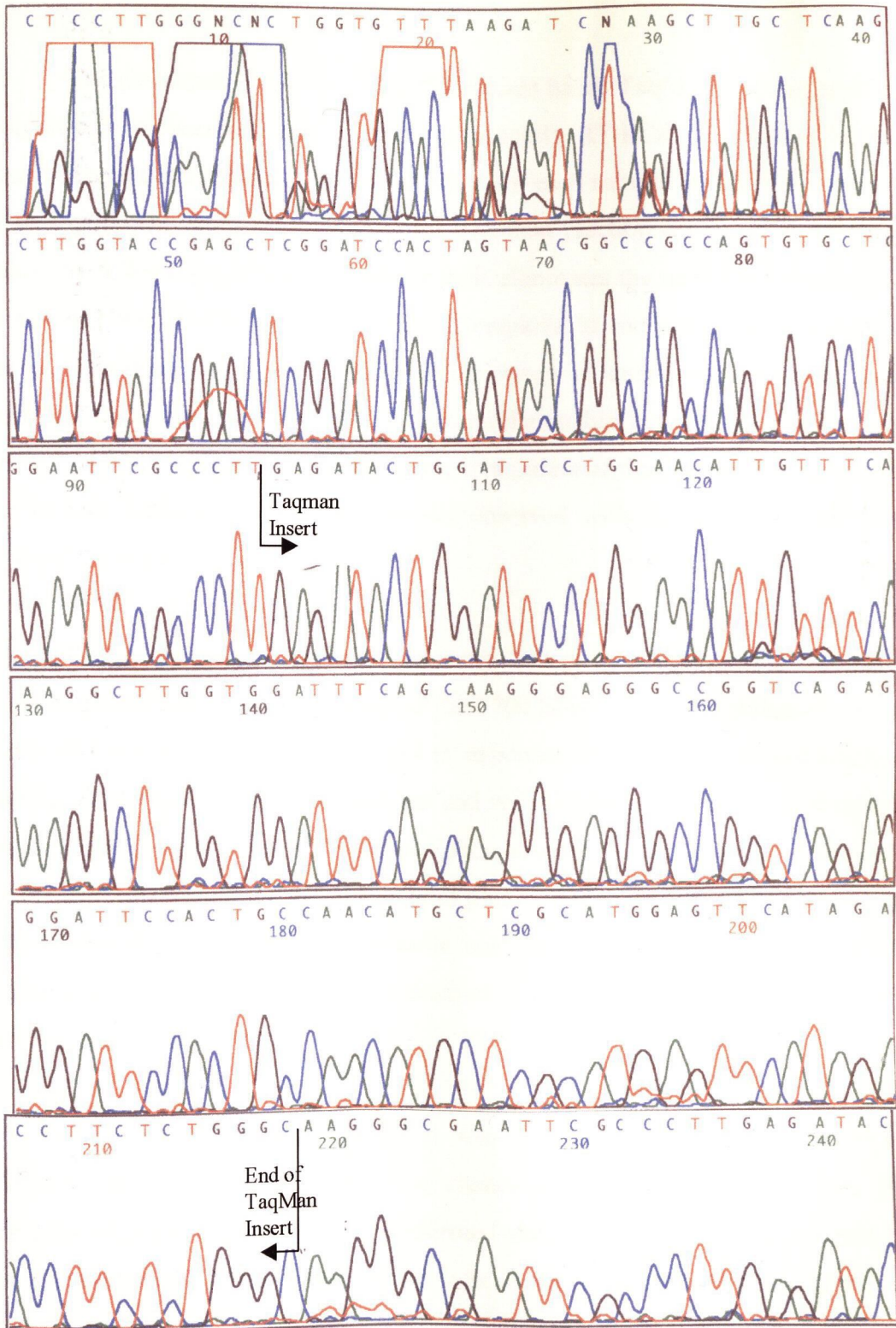
Figure 4.12 Big Dye™ Terminator Sequencing of c-*abl* TaqMan® Product. This figure illustrates the sequencing results obtained from the ABI Prism® 310 Genetic Analyser using the methods described in section 4.2.5.3. All plasmids were sequenced bi-directionally and in triplicate, and results compared to published sequences.

4.4   DISCUSSION

The development of Real-Time fluorescent based TaqMan® Assays represents a significant advancement in the field of quantitative RT-PCR. Real-Time TaqMan® assays record the threshold cycle, or Ct value, for each sample which enables the data to be interpreted using the comparative Ct method (section 4.1.4). Determining Ct values by following real-time kinetics of PCR eliminates the need for a competitor to be co-amplified with the target template. Compared to end-point measurements, the use of Ct values also expands the dynamic range of quantitation because data is collected for every cycle of PCR. A linear relationship between Ct and the initial amount of RNA has been demonstrated for five orders of magnitude, compared to the one or two orders of magnitude typically observed with an end-point assay (ABI PRISM® 7700 SDS data).

The early cycles of the PCR are characterised by an exponential increase in target amplification. A key advantage if the 7700 SDS® is that the threshold cycle is observed when the amplification is still in exponential phase and has not reached a plateau. Thus the Ct is a more accurate and reliable indication of the starting copy number than the amount of PCR product accumulated. As the reaction components are not rate limiting during the exponential phase of the reaction, Ct values are very reproducible for reactions with the same starting gene copy number. Thus, the precision and sensitivity of RNA quantitation is enormously enhanced compared to standard end-point detection.

Using the 7700 SDS® system, it was possible to amplify both c-*abl* and GAPDH mRNA in all fourteen cases of chondrosarcoma studied (Table 4.4). For each case, multiple extractions were performed and analysed, yielding consistent and reproducible results. This is in total contrast to the data obtained using End-Point determinations in which amplification was recorded in only 25% of cases (Table 3.3). Table 4.5 shows normalised c-*abl* expression in each grade of chondrosarcoma. Grade 1 chondrosarcoma are used as the reference population resulting in an index value of 1 for this group. There is little difference between c-*abl* expression in grade 1 and grade 2 chondrosarcoma which have an Index value of 0.97. These two grades

of chondrosarcoma are also relatively close morphologically. Grade 3 chondrosarcoma, however, appears to have significantly reduced levels (Index = 0.02) of c-*abl* mRNA compared to the grade 1 tumours. This correlates specifically with the findings in Chapter 2 in which grade 1 tumours displayed intense staining for the Abl oncoprotein but the more poorly differentiated chondrocytes of grade 3 chondrosarcoma showing minimal and more diffuse Abl expression (section 2.4.2).

In order to perform statistical analysis on the data obtained, the experimental design would have to incorporate multiple RNA extractions (min. n=3) of each sample, and analysis of each RNA in triplicate by TaqMan® RT-PCR. In this study, RNA was extracted from 5 consecutive sections (n=5) of the paraffin embedded tissue of interest. Unfortunately, due to the extremely low concentrations of mRNA in each extraction, it was not possible to perform multiple analyses on each extraction. Consequently, it was not possible to apply the one sided paired Student t-test which is normally used to analyse data generated on the 7700 SDS® system. Based on standard deviation calculations, however, it was possible to determine that at least two of the grade 3 chondrosarcoma had significantly lower c-*abl* mRNA levels than the grade 1 chondrosarcoma.

RNA was successfully extracted and amplified in 10 of 11 cases of gastric carcinoma investigated for c-*abl* expression. Only 8 of these cases could be amplified and detected using end-point assays (Table 3.3). In total, the study comprised 6 cases of diffuse type signet ring carcinoma of stomach and 5 cases of intestinal type gastric adenocarcinoma. The diffuse type signet ring adenocarcinoma show index values ranging from 0.15 to 1.14 (mean 0.614, std. deviation 0.43). This is considerably higher than the index values of intestinal type adenocarcinoma, which range from 0.005 to 0.30 (mean 0.17, std. deviation 0.11). This again correlates with the observations of Abl protein expression in which intense Abl immunoreactivity was observed in diffuse carcinoma of the stomach with weaker Abl staining associated with the intestinal type (section 2.3.5).

The effect of tissue type on RNA yields have previously been discussed and it has been demonstrated that least success was achieved in extracting and amplifying RNA from formalin fixed paraffin embedded liposarcoma (section 3.3.6). End-point

determinations succeeded in detecting c-*abl* mRNA in only 2 of 15 cases (Table 3.3). Using Real-Time 7700 TaqMan® RT-PCR it was possible to amplify c-*abl* in 100% of liposarcoma cases. Data was analysed using the comparative Ct method. No statistically significant difference in c-*abl* expression was noted between the different grades of liposarcoma tumour. This is not surprising given that although there were differences in Abl immunostaining between high and low grade liposarcoma (section 2.3.3), the contrast was not as significant as that observed between the different grades of chondrosarcoma. I have also commented previously on the relatively small number of mature adipocytes per section of liposarcoma, thus limiting the amount of RNA available for extraction. As such, a considerable upregulation of c-*abl* expression in each cell would be required to significantly alter total net c-*abl* measured.

The PCR products generated were cloned into Topo TA™ cloning vectors (Invitrogen Inc.) according to the manufacturers protocol and sequenced on the ABI PRISM® 310 genetic analyser to confirm the specificity of the amplification. Figure 4.12 shows a sample printout from the ABI Prism 310 genetic analyser. In this sample, the plasmid contains an insert of the cDNA generated using a primer set which flank the 'abl TaqMan amplicon'. Sequencing was performed independently using both the forward and reverse sequencing primers from the Invitrogen Topo™ TA cloning kit. Bases are determined by the accompanying Sequence Analysis Software (PE Biosystems). The results confirmed that the c-*abl* product amplified during TaqMan® RT-PCR is as expected for the given primer set used.

In conclusion, Real-Time 7700® TaqMan RT-PCR offers a sensitive, reliable and accurate method of gene quantitation. It has facilitated measurement of c-*abl* mRNA in a series of archival paraffin embedded tissues that could not previously be quantitated using end-point assay systems. I have successfully demonstrated that c-*abl* mRNA is significantly lower in high-grade chondrosarcoma than in low-grade chondrosarcoma. The results support the expression of Abl oncoprotein in chondrosarcoma described in section 2.3.2. I have also shown that c-*abl* mRNA levels are higher in diffuse (signet ring) carcinoma of the stomach relative to intestinal type gastric adenocarcinoma. This is again in keeping with the immunohistochemical staining patterns for Abl protein in this tumour group. In an early part of this study

(section 3..6), liposarcoma proved to be the most difficult tissue from which to extract amplifiable mRNA. Using the 7700 SDS®, we have achieved 100% success in amplifying c-*abl* and GAPDH mRNA from formalin fixed paraffin embedded liposarcoma.

The specificity of the amplification has been verified by sequencing products formed using Big Dye™ terminator sequencing reactions and the ABI PRISM® 310 genetic analyser. It is not possible to sequence TaqMan® assay products directly as the reporter and quencher molecules interfere with the fluorescence dyes used in Big Dye™ terminator sequencing (e.g. Rox, Tamra). Consequently, parallel PCR reactions were run with the omission of the TaqMan® probe and these reaction products were sequenced using the ABI PRISM® 310 instrument. All products were sequenced bi-directionally and in triplicate. Figure 4.12 shows the output data from the sequencing of a c-*abl* TaqMan® amplicon.

The ability to identify the exact contribution of individual cell types to the total mRNA extracted from a tissue section would provide valuable information on cell specific gene expression patterns. Attempts were made to localise c-*abl* mRNA to individual cells using Laser Capture Microdissection (LCM). LCM is based on the adherence of visually selected cells to a thermoplastic membrane, which overlies the dehydrated tissue section and is focally melted by triggering of a low energy infrared laser pulse. The melted area forms a composite with the selected cells, which can then be simply removed by lifting the membrane. Although the laser transiently raises the temperature of the transfer film to 90°C, its energy is absorbed by the film and is poorly absorbed by biological tissue. Nucleic acids and proteins recovered from these cells should not therefore be degraded by heat conduction (Goldstein *et al*, 1998). Unfortunately, analysis of mRNA post-LCM proved unsuccessful in our hands. It is believed that the minute quantities of mRNA from the selected individual cells are lost during the extraction process. This is not unexpected given the very low signals attainable from RNA which has been extracted from two consecutive 10μm sections of formalin fixed paraffin embedded tissues. An alternative method of determining expression of c-*abl* mRNA in specific cell types within a tissue section is

in-situ RT-PCR. It is proposed to further investigate *c-abl* gene expression in tumour cells and the endothelial cells of tumour microvessels using in-cell amplification.

5.   C-*ABL* MRNA DETECTION BY *IN-SITU* RT-PCR

5.1   INTRODUCTION

Thus far, Abl protein expression has been investigated in a variety of normal tissue and tumour types by immunohistochemistry. Staining patterns observed suggest possible roles for Abl in tumour cell differentiation, inhibition of apoptosis and angiogenesis. Real-Time quantitative RT-PCR has enabled us to confirm c-*abl* upregulation at the mRNA level, following extraction of RNA from tissue sections. Of greater significance, however, would be the ability to localise c-*abl* mRNA expression to individual cells within the tissue sections. It is hypothesised that *in-situ* RT-PCR may provide the means by which identification of c-*abl* expression in specific cells can be achieved.

5.1.1   BACKGROUND

Solution phase polymerase chain reaction is a highly specific and sensitive technique for the detection of nucleic acid sequences *in vitro*. It has the ability to amplify single copy genes, which may then be detected by such methods as Southern blotting, agarose gel electrophoresis and TaqMan® PCR. A prerequisite to this methodology is the necessity to extract the nucleic acid from the tissue or biological sample through destruction of the individual cells. In the case of tissues where a mixed population of cells may be present, it is impossible to determine the contribution of each cell type to the total mRNA extracted. Thus a major limitation of solution phase PCR is the inability to visualise and localise amplified product within cellular and tissue specimens. In addition, data previously presented (section 3.4.4) highlights the difficulties encountered in extracting RNA from tissues which have been formalin fixed and paraffin embedded.

In-situ Hybridisation (ISH) can be used to detect both DNA and RNA targets at the cellular level by the hybridisation of a specifically designed nucleotide probe. This technique boasts high specificity and preserves tissue morphology enabling precise localisation of nucleic acids in intact cells. The draw-back with the *in-situ* hybridisation

technique is the relatively low detection limits, the threshold level for non-isotopic ISH estimated to be about 20 copies per cell (Nuovo *et al*, 1991a; Bates *et al*, 1997).

5.1.2   PRINCIPLES OF IN-SITU PCR

The *in-situ* PCR technique allows the polymerase chain reaction to be performed in non-disrupted cells and tissue sections, increasing nucleic acid copy numbers to levels readily detectable by ISH or immunohistochemistry. As a result, the technique offers the combined sensitivity of the PCR with the sub-cellular localisation of ISH using a target specific probe. *In-situ* amplification of RNA templates provides a means by which cytoplasmic message can be localised, permitting evaluation of gene expression in different cells and tissues.   The first person to report a successful PCR *in-situ* hybridisation technique was Dr. Ashley Haase. This pioneering work, which employed radioactive probes, multiple primer pairs and a fixed cell suspension, was described in 1990 (Haase *et al*, 1990). Non-radioactive labels such as biotin, digoxigenin or fluorescein are now taking preference in most laboratories over radioactive labels (^{32}P, ^{35}S), primarily for safety reasons. In general, two different strategies employed for *in-cell* amplification: direct and indirect (Figure 5.1).

5.1.3   DIRECT IN-SITU PCR

Direct *in-situ* PCR involves the incorporation of a label directly into the amplicon during the thermal cycling process. This may be achieved through use of a hapten label attached to a nucleoside analogue (e.g. biotin-11-dUTP, digoxigenin-11-dUTP or fluorescein) or via hapten labelled primers (Figure 5.1). Direct labelling incorporation results in the labelling of all nucleic acids that are synthesised during the PCR process, resulting in high sensitivity and single copy gene detection. It also obviates the need for a hybridisation step. However, incorporation of the hapten-labelled nucleoside into damaged or 'nicked' DNA by Taq polymerase can lead to very high background signals or even false positive results. Using labelled primers does help to reduce this phenomenon but as there is less hapten per PCR product, this method tends to be less

Schematic of *In-Situ* PCR

Sample

↓

Fixation

↓

Pretreatment

Reverse Transcription
of mRNA

↓

cDNA

Direct *In-Situ* PCR	Indirect *In-Situ* PCR	*In-Situ* TaqMan® PCR

Amplification **Amplification** **Amplification**

■ dNTP   or
■ Primer

TaqMan® probe:
R = Reporter Dye (FAM)
Q = Quencher Dye (Tamra)

Probe Hybridisation

Immunodetection

Fluorescent Signal

Immunodetection

Visualisation

Visualisation

Visualisation

Figure 5.1 Principal stages of in-cell amplification techniques

sensitive. Where fluorescein has been incorporated onto the oligonucleotides it has been observed that autofluorescence, which increases with every round of PCR, is difficult to overcome (Embleton *et al*, 1992).

5.1.4   *INDIRECT PCR-ISH*

The indirect method, PCR *in-situ* hybridisation or PCR-ISH, requires amplification of the target sequence in the absence of any labels followed by *in-situ* hybridisation of the amplified product with a labelled probe (Figure 5.1). RT-PCR-ISH refers to the amplification of mRNA sequences, first requiring generation of cDNA (copy DNA) template using reverse transcriptase, followed by a brief fixing of the specimen to maintain localisation of PCR product. The amplicon may then be detected using a suitably labelled probe. The indirect method overcomes the problem of DNA repair and mis-priming, however it may be prone to high backgrounds due to non-specific probe hybridisation.   RT-PCR may be performed in two single steps or using a one-step approach. The former employs a reverse transcriptase enzyme such as MMLV or AMV to generate the cDNA strand from the mRNA template and the cDNA is then amplified using Taq polymerase.   The one-step approach utilises the recombinant *Thermus thermophilus* (rTth) polymerase, which possesses both reverse transcriptase and DNA polymerase activities.   Indirect RT-PCR-ISH generally takes longer than the direct labelling method to perform due to the additional hybridisation and stringent washes which must be performed.

5.1.5   *IN-SITU TAQMAN® PCR*

TaqMan® PCR enables detection of low copy number specific nucleic acid sequences, based on a 5' exonuclease assay system (section 3.1.5.3). Hybridisation of the fluorescently labelled probe within the target sequence occurs in real time and the signal generated is proportional to the quantity of original starting material. Thus *'in cell'* TaqMan® RT-PCR (Figure 5.1) provides a method of measurement of gene expression within cells, once again combining the sensitivity of PCR with the specificity of *in-situ* hybridisation techniques. The generation of fluorescence signal within the cells is

monitored by fluorescent microscopy. Slides must be photographed as soon as possible after thermal cycling as the signal fades with time and fluorophores can diffuse from the cell. This is in contrast to the *in-situ* techniques employing hapten labels such as dig-11-dUTP in which the slides can be stored long term without any signifcant fading of signals.

Using these methods of direct *in-situ* RT-PCR, RT-PCR-ISH and in-cell TaqMan® RT-PCR, it is proposed to localise c-*abl* expression to individual cells within formalin fixed paraffin embedded tissue sections.

5.2 MATERIALS & METHODS

5.2.1 CELL PREPARATION

Tissue culture cells or other single cell suspensions can be used for *in-situ* RT-PCR. Cells must be washed twice in 1X PBS, pH7.4. The cells are the resuspended in 1X PBS, pH7.4 at a concentration of 2×10^6 cells/ml. Approximately 25µl of cell suspension is added to each area of the slide using a micropipette and spread evenly across the surface of the slide. Alternatively, cell cytospins can be prepared. The slides are allowed to air-dry in a laminar-flow hood. Cells are then fixed and permeabilised using ORTHO PermeaFix (ORTHO Diagnostic Systems) according to the following protocol:

- Slides are incubated in 1X ORTHO PermeaFix for 90min

- The following washes must then be performed:
    40%v/v ethanol   x 30min
    60%v/v ethanol   x 30min
    80%v/v ethanol   x 30min
    100%v/v ethanol   x 30min

Slides are stored in 100%v/v ethanol at −70°C for up to one month until ready for staining. Slides must be allowed to air-dry fully before applying PCR mix.

5.2.2 FROZEN SECTIONS

Frozen sections (6µm) are cut and mounted on APES coated PE *In-Situ* PCR glass slides. Sections are washed twice in sterile 1X PBS, pH7.4 at 4°C to remove all traces of the embedding medium (OCT compound). This material binds many of the detection reagents and normally results in very high backgrounds. Sections may be fixed and permeabilised in ORTHO PermeaFix as outlined in section 5.2.1. Alternatively, sections can be fixed in 4%w/v paraformaldehyde in PBS for 30min. After fixation, slides are rinsed in 1X PBS, pH7.4 for 5min. Slides are then immersed in 0.1M Tris-HCl, pH7.2 containing 0.25%v/v Triton X-100 for 5min. Sections are

digested with 0.4mg/ml proteinase K for 15 min at 37°C. Slides are then washed in 0.1M Tris-HCl, pH7.2 for 5min. Slides are briefly immersed in 20%v/v aqueous acetic acid at 4°C for 15sec. Once again, slides are washed in 0.1M Tris-HCl, pH7.2 for 5min. Finally, slides are rinsed in two changes of DEPC treated water for 10min each.

5.2.3 *PARAFFIN-EMBEDDED TISSUES*

'Cross-linking' fixatives such as formalin or paraformaldehyde necessitate considerable pretreatment of tissue sections before they become permeable to PCR reagents. The following steps are those that permit reagent entry to the cells while also favouring preservation of morphology and retention of signal:

- Sections (6μm) are cut onto APES coated *In-Situ* PCR glass slides (PE Biosystems)
- Slides are incubated on a hotplate for 1hr at 50°C and then overnight in a dry oven, again at 50°C, to achieve maximum section adhesion
- The following washes are performed at room temperature unless otherwise stated:

  - Xylene (2x10min)
  - 100%v/v ethanol (2x5min)
  - 75%v/v ethanol (2min)
  - 50%v/v ethanol (2min)
  - 0.1%v/v DEPC water (5min)
  - 0.2M HCl (10min)

  (At this point, the Proteinase K solution (300μg/ml) should be prepared and and pre-heated to 37°C)

  - 1X PBS, pH7.2 (2min)
  - 0.01%v/v Triton X-100 (2min)
  - 1X PBS, pH7.2 (2min)
  - Proteinase K solution (18.5min at 37°C)
  - 0.2%w/v glycine (5min)

- • 1X PBS, pH7.2 (15min)
- • 20%v/v acetic acid (15sec)
- • 0.01%v/v DEPC water (2 x 10min)
- Slides must be allowed to air-dry fully before applying PCR mix

5.2.4 PROBE GENERATION

DNA probes can be generated using previously optimised solution phase PCR conditions and a labelled nucleotide analogue such as biotin-11-dUTP or dig-11-dUTP (Enzo Diagnostics Inc.). Dig-11-dUTP is used as a substrate for Taq DNA polymerase and reverse transcriptase (AMV and MuLV) and can replace dTTP in nick translation reactions and in random primed DNA labelling (Feinberg *et al*, 1983). The PCR reaction should contain a ratio of 35% dig-11-dUTP and 65% dTTP. Separation of unincorporated nucleotides from labelled probes can be achieved using a simple ethanol precipitation step.

5.2.5 AMPLIFICATION

The concentrations of many of the reagents in the amplifying solution for RT-PCR *in-situ* hybridisation differ greatly to those for solution phase RT-PCR. The enzyme buffer is the exception with the same concentration used for both techniques. The following is the approximate composition of the amplifying solution, which must be further optimised for each primer set or individual assay:

$Mn(Oac)_2$	1.0-5.0mM
Buffer (1X)	50mM Bicine, 115mM potassium acetate, 40%w/v glycerol, pH8.2
dNTP's	200-400μM
Primers	0.2-1.0μM each
EZrTth	5-10U/50μl reaction

Sufficient mastermix is prepared to enable 50μl to be added to each well of the slides.

5.2.6 MASTERMIX COMPOSITION FOR IN SITU RT-PCR: ABL (A+C) PRIMERS

Reagent	Stock Conc.	Volume	Final Conc.
Forward Primer (MWG Biotech)	30pmol/µl	2µl	0.24µM
Reverse Primer (MWG Biotech)	30pmol/µl	2µl	0.24µM
5X rTth Buffer (PE Biosystems)	5X	10µl	1X
EZrTth Polymerase (PE Biosystems)	2.5U/µl	3µl	7.5U
dNTP mix	*	8µl	100µM
Manganese Acetate (PE Biosystems)	25mM	7µl	3.5mM
SF dH$_2$O	-	18µl	-
Final Volume	-	50µl	-

Table 5.1 Mastermix composition for in-situ RT-PCR using Abl (A+C) Primers

*Labelled dNTP mix prepared as follows:

    12µl x 2.5mM dATP

    12µl x 2.5mM dGTP

    12µl x 2.5mM dCTP

    8µl x 2.5mM dTTP

    4µl x dig-11-dUTP (1nmol/µl, Boehringer Mannheim)

*Unlabelled dNTP mix prepared as follows:

    12µl x 2.5mM dATP

    12µl x 2.5mM dGTP

    12µl x 2.5mM dCTP

    12µl x 2.5mM dTTP

5.2.6.1 Thermal Cycling conditions for *In situ* RT-PCR: Abl (A+C) primers

Slides are reverse transcribed at 58°C for 45min and denatured for 1min at 94°C. This is followed by 25 cycles of 94°C for 45sec, 58°C for 45sec and 72°C for 1min. A final elongation step of 72°C for 3min is then performed before holding slides at 4°C until ready for detection.

5.2.7 MASTERMIX COMPOSITION FOR IN SITU TAQMAN® RT-PCR: ABL TAQMAN® PRIMERS

The optimal reaction component concentrations for *in-situ* TaqMan® RT-PCR using the c-*abl* primer and probe set are given in Table 5.2 The reactions are performed using a one-step approach employing the EZrTth polymerase enzyme.

Reagent	Stock Conc.	Volume	Final Conc.
Forward Primer	10pmol/µl	2µl	0.42µM
Reverse Primer	10pmol/µl	2µl	0.42µM
5X rTth Buffer	5X	10µl	1X
EZrTth Polymerase	2.5U/µl	3µl	7.5U
dNTP's (A, G, C & U)	2.5mM each	8µl	100µM
Manganese Acetate	25mM	7µl	3.5mM
TaqMan® Probe	5µM	1.5µl	150nM
SF dH$_2$O	-	16.5µl	-
Final Volume	-	50µl	-

Table 5.2 Mastermix composition for in-situ TaqMan® RT-PCR. All reagents supplied by PE Applied Biosystems, U.K.

5.2.8 THERMAL CYCLING CONDITIONS FOR IN SITU TAQMAN® RT-PCR: C-ABL TAQMAN® PRIMER AND PROBE SET

Slides are reverse transcribed at 58°C for 45min and denatured for 5min at 94°C. Samples are then subjected to 25-30 cycles of 94°C for 15sec followed by 60°C for 60sec. Slides are held at 4°C until ready for detection.

5.2.9   SIGNAL DETECTION

Following thermal cycling, the amplicover clip/discs are disassembled and the slides transferred to preheated 2X SSC at 37°C for 10min followed by 5min in 4X SSC at room temperature. Slides that have undergone in situ TaqMan® RT-PCR are rinsed in DEPC treated water and mounted in 25µl of a water-based fluorescent microscopy mounting medium. In order to preserve fluorescence for short-term storage, slides can be wrapped in tinfoil and stored at 4°C in the dark. Slides which have been labelled directly with dig-11-dUTP or have still to undergo a probe hybridisation step need to be dehydrated through graded alcohols: 50%v/v ethanol (2min), 75%v/v ethanol (2min) and 100%v/v ethanol (5min). Allow slides to air-dry before applying the probe hybridisation mixture or detection reagents.

5.2.9.1   Probe Hybridisation (RT-PCR-ISH)

Ideally, sections should be covered with 50µl of a labelled oligonucleotide probe (section 5.2.4) at a concentration of 1-1.5ng/ml. Probes are prepared in hybridisation (Blotto) buffer containing:

1ml	4%w/v dried milk powder in distilled water
5ml	5%w/v dextran sulphate
2ml	20X SSC
2ml	Distilled water
10ml	Formamide

The probe should be applied directly onto sections and coverslipped to prevent evaporation. Slides are placed onto a preheated hot plate and incubated at 90-95°C for 10min to denature both probe and target. The slides can then be transferred to a humidified chamber and incubated overnight at 37-42°C.

5.2.9.2   Post-hybridisation Washes

Following removal of the coverslips, the sections are subjected to a series of stringent washes:

2X SSC	at RT for 10min
2X SSC	at 60°C for 10min
0.2X SSC	at 55°C for 5min
0.2X SSC	at 42°C for 5min
0.1X SSC	at RT for 5min

This is followed by 10min incubation in blocking buffer (5%w/v BSA in 0.1M Tris-HCl, pH9.5, 0.1M NaCl, 50mM, $MgCl_2$).

5.2.9.3 Detection of digoxigenin-labelled probes

Slides are incubated in alkaline-phosphatase conjugated anti-digoxigenin antibody (Boehringer Mannheim, diluted 1/600 in TBT) for 30min at room temperature. Two washes in TBS for 5min each are then performed. Signals are developed using Sigma *FAST*™, Fast Red TR/Napthol AS-MX Alkaline Phosphatase substrate tablets, for 10min and washed under running tap water for 10min. Finally, slides are coverslipped with aqueous mountant and viewed by light microscopy.

5.3 RESULTS

5.3.1 IN-SITU RT-PCR IN HL60 CELLS

In-situ RT-PCR techniques were successfully applied to HL60 leukemic cells which had been fixed and permeabilised in ORTHO PermeaFix™ as outlined in section 5.2.1. Direct incorporation of dig-11-dUTP during amplification of c-*abl* is illustrated in Figure 5.4. The signal specificity is confirmed by the absence of staining in the corresponding negative control (Figure 5.2). Indirect *in-situ* RT-PCR was also performed on HL60 cells using a digoxigenin labelled c-*abl* specific probe (section 5.2.4). Optimisation of the cell permeabilisation step is critical to ensure entry of the labelled probe, without resulting in diffusion of PCR products from the cells. Figure 5.3 shows c-*abl* expression in HL60 cells by indirect *in-situ* RT-PCR. The absence of any background staining confirms the target specificity of the dig-labelled c-*abl* probe.

5.3.2 IN-SITU RT-PCR IN FORMALIN-FIXED PARAFFIN EMBEDDED TISSUES

Application of the direct and indirect *in-situ* RT-PCR techniques to formalin-fixed paraffin embedded tissues required the addition of numerous tissue pre-treatment steps (section 5.2.3). Despite extensive optimization however, these additional steps often proved detrimental to tissue morphology and adherence to the PCR slides. In practice, results could only be generated on formalin-fixed paraffin embedded tissues using the direct labeling method. c-*abl* mRNA was detected in breast carcinoma cells and tumour microvessels using direct *in-situ* RT-PCR (Figures 5.5 & 5.7). c-*abl* mRNA was also detected in the villi of early (6-7wks) placenta (Figure 5.6), in the nuclei of mature adipocytes of well-differentiated liposarcoma (Figure 5.8) and arterial endothelial cells in gastric carcinoma (Figure 5.9).

5.3.3 IN-SITU TAQMAN® RT-PCR

In-situ TaqMan® RT-PCR (section 5.2.8) was successfully performed on HuVec endothelial cells which had been fixed and permeabilised in ORTHO PermeaFix™ (section 5.2.1). Maximum signal intensity was observed after 30 cycles of PCR (Figure 5.10, panel D). Subsequent cycles result in quenching of the fluorescence signal due to the close proximity of the reporter and quencher molecules within the cell. Once again, this technique proved extremely difficult to transfer onto formalin-fixed paraffin embedded tissues. The repeated thermal cycling of tissues resulted in considerable auto-fluorescence within the tissue sections, which made it impossible to accurately interpret the results (data not shown). Consequently, in-cell TaqMan® RT-PCR proved unsuitable for the detection of c-*abl* mRNA in formalin-fixed tissues for the purpose of this study.

Figure 5.2   c-*abl* mRNA expression in HL60 cells by direct labelling *in-situ* RT-PCR: negative control.
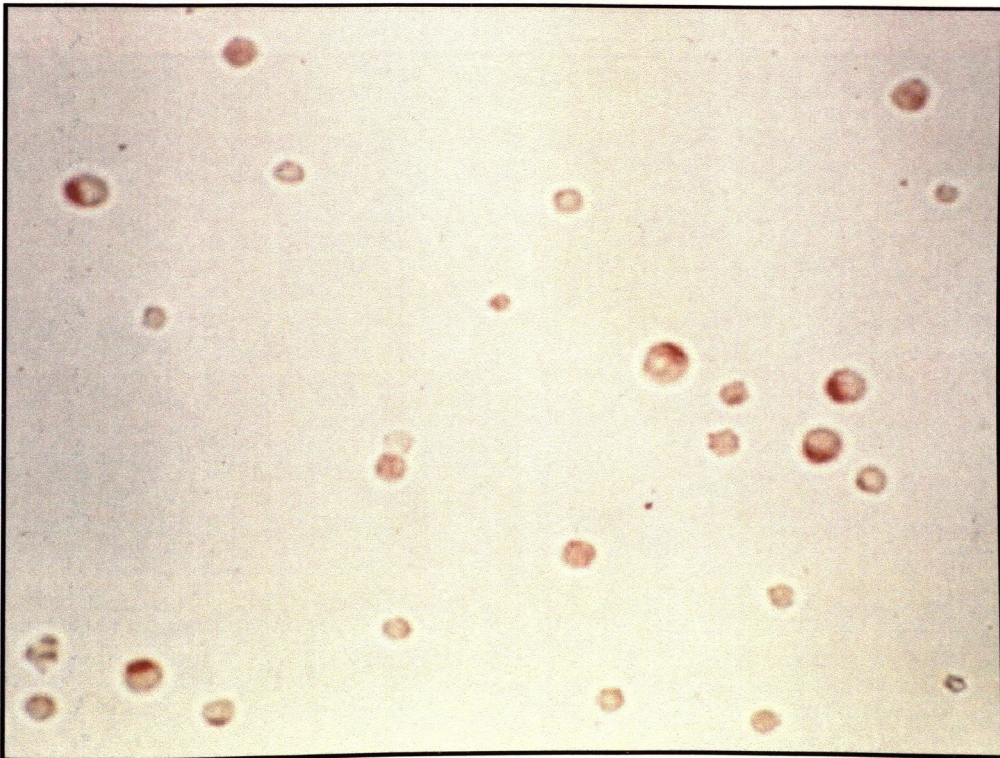
Figure 5.3   c-*abl* mRNA expression in HL60 cells by indirect RT-PCR-ISH using a digoxigenin labelled probe.
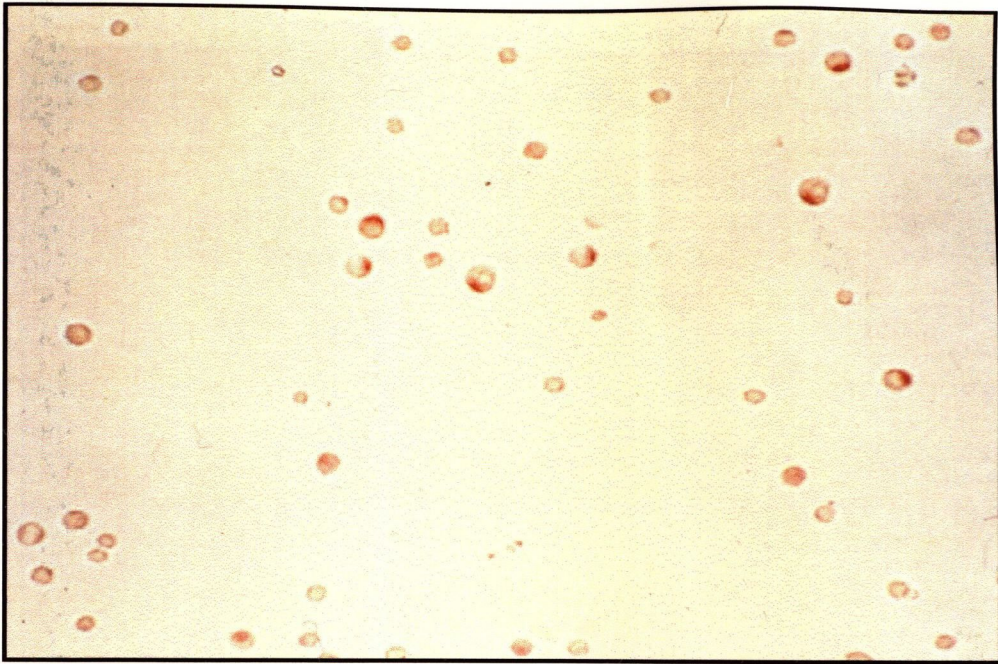
Figure 5.4   c-*abl* mRNA expression in HL60 cells by direct labelling *in-situ* RT-PCR, using dig-11-dUTP (Boehringer Mannheim).
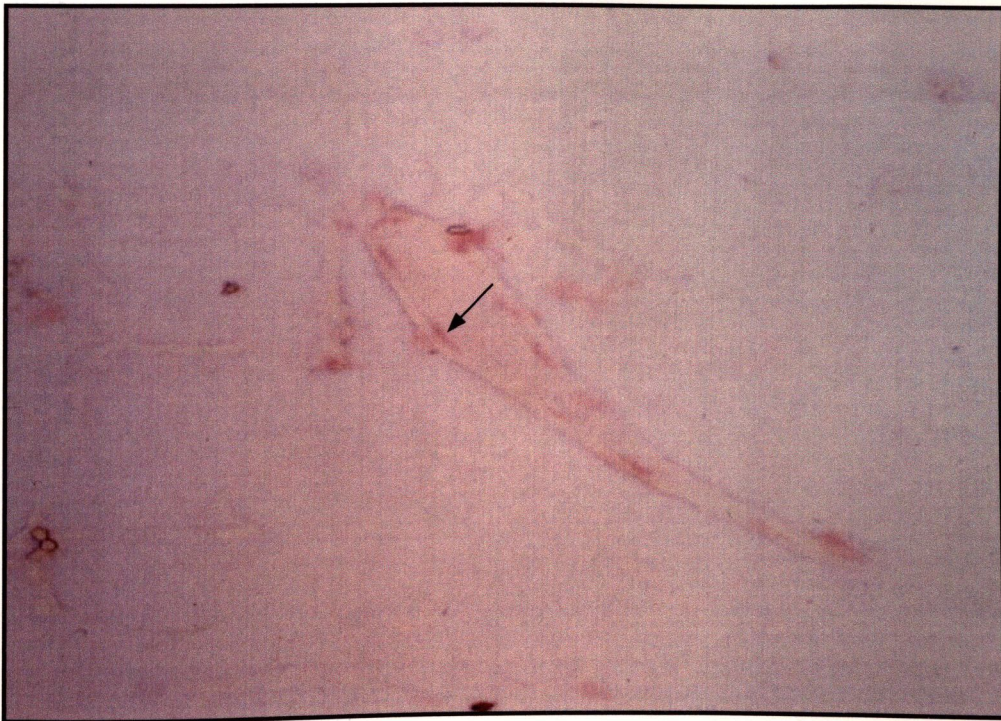
Figure 5.5   Localisation of c-*abl* mRNA expression to the endothelium of a tumour microvessel in breast carcinoma. Arrow indicates nuclear staining in endothelial cells.
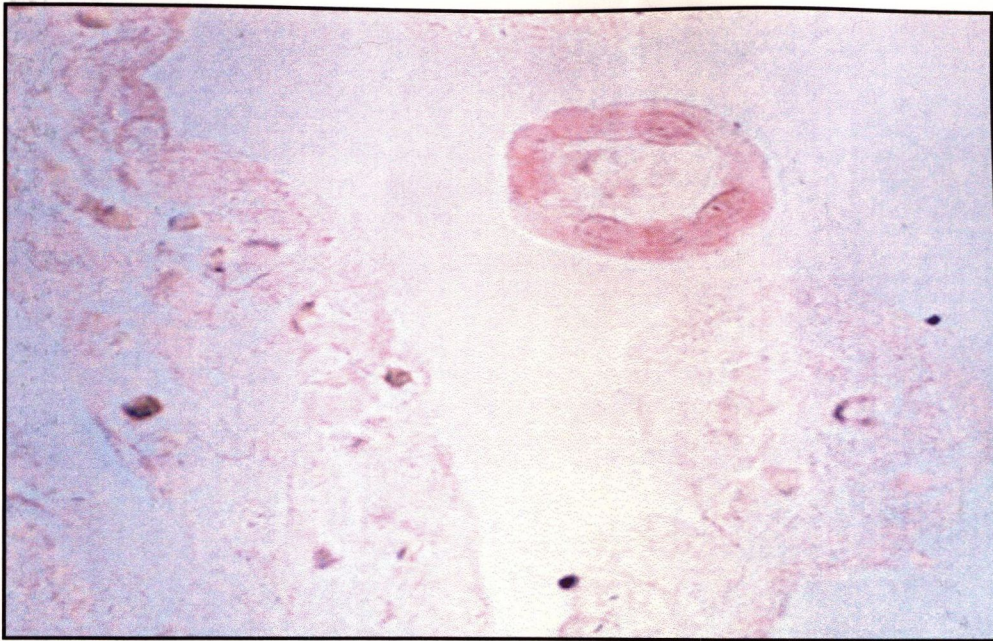
Figure 5.6   c-*abl* mRNA expression human placenta.   Intense nuclear staining is observed in villus of early placenta (7wks)
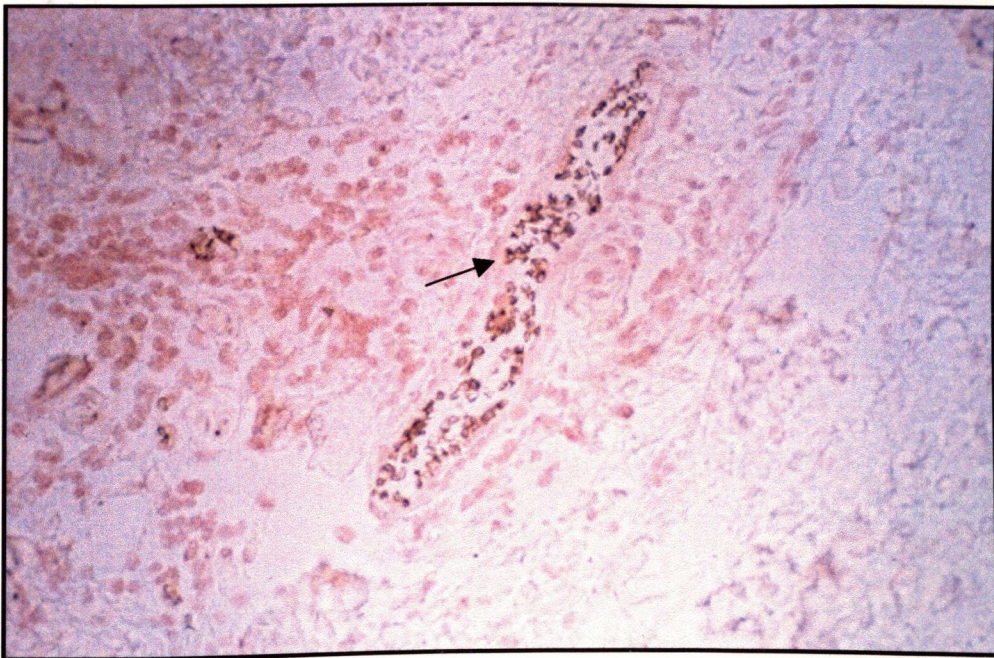
Figure 5.7   c-*abl* mRNA expression in nucleus of breast carcinoma tumour cells. There is weak staining of the endothelial cells of the tumour microvessel (arrow).
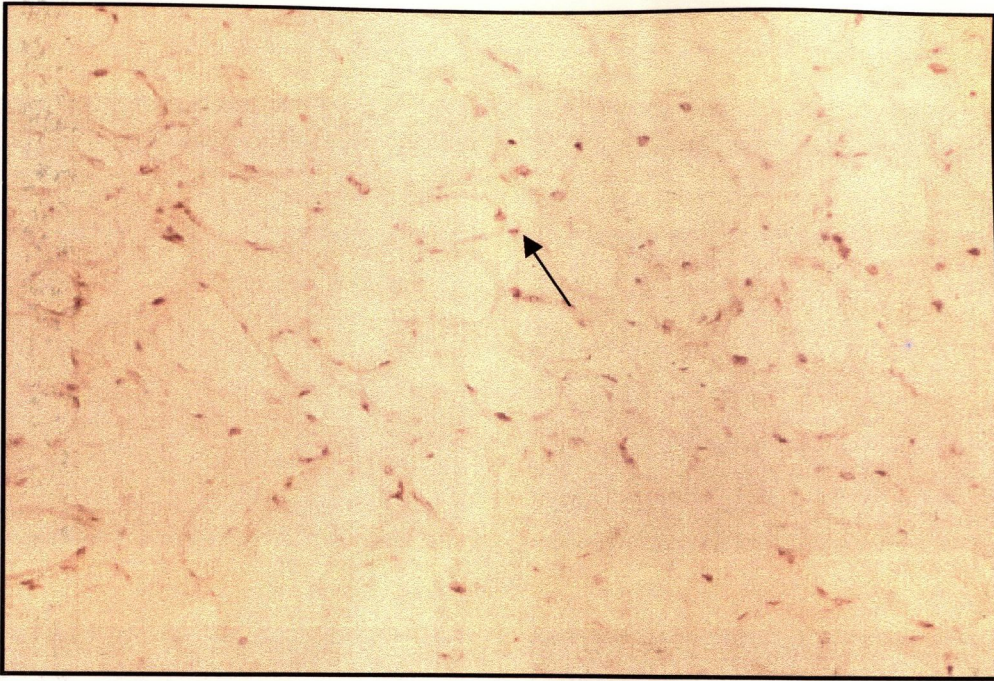
Figure 5.8 c-*abl* mRNA expression in well differentiated liposarcoma using direct labelling *in-situ* RT-PCR. Arrow indicates nuclear staining of mature adipocytes.
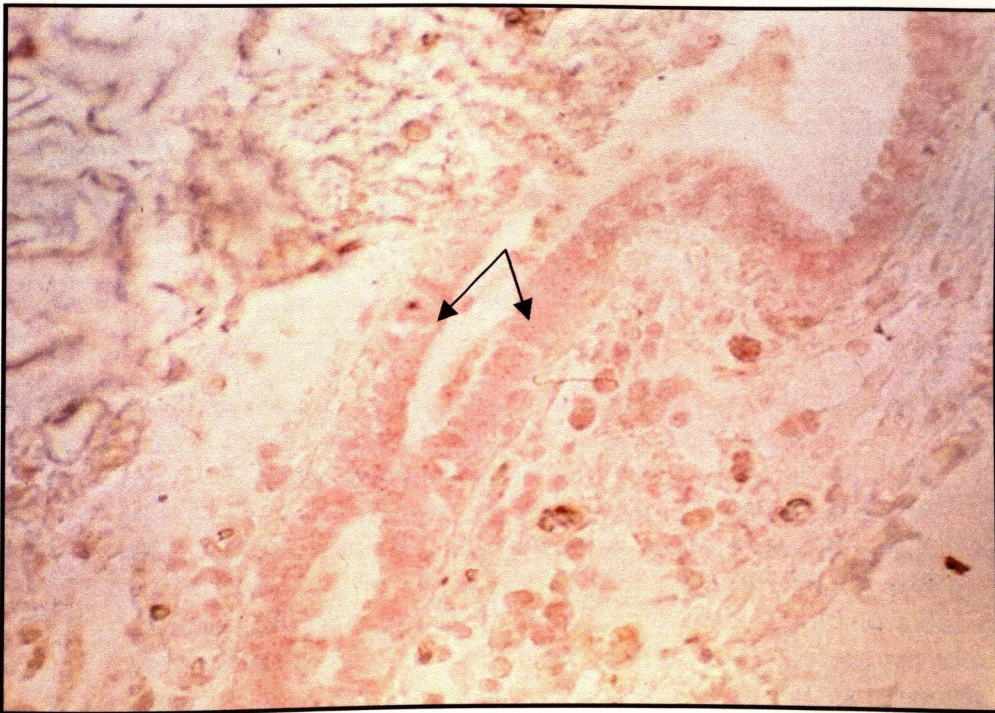
Figure 5.9 c-*abl* expression in gastric carcinoma by direct *in-situ* RT-PCR. Localisation of c-*abl* mRNA to arterial endothelial cells.
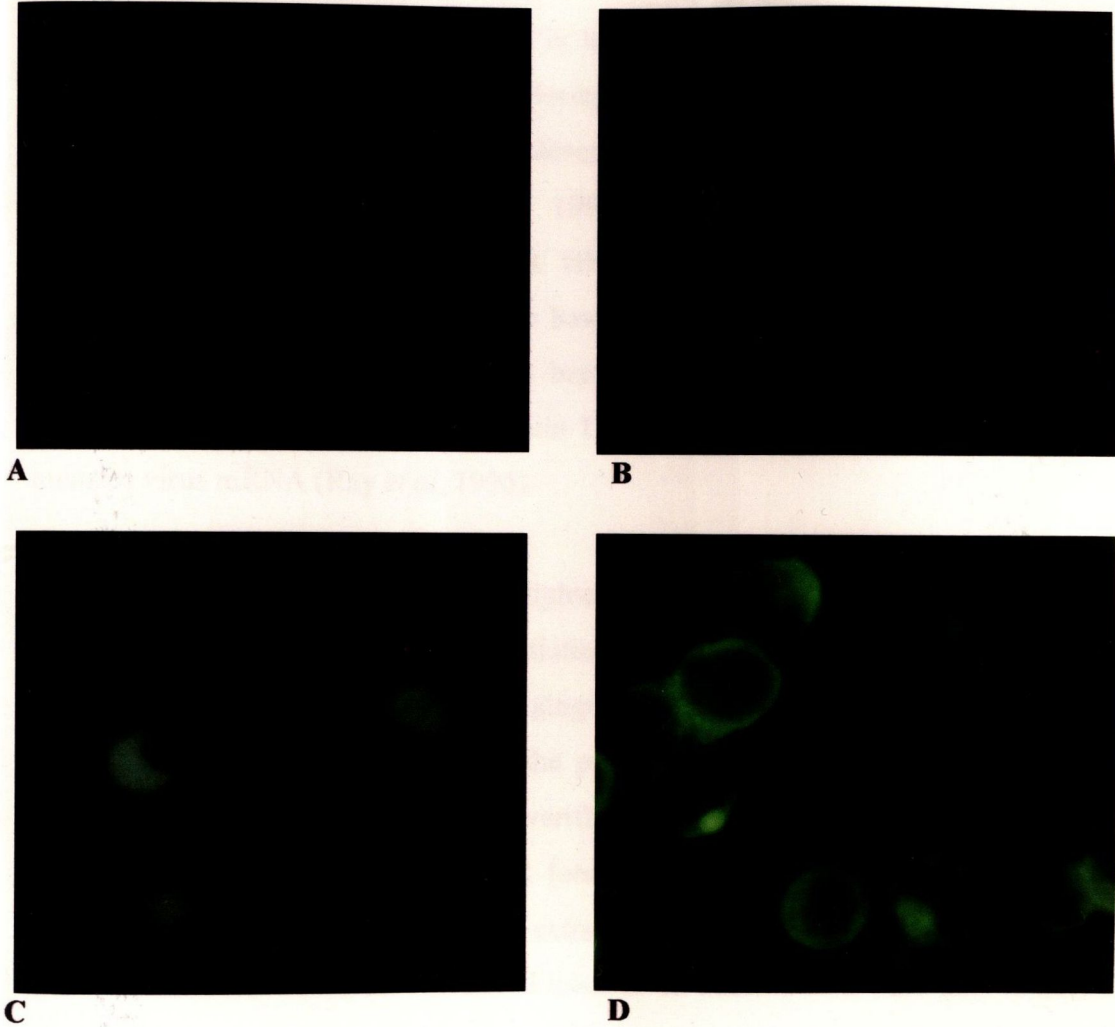
Figure 5.10   c-*abl* expression in HuVec endothelial cells by *in-situ* TaqMan® RT-PCR
        A.   Negative control, omission of Taq® polymerase
        B.   Fluorescence signal after 20 cycles of TaqMan® RT-PCR
        C.   Fluorescence signal after 25 cycles of TaqMan® RT-PCR
        D.   Fluorescence signal after 30 cycles of TaqMan® RT-PCR
After 30 cycles, the close proximity of released reporter and quencher molecules due to the spacial confines of the cell, results in a decrease in signal intensity due to quenching. Diffusion of fluorescent molecules from the cell is also observed. The results show that, as expected, c-*abl* mRNA is predominantly localised to the nucleus of endothelial cells.

5.4 DISCUSSION

The ability to detect target sequences within individual cells and within sub-populations of cells is a valuable tool in the study of cell specific gene expression, latent viral infections and in the monitoring of disease progression. Various *in-situ* PCR methods have been successfully described for the detection of DNA sequences including lentivirus (Haase *et al*, 1990), hantavirus (Nuovo *et al*, 1996), papillomavirus (O'Leary *et al*, 1994), HHV-8 (O'Leary *et al*, 2000) and KSHV (Boshoff *et al*, 1995). Although there have been fewer reports for the detection of RNA sequences, *in-situ* RT-PCR has been described for pyruvate dehydrogenase mRNA (Uhlmann *et al*, 1998b), vitamin D receptor mRNA (Mee *et al*, 1997) and measles virus mRNA (Ray *et al*, 1996).

Data previously presented highlighted variations in c-*abl* mRNA expression in some tumour cells, during cell differentiation and apoptosis and in the neovasculature during enchondral ossification and angiogenesis. Localisation of differential c-*abl* expression was initially described at the protein level using immunohistochemistry (section 2.2.7.4). Subsequent studies verified these observations at the mRNA level by solution phase TaqMan® RT-PCR (section 4.4). However, Chapter 3 clearly outlines the difficulties encountered in extracting and successfully amplifying mRNA from formalin-fixed paraffin embedded tissues. In addition, the data fails to address the contribution of each cell type in a tissue section to the overall levels of c-*abl* mRNA measured. Of particular interest to this study was the possibility of detecting c-*abl* message in the endothelial cells of tumour microvessels. Given the limited sensitivity of existing *in situ* hybridisation techniques, it was hypothesised that *in-situ* RT-PCR might provide a more sensitive alternative for detecting c-*abl* mRNA transcripts in tissue sections.

Although there are many publications on the technique, *in-situ* RT-PCR on paraffin wax-embedded material remains difficult, labour intensive and technically challenging. It seems that no universally applicable protocol is available and considerable optimisation of reaction conditions is required. A key step in the procedure is controlled proteinase treatment to permeabilise cells, permitting entry of

higher concentrations of primers, Magnesium and/or DNA polymerase when compared to traditional PCR protocols (section 5.2.5). The use of "PermeaFix" for cell fixation and permeabilisation, the use of rTth DNA polymerase and an exon junctional primer approach, all help to reduce the time required to perform in cell RNA amplification.

One possible criticism of IS-RT-PCR is that, as amplification is required to detect mRNA, the original levels of transcripts are insignificant with respect to cellular function and any positive results are therefore meaningless. However, previous evidence (Komminoth et al, 1992a; Uhlmann et al, 2000; O'Leary et al, 2000) has suggested that amplification is not as efficient as that obtained in conventional SP-PCR and follows a more linear amplification of template.

Accurate interpretation and meaningful comparisons of the results obtained from different published in-situ PCR protocols require adequate consideration of technical difficulties including type of starting material, quality and type of target sequence, amplification system, detection system and the use of adequate controls. Uhlmann et al, 1998a, provide a comprehensive review of in cell amplification techniques and give expert analysis of the stages involved, problems encountered and controls required.

Figures 5.3 – 5.4, demonstrate that c-abl mRNA has been successfully amplified in-situ in the HL60 leukemia cell line using both the indirect and direct labelling methods respectively. Evidently, the permeabilisation step is sufficiently optimised to ensure entry of reagents into the cells without resulting in diffusion of PCR products from the cells. The negative controls show no signal for both the direct and indirect labelling techniques (Figure 5.2). High background staining would not be expected in cell lines if the cells have been fixed correctly, as there should be little degradation or 'nicks' in the nucleic acids. The absence of staining in the control for ISH method would indicate that the digoxigenin labelled Abl probe generated (section 5.2.4) displays a high level of specificity for its target sequence.

Figure 5.10 shows c-abl mRNA expression in endothelial cells by TaqMan® RT-PCR. Target amplification is monitored by fluorescent microscopy at five cycle

intervals. Nuclear localisation of c-*abl* is clearly evident after 20 cycles of PCR (Figure 5.10, B), with signal intensities increasing over the next 10 cycles (Figure 5.10, C+D). The optimal number of cycles depends on the individual assay, although where possible cycle number is kept to a minimum in order to prevent diffusion problems and preserve tissue or cell morphology. In addition, as the cycle number increases, the proximity of the free reporter and quencher molecules within the limited volume of the cell increases and can lead to a reduction of signal strength.

Once the amplification and detection methods had been fully optimised on cell lines, the three different strategies were then applied to formalin-fixed paraffin embedded tissues (section 5.2.3). Despite extensive optimisation of tissue pre-treatment steps, extreme difficulty was encountered in preserving tissue morphology and preventing tissue sections from lifting off the slides during the thermal cycling process. This was particularly true in the cases of chondrosarcoma and liposarcoma. Insufficient protease digestion resulted in reaction failure, yet increased digestion was at the expense of morphology. *In-cell* TaqMan® RT-PCR proved unsuitable for use on formalin-fixed paraffin embedded tissues due to an unacceptable signal-to-noise ratio. This was due to the high levels of autofluorescence within the tissue sections, which increased with thermal cycling. The direct labelling technique proved most successful in our hands, due to the fact that the slides did not have to be subjected to the additional processing steps incurred during the ISH stages. However it must be noted that non-specific incorporation of nucleotides by *Taq* polymerase into damaged DNA is undoubtedly a major contributor to false positive results using the direct *in-situ* RT-PCR technique.

The results obtained demonstrate that we have successfully detected c-*abl* mRNA in breast cancer cells and in the adjacent endothelial cells of a tumour microvessel (Figure 5.7). We have also demonstrated intense nuclear staining for c-*abl* in the villi of early placental villi (Figure 5.6), a finding which is in keeping with the intense c-Abl protein expression in develeloping endothelium and connective tissues in placenta at 7wks. (section 2.3.6). In gastric carcinoma, it was possible to detect c-*abl* mRNA in the endothelium of blood vessels as illustrated in Figure 5.9. Possibly the most striking evidence of c-*abl* mRNA in endothelial cells is seen in Figure 5.5 which illustrates strong nuclear staining for c-*abl* in the endothelial cells of

a tumour microvessel in breast carcinoma. Overall, the results serve to validate, at the molecular level, that c-*abl* is upregulated in certain tumour cell types, during cellular differentiation and in endothelial cells during tumour angiogenesis.

6. IN-VITRO ASSESSMENT OF C-*ABL* EXPRESSION IN HUVEC ENDOTHELIAL CELLS

6.1 INTRODUCTION

Angiogenesis is the process which results in the formation of new blood vessels. In normal life, angiogenesis plays a vital role in reproduction, embryogenesis, menstruation and wound healing and repair. Under normal physiological conditions, vascular endothelial cells are quiescent and the process of angiogenesis is strictly controlled (Hobson *et al*, 1984; Chavakis & Dimmeter, 2002). A significant body of work indicates that neoplastic lesions must develop angiogenic ability to progress. Its importance was first recognised by Folkman in 1971, when he suggested that the continued growth of tumours was dependent on angiogenesis. Without neovascularization, solid tumours would grow only until passive diffusion was unable to provide the tumour cells with the necessary conditions for proliferation. In the absence of angiogenesis, tumour spheroids *in vivo* only grow to a size of approximately 2mm (Gimbrone *et al*, 1972; Beecken *et al*, 2002). Further growth does not occur unless the spheroids become vascularised. However, this hypothesis has recently been challenged (Pezzella *et al*, 2001) with evidence that if a tumour can obtain a sufficient nutrients from the existing blood supply then it could grow without the need for production of new vessels. This has important implications in the design of anti-angiogenic therapies for the treatment of both primary tumour growth and metastatic spread.

Receptor tyrosine kinases and their ligands have important roles in the regulation of normal and tumour angiogenesis. Following specific stimuli, endothelial cells have the ability to re-enter the cell cycle, dissolve their underlying basement membrane, proliferate and migrate to form capillary outgrowths projecting into the surrounding tissue (Mustonen & Alitalo, 1995). A number of tyrosine kinases may contribute to angiogenesis and/or endothelial cell function including vascular endothelial growth factor (VEGF), fibroblast growth factor receptor (FGFR) and platelet derived growth factor receptor β (PDGFRβ), which are all widely expressed (Kolibaba & Druker, 1997; Rosen, 2002). Others such as TIE (tyrosine kinase with immunoglobulin and epidermal growth factor homology domains; Partanen *et al*, 1990) and TEK (tunica internal endothelial kinase; Dumont *et al*, 1992) are expressed predominantly in endothelial cells. However, despite the

apparent importance of tyrosine kinases in angiogenesis, no particular role for c-Abl in angiogenesis has been identified to date.

I have presented evidence that the Abl oncoprotein is selectively expressed in physiological angiogenesis, during early placental villi and in the proliferating vessels during enchondral ossification. We have also demonstrated intense Abl expression in tumour microvessels of liposarcoma, breast carcinoma and gastric adenocarcinoma. The results support a previously undescribed role for Abl as either a direct or an indirect modulator of angiogenesis. It is proposed to examine expression of c-*abl* in endothelial cells following exposure to a number of external stimuli.

c-Abl tyrosine kinase activity is tightly regulated *in vivo*. c-Abl can be triggered by stimuli such as DNA damaging agents (Kharbanda *et al*, 1995a; Liu *et al*, 1996) and integrin mediated cell adhesion (Lewis, 1996). An important factor of c-Abl activation is cell cycle arrest: overexpression of c-Abl blocks cell cycle G_1/S transition (Sawyers *et al*, 1994) and cells with compromised c-Abl function have deregulated cell cycle (Daniel *et al*, 1996). Another important factor of c-Abl activation is induction of apoptosis. Overexpression of c-Abl induces apoptosis, and c-Abl is apparently required for DNA-damage induced apoptosis (Yuan *et al*, 1997, 1998 & 1999).

Cells exposed to ionizing radiation and other DNA damaging agents respond with activation of c-Abl (Kharbanda *et al*, 1995(a), (b) & 1996; Liu *et al*, 1987; Yoshida *et al*; 2002). The activation of c-Abl in response to genotoxic stress is associated with the interaction of c-Abl with the p53 protein, and its homolog p73, in the G1 arrest response (Yuan *et al*, 1999). Signals downstream of c-Abl activation include induction of the stress-activated proapoptotic SAPK/JNK and p38 mitogen-activated protein kinase (Kharbanda *et al*, 1995b; Pandey *et al*, 1996). One issue concerning the genotoxic stress response is how DNA damage is converted into informational intracellular signals that effect behaviour. In a potential feedback mechanism, c-Abl phosphorylates and inhibits DNA-PK activity (Kharbanda *et al*, 1997). In addition, it has been demonstrated that c-Abl interacts with the ATM gene and that ATM may be responsible for the activation of c-Abl in response to genotoxic stress (Baskaran *et al*, 1997; Shafman *et al*, 1997). It was proposed to expose HuVec

endothelial cells to heat shock and serum deprivation to determine the effect on expression of c-*abl*.

The DNA-PK and ATM are related to members of the phospatidylinositol-3 (PI-3) kinase family (Hartley *et al*, 1995) involved in cell cycle control and DNA repair. PI-3K is tyrosine phosphorylated, and subsequently activated, by various RTKs and receptor-associated PTKs. PI-3K is a heterodimeric protein containing an 85 kDa and 110 kDa subunits. The p85 subunit contains SH2 domains that interact with activated receptors or other receptor-associated PTKs and is itself subsequently tyrosine phosphorylated and activated. The 85 kDa subunit is non-catalytic, however, it does contain a domain homologous to GTPase activating (GAP) proteins. It is the 110 kDa subunit that is enzymatically active. PI-3K associates with and is activated by, the PDGF, EGF, insulin, IGF-1, HGF and NGF receptors.

Studies have shown that c-Abl phosphorylates p85 and thereby inhibits PI-3K activity in the apoptotic response to DNA damage (Yuan *et al*, 1987). Wortmannin has been shown to have an inhibitory effect on PI-3 kinase at nanomolar concentrations (Arcaro *et al*, 1993), with a reported IC_{50} value between 1 and 10nM (Woscholski *et al*, 1994). BCR/ABL binds to adaptor proteins Grb-2 and Shc resulting in p21ras activation and also activation of the PI 3-kinase pathway. In this way BCR-ABL could influence the expression of genes belonging to the PI 3-kinase family such as ATM and DNA-PKcs (Skorski *et al*, 1992). Wortmannin, a potent inhibitor of the p110 catalytic subunit of PI3-kinase, inhibits proliferation of Ph[+] cell lines and colony formation by CML primary cells (Skorski *et al*, 1995). Inhibition of PI3K blocks proliferation of BCR-ABL-dependent cells, establishing the importance of PI3K for BCR-ABL activity.

A recent study, (Manna *et al*, 2000) has shown that the inhibitory effect of wortmannin is found not to be cell type-specific. Wortmannin has also been reported to inhibit a number of other kinases (Bonser *et al*, 1991; Cross *et al*, 1995) but only at concentrations greater than those reported to inhibit PI 3-kinase (100nM range). It is proposed to investigate the effect of wortmannin on c-*abl* expression in endothelial cells by TaqMan® RT-PCR.

The production of reactive oxidative species (ROS) is a natural by-product of cellular metabolism. The cellular response to genotoxic stress includes release of mitochondrial cytochrome C and then induction of apoptosis (Kharbanda *et al*, 1997; Takeyama *et al*; 2002). Sun *et al*, 2000(b), demonstrates that the cytoplasmic but not nuclear c-Abl is activated in COS7 cells by treatment with reactive oxidative species. In addition, cytoplasmic H_2O_2 induces cytochrome C release by a c-Abl dependent mechanism. Recent work has shown that c-Abl phosphorylates protein kinase C (PKC) δ in COS7 cells treated with H_2O_2 (Sun *et al*, 2000(a)). It is proposed to investigate the effect of reactive oxidative species on c-*abl* mRNA and c-Abl kinase activity in endothelial cells using TaqMan® RT-PCR and phosphotyrosine immunoblotting respectively.

The presence of the c-Abl protein in the neovasculature during enchondral ossification and in tumour microvessels was an unexpected and significant finding. The aim of this part of the study was to investigate more fully the events leading to c-Abl upregulation in endothelial cells *in vitro*. A number of external stimuli were investigated including heat shock, serum deprivation, reactive oxidative species (H_2O_2) and wortmannin. The secretion of a number of growth factors and other by-products of metabolism from tumour cells themselves may play a role in the modulation of c-Abl in adjacent endothelial cells. To investigate this, endothelial cells were cultured in media from a number of tumour cell lines and the effect on c-Abl expression established.

6.2   MATERIALS & METHODS

6.2.1   SOURCE OF CELL LINES

Cell lines were obtained from the European Collection of Animal Cell Cultures (ECACC), Porton Down, Salisbury, UK, as outlined in Table 6.1.

Designation	Source	Number	Description	Medium
CRL-1596.2	ECACC	U-937	Histiocytic Lymphoma	RPMI 1640
ECV304	ECACC	HuVEC	Human Endothelial	Medium 199
K562	ECACC	K562	Leukemia, Human Myeloid	RPMI 1640
HL60	ECACC	HL60	Leukemia, Human	RPMI 1640

Table 6.1   Designated cell lines, source and media used for *in vitro* studies.

6.2.1.1   Initiation of Cultures

Upon receipt, frozen cultures are stored in liquid nitrogen vapour phase until ready for use. The vial is thawed by gentle agitation in a 37°C water bath or incubator. Thawing should be rapid (less than 2min). Vials are decontaminated by spraying with 70%v/v ethanol. Cells are added to sterile universal and 10ml resuscitation medium (culture medium + 10%v/v FCS) is added drop-wise on ice. The cryoprotective agent is removed by centrifuging cells at 125g for 5min. Supernatant is discarded and the pellet resuspended in 1ml resuscitation media. An appropriate volume of fresh medium is added and cells transfered to an appropriate size vessel.

6.2.1.2   Maintenance of Cell Cultures

Cells are maintained in tissue culture flasks at 37°C in 5%v/v CO_2 and inspected daily by phase contrast microscopy. Depending on seeding densities, cells are split every 2-4 days or harvested for experimental purposes. Once the adherent cell lines become confluent they are trypsinised in 1X trypsin EDTA. Cells must first be rinsed in serum free media as B.S.A. is known to inhibit the activity of trypsin. Cells are incubated in the trypsin for 15min at 37°C or until the cells have detached from the base of the flask. 5ml of growth media containing B.S.A. is added to each flask to halt the activity of the trypsin and prevent cell damage. The contents of each flask are pelleted by centrifugation at 1200g for 10min and cell number and viability assessed as outlined in section 6.2.1.3.

6.2.1.3   Enumeration of Cells and Cell viability

Ethidium bromide and acridine orange staining (EB/AO) staining (Lee *et al*, 1975) is employed to assess cell viability and number. Cells are pelleted by centrifugation at 1200g for 8min and resuspended in an appropriate volume of culture medium. Cells are mixed with EB/AO dye solution (1.6μg/ml EB and 0.4μg/ml AO in 0.1M PBS pH7.3) in a 1:2 ratio and immediately loaded under a coverslip on a Neubauer haemocytometer (Hudson and Hay, 1976). Fluorescent cells are viewed using a Leitz Dialux 20 EB microscope with UV filter. Under UV light viable cells fluoresce green due to the presence of EB while non-viable cells emit red fluorescence due to the presence of AO.

6.2.2 *ISOLATION OF PROTEINS FOR PROTEIN TYROSINE PHOSPHORYLATION ASSAY*

Approximately 5×10^6 cells per sample are harvested by centrifugation at 600g for 5min. Cell pellets are washed in PBS, pH7.2, containing 1mM sodium orthovanadate and centrifuged for 5min at 600g. The supernatant is discarded and the cell pellet is resuspended in 100μl ice-cold lysis buffer (1X, New England BioLabs Inc.). Lysates are incubated on ice for 20min and then centrifuged at top speed for 10min. Following centrifugation, the supernatant should be removed and transferred to a fresh tube. Samples can be frozen and stored at −70°C for up to two weeks.

6.2.3 ISOLATION OF RNA FOR TAQMAN® RT-PCR ANALYSIS

Total RNA is extracted from cell lines using the QIAshredder unit and RNeasy Mini Kit (Qiagen Ltd.) as described in section 3.2.2. All extractions are performed in triplicate. RNA samples are stored at -70°C in RNase free water.

6.2.4 PREPARATION OF CELL SMEARS FOR IMMUNOHISTOCHEMISTRY AND IN SITU RT-PCR ANALYSIS

Cell are washed twice in 1X PBS, pH7.4 at 37°C centrifuged for 5min at 600g. Pellets are resuspended in 1X PBS, pH7.4 at a concentration of 2×10^{6}cells/ml. Approximately 25µl of cell suspension is applied directly onto either APES coated glass microscopy slides (*Select* Propper Ltd) or APES coated PE *In-Situ* PCR glass slides. Alternatively, cell cytospins can be prepared. Slides can be left to air-dry in a laminar flow hood.

6.2.5 BRADFORD ASSAY FOR PROTEIN DETERMINATION

A stock B.S.A. solution at a concentration of 10mg/ml is prepared in dH$_2$O. From this, a 1:100 dilution in dH$_2$O is prepared giving a working stock of 100µg/ml B.S.A. A range of B.S.A. standards (0-50µg/ml) are prepared in duplicate in dH$_2$O. At this point, 500µl of each standard is added to 500µl of Bradford reagent (Sigma) and mixed thoroughly. Standards (100µl) are pipetted in duplicate into a 96 well plate and the absorbance measured at 595nm. Absorbance readings must be taken within 60min of addition of the Bradford Reagent.

6.2.6 MOLECULAR WEIGHT STANDARDS AND SAMPLE PREPARATION FOR SDS-PAGE

Molecular Weight (Kaleidoscope Prestained) standards were obtained from Bio-Rad, the composition of which is given in Table 6.2

Protein	Molecular Weight (Da)
Aprotinin	7,600
Lysozyme	17,000
Soybean trypsin inhibitor	32,000
Carbonic anhydrase	43,800
Bovine serum albumin	86,000
β-galactosidase	132,000
Myosin	212,000

Table 6.2 Composition of molecular weight standards for SDS-PAGE

Protein samples for SDS-PAGE are isolated as outlined in section 6.2.2. Samples and standards are resuspended in an equal volume (check) of 1X sample buffer (composition) and aliquoted in 20µl volumes. Incubate at 95°C in a water bath for 5-10min and then centrifuge briefly to precipitate any dissolved solids. Samples and standards can be stored at –20°C until required.

6.2.7 *PREPARATION OF SDS-PAGE GELS*

Glass plates should be washed thoroughly with 100%v/v ethanol to remove traces of proteins, which might interfere with the running of the gel, and are allowed to air-dry. The composition of the gel mix is dependent on the molecular weight of the protein(s) of interest, however in this case a 10%w/v gel is sufficient.

Component	Resolving Gel (ml)	Stacking Gel (ml)
30%v/v Acrylamide mix	13.3	1.3
1.5M Tris, pH8.8	10.0	-
1.0M Tris, pH6.8	-	1.0
Distilled water	15.9	5.5
10%w/v SDS	0.4	0.08
10%w/v Ammonium persulfate	0.4	0.08
TEMED	0.016	0.008

Table 6.3 Composition of 10%w/v SDS-PAGE Gel mix (sufficient for 4 gels).

The APS solution must be prepared fresh on a daily basis. The APS and TEMED are added last with gentle swirling as excessive agitation incorporates oxygen which inhibits polymerisation. The resolving gel is first poured into the cast and covered in a layer of water-saturated butanol preventing contact with oxygen. Gel polymerisation takes up to 1hr at room temperature. The butanol water is poured off and the top of the gel washed with water until no traces of butanol remain. Stacking gel is then prepared as in Table 6.3 and each cast filled to overflowing and a clean comb inserted into the polymerising gel. Stacking gel polymerisation takes up to 30min. Before electrophoresis, the comb, rubber seal and clips are removed. Unpolymerised gel is removed by gently rinsing the wells with distilled water, and the wells are straightened using a gel-loading tip.

6.2.8 WESTERN BLOT MEASURE OF PROTEIN TYROSINE PHOSPHORYLATION

Protein concentration in each sample is determined using a standard Bradford assay (Bradford, 1976). Equal amounts of protein (40-50µg) are loaded onto a 10%w/v SDS-polyacrylamide gel and run at 80V through the stacking gel and 120V through the resolving gel. The proteins are transferred onto PVDF membrane using a wet transfer gel apparatus. The gel is first equilibrated in transfer buffer (25mM tris, 192mM glycine, 10%v/v methanol) for 15min at room temperature. PVDF membrane is cut to size and soaked in 100%v/v methanol for 15sec, washed in UPH$_2$O for 2min before soaking in transfer buffer for 5min. The transfer sandwich is assembled and proteins transferred at 30V, 90mAmp overnight at 4°C with constant agitation of the transfer buffer using a stirring bar. Once the transfer is complete, the PVDF membrane and gel are processed seperately. Efficiency of transfer can be assessed by Coomassie staining the gel post transfer (section 6.2.8.1). The membrane is blocked for 2hr at room temperature with TBS containing 5%w/v fatty acid free BSA. After blocking, the membrane is washed in two changes of TBST for 2min each. Membranes are probed at room temperature for 2hr with anti-phosphotyrosine primary antibody (PT-03, Calbiochem), diluted 1/100 in TBST containing 1%w/v fatty acid free BSA. Three further washes in TBST are performed (2x5min, 1x10min). Membranes are then probed with secondary biotinylated antibody (goat anti-mouse IgG, diluted 1/1000 in TBST containing 1%w/v BSA) for 1hr at room

temperature. Wash membranes 2x5min, 1x10min, 2x5min in TBST, followed by a final wash in TBS for 5min. Enhanced Chemiluminescence Detection (ECL, Amersham) is used to visualize the cross-reacting bands.

6.2.8.1 Coomassie Blue Staining of PAGE Gel

The stacking gel is removed and the resolving gel placed in a plastic tray containing 0.1%w/v Coomassie Blue R-250 and allowed to stain overnight at room temperature. Approximately 10 volumes of stain per gel are recommended. After staining is complete, excess stain is removed by diffusion destaining. The destaining solution (40%v/v MeOH, 7%v/v Acetic Acid, 53%v/v H_2O) is renewed until an acceptable level of background is achieved. Destained gels can be stored in sealed plastic bags containing 7%v/v acetic acid.

6.2.8.2 Ponceau S Staining

Equal protein loading per well and even transfer to the membrane may be verified by briefly staining the membrane in Ponceau S stain, immediately after transfer and before any antigen detection takes place.

6.2.8.3 Enhanced Chemiluminescence Detection (ECL)

Membranes are blocked with 1%w/v BSA in PBS/Tween for 1hr with mixing on a platform. The membrane is rinsed briefly in two changes of PBS/Tween, and then one wash of 15min and two of 5min in fresh changes of the wash buffer. Following incubation with appropriate primary and secondary antibodies (section 6.2.8), blots are washed in two changes of PBS for 15min each. ECL detection kits (Amersham) are then used to detect signals. Briefly, solutions A and B are mixed in a 1:40 ratio, and 5ml placed on thmembranes for up to 10min. Membranes are placed face down in cling film, any air bubbles carefully excluded and the membrane carefully wrapped. Expose blots to X-ray film (Sigma) for 5-30sec. Exposed films are then developed, fixed and allowed to air-dry.

6.2.9 C-abl REAL-TIME 7700SDS TAQMAN® ASSAY

The TaqMan® assay is as described in section 4.1.2. However, the introduction of the PE Applied Biosystems Universal TaqMan® Mastermix considerably simplifies sample set-up (Table 6.4). Incorporation of AmpErase® uracil N-glycosylase and dUTP provide protection against carryover contamination.

Component	Concentration/Volume
c-*abl* Forward Primer	300nM
c-*abl* Reverse Primer	300nM
c-*abl* TaqMan® Probe	100nM
Universal Mastermix (2X)	12.5µl
cDNA	2µl
dH$_2$O	As required
Final Volume	25µl

Table 6.4 c-*abl* TaqMan® Assay set-up using Universal Mastermix (PE Applied Biosystems)

6.2.10 STATISTICAL ANALYSIS OF ABI PRISM 7700 SDS® DATA

All samples analysed on the ABI Prism 7700 SDS® were performed in triplicate. Relative quantitation data can be statistically analysed using one-sided test as described by Walpole and Meyers in "Probability and Statistics for Engineers and Scientists", Macmillan Publishing, 1972. The formula is:

$$\textbf{Test} = (x1 - x2) - TS\left(sqr(1/n1 + 1/n2) \right)$$

Where: x1 = mean of group 1

x2 = mean of group 2

T = t value

$S = sqr\left(\left((n1\text{-}1)S1^2 + (n2\text{-}1)S2^2 \,/\, (n1 + n2 - 2) \right)\right.$

Sqr = square root

n1 = number in group 1

n2 = number in group 2

S1 = standard deviation of group 1

S2 = standard deviation of group 2

If the result of the equation is less than or equal to zero, then the observed differences are not considered to be statistically significant. In other words, the likelihood that the results were caused by a significant event cannot be distinguished from the likelihood that the results were merely the result of random variation in the assay. If the result is found to be greater than zero, the differences are considered statistically significant.

6.3 RESULTS

6.3.1 CONTROL GENE EXPRESSION

c-*abl* expression in a series of samples (section 2.2) was assessed using the 7700 SDS®. Expression of three different proposed control genes: Glyceraldehyde-3-phosphate dehydrogenase (GAPDH), β-2-microglobulin (β2M) and human phosphoglycerokinase (PGK), was also examined in these samples by 7700 TaqMan® RT-PCR. The raw data is shown in Figure A2.1 and A2.2 (Appenix A2). Table 6.5 summarises the Index value calculated for each sample using the comparative Ct method of analysis (section 4.1.4). The statistical significance of the results is determined using a one-sided paired T-test as described previously (section 6.2.9).

SAMPLE	CONTROL GENE		
	GAPDH	(β2M)	PGK
H$_2$O$_2$ treated endothelial cells	1.058[*]	1.055[#]	1.031[*]
H$_2$O$_2$ control	0.561[*]	0.619[#]	0.471[*]
Serum deprived endothelial cells	1.038	1.143	1.004
Serum control	1.322	1.391	1.208
Heat shocked endothelial cells	1.092	0.991	0.941
Heat shock control	1.434	0.769	1.210

Table 6.5 Evaluation of endogenous reference genes for use in TaqMan® Assays. Table 6.5 shows c-*abl* Index values normalised against three different proposed house keeping genes. [*]Results are statistically significant, i.e. there is a significant increase in c-*abl* expression in endothelial cells treated with 1.0mM H$_2$O$_2$ for 30min, using either GAPDH or PGK as controls. [#]The result obtained using β2M as control is not statistically significant, due primarily to a lot of variation between replicates (raw data in Appendix A2). All other results show no changes in c-*abl* expression between treated cells and untreated controls, regardless of housekeeping gene used to normalise results. Corresponding Figure 6.1 illustrates the c-*abl* TaqMan® amplification plots in these six test samples.

Using the same data, it is possible to confirm that GAPDH expression is unaffected by the selected experimental treatments by normalising the GAPDH Ct against PKG Ct values. Table 6.6 shows GAPDH indices calculated using the comparative Ct method using PKG as the reference.

SAMPLE	GAPDH (INDEX)
H_2O_2 treated endothelial cells	1.13
H_2O_2 control	1.16
Serum deprived endothelial cells	0.96
Serum control	0.91
Heat shock endothelial cells	0.86
Heat shock control	0.88

Table 6.6 Comparison of GAPDH levels in treated and untreated endothelial cells, using PKG as an endogenous reference gene. The results clearly indicate that GAPDH is unaffected by any of the experimental conditions under investigation. GAPDH levels remained constant even in those samples which previously displayed significant increases in c-*abl* expression in response to treatment with H_2O_2 (Table 6.5).

6.3.2 C-abl BASELINE DETERMINATION

It is important to ascertain if there are any variations in c-*abl* expression in endothelial cells due to culture, RNA extraction, cDNA synthesis or any other experimental variable. Endothelial cells were cultured in 6 well plates until confluent and RNA extracted in duplicate from each well. cDNA was prepared in duplicate from each RNA sample under identical experimental conditions. Each cDNA was then analysed, in triplicate, for GAPDH and c-*abl* using TaqMan® PCR as previously described (section 4.2.2 and 4.2.2). Figure 6.2 shows the raw spectra obtained, raw data not shown. All data was analysed using the comparative Ct method and statistical significance evaluated based on the one-sided paired T-test. Normalising each sample to its own replicate RNA sample yielded the data shown in Table 6.7
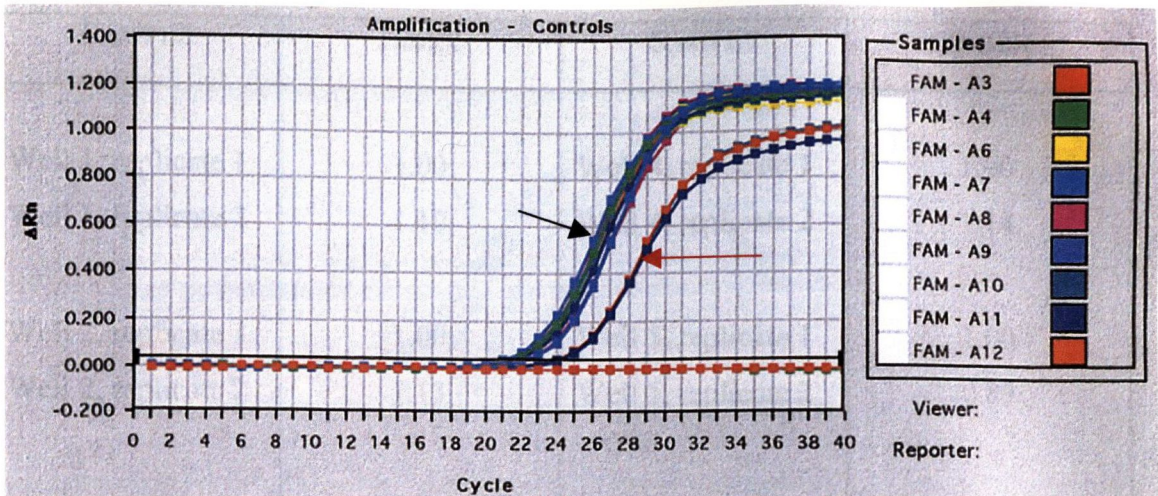
Figure 6.1 TaqMan® amplification curves for c-*abl* expression in three different test and control samples (outlined in Table 6.5). The red arrow indicates the H_2O_2 treated sample (in triplicate), which has an average Ct value of 24.16. The black arrow points to all the other amplification plots whose Ct values range from 20.12 to 21.85. This group includes the corresponding untreated control for the H_2O_2 treated samples. The figure clearly illustrates a significant decrease in c-*abl* mRNA following treatment with H_2O_2 (corresponding with index values shown in Table 6.5)
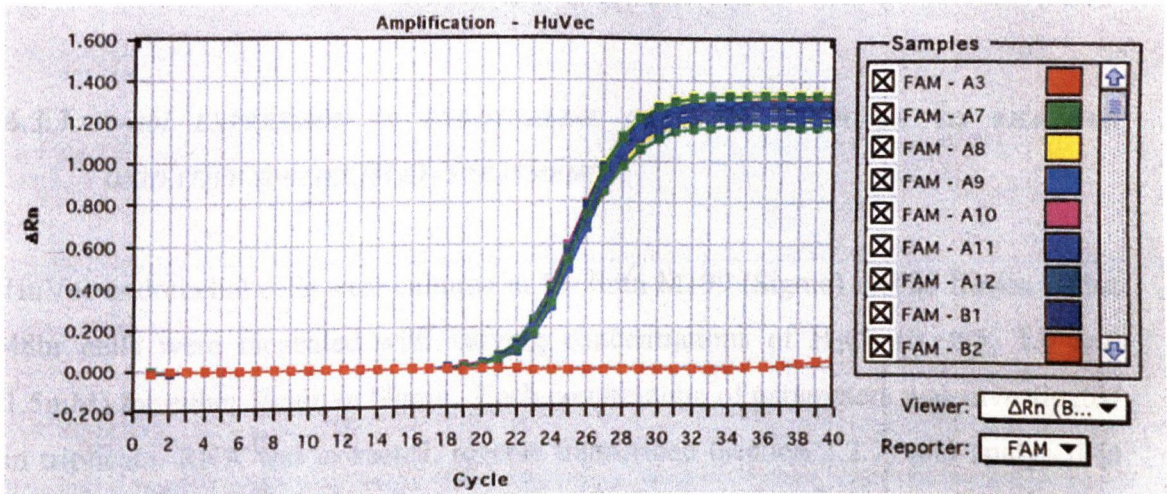
Figure 6.2 c-*abl* baseline expression TaqMan® amplification curves. This figure illustrates the amplification plots observed from 12 replicate endothelial cell RNA samples, assayed in triplicate for c-*abl* mRNA. All Ct values range from 20.29 to 20.61 (raw data not shown). Table 6.7 displays sample indices calculated using the comparative Ct method.

SAMPLE	INDEX	SAMPLE	INDEX
Well 1, replicate 1	1.00	Well 4, replicate 1	1.00
Well 1, replicate 2	1.10	Well 4, replicate 2	1.14
Well 2, replicate 1	1.00	Well 5, replicate 1	1.00
Well 2, replicate 2	1.13	Well 5, replicate 2	0.89
Well 3, replicate 1	1.00	Well 6, replicate 1	1.00
Well 3, replicate 2	1.13	Well 6, replicate 2	0.91

Table 6.7 Baseline c-*abl* expression in endothelial cells under standard cell culture conditions. The results indicate that there is no statistically significant difference in c-*abl* mRNA levels as a result of any constant experimental variable. Normalising all replicates against well 1, replicate 1 further confirms that a steady baseline of c-*abl* expression exists under normal culture conditons.

6.3.3 c-abl EXPRESSION IN ENDOTHELIAL CELLS IN RESPONSE TO REACTIVE OXIDATIVE SPECIES (H_2O_2 TREATMENT)

HuVec endothelial cells were cultured in Medium M199 (Sigma) in T25 flasks. After 48hr cells were incubated with varying concentrations of H_2O_2 (0, 0.5, 1.0 and 1.5mM) for either 30min or 60min. Each combination of parameters was investigated in triplicate. RNA was extracted, reverse transcribed (section 3.2.7) and analysed in triplicate for GAPDH and c-*abl* using the 7700 SDS TaqMan® assays. Index values for c-*abl* expression normalised against GAPDH are calculated using the comparative Ct method and statistical analysis of Indices performed using the paired student t-test (section 6.2.9). Table 6.8 summarises the results obtained.

H$_2$O$_2$ CONC.	INDICES (AVE. OF TRIPLICATES)	ONE-SIDED T-TEST	INDEX (AVE.)
30min. 0mM	0.9839 0.8753 0.8608	Reference -0.43 -0.83	0.9066 (control)
0.5mM	0.3866 0.3359 0.3151	+0.08 +0.07 +0.14	0.3459 Significant
1.0mM	0.4079 0.3808 0.4094	+0.07 +0.12 +0.03	0.3994 Significant
1.5mM	0.3189 0.2853 0.3863	+0.13 +0.17 +0.07	0.3302 Significant
60min. 0mM	0.9696 1.0229 1.0308	Reference -0.73 -0.55	1.0077 (control)
0.5mM	0.5207 0.5307 0.5805	-0.11 -0.07 -0.15	0.5440 Not Significant
1.0mM	0.3386 0.1376 0.2934	+0.18 +0.38 +0.22	0.2565 Significant
1.5mM	0.2019 0.2012 0.1591	+0.12 +0.29 +0.35	0.1874 Significant

Table 6.8 c-*abl* expression in endothelial cells following treatment with H$_2$O$_2$.
Normalisation of c-*abl* results with GAPDH endogenous control gene using the untreated control (0mM) as a calibrator to give an overall average index value. Applying the one-sided t-test to relative quantitation yields a test value which if negative or zero the result is **not** significant. If the test value is positive then the index is deemed statistically significant (99% Confidence Interval). The data presented clearly demonstrates a marked decrease in c-*abl* mRNA in response to reactive oxidative species at all concentrations of H$_2$O$_2$ investigated after 30min. After 60min, the levels of c-*abl* has increased marginally in the 0.5mM sample, such that the observed decrease in expression is no longer statistically significant. However, at the

higher concentrations of H_2O_2, c-*abl* has decreased even more dramatically after 60min than after 30min.
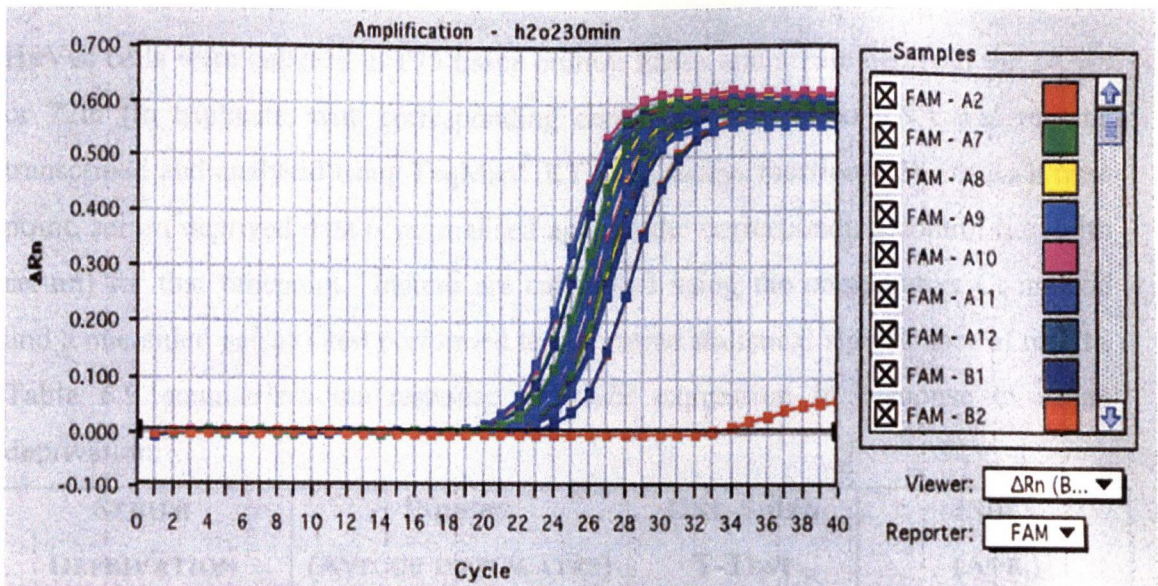
Figure 6.3 c-*abl* TaqMan® amplification plots following treatment of endothelial cells with varying concentrations of H_2O_2 (0-1.5mM) for 30min. Ct values range from 20.89 to 23.87 (raw data not shown). Each sample was normalised against GAPDH (Figure 6.4) and Indices calculated using the comparative Ct method (Table 6.8). The slight increase in baseline Rn value in the last 5 cycles is due to partial degradation of the TaqMan® probe due to long term storage of the probes which have a limited 'shelf-life' of approximately 6mths.
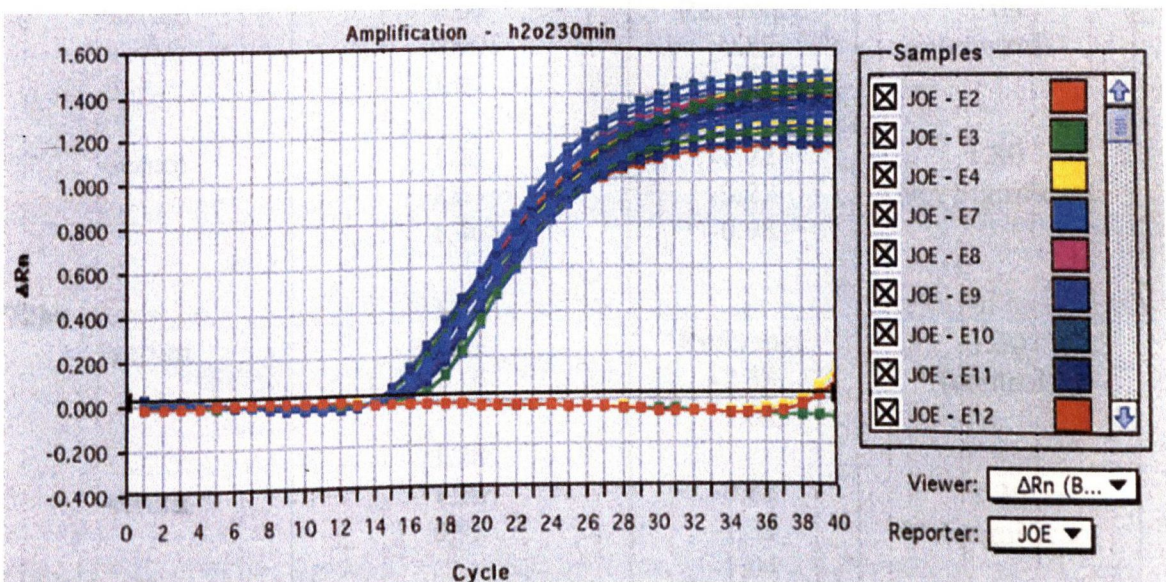
Figure 6.4 GAPDH TaqMan® amplification plots following treatment of endothelial cells with varying concentrations of H_2O_2 (0-1.5mM) for 30min. Ct values range from 15.76 to 16.03 (raw data not shown). Indices calculated are shown in Table 6.8

6.3.4 c-abl EXPRESSION IN ENDOTHELIAL CELLS IN RESPONSE TO SERUM DEPRIVATION

HuVec cells were cultured in T75 tissue culture flasks and serum deprived for 24, 48 or 72hr (in triplicate, with corresponding controls). Harvested RNA was reverse transcribed and analysed using TaqMan® RT-PCR assays (section 4.2). At each time point, serum deprived data is normalised against the corresponding control (i.e. with serum) for that timepoint. Indices are calculated using the comparative Ct method and a one-sided paired t-test performed to determine statistical significance of results. Table 6.9 summarises the response of c-abl expression in response to serum deprivation.

SERUM DEPRIVATION	INDICES (AVE. OF TRIPLICATES)	ONE-SIDED T-TEST	INDEX (AVE.)
24hr			
+serum	1.05	Reference	1.01
	0.96	-0.81	(control)
	1.03	-1.09	
-serum	1.20	-0.77	1.32
	1.29	-0.87	Not Significant
	1.48	-1.09	
48hr			
+serum	1.09	Reference	1.03
	0.90	-0.82	(control)
	1.01	-1.02	
-serum	1.22	-1.22	1.80
	2.61	-3.22	Not Significant
	1.46	-0.98	
72hr	1.00		
+serum	1.82	Reference	1.30
	1.10	-2.38	(control)
		-1.04	
	1.28		
-serum	1.86	-0.82	1.35
	0.92	-1.39	Not significant
		-1.04	

Table 6.9 c-abl expression in endothelial cells in response to serum deprivation. The results celarly indicate that serum starvation does not result in any significant change in c-abl mRNA levels in endothelial cells as determined by Real-Time

TaqMan® RT-PCR. Corresponding Figure 6.5 and Figure 6.6 illustrate approximate c-*abl* Ct values of 23 for all samples and GAPDH Ct values of 16.
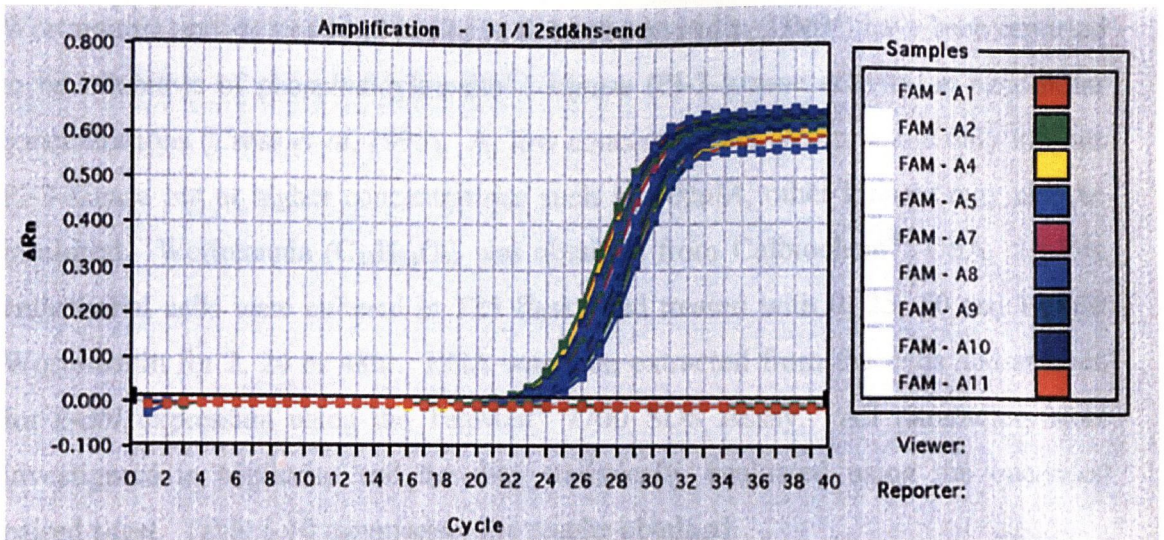
Figure 6.5 c-*abl* TaqMan® amplification plots following treatment of endothelial cells with Serum Deprivation for 0, 24,48 and 72hr, and the corresponding controls. All samples were assayed in triplicate and showed approximate average Ct values of 23. Index values for each sample are shown in Table 6.9
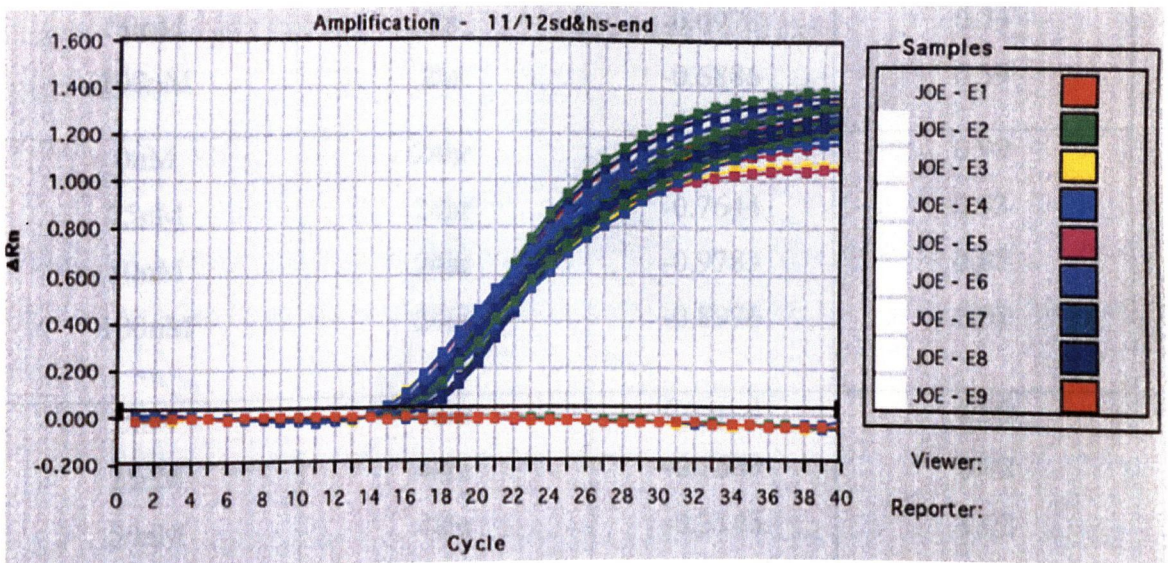
Figure 6.6 GAPDH TaqMan® amplification plots following treatment of endothelial cells with Serum Deprivation for 0, 24,48 and 72hr, and the corresponding controls. All samples were assayed in triplicate and showed approximate average Ct values of 16. Index values for each sample are shown in Table 6.9

6.3.5 *c-abl* EXPRESSION IN ENDOTHELIAL CELLS IN RESPONSE TO TREATMENT WITH WORTMANNIN

Wortmannin and its structural analogue demethoxyviridin (DMV) have been reported to be inhibitors of phosphatidylinositol-3-kinase (PI-3-kinase activity) at nanomolar concentrations (Cross *et al*, 1995). At low concentrations, Wortmannin only inhibits PI-3-kinase but at higher concentrations such as 100nM, other kinases may also be inhibited. Wortmannin ($C_{23}H_{24}O_8$) was obtained from Calbiochem®, USA. HuVec endothelial cells were cultured in T25 flasks and treated with 0, 25, 50 and 100nM Wortmannin for 2, 24 or 48hr. RNA was then extracted from the cells and assayed for c-*abl* expression using the TaqMan® 7700 SDS Assay. All parameters were investigated in triplicates and the data statistically evaluated using the one-sided paired t-test. Table 6.10 summarises the results obtained.

Wortmannin concentation	Treatment time	T-test	Index (Average)
0nM	2hr	Control	1.03
25nM	2hr	-0.0969	0.87
50nM	2hr	-0.0978	0.73
100nM	2hr	-0.6886	0.59
0nM	24hr	Control	0.99
25nM	24hr	-0.7644	0.93
50nM	24hr	-0.9783	0.85
100nM	24hr	-0.8976	0.62
0nM	48hr	Control	0.99
25nM	48hr	-0.1639	0.92
50nM	48hr	-0.3145	1.03
100nM	48hr	+0.3145[*]	0.54[*]

Table 6.10 c-*abl* expression in endothelial cells in response to treatment with Wortmannin. [*]A two-fold decrease in c-*abl* expression (99% confidence interval) is

observed when endothelial cells are incubated with 100nM Wortmannin for 48hr. Although a decrease in expression is observed with 100nM Wortmannin at the earlier sampling times, the effect did not approach statistical significance.

6.3.6   *C-abl EXPRESSION IN ENDOTHELIAL CELLS IN RESPONSE TO HEAT SHOCK*

Endothelial cells were cultured in T25 flasks and subjected to heat-shock at 40°C for 60sec (parameters selected based on preliminary study in which U-937 lymphoma cells were subjected to heat shock for 0, 15, 30, 45, 60, 90 and 120sec at 40°C, 42°C, 45°C and 50°C; data not shown).   U-937 lymphoma cells demonstrate a 5-fold increase in c-*abl* mRNA after 8hrs when heat shocked at 40°C for 60sec).   Following heat-shock, cells were returned to incubator and RNA harvested after 1, 8, 12 and 24hr.   c-*abl* and GAPDH levels were assessed using the 7700 SDS TaqMan® assays. The results obtained are outlined in Table 6.11.

Sample	1hr Index (Ave.)	8hr Index (Ave.)	12hr Index (Ave.)	24hr Index (Ave.)
Control	1.10	1.09	1.05	0.99
Heat-shock	1.15	0.77	1.06	1.03
T-test	*-0.11*	*-0.29*	*-2.26*	*-0.68*

Table 6.11   c-*abl* expression endothelial cells in response to heat-shock.   The results indicate that c-*abl* mRNA levels are unaffected by subjecting HuVec endothelial cells to temperatures of 40°C for 60sec.

6.3.7   *c-abl EXPRESSION IN ENDOTHELIAL CELLS FOLLOWING TUMOUR MEDIA TITRATION*

In this experiment, endothelial cells were cultured in culture media obtained from a number of other different cell lines including PC3 (prostate adenocarcinoma cell line), MCF-7 (human breast tumourigenic cell line), U-937 (histiocytic lymphoma cell line), K562 and HL60 (leukemic cell lines).   All of these cell lines are cultured in

RPMI 1640, as are the ECV-304 endothelial cell line. Cell lines were intiated and grown in fresh media until cultures were firmly established. Media was removed from the above-mentioned cell lines and any cells or cellular debris removed by centrifugation at 600g for 5min. The supernatant ('tumour cell line media') was then placed into the flasks containing proliferating endothelial cells. Initial experiments (data not shown), demonstrated that a 50:50 ratio of fresh RPMI 1640 to tumour cell line media is sufficient to maintain cell growth while allowing the desired effects to be observed. Endothelial cells were then harvested after 16, 24, and 48hr and the effect of tumour media titration expression in c-*abl* expression evalutated by TaqMan $^{®}$ RT-PCR.

As with all of the gene expression studies described in this thesis, all experiments were performed in triplicate. Unfortunately however, the results from the repeated sets of experiments proved extremely variable and unreproducible. Table 6.12 summarises the range of results obtained, and whether the observed changes in c-*abl* expression in each TaqMan$^{®}$ assay were statisitically significant. The Index values shown were calculated using the Comparative Ct Method (section 4.1.4), using average Ct values for each sample. Statisitical significance was determined using the one-sided paired T-test (section 6.2.9). A negative or zero Test result indicates that the result is not significant, a positive results means that the result is significant at 99% Confidence Interval (raw data not shown).

CELL LINE MEDIA	TIME	REPLICATE	INDEX (AVERAGE)	RESULT
ECV-304 (Control)	18hr	A	1.02	Control
		B	1.13	
		C	1.06	
PC3	18hr	A	0.32	Significant
		B	0.96	Not Significant
		C	0.70	Significant
MCF-7	18hr	A	1.14	Not Significant
		B	1.05	Not Significant
		C	0.37	Significant
U-937	24hr	A	0.68	Significant
		B	1.10	Not Significant
		C	0.98	Not Significant
HL60	24hr	A	1.81	Significant
		B	1.07	Not significant
		C	1.33	Not significant
K562	24hr	A	1.03	No Significant
		B	1.64	Significant
		C	1.99	Significant

Table 6.12 c-*abl* expression in endothelial cells following tumour media titration. The data presented in this table are the average results of three independent repeat experiments (A, B & C). Within each individual experiment (A, B or C) each variable was assayed in triplicate and each sample in turn assayed in triplicate by TaqMan® RT-PCR (giving rise to the average Index values shown above). No intra-sample variations in Ct value was observed. However, under these identical experimental conditions, significant changes in c-*abl* mRNA were detected in some samples by TaqMan® RT-PCR, while repeat experiments showed no change in c-*abl* expression in corresponding samples.

6.3.8 ABL ACTIVITY DETERMINATION BY PHOSPHOTYROSINE IMMUNOBLOTTING

6.3.8.1 Optimisation of blocking step of phosphotyrosine western blots

Initial attempts to detect phosphorylation of tyrosine residues using the PT03 antiphosphotyrosine antibody, Calbiochem, resulted in very high levels of background signal. In order to ascertain the suitability of the blocking buffer used, a sample was run on three different lanes of a SDS-PAGE gel and transferred onto PVDF membrane which was then cut in three 'mini-blots'. Each mini-blot was blocked in either **A.** 5%w/v milk, **B.** 5%w/v BSA or **C.** 5%w/v Fatty Acid Free BSA. All three blots were then washed and processed simultaneously under identical conditions.
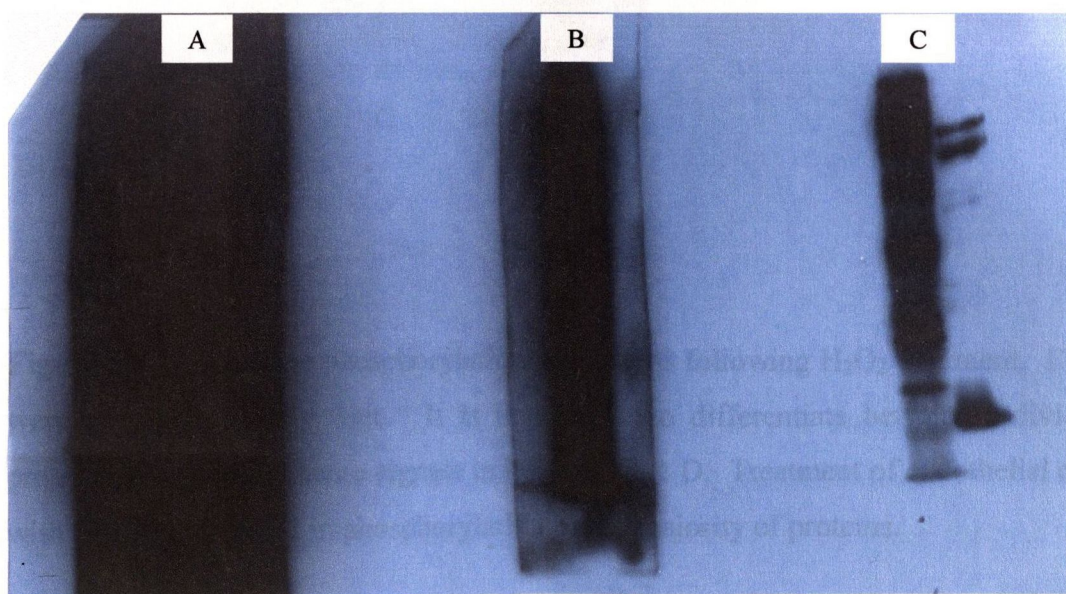
Figure 6.7 Optimisation of blocking buffer for use with PT03 antiphosphotyrosine antibody, Calbiochem. Three different buffers were assessed to determine the effect on background signal, **A.** 5%w/v milk, **B.** 5%w/v BSA or **C.** 5%w/v Fatty Acid Free BSA. The results clearly show that Fatty Acid Free BSA is the optimal blocking buffer for use with the PTO3 antibody.

6.3.8.2   **Abl phosphotyrosine status following treatment with H_2O_2**

Lane A: 0.0mM H_2O_2	
Lane B: 0.5mM H_2O_2	
Lane C: 1.0mM H_2O_2	
Lane D: 1.5mM H_2O_2	
Lane E: MrW Standards	
(Table 6.2)	

212kDa
132kDa
86kDa
43.8kDa
32kDa

A   B   C   D   E
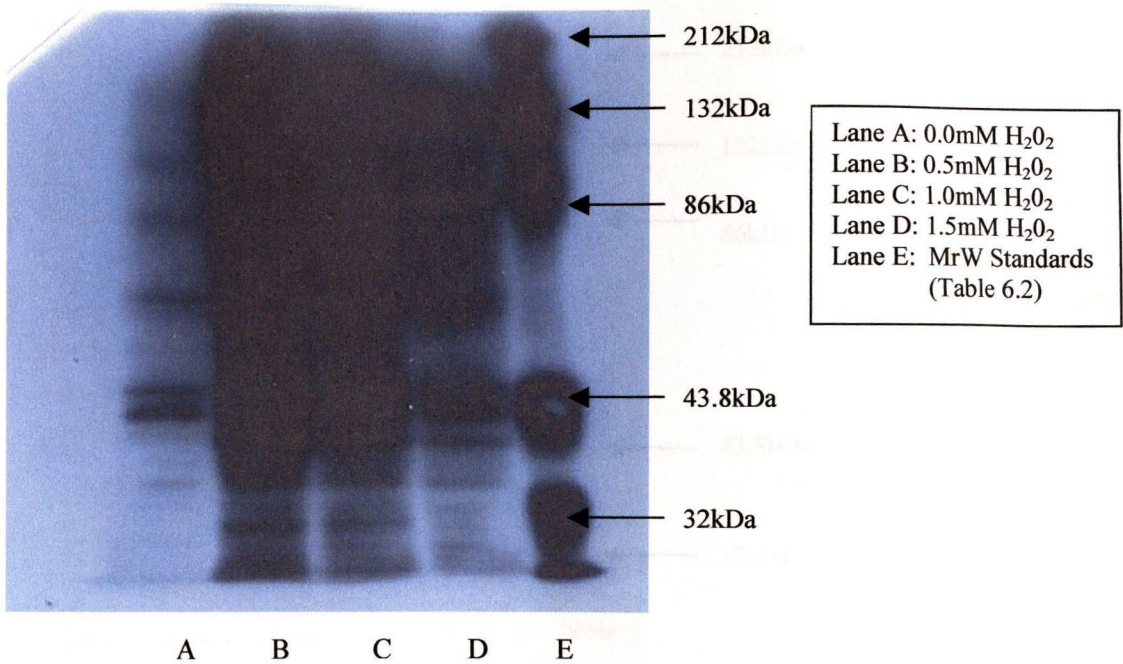
Figure 6.8   Tyrosine phosphorylation of proteins following H_2O_2 treatment. Films were exposed for only 3sec. It is impossible to differentiate between individual protein bands due to intense signals in lanes B, C & D. Treatment of endothelial cells with H_2O_2 has resulted in phosphorylation of the majority of proteins.

6.3.8.3 Ponceau S staining of Western blots to verify equal protein loading and efficiency of transfer

212kDa
132kDa
86kDa
43.8kDa
32kDa
A
B
C
D
E

Lane A: 0.0mM H_20_2
Lane B: 0.5mM H_20_2
Lane C: 1.0mM H_20_2
Lane D: 1.5mM H_20_2
Lane E: MrW Standards
(Table 6.2)
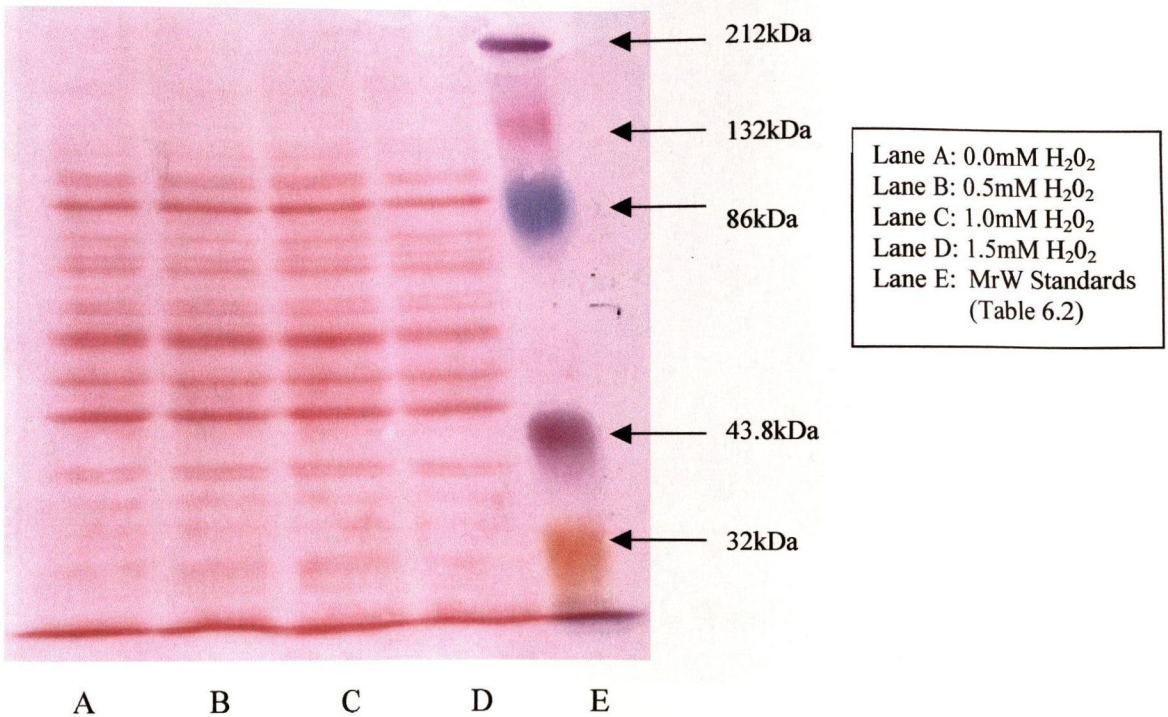
Figure 6.9 Ponceau S stain of H_20_2 treated endothelial cell protein extracts. The staining confirms that all lanes contain equal protein loading and that the wet transfer was successful. Equal loading was further confirmed by probing the blot for actin (data not shown).

6.3.8.4   **Abl phosphorylation following heat-shock treatment**

210kb, Abl

Lane A: 0.0mM H_2O_2
Lane B: 0.5mM H_2O_2
Lane C: 1.0mM H_2O_2
Lane D: 1.5mM H_2O_2
    MrW Standards
    (Table 6.2)
Lane E: 1hr
Lane F: 4hr
Lane G: 8hr
Lane H: 18hr

A   B   C   D   E   F   G   H
H_2O_2 Treated Samples   Heat Shock Samples
                                      $40^{\circ}C/30sec$

MrW Markers
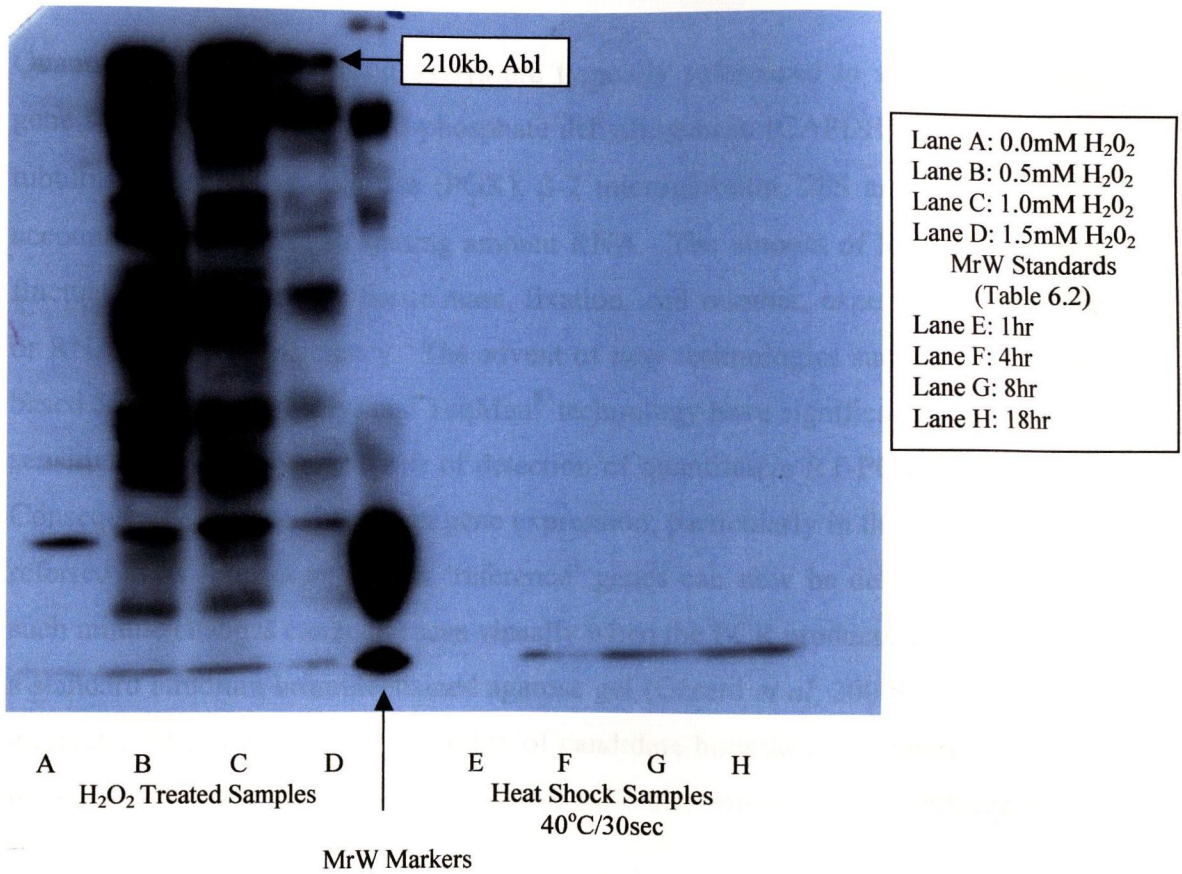
Figure 6.10   Abl tyrosine phosphorylation status following Heat-Shock treatment. The left hand side of this immunoblot illustrates another series of samples which have been treated with 0-1.5mM H_2O_2 for 60min. The results mirror those seen in Figure 6.8. The right hand side of the blot shows protein extracts from a series of samples subjected to heat shock at $40^{\circ}C$ for 60sec after 1, 4, 8 and 18hr. No change in phosphotyrosine levels are detected following heat shock of endothelial cells.

6.4   DISCUSSION

6.4.1   CONTROL GENE EXPRESSION

Quantitative gene expression assays are typically referenced to an internal control gene such as glyceraldehyde-3-phosphate dehydrogenase (GAPDH), albumin, actins, tubulins, phosphoglycerokinase (PGK), β-2 microglobulin, 28S and 18S rRNAs, to account for differences in starting amount RNA. The amount of RNA assayed may fluctuate to differences in tissue mass, fixation, cell number, experimental treatment or RNA extraction efficiency. The advent of new technologies such as fluorescence based 5'exonuclease assays and TaqMan® technology have significantly improved the sensitivity, selectivity and limits of detection of quantitative RT-PCR measurements. Consequently, minute changes in gene expression, particularly in those genes hitherto referred to as 'housekeeping' or 'reference' genes can now be detected. Invariable such minute changes cannot be seen visually when the PCR products are visualised on a standard ethidium bromide-stained agarose gel (Gerard *et al*, 2000). It would seem imperative therefore that the suitability of candidate housekeeping genes be assessed for each individual study and that, where possible, more than one reference gene should be employed.

Ideally, the conditions of the experiment should not influence the expression of the internal control gene. Glyceraldehyde-3-phosphate dehydrogenase (GAPDH) is a key enzyme involved in the regulation of glycolysis, catalysing the formation of 1,3-bisphosphoglycerate, and has been commonly considered as a constitutive housekeeping gene on the basis that its level of expression is unaffected by experimental or physiological conditions. However, evidence exists that GAPDH is involved in several key biological processes such as endocytosis, control of gene expression, DNA replication and repair in neuronal apoptosis (Sirover, 1997). In addition, it has been demonstrated that GAPDH expression is substantially increased in human cancers of various origins such as the lung (Tokunaga *et al*, 1987), pancreas (Schek *et al*, 1988) and cervix (Kim *et al*, 1998). Recent reports have expressed concern at the use of GAPDH as a suitable endogenous control for human carcinoma gene expression analysis (Revillion *et al*, 1998 & 2000). In order to ascertain the suitability of GAPDH as a control gene for the ensuing experiments, a series of

experiments were performed. RNA was extracted and analysed from endothelial cells which had been treated with hydrogen peroxide, serum deprivated or exposed to heat shock (section 6.3). Real-time 7700 TaqMan® analysis was performed using primer/probe sets for the detection of c-*abl*, GAPDH, Human PKG and β-2-microglobulin. H_2O_2 is a treatment which we have previously shown to cause changes in c-*abl* mRNA levels (data not shown), whereas serum deprivation and heat shock do not appear to affect c-*abl* expression. Table 6.5 summarises the result obtained. A high degree of variation between replicates was observed when using the β-2-microglobulin primer set, particularly in the H_2O_2 treated cell samples and in the 72hr serum deprived samples (raw data not shown). Consequently, β-2-microglobulin would not be considered a suitable reference gene for subsequent assays. Abl, Human PKG and GAPDH primers all gave very tight, reproducible result (raw data not shown). Firstly, c-*abl* expression was evaluated using Human PKG and GAPDH as control genes (Table 6.5) with both sets of results yielding identical results. Secondly, GAPDH expression was evaluated using Human PKG as the control gene (Table 6.6). No variation in GAPDH was observed between treated and untreated samples, even in those where changes in abl were recorded. It was therefore concluded that GAPDH is a suitable control gene for the proposed experiments.

6.4.2   c-abl BASELINE EXPRESSION IN ENDOTHELIAL CELLS

All experiments using the 7700 SDS® were specifically designed such that all parameters were investigated in triplicate and analysed in triplicate via the TaqMan® 96-well plate assay format to eliminate variability in standard deviations. It was important to establish the extent, if any, of c-*abl* mRNA variation between replicates. The students-t-test (T-test) was used with statistical confidence interval of 99% in a one-sided statistical test equation (section 6.2.9). Table 6.7 clearly illustrates that c-*abl* mRNA expression levels are unaffected by normal cell culture conditions. There are no variations in experimental replicates, or are there any variations attributable to any assay variable. Consequently, it will be possible in subsequent experiments to accredit with confidence any statistically significant changes in c-*abl* expression to the experimental parameter under investigation.

6.4.3 *c-abl* IN RESPONSE TO REACTIVE OXIDATIVE SPECIES

In this study, endothelial cells were exposed to a range of concentrations of H_2O_2 (0.5-1.0mM) for either 30 or 60min. RNA was extracted and analysed using TaqMan® RT-PCR. After 30min there was significant decrease in the c-*abl* mRNA at all concentrations of hydrogen peroxide tested (Table 6.8). Loss of c-*abl* in cells about to undergo apoptosis is expected given our earlier observations in which hypertrophic chondrocytes at the growth plate showed a loss of Abl protein expression relative to maturing chondrocytes in the bone shaft (section 2.2.1). At this time point there was little difference in the amounts of c-*abl* message observed at the different concentrations of H_2O_2 (section 6.3.3). After 60min, it appears as if the endothelial cells treated with the lowest concentration of H_2O_2 are beginning to recover, as the levels of c-*abl* mRNA are no longer significantly lower than the untreated control samples (Table 6.8). At the higher concentrations however, the levels of c-*abl* are even lower than those observed after 30min. The 1.0mM treated sample has decreased from 0.3994 to 0.2565, while the 1.5mM sample has decreased from 0.1874 (Table 6.8). The results clearly demonstrate that c-*abl* is reduced in endothelial cells in response to reactive oxidative species. Sun *et al*, 2000, demonstrate that cytochrome *c* is released in response to H_2O_2 and that this effect is mediated by a c-Abl –dependent mechanism. Kumar *et al*, 2003, show that the cell death response to oxidative stress can be abrogated through c-Abl inhibition using the tyrosine kinase inhibitor STI571.

To determine whether the phosphorylation status of c-Abl is altered in response to treatment with H_2O_2, protein extracts from treated cells were assayed for tyrosine phosphorylation by western blotting (section 6.2.8). Figure 6.8 illustrates significant increases in tyrosine phosphorylation of the majority of proteins in the cellular extracts following treatment with 0.5 or 1.0mM hydrogen peroxide for 30minutes. At higher concentrations of H_2O_2 (1.5mM) a lesser degree of tyrosine phosphorylation was detected, in contrast with the mRNA results (Table 6.8) in which the apparent decrease in c-*abl* mRNA is greater in the 1.5mM treated cells. It is likely that at this higher concentration of H_2O_2, the cells were severely injured to such an extent that the apoptotic pathways gave way to necrosis and as a result, the role of the protein tyrosine kinases is diminished.

6.4.4 c-abl EXPRESSION IN ENDOTHELIAL CELLS IN RESPONSE TO SERUM DEPRIVATION

Endothelial cells were subjected to serum deprivation for 24, 48 or 72hr using appropriate controls. c-abl mRNA analysis by TaqMan® RT-PCR showed no significant difference in expression of c-abl as a result of serum deprivation (Table 6.9). Although not statitistically significant, it is interesting to note an upward trend in c-abl expression, particularly after serum deprivation for 48hr (Index values of 1.22, 2.61 and 1.46). However, even after 72hr, the endothelial cells did not show any morphological signs of apoptosis and remained adhered to the tissue culture flask. This is in contrast to the observations made after treating the cells with 1.0mM or 1.5mM H_2O_2 where some loss of adherence was noted after 60min. It was not possible to serum deprive the endothelial cells for any longer than 72hr as the cells have already reached confluency at that point. Phosphotyrosine immunoblotting (section 6.2.8) showed no change in c-Abl tyrosine phosphorylation status following serum deprivation. Therefore, it may be concluded that serum deprivation *in vitro* has no affect on c-Abl expression or activity in endothelial cells.

6.4.5 c-abl EXPRESSION IN RESPONSE TO TREATMENT WITH WORTMANNIN

In order to determine the effect of wortmannin on c-abl expression in endothelial cells, we incubated ECV-304 HuVec cells in growth media containing 0-100nM wortmannin for 2, 24 and 48hrs. At concentrations of 0, 25 or 50nM wortmannin, no significant change in c-abl expression was observed by TaqMan® RT-PCR. A two-fold decrease in c-abl expression (99% confidence interval) is observed when endothelial cells are incubated with 100nM Wortmannin for 48hr (Table 6.10). Although a decrease in expression is observed with 100nM Wortmannin at the earlier sampling times, the effect did not approach statistical significance (Table 6.10). As discussed previously, wortmannin is known to be a potent inhibitor of PI 3-kinase activity (Arcaro *et al*, 1993). Wortmannin has also been reported to inhibit a number of other kinases (Bonser *et al*, 1991; Cross *et al*, 1995) but only at concentrations greater than those reported to inhibit PI 3-kinase (100nM range). We have demonstrated a reduction in c-abl expression in endothelial cells at a concentration of 100nM wortmannin. The results cannot confirm whether

wortmannin has directly inhibited c-*abl* or whether the observed decrease in c-*abl* is a downstream effect of PI-3 kinase inhibition. However, given that PI-3 kinase is likely to be inhibited even at the lower concentrations of wortmannin tested, and no inhibition of c-*abl* is evident in these samples, it is likely that wortmannin has directly caused a reduction in c-*abl* levels in endothelial cells. BCR-ABL has been linked to activation of PI-3 kinase (Skorski *et al*, 1995). Inhibition of PI3K blocks proliferation of BCR-ABL-dependent cells, establishing the importance of PI3K for BCR-ABL activity. The ability to inhibit normal c-*abl*, suppressing its anti-apoptotic function, could conceivably be exploited in the development of apoptosis based treatments for malignancy.

6.4.6   c-abl *IN RESPONSE TO HEAT SHOCK*

HuVec endothelial cells were subjected to heat shock for 60sec and c-*abl* mRNA levels measured after 0, 1, 8, 12 and 24hr. In our hands, a five fold increase in c-*abl* expression was noted in U-937 cells after 8hrs following heat shock at 40°C for 60sec, (preliminary study, data not shown). However, our results indicate that no significant changes in c-*abl* expression are observed in HuVec endothelial cells in response to heat-shock. On careful examination of the data obtained after 8hrs, an apparent decrease in c-*abl* expression is observed (Index = 0.77), and while this result is not statistically significant, the downward trend was observed in all three replicate experiments performed. However, no change in Abl tyrosine phosphorylation status was observed in any of the samples by western blot analysis (Figure 6.10). The results therefore would suggest that c-*abl* expression, but in particular c-Abl activity, in endothelial cells is unaffected by heat shock. In addition, the results would seem to indicate that the response of c-*abl* mRNA levels to heat shock is cell type specific. The results are surprising given that heat-shock is a model form of stress shown to inhibit cell cycle progression (Li & Cai, 1999; Nitta *et al*, 1997). Heat-shock has been shown to activate ERK1/2 (MAP kinase) and induces extensive CTD phosphorylation (Venetianer *et al*, 1995). It is likely that the hyperphosphorylated form of CTD contributes to the altered gene expression patterns characteristic of heat shock (Dubois, 1999). Both ERK1/2 and c-*abl* tyrosine kinase are CTD kinases implicated in cell cycle regulation, and similar responses to stress factors would be expected.

6.4.7 c-abl IN RESPONSE TO TUMOUR MEDIA TREATMENT

The ability to induce and sustain angiogenesis seems to be an essential step during tumour development. Counterbalancing positive and negative regulatory signals can encourage or block angiogenesis (Hanahan and Folkman, 1996). At present there are more than two dozen angiogenic inducer and inhibitor factors known (Hanahan & Weinberg, 2000), including integrins, adhesion molecules and numerous growth factors such as VEGF (vascular endothelial growth factor) and FGF (fibroblast growth factor). The dependence of tumour cells on nearby capillaries for survival raises the possibility that the tumour cells themselves may develop the ability to encourage new blood vessel formation. We investigated the effect of culturing HuVec endothelial cells in the presence media obtained from a variety of tumour cell lines to determine the effect, if any, on c-abl expression (section 6.3.7).

The results obtained were inconclusive, given the high degree of variability between replicate experiments. The observed differences in c-abl mRNA expression were not reproducible under apparently identical experimental conditions. The control samples in which HuVec cells were cultured in ordinary growth media showed no variations in c-abl expression (Table 6.12). This is expected following the c-abl baseline experiments performed previously (section 6.4.2). It is particularly interesting to note the differences in the trends observed between the leukaemic cell lines and those of solid tumours. Where significant, the solid tumour cell line media all resulted in a decrease in c-abl expression in endothelial cells (Table 6.12). The PC3 prostate carcinoma cell line caused resultant Index values of 0.32 and 0.70; the MCF-7 breast tumourigenic cell line gave an Index Value of 0.37; and the histiocytic lymphoma cell U-937 line gave an Index value of 0.68. In contrast, the HL60 and K562 cell lines resulted in increased expression of c-abl in endothelial cells, yielding index values of 1.81 and 1.64 or 1.99 respectively (Table 6.12). However, it must be emphasised that these observations, while worthy of note, could not be reliably reproduced in replicate experiments.

Increased angiogenesis is important in the pathophysiology of solid tumours (Chavakis & Dimmeter, 2002; Beecken et al, 2002). Recent studies have shown that angiogenesis and angiogenic factors may also play an important role in

haematological malignancies (Aguayo *et al*, 2000; Bertolini *et al*, 2000). Both acute myeloid leukaemia (AML) and myelodysplastic syndrome (MDS) are associated with a substantial increase in vascularity of the bone marrow and increased levels of various angiogenic factors (Albitar, 2001). AML cells produce pro-angiogenic factors such as VEGF, a potent inductor of angiogenesis (Hussong *et al*, 2000). Furthermore, elevated levels of basic fibroblast growth factor (b-FGF) are detected in patients with acute lymphoblastic leukaemia (Perez-Atayde *et al*, 1997). The Bcr/abl fusion gene is found in the majority of patients with CML. The fusion gene has recently been reported in the circulating endothelial cells of patients with CML, thus showing that the chromosomal translocation has occurred in medullary hemangioblasts (Hussong *et al*, 2000). These observations suggest that medullar angiogenesis may play a role in the proliferation of leukaemic cells. Litwin *et al*, 2002, suggest that angiogenesis in AML is likely to represent a response to micro-environmental factors *in vivo* rather than being an intrinsic property of leukaemic cells. Albitar, 2001, demonstrate that most angiogenic factors secreted by haematopoietic cells appear to promote growth and proliferation of the leukaemic cells in an autocrine fashion. The results of this study support this finding, showing that the angiogenic factors secreted by both the HL60 and K562 leukaemic cell line resulted in an increase in c-*abl* expression in HuVec endothelial cells *in vitro*.

7. DISCUSSION

7. DISCUSSION

The fundamental elements that define the pathology of human cancer include limitless replicative potential, sustained angiogenesis and evasion of apoptosis (Hanahan & Weinberg, 2000). A complex and rigorously controlled series of events govern the cell cycle and ultimately the fate of the individual cell. A map for cell cycle control and DNA repair has been published recently (Kohn, 1999). It is clear that such control is as a result of a network of interacting genes and pathways, encompassing a multitude of signalling molecules, receptors, growth factors and cell-to-cell adhesion/interaction molecules. Tumourigenesis is characterised by the loss of function of any of these key molecules which normally either sense DNA damage or commit cells to the apoptotic pathway.

This study focuses on the role of the c-*abl* proto-oncogene in cellular differentiation, apoptosis and tumour angiogenesis. At the outset, it was proposed to address three key questions regarding c-*abl* function *in vivo*:

1. IN WHAT TISSUES IS c-*abl* EXPRESSED AND WHAT ROLE DOES ABL PLAY IN APOPTOSIS, TUMOURIGENESIS AND ANGIOGENESIS IN NON-HAEMATOPOIETIC TUMOURS?

Initially, Abl protein expression was determined immunohistochemically in a series of formalin fixed paraffin embedded tissues and tumours. Our findings suggest that Abl is involved in differentiation and the inhibition of apoptosis in chondrocytes in normal fetal cartilage. In addition, Abl is observed in proliferating osteoblasts and the formation of new blood vessels at the growth plate (section 2.3.1). It can be concluded therefore that Abl may play a pivotal role in the events leading to enchondral ossification at the growth plate in human fetal cartilage.

Expression of the c-Abl/Bcr-Abl oncoprotein in chondrosarcoma and liposarcoma correlated directly with tumour cell differentiation and apoptosis. Low grade, well-differentiated tumours showed strong Abl expression and minimal apoptosis. High grade, poorly differentiated tumours showed weak or negative Abl staining and noticeably higher levels of apoptosis (section 2.3.2). Thus, the

importance of c-Abl in cellular differentiation and regulation of apoptosis is further substantiated by the observations of Abl expression in chondrosarcoma and liposarcoma. Differential expression of Abl in differentiating chondrocytes, adipocytes and also in the umbilical cord strongly supports a role for c-Abl in the survival of specific connective tissues.

Despite the importance of tyrosine kinase family members in general to angiogenesis, no particular role for c-Abl in angiogenesis has been identified to date. This thesis however, presents strong evidence that c-Abl may be either directly or indirectly angiogenic. Strong Abl expression is observed in the tumour microvessels of liposarcoma, breast carcinoma and diffuse type signet ring carcinoma of the stomach (section 2.3.3-2.3.5). Abl expression has been demonstrated in early placental villi and in umbilical cord blood vessels (section 2.3.6) and also in the neovasculature during enchondral ossification (section 2.3.1). Previous work by our group has confirmed that c-Abl is not usually expressed in normal adult blood vessels (O'Neill *et al*, 1997).

In summary, it may be concluded that c-Abl is an important factor in apoptosis inhibition, cellular differentiation and angiogenesis in certain non-haematopoietic tumours.

2. IS DIFFERENTIAL REGULATION OF c-*abl* EXPRESSION OBSERVED AT BOTH THE PROTEIN AND MRNA LEVEL?

Thus far, differential regulation of c-Abl protein expression has been observed using immunohistochemistry. The ability to assess gene expression at the mRNA level would provide valuable information as to whether such regulation is occurring at the level of transcription or translation. All of the material used in this study is comprised of histological formalin-fixed paraffin embedded tissues. The technical difficulties arising from fixation effects and template degradation have been discussed previously (section 3.1.1) and were highlighted by the poor success rates initially encountered in extracting and amplifying RNA from the formalin fixed specimens. This study presents a comprehensive evaluation of a number of RNA extraction

protocols. The main objective was to establish an extraction protocol, which would be most conducive to subsequent analysis of short mRNA sequences by RT-PCR. If routine use of the polymerase chain reaction on histological samples is to be realised, a technique which is easily introduced into the diagnostic laboratory must be developed. Previous attempts at performing molecular biological studies on formalin fixed paraffin embedded tissues have involved lengthy and labour intensive extraction procedures unsuitable for routine use (Goelz *et al*, 1985; Warford *et al*, 1988). This thesis describes a procedure for rapid and reliable extraction of RNA from the archival material using the Gentra Pure*Script*™ RNA isolation kit (section 3.2.3).

The results also demonstrate the increased sensitivity and limits of detection attainable with recent advances in fluorescence based Quantitative RT-PCR instruments (section 3.1.5). Initial attempts to analyse the extracted RNA using conventional SP-PCR proved unsuccessful, primarily due to amplicon size (section 3.3.2). Advances in fluorescence based 5' exonuclease assays resulted in the introduction of the TaqMan® 7200 End-point Sequence Detection System. This system offered the combined sensitivity of the polymerase chain reaction with specificity of the TaqMan® probe hybridisation and a smaller amplicon size generated during TaqMan® PCR. All of these features enabled us to detect mRNA transcripts in extracts from formalin fixed paraffin embedded samples which could not be detected by solution phase PCR (section 3.3.6). End-point determinations did not however permit quantitative analysis of c-*abl* levels within these samples. Ultimately, the evolution of the real-time TaqMan® 7700 Sequence Detection System enabled quantification of c-*abl* mRNA expression in tissues which had failed previously to be evaluated by alternative preceding technologies (section 3.3.6). The precision and sensitivity of RNA quantitation is enormously enhanced using real-time data acquisition compared to standard end-point detection.

Primer Express™ software was used to design suitable primers and probe for the analysis of c-*abl* mRNA by TaqMan® RT-PCR. Subsequent to this, an efficient and reproducible c-*abl* TaqMan® assay was developed which was suitable for use with the 7700 SDS®. Using this assay, c-*abl* was successfully amplified in all but one of the formalin fixed paraffin embedded tissues under investigation. Given the fact that some of the chondrosarcoma blocks had been acid decalcified and other tissue

blocks had been stored for up to 44yr, the successful extraction and amplification of RNA from these samples was particularly remarkable.

The results of the c-*abl* TaqMan® analysis demonstrated that c-*abl* mRNA is significantly lower in high-grade chondrosarcoma than in low-grade chondrosarcoma. This result mirrors the observed expression of Abl oncoprotein in chondrosarcoma described previously, thus further supporting a role or c-*abl* in differentiation and apoptosis modulation in chondrosarcoma. No statistically significant difference in c-*abl* expression was noted between the different grades of liposarcoma investigated. The raw data shown in Table 4.8 however illustrates the wide range of ΔCt values recorded within each sub-classification of liposarcoma, and consequently an average value for each grade tumour was calculated for comparison purposes. In addition, considerably lower yields of mRNA were obtained from liposarcoma cases than other tumour types as discussed previously (section 3.4.4). The levels of c-*abl* mRNA have been shown to be higher in diffuse (signet ring) carcinoma of the stomach relative to intestinal type gastric adenocarcinoma. This is again in keeping with the immunohistochemical staining patterns for Abl protein in this tumour group.

In conclusion, real-time TaqMan® RT-PCR has enabled us to confirm that the differential expression in c-*abl* observed at the protein level can also found at the mRNA level, although it does not indicate precisely which cells have this *abl* mRNA.

Consequently, the question of which precise cells are contributing to the net yield of c-*abl* mRNA needed to be addressed. Initial attempts to localise c-*abl* mRNA to individual cells in a tissue section involved laser capture microdissection. Unfortunately, the yields of mRNA obtainable using this technology were below the limits of detection of the subsequent mRNA assay techniques. As it was believed that the transcripts were being lost during the RNA extraction stages, it was hypothesised that *in-situ* RT-PCR would prove to be a more suitable alternative due to the fact that the target template does not have to be extracted from the relevant cells.

In-situ RT-PCR is a relatively new technique (Haase, 1990), which offers the combined sensitivity of gene amplification techniques with the localisation benefits of

in-situ hybridisation techniques. A number of different *in cell* amplification strategies were assessed in this study: direct *in-situ* RT-PCR, RT-PCR-ISH and *in cell* TaqMan® RT-PCR. All three methods were shown to be effective and reproducible when applied to cell cytospins prepared from a number of different cell lines. However, a number of technical difficulties were encountered in applying the same techniques to formalin fixed paraffin embedded tissues. Despite extensive optimisation of the protease digestion and tissue pretreatment steps, loss of morphology and lifting of tissue sections from the slides during thermal cycling proved most problematic. In practice, the direct labelling method was the only strategy that worked repeatedly in our hands. The results obtained confirmed the presence of c-*abl* mRNA in breast cancer cells and adjacent tumour microvessels. c-*abl* mRNA was detected in the villi, developing endothelium and connective tissues in placenta at 7wks gestation. c-*abl* mRNA was also localised to the tumour microvessels of gastric carcinoma using direct *in-situ* RT-PCR. Overall, the results served to corroborate the findings observed immunohistochemically using the c-Abl/BCR-Abl antibody. The importance of c-Abl in angiogenesis is further substantiated through identification of c-*abl* mRNA transcripts in the endothelium of early placenta and in the neovasculature of breast and gastric carcinoma.

3. IS c-*abl* mRNA IN ENDOTHELIAL CELLS MODULATED IN RESPONSE TO SPECIFIC STRESS FACTORS?

It has previously been reported that a number of stimuli including heat shock, reactive oxidative species and chemotherapeutic agents appear to mediate apoptosis in a death receptor independent manner via the mitochondrial pathway (Kroemer *et al* 1997 & 1998). This study aimed to investigate the effect of such stress factors on the level of c-*abl* expression in HuVec endothelial cells. c-*abl* mRNA levels were assessed using the Real-Time TaqMan® RT-PCR Assay system and using GAPDH as a control gene. The results demonstrate that c-*abl* mRNA expression decreases in response to reactive oxidative species. However, analysis of parallel protein extract illustrates an increase in Abl tyrosine phosphorylation status following treatment with H_2O_2, which indicates an increase in c-Abl tyrosine kinase activity. However, the majority of proteins visualised on the SDS-PAGE gels showed increased

phosphorylation and as such, no direct relationship between H_2O_2 and Abl activation could be established using this assay technique. An alternative method of determining c-Abl tyrosine kinase activation is through incubation of anti-c-Abl antibody immunoprecipitates with the GST-Crk (120-225) fusion protein (Feller *et al*, 1994; Ren *et al*, 1994). Activation of c-Abl results in phosphorylation of GST-Crk which can be detected by immunoblot analysis. This would provide a more specific assay for c-Abl activity measurements for future experiments. Sun *et* al, 2000, show that both nuclear and cytoplasmic c-Abl are activated by oxidative stress, a finding substantiated by Kumar *et al*, 2001. Sun *et al*, 2000, also demonstrate that cytochrome *c* is released in the cellular response to H_2O_2 and that the effect is mediated by a c-Abl dependent mechanism. A recent study (Kumar *et al*, 2003) utlises STI571, an inhibitor of Bcr-Abl in chronic myelogenous leukemia, to block the response of U-937 myeloid leukemia cells and mouse embryo fibroblasts to hydrogen peroxide. The results demonstrate that STI571 attenuates H_2O_2-induced loss of mitochondrial transmembrane potential. Consequently, STI571 inhibits the death response to H_2O_2 exposure by 40 to 80% depending on cell type (Kumar *et al*, 2003). These findings support a role for c-*abl* in mitochondrial dysfunction and cell death in response to reactive oxidative species. The data presented in this study showed no evidence of c-*abl* activation in response to either heat-shock or serum deprivation of endothelial cells. Decreased c-*abl* mRNA expression in endothelial cells was noted following treatment with high levels of wortmannin, although no concomitant change in c-Abl tyrosine phosphorylation status was observed. It may be interesting to investigate the stress-induced regulation of c-Abl in diseases such as atheroschlerosis in which apoptosis of endothelial and smooth muscle cells is central to disease progression. The effect of mechanical force and pulse pressure on c-Abl expression in endothelial cells may provide a greater insight into the role of Abl in non-malignant diseases.

The results obtained following incubation of endothelial cells with tumour cell line media were particularly interesting, although further investigations are required due to the high degree of variability of the data. The data showed an increase in c-*abl* following incubation with media from the HL60 and K562 leukaemic cell lines. In total contrast, a significant decrease in c-*abl* expression was noted following treatment with media from various solid tumour cell lines. The importance of angiogenesis for

the continued growth of solid tumours and in many forms of leukaemia has been discussed previously. PDGF is one of many tyrosine kinases known to play a pivotal role in endothelial cell function (Rosen, 2002). PDGF signalling can vary from autocrine stimulation of cancer cell growth to more paracrine interactions involving adjacent stroma and even angiogenesis (George, 2001). Interestingly, the tyrosine kinase inhibitor imatinib mesylate (formerly ST571, [Gleevec]) used to block BCR-Abl oncoprotein activity in CML, is also a potent inhibitor of PDGFR kinase. Imatinib mesylate is currently being evaluated for the treatment of PDPGF responsive tumours such as prostate cancer (Cross & Reiter, 2002).

The work presented in this thesis confirms a role for c-Abl in tumour cell differentiation and inhibition of apoptosis. In addition, a hitherto undefined role for c-Abl in angiogenesis has also been investigated. The development and optimisation of RNA extraction techniques has provided a valuable tool for retrospective analysis of nucleic acids in archival histological samples. The sensitivity of such analyses has been greatly enhanced with the advancements in Real-Time Quantitative RT-PCR, TaqMan® technology and *in-situ* RT-PCR methodologies. The response of c-Abl in endothelial cells to various stress factors suggests a possible role for Abl in the mitochondrial apoptotic pathway. Ito *et al*, 2001, have shown c-Abl involvement in signalling from the endoplasmic reticulum (ER) to the mitochondria, and thereby in the apoptotic stress response to ER stress. Recently (Li *et al*, 2002), a novel c-Abl interacting protein, Aph2, has been identified with a unique cysteine rich motif (zf-DHHC) and a 53aa stretch sharing homology with the creatine kinase. Deletion and over-expression studies have demonstrated that Aph2 may be involved in ER stress-induced apoptosis in which c-Abl plays an important role.

7.1   CONCLUDING REMARKS

Significant progress has been made in recent years in understanding the complex, multi-faceted role of c-Abl. Despite this progress, the precise functions remain unclear and a single comprehensive model is not available. Roles for c-Abl in cell cycle regulation, stress responses, integrin signalling and neural development are likely. The information on c-Abl accumulated through this study has provided several further avenues of investigation in the pursuit of understanding this complex tyrosine

kinase. Regarding the nuclear function of c-Abl, it will be important to identify c-Abl regulated promoters in order to define the role of c-Abl in DNA synthesis and repair. The potential for *abl* to phosphorylate other apoptosis modulating genes could be investigated using a temperature sensitive *v-abl* mutant used in previous studies (McGahon *et al*, 1994). The use of such a mutant enables the expression of the *abl* tyrosine kinase to be carefully controlled and the interaction of *abl* with other genes to be investigated. Traditional methods in molecular biology generally work on a 'one gene in one experiment' basis, providing limited information on the complicated way in which genes and their products interact. Advances in DNA chip or gene array technology potentially allows the analysis and comparison of thousands of genes on a single chip, providing researchers with a better picture of the interactions among all of these genes simultaneously. In addition, the field of proteomics has rapidly expanded over the last decade. Proteomics employs a multitude of techniques to resolve, quantitate and rapidly identify proteins, as well as to identify their interacting proteins. In combination with DNA microarrays, this technology promises to contribute significantly to our understanding of the role of c-*abl* and its interplay with other genes involved in apoptosis, angiogenesis and the development of cancer.

8.   APPENDIX

A1 COMPARATIVE C_T METHOD (MULTIPLEX/SINGLE TUBE) FORMULA FOR QUANTITATIVE GENE EXPRESSION ANALYSIS:

The equation for the amount of target, normalized to an endogenous reference and relative to a calibrator, is given by:

$$2^{-\Delta\Delta C_T}$$

Derivation of the Formula

The equation that describes the exponential amplification of PCR is:

$$X_n = X_o \times (1 + E_X)^n$$

where:

X_n	=	number of target molecules at cycle n
X_o	=	initial number of target molecules
E_X	=	efficiency of target amplification
N	=	number of cycles

The threshold cycle (C_T) indicates the fractional cycle number at which the amount of amplified target reaches a fixed threshold. Thus,

$$X_T = X_o \times (1 + E_X)^{C_{T,X}} = K_X$$

X_T	=	threshold number of target molecules
$C_{T,X}$	=	threshold cycle for target amplification
K_X	=	Constant

A similar equation for the endogenous reference reaction is:

$$R_T = R_o \times (1 + E_R)^{C_{T,R}} = K_R$$

where:

R_T	=	threshold number of reference molecules
R_o	=	initial number of reference molecules
E_R	=	efficiency of reference amplification
$C_{T,R}$	=	threshold cycle for reference amplification
K_n	=	constant

Dividing X_T by R_T gives the following expression:

$$\frac{X_T}{R_T} = \frac{X_o \times (1 + E_X)^{C_{T,X}}}{R_o \times (1 + E_R)^{C_{T,R}}} = \frac{K_X}{K_R} = K$$

The exact values of X_T and R_T depend on a number of factors, including:
- Reporter dye used in the probe
- Sequence context effects on the fluorescence properties of the probe
- Efficiency of probe cleavage
- Purity of the probe
- Setting of the fluorescence threshold.

Therefore, the constant K does not have to be equal to one.

Assuming efficiencies of the target and the reference are the same: $E_X = E_R = E$,

$$\frac{X_o}{R_o} \times (1 + E_X)^{C_{T,X} - C_{T,R}} = K$$

or

$$X_N \times (1 + E)^{\Delta C_T} = K$$

where:

$$X_N \quad = \quad \text{the normalized amount of target}$$

$$\Delta C_T \quad = \quad \text{the difference in threshold cycles for target and reference}$$

Rearranging gives the following expression:

$$X_N = K \quad x \quad (1 + E)^{\Delta C_T}$$

The final step is to divide the X_N for any sample q by the X_N for the calibrator (cb):

$$\frac{X_{N,q}}{X_{N,cb}} = \frac{K \ x \ (1 + E)^{-}}{K \ x \ (1 + E)^{-\Delta_{CT,cb}}} = (1 + E)^{-\Delta\Delta C_T}$$

where:

$$\Delta\Delta C_T = \Delta C_{T,q} - \Delta C_{T,cb}$$

For amplicons designed and optimized according to Applied Biosystems guidelines (amplicon size < 150 bp), the efficiency is close to one. Therefore, the amount of target, normalized to an endogenous reference and relative to a calibrator, is given by:

$$2^{-\Delta\Delta C_T}$$

A2   CONTROL GENE EXPRESSION BY 7700 TAQMAN REAL-TIME SDS® TECHNOLOGY.

PE Applied Biosystems

Sequence Detection Systems
1.6.3

File Name:Controls
User:Jen
Date:Wed, Dec 13, 2000
Comments:Jennifer Control Plate - Beta 2-microglobulin

Plate Type:7700 Single Reporter☐
PCR Volume:25

Thermal Cycle Conditions

Cycle	Temperature	Time	Repeat	Ramp Time	Auto Increment
Hold	50.00	2:00		Auto	
Hold	95.00	10:00		Auto	
Cycle	95.00	0:15	40	Auto	
	60.00	1:00		Auto	

Standard Curve

Slope: 0.00
Intercept: 0.00
Fit R: 0.00

Threshold: 0.05
Baseline Range: (3 , 15)

Sample Information

Well	Type	Sample Name	Replicate	Ct	Quantity	Std. Dev.	Mean
E7	UNKN	H2O2 untreated		20.29		0.00	0.00
E8	UNKN	H2O2 untreated		20.52		0.00	0.00
E9	UNKN	H2O2 untreated		20.29		0.00	0.00
E10	UNKN	H2O2 1.0mM, 30min.		22.13		0.00	0.00
E11	UNKN	H2O2 1.0mM, 30min.		21.48		0.00	0.00
E12	UNKN	H2O2 1.0mM, 30min.		20.98		0.00	0.00
F1	UNKN	SD 72+ cont.		19.64		0.00	0.00
F2	UNKN	SD 72+ cont.		20.00		0.00	0.00
F3	UNKN	SD 72+ cont.		19.69		0.00	0.00
F4	UNKN	SD 72-		18.16		0.00	0.00
F5	UNKN	SD 72-		20.07		0.00	0.00
F6	UNKN	SD 72-		20.10		0.00	0.00
F7	UNKN	HS 8hr cont.		20.13		0.00	0.00
F8	UNKN	HS 8hr cont.		19.86		0.00	0.00
F9	UNKN	HS 8hr cont.		20.07		0.00	0.00
F10	UNKN	HS 8hr 60sec.		19.00		0.00	0.00
F11	UNKN	HS 8hr 60sec.		19.11		0.00	0.00
F12	UNKN	HS 8hr 60sec.		19.03		0.00	0.00
E1	NTC	E1	NTC	40.00		0.00	0.00
E2	NTC	E2	NTC	40.00		0.00	0.00
E3	NTC	E3	NTC	40.00		0.00	0.00
E4	NTC	E4	NTC	40.00		0.00	0.00
E5	NTC	E5	NTC	40.00		0.00	0.00
F6	NTC	F6	NTC	40.00		0.00	0.00

Figure A2.1 Beta-2-microglobulin assessment in six different samples by TaqMan®
7700 RT-PCR. The raw data shows a high degree of variation between triplicates.
For example, wells E10-E12 contain RNA extracted from HuVec endothelial cells
treated with 1.0mM H_2O_2 for 30min. The Ct values recorded are 22.13, 21.48 and
20.98. This is in contrast to the GAPDH readings illustrated in corresponding Figure
A1.2 in which replicates are extremely tight.

PE Applied Biosystems

Sequence Detection Systems
1.6.3

File Name:Controls
User:Jen
Date:Wed, Dec 13, 2000
Comments:Jennifer Control Plate - GAPDH

Plate Type:7700 Single Reporter☐
PCR Volume:25

Thermal Cycle Conditions

Cycle	Temperature	Time	Repeat	Ramp Time	Auto Increment
Hold	50.00	2:00		Auto	
Hold	95.00	10:00		Auto	
Cycle	95.00	0:15	40	Auto	
	60.00	1:00		Auto	

Standard Curve

Slope: 0.00
Intercept: 0.00
Fit R: 0.00

Threshold: 0.04
Baseline Range: (3 , 15)

Sample Information

Well	Type	Sample Name	Replicate	Ct	Quantity	Std. Dev.	Mean
C7	UNKN	H2O2 untreated		16.11		0.00	0.00
C8	UNKN	H2O2 untreated		16.10		0.00	0.00
C9	UNKN	H2O2 untreated		16.06		0.00	0.00
C10	UNKN	H2O2 1.0mM, 30min.		17.02		0.00	0.00
C11	UNKN	H2O2 1.0mM, 30min.		17.02		0.00	0.00
C12	UNKN	H2O2 1.0mM, 30min.		17.07		0.00	0.00
D1	UNKN	SD 72+ cont.		14.77		0.00	0.00
D2	UNKN	SD 72+ cont.		14.84		0.00	0.00
D3	UNKN	SD 72+ cont.		14.71		0.00	0.00
D4	UNKN	SD 72-		15.15		0.00	0.00
D5	UNKN	SD 72-		15.11		0.00	0.00
D6	UNKN	SD 72-		15.15		0.00	0.00
D7	UNKN	HS 8hr cont.		15.30		0.00	0.00
D8	UNKN	HS 8hr cont.		15.31		0.00	0.00
D9	UNKN	HS 8hr cont.		15.38		0.00	0.00
D10	UNKN	HS 8hr 60sec.		15.11		0.00	0.00
D11	UNKN	HS 8hr 60sec.		15.12		0.00	0.00
D12	UNKN	HS 8hr 60sec.		15.12		0.00	0.00
C1	NTC	C1	NTC	40.00		0.00	0.00
C2	NTC	C2	NTC	40.00		0.00	0.00
C3	NTC	C3	NTC	40.00		0.00	0.00
C4	NTC	C4	NTC	40.00		0.00	0.00
C5	NTC	C5	NTC	40.00		0.00	0.00

Figure A2.2 GAPDH assessment in six different samples by TaqMan® 7700 RT-PCR. The raw data shows a high degree of reproducibility between triplicates. For example, wells E10-E12 contain RNA extracted from HuVec endothelial cells treated with 1.0mM H_2O_2 for 30min. The Ct values recorded are 17.02, 17.02 and 17.07. This is in contrast to the beta-2-microglobulin readings illustrated in corresponding Figure A1.1 in which replicates show variable Ct values.

A3   LIST OF PRESENTATIONS & PUBLICATIONS RELATED TO THIS THESIS

PRESENTATIONS:

Galway, Ireland, April 14th, 2000. Joint Irish Association for Cancer Research and Irish Society of Medical Oncology Meeting. **Russell JM**, Uhlmann V, O'Leary JJ, Lawler M, Gaffney EF. In-cell amplification for the detection of c-abl mRNA in cell lines and tissue sections (poster).

London, UK, January 20th, 2000. Pathological Society of Great Britain and Ireland. Uhlmann V, Luttich K, O'Donovan M, Bermingham N, Silva I, Kenny C, Ring M, Sweeney M, Howells D, Picton S, **Russell JM**, Sheils O, O'Leary JJ. Novel in-cell amplification for the detection of DNA and RNA in tissue sections (oral).

Belfast, Northern Ireland, April 14th, 1999. Irish Association for Cancer Research Meeting. **Russell JM**, Sheils O, O'Leary JJ, Cotter T, Lawler M, Gaffney EF. Feasibility of gene expression studies in archival material using TaqMan RT-PCR (poster).

San Francisco, USA, March 22nd, 1999. United States and Canadian Academy of Pathology Meeting. O'Donovan M, **Russell JM**, Cotter TG, Lawler M, Fletcher CDM, O'Leary JJ, Gaffney EF. Abl and *abl* mRNA expression in liposarcoma: Correlation with tumour cell differentiation, angiogenesis and extent of apoptosis (poster).

Kilkenny, Ireland, Feb 6th, 1999. Academy of Medical Laboratory Science. **Russell JM**, Cotter TG, O'Leary JJ, Lawler M, Gaffney EF. mRNA analysis in archival material using TaqMan RT-PCR (oral).

Leicester, UK, July 1st, 1998. Pathological Society Meeting of Great Britain and Ireland. **Russell JM**, Dunne BM, O'Donovan M, O'Neill AJ, Cotter TG, Lawler M, Fletcher CDM, O'Leary JJ, Gaffney EF. Abl expression, angiogenesis and apoptosis in diffuse gastric adenocarcinoma and liposarcoma (oral).

Dublin, Ireland, June 21st, 1998. Joint British Association and Irish Association Cancer Research Meeting. **Russell JM**, O'Neill AJ, Dunne BM, O'Donovan M, Fletcher CDM, Lawler M, Gaffney EF. Abl expression in liposarcomas with particular reference to angiogenic tumour microvessels (poster).

Dublin, Ireland, June 21st, 1998. Joint British Association and Irish Association Cancer Research Meeting. **Russell JM**, O'Neill AJ, Dunne BM, O'Donovan M, Gillan JE, Cotter TG, Lawler M, Gaffney EF. Expression of the Abl oncoprotein in the neovasculature during enchondral ossification and in tumour angiogenesis (poster).

Belfast, Northern Ireland, May 2nd, 1998. Euro Cell Path Meeting. **Russell JM**, O'Neill AJ, Dunne BM, O'Donovan M, Gillan JE, Cotter TG, Lawler M, Gaffney EF.

Expression of the Abl oncoprotein during enchondral ossification and in tumour angiogenesis (poster).

Dublin, Ireland, March 27th, 1998. National Scientific Medical Meeting. **Russell JM**, O'Neill AJ, Dunne BM, O'Donovan M, Gillan JE, Cotter TG, Lawler M, Gaffney EF. Expression of the Abl oncoprotein during enchondral ossification and in tumour angiogenesis (poster).

Sheffield, UK, July 2nd, 1997. Pathological Society of Great Britain and Ireland. **Russell JM**, O'Donovan M, O'Neill AJ, Dunne BM, Cotter TG, Gillan J, Dervan PA, Lawler M, Gaffney EF. Abl expression in developing fetal cartilage and chondrosarcoma; relationship to chondrocyte differentiation and inhibition of apoptosis (oral).

Kinsale, Ireland, April 12th, 1997. Irish Association for Cancer Research. **Russell JM**, O'Neill AJ, Dunne BM, Cotter TG, Gillan J, Dervan PA, Lawler M, Gaffney EF. The c-Abl protein is required for differentiation and inhibition of apoptosis in fetal and neoplastic chondrocytes (oral).

PAPERS:

Uhlmann V, O'Leary JJ, Kennedy M, Luttich K, Silva I, **Russell JM**, Sheils O, Ring M, Sweeney M, Kenny C, Bermingham N, Howells D, Picton S, Lucas SB. Improved in-situ detection method for telomeric tandem repeats in metaphase spreads and interphase nuclei. *J Clin Pathol: Mol Pathol* 2000; **53**: 48-50

O'Donovan M, **Russell JM**, O'Leary JJ, Gillan JA, Lawler MP, Gaffney EF. Abl expression, tumour grade and apoptosis in chondrosarcoma. *J Clin Pathol: Mol Pathol* 1999; **52**(6): 341-344

O'Neill AJ, Cotter TG, **Russell JM**, Gaffney EF. Abl expression in human fetal and adult tissues, tumours and tumour microvessels. *J Pathol* 1997: 183; 325-329

ABSTRACTS:

Russell JM, O'Neill AJ, Dunne BM, O'Donovan M, Gillan JE, Cotter TG, Lawler M, Gaffney EF. Expression of the Abl oncoprotein in the neovasculature during enchondral ossification and in tumour angiogenesis. *Br J Cancer* 1998; 78(Suppl 1): P99

Russell JM, O'Neill AJ, Dunne BM, O'Donovan M, Gillan JE, Cotter TG, Lawler M, Gaffney EF. Expression of the Abl oncoprotein during enchondral ossification and in tumour angiogenesis. *Irish Journal of Medical Science* 1998; 167(Suppl 5): P38

Russell JM, O'Neill AJ, Dunne BM, O'Donovan M, Fletcher CDM, Lawler M, Gaffney EF. Abl expression in liposarcomas with particular reference to angiogenic tumour microvessels. *Br J Cancer* 1998; 78(Suppl 1): P98

Russell JM, O'Donovan M, O'Neill AJ, Dunne BM, Cotter TG, Gillan J, Dervan PA, Lawler M, Gaffney EF. Abl expression in developing fetal cartilage and chondrosarcoma; relationship to chondrocyte differentiation and inhibition of apoptosis. *J Pathol* 1997; 18(suppl): 24A

OTHER PRESENTATIONS AND PUBLICATIONS

O'Leary JJ, Kennedy M, Howells D, Silva I, Uhlmann V, Luttich K, Biddolph S, Lucas SB, **Russell JM**, Bermingham N, Ring M, Kenny C, Sweeney M, Sheils O, Isaacson P, Picton S, Gatter K. Cellular localisation of HHV 8 in Castlemans Disease: is there a link with lymph node vascularity? *J Clin Pathol: Mol Pathol* In Press

O'Leary JJ, Kennedy M, Luttich K, Uhlmann V, Silva I, **Russell JM**, Sheils O, Ring M, Sweeney M, Bermingham N, Howells D, Picton S, Lucas SB. Localisation of HHV 8 in AIDS related lymphadenopathy. *J Clin Pathol: Mol Pathol* 2000; **53**: 43-47

London, UK, January 20th, 2000. Pathological Society of Great Britain and Ireland. O'Donovan M, Bermingham N, Silva I, Luttich K, Howells D, Picton S, Uhlmann V, Ring M, Sweeney M, Kenny C, **Russell JM**, Sheils O, Lucas S, O'Leary JJ. Genome wide evaluation of Kaposi's sarcoma derived primary spindle cultures and HHV 8 transformed endothelial cells (poster).

Dublin, Ireland, November 26th, 1999. Irish Society of Gastroenterology. Lynch S, Dunne J, Abuzakouk M, **Russell JM**, Weir DG, Feighery C. Quantitation of IL-15 mRNA levels in the epithelial and lamina propria layers of human control and coeliac biopsies using TaqMan RT-PCR (poster).

9. REFERENCES

Abrams JM, White K, Fessler LI, Steller H. Programmed cell death during Drosophilia embryogenesis. *Development* 1993; **117**(1): 29-43

Adams JM. Oncogene activation by fusion of chromosomes in leukaemia. *Nature* 1985; **315**(6020): 542-543

Afford S, Randhawa S. Apoptosis [Review]. *Mol Pathol* 2000; **53**(2): 55-63

Agami R, Shaul Y. The kinase activity of c-Abl but not v-Abl is potentiated by direct interaction with RFXI, a protein that binds the enhancers of several viruses and cell-cycle regulated genes. *Oncogene* 1998; **16**: 1779-1788

Aguayo A, Kantarjian H, Manshouri T, Gidel C, Estey E, Thomas D, Koller C, Estrov Z, O'Brien S, Keating M, Freireich E, Albitar M. Angiogenesis in acute and chronic leukemias and myelodysplastic syndromes. *Blood* 2000; **96**(6): 2240-2245

Albitar M. Angiogenesis in acute myeloid leukemia and myelodysplastic syndrome. *Acta Haematol* 2001; **106**(4): 170-176

Alison MR. Identifying and quantifying apoptosis: a growth industry in the face of death. *J Pathol* 1999; **188**: 117-118

Ameisen JC, Capron A. Cell dysfunction and depletion in AIDS: the programmed cell death hypothesis. *Immunology Today* 1991; **12**(4): 102-105

Anderson JJ, Tiniakos DG, McIntosh GG, Autzen P, Henry JA, Thomas MD, Reed J, Horne GM, Lennard TWJ, Angus B, Horne CHW. Retinoblastoma Protein in human breast carcinoma: Immunohistochemical study using a new monoclonal antibody effective on routinely processed tissues. *J Pathol* 1996; **180**: 65-70

Arcaro A Wymann MP. Wortmannin is a potent phosphatidylinositol 3,4,5-triphosphate in neutrophil responses. *J Biochem* 1993; **296**: 297-301

Arends MJ, McGregor AH, Wyllie AH. Apoptosis is inversely related to necrosis and determines growth in tumors bearing constitutively expressed *myc*, *ras*, and HPV Oncogenes. *Am J Pathol* 1994; **144**(5): 1045-1057

Ashkenazi A, Dixit VM. Death receptors: signaling and modulation. *Science* 1998; **281**: 1305-1308

Bamberger ME, Landreth GE. Inflammation, apoptosis, and Alzheimer's disease. *Neuroscientist* 2002; **8**(3): 276-83.

Bankfalvi A, Navabi H, Bier B, Bocker W, Jasani B, Schmid KW. Wet autoclave pretreatment for antigen retrieval in diagnostic Immunohistochemistry. *J Pathol* 1994; **174**: 223-228

Barila D, Superti-Furgi G. An intramolecular SH3-domain interaction regulates c-Abl activity. *Nature Genetics* 1998; **18**: 280-282

Bartek J, Lukas J, Bartkova J. Perspective: Defects in cell cycle control and cancer. *J Pathol* 1999; **187**: 59-99

Bartova E, Kozubek S, Kozubek M, Jirsova P, Lukasova E, Skalnikova M, Buchnickova K. The influence of the cell cycle, differentiation and irradiation on the nuclear location of the *abl, bcr* and *c-myc* genes in human leukemic cells. *Leukemia Research* 2000; **24**: 233-241

Bartram CR, DeKlein A, Hagemeyer A, Van Agthoven T, Van Kessel AG, Bootsma D, Grosveld G, Ferguson-Smith MA, Davies T, Stone M. Translocation of *c-abl* oncogene correlates with the presence of the Philadelphia chromosome in chronic myelocytic leukemia. *Nature* 1983; **306**: 277-280

Baskaran R, Chiang GG, Wang JYJ. Identification of a Binding Site in c-Abl Tyrosine Kinase for the C-Terminal Repeated Domain of RNA Polymerase II. *Mol Cell Biol* 1996; **16**(7): 3361-3369

Baskaran R, Dahmus ME, Wang JYJ. Tyrosine phosphorylation of mammalian RNA polymerase II carboxy-terminal domain. *Proc Natl Acad Science USA* 1993; **90**(23): 11167-11171

Baskaran R, Wood LD, Whitaker LL, Canman CE, Morgan SE, Xu Y, Barlow C, Baltimore D, Wynshaw-Boris A, Kastan MB, Wang JYJ. Ataxia telangiectasia mutant protein activates c-Abl tyrosine kinases in response to ionizing radiation. *Nature* 1997; **387**: 516-519

Bates PJ, Sanderson G, Holgate ST, Johnston SL. A comparison of RT-PCR, in-situ hybridisation and in-situ RT-PCR for the detection of rhinovirus infection in paraffin sections. *J Virol Meth* 1997; **67**: 153-160

Battifora H, Kopinski M. The influence of protease digestion and duration of fixation on the immunostaining of keratins. A comparison of formalin and ethanol fixation. *J Histochem Cytochem* 1986; **34**(8): 1095-1100

Bedi A, Shakis SJ. Mechanisms of cell commitment in myeloid cell differentiation. [Review] *Current Opinion in Hematology* 1995; **2**(1): 12-21

Beecken WD, Kramer W, Jons D. New molecular mediators in tumour angiogenesis. *J Cell Mol Med* 2002; **4**(4): 262-269

Ben-Ezra J, Johnson DA, Rossi J, Cook N, Wu A. Effect of Fixation on the Amplification of Nucleic Acids from Paraffin-embedded Material by the Polymerase Chain Reaction. *J Histochem Cytochem* 1991; **39**(3): 351-354

Ben-Neriah Y, Bernards A, Paskind M, Daley GQ, Baltimore D. Alternative 5' Exons of c-*abl* mRNA. *Cell* 1986; **44**: 577-586

Bertolini F, Mancuso P, Gobbi A, Pruneri G. The thin red line: Angiogenesis in normal and malignant hematopoiesis. *Experimental Hematology* 2000; **28**: 993-1000

Bicknell GR, Shaw JA, Pringle JH, Furness PN. Amplification of specific mRNA from a single human renal glomerulus, with an approach to the separation of epithelial cell mRNA. *J Pathol* 1996; **180**: 188-193

Bjornsson J, McLeod RA, Unni KK. Primary chondrosarcoma of the long bones and limb girdles. *Cancer* 1998; **83**: 2105-2109

Blow JJ. The regulation of chromosome replication. *J Pathol* 1992; **167**: 175-179

Bonser RW, Thompson NT, Randall RW, Tateson JE, Spacey GD, Hodson HF, Garland LG. Demethoxyviridin and wortmannin block phospholipase C and D activation in the human neutrophil. *Br J Pharmacol* 1991; **103**: 1237-1241

Boom R, Sol CJA, Salimans MMM, Jansen CL, Wertheim-van Dillen PME, Van der Noordaa J. Rapid and Simple Method for Purification of Nucleic Acids. *J Clinical Microbiology* 1990; **28**(3): 495-503

Boshoff C, Schulz TF, Kennedy MM, Graham AK, Fisher C, Thomas A, McGee JO'D, Weiss RA, O'Leary JJ. Kaposi's sarcoma-associated herpesvirus infects endothelial and spindle cells. *Nature Medicine* 1995; **1**(12): 1274-1278

Bradford MM. A rapid and sensitive method for the quantitation of microgram quantities of protein utilizing the principle of dye binding. *Anal biochem* 1976; **72**: 248

Bramwell NH, Burns B. The effects of fixative type and fixation time on the quantity and quality of extractable DNA for hybridization studies in lymphoid tissue. *Exp Haem* 1988; **16**(8): 730-732

Brighton CT. Growth Plate: Structure and Physiology. *In* Orthopedics, Section XXIV, Chapter 162: 1994; 1643-1649

Brown A, Browes C, Mitchell M, Montano X. c-abl is involved in the association of p53 and trk A. *Oncogene* 2000; **19**: 3032-3040

Brown L, McCarthy N. A sense-abl response? *Nature* 1997; **387**: 450-451

Cance WG, Brennan MF, Dudas ME, Huang C-M, Cordon-Cardo C. Altered expression of the retinoblastoma gene product in human sarcomas. *N Engl J Med* 1990; **323**(21): 1457-1463

Carr NJ, Talbot IC. In situ end labelling: effect of proteolytic enzyme pretreatment and hydrochloric acid. *J Clin Pathol* 1997; **50**: 160-163

Chavakis E, Dimmeter S. Regulation of endothelial cell survival and apoptosis during angiogenesis. *Arterioscler Thromb Vasc Biol* 2002; **22**(6): 887-893

Chen X. The p53 family: same response, different signals? *Mol Med Today* 1999; **5**: 387-392

Chiu KP, Cohen SH, Morris DW, Jordan GW. Intracellular amplification of proviral DNA in tissue sections using the polymerase chain reaction. *J Histochem Cytochem* 1992; **40**(3): 333-341

Chomiczynski P, Sacchi N. Single step method of RNA isolation by acid guanidium thiocyanate-phenol-chloroform extraction. *Anal Biochem* 1987; **162**: 156-159

Coates PJ, D'Ardenne AJ, Khan G, Kangro HO, Slavin G. Simplified procedures for applying the polymerase chain reaction to routinely fixed paraffin waxed sections. *J Clin Pathol* 1991; **44**: 115-118

Cohen GM, Sun XM, Snowden T, Dinsdale D, Skilleter DN. Key morphological features of apoptosis may occur in the absence of internucleosomal DNA fragmentation. *Biochem J* 1992; **286**: 331-334

Cong F, Goff SP. c-Abl-induced apoptosis, but not cell cycle arrest, requires mitogen-activated protein kinase kinase 6 activation. *Proc Natl Acad Sci, USA* 1999; **96**(24): 13819-13824

Cooper JA. The src family of protein tyrosine kinsaes. In: *Peptides and Protein Phosphorylation* (B.Kemp, ed.). 1990; pp.85-113. Boca Raton, FL: CRC Press

Corradini P, Inghirami G, Astolfi M, Ladetto M, Voena C, Ballerini P, Gu W, Nilsson K, Knowles DM, Boccadoro M, Pileri A, Dalla-Favera R. Inactivation of Tumor Suppressor Genes, p53 and Rb1, in Plasma Cell Dyscrasias. *Leukemia* 1994; **8**(5): 758-767

Cortez D, Kadlec L, Pendergast AM. Structural and signalling requirements for BCR-ABL-mediated transformation and inhibition of apoptosis. *Mol Cell Biol* 1995; **15**(10): 5531-5541

Cotter TG. BCR-ABL: an anti-apoptosis gene in chronic myelogenous leukemia. *Leuk Lymphoma* 1995; **18**: 231-236

Cross MJ, Stewart A, Hodgkin MN, Wakelam MJ. Wortmannin and its structural analogue demothoxyviridin inhibit stimulated phospholipase A2 activity in Swiss 3T3 cells. Wortmannin is not a specific inhibitor of phosphatidylinositol 3-kinase. *J Biol Chem* 1995; **270**(43): 25352-25355

Cross NC, Reiter A. Tyrosine kinse fusion genes in chronic myeloproliferative diseases. *Leukemia* 2002; **16**(7): 1207-1212

Curran S, McKay JA, McLeod HL, Murray GI. Laser capture microscopy. *J Clin Pathol: Mol Pathol* 2000; **53**: 64-68

Dada MA, Chetty R, Biddolph SC, Schneider JW, Gatter KC. The immunoexpression of bcl-2 and p53 in Kaposi's sarcoma. *Histopathology* 1996; **29**: 159-163

Dai Z, Pendergast AM. Abi-2, a novel SH3-containing protein interacts with the c-Abl tyrosine kinase and modulates c-Abl transforming activity. *Genes Dev.* 1995; **9**: 2569-2582

Daley GQ, Van Etten RA, Jackson PK, Bernards A, Baltimore D. Nonmyristoylated Abl proteins transform a factor-dependent hematopoietic cell line. *Mol Cell Biol* 1992; **12**(4):1864-1871

Dan S, Naito M, Seimiya H, Kizaki A, Mashima T, Tsuruo T. Activation of c-Abl tyrosine kinase requires caspase activiation and is not involved in JNK/SAPK activation during apoptosis of human monocytic leukemia cells. *Oncogene* 1999; **18**: 1277-1283

Danial NN, Losman A, Lu T, Yip N, Krishnan K, Krolewski J, Goff SP, Wang JYJ, Rothman PB. Direct Interaction of Jak1 and *v*-Abl is Required for *v*-Abl-Induced Activation of STATs and Proliferation. *Mol Cell Biol* 1998; **18**(11): 6795-6804

Daniel R, Wong PMC, Chung SW. Isoform-specific functions of c-abl: Type I is Necessary for Differentiation, and type IV is Inhibitory to Apoptosis. *Cell Growth and Differentiation* 1996; **7**: 1141-1148

David-Cordonnier MH, Hamdane M, Bailly C, D'Halluin JC. Determination of the human c-Abl consensus DNA binding site. *FEBS Letters* 1998; **424**: 177-182

David-Cordonnier MH, Payet D, D'Halluin JC, Waring MJ, Travers AA, Bailly C. The DNA-binding domain of human c-Abl tyrosine kinase promotes the interaction of a HMG chromosomal protein with DNA. *Nucl Acids Research* 1999; **27**(11): 2265-2270

Dei Tos AP, Doglioni C, Piccinin S, Maestro R, Mentzel T, Barbareschis M, Boiocchi M, Fletcher CDM. Molecular abnormalities of the p53 pathway in dedifferentiated liposarcoma. *J Pathol* 1997; **181**: 8-13

Desagher S, Martinou JC. Mitochondria as the central control point of apoptosis [Review]. *Trends in Cell Biology* 2000; **10**: 369-377

Dhut S, Chaplin T, Young BD. BCR/ABL and BCR proteins: biochemical characterisation and localisation. *Leukemia* 1990; **4**: 745-750

Dhut S, Dorey EL, Hortan MA, Ganesan TS, Young BD. Identification of two normal bcr gene products in the cytoplasm. *Oncogene* 1988; **3**: 561-566

DiGiuseppe JA, Kastan M. Apoptosis in haematological malignancies. *J Clin Pathol* 1997; **50**: 361-364

Dirnhofer S, Berger C, Untergasser G, Geley S, Berger P. Human β-actin retropseudogenes interfere with RT-PCR. *Trends in Genetics* 1995; **11**(10): 380-381

Doyle CT, O'Leary JJ. The search for the universal fixative or 'Magic Juice'. *J Pathol* 1992; **166**: 331-332

Dragovich T, Rudin CM, Thompson CB. Signal transduction pathways that regulate cell survival and cell death. *Oncogene* 1998; **17**: 3207-3213

Druker BJ, Lydon NB. Lessons learned from the development of an Abl tyrosine kinase inhibitor for chronic myelogenous leukaemia. *J Clin Invest* 2000; **105**(1): 3-7

Dubois MF, Marshall NF, Nguyen VT, Dahmus GK, Bonnet F, Dahmus ME, Bensaude O. Heat shock of HeLa cells inactivates a nuclear protein phosphatase specific for dephosphorylation of the C-terminal domain of RNA polymerase II. *Nucleic Acids Res* 1999; **27**:1338-1344

Dumont DJ, Yamaguchi TP, Conlon RA, Rossant J, Breitman ML. tek, a novel tyrosine kinase gene located on mouse chromosome 4, is expressed in endothelial cells and their presumptive precursors. *Oncogene* 1992; **7**: 1471-1480

Ebina M, Steinberg SM, Mulshine JL, Linnoila RI. Relationship of p53 Overexpression and Up-regulation of Proliferating Cell Nuclear Antigen with the clinical course of Non-Small Cell Lung Cancer. *Cancer Res* 1994; **54**: 2496-2503

Embleton MJ, Gorochov G, Jones PT, Winter G. In-cell PCR from mRNA:amplifying and linking the rearranged immunoglobulin heavy and light chain V-genes within single cells. *Nucl Acids Res* 1992; **20**: 3831-3837

Erlich HA, Gelfand D, Sninsky JJ. Recent advances in the polymerase chain reaction. *Science* 1991; **252**(5013): 1643-1651

Evans PAS, Short MA, Jack AS, Norfolk DR, Child JA, Shiach CR, Davies F, Tobal K, Liu Yin JA, Morgan GJ. Detection and quantitation of the CBFβ/MYH11 transcripts associated with the inv(16) in presentation and follow-up samples from patients with AML. *Leukemia* 1997; **11**: 364-369

Fabbri M, Bannkyh S, Balch WE. Export of protein from the endoplasmic reticulum is regulated by a diacylglycerol/phorbol ester binding protein. *J Biol Chem* 1994; **269**: 26848-26857

Faderl S, Talpaz M, Estrov Z, O'Brien S, Kurzrock R, Kantarjian HM. The biology of chronic myeloid leukemia. *N Eng J Med* 1999; **341**(3): 164-172

Fainstein E, Marcella C, Rosner A, Canaani E, Gale RP, Dreazen O, Smith SD, Croce CM. A new fused transcript in Philadelphia chromosome acute lymphocytic leukemia. *Nature* 1987; **330**: 386-388

Farnum CE, Wilsman NJ. Cellular turnover at the chondo-osseous junction of growth plate cartilage: analysis by serial sections at the light microscopical level. *J Ortho Res* 1989; **7**(5): 654-666

Feinberg AP, Vogelstein B. A technique for radiolabeling DNA restriction endonuclease fragments to high specific activity. *Anal Biochem* 1983; **132**: 6-13

Feller SM, Ren R, Hanafusa H, Baltimore D. SH2 and SH3 domains as molecular adhesives: the interactions of Crk and Abl. *Trends in Biochemical Sciences* 1994; **19**(11): 453-458

Fend F, Raffeld M. Laser capture microdissection in pathology. *J Clin Pathol* 2000; **53**: 666-672

Fernandes RS, Gorman AM, McGahon A, Lawlor M, McCann S, Cotter TG. The repression of apoptosis by activated abl oncogenes in chronic myelogenous leukaemia. *Leukemia* 1996; **10**(2s): 17-21

Finke J, Fritzen R, Ternes P, Lange W, Dolken G. An Improved Strategy and a Useful Housekeeping Gene for RNA Analysis from Formalin-Fixed, Paraffin-Embedded Tissues by PCR. *BioTechniques* 1993; **14**(3): 448-453

Flaman JM, Waridel F, Estreicher A, Vannier A, Limacher JM, Gilbert D, Iggo R, Frebourg T. The human tumour suppressor gene p53 is alternatively spliced in normal cells. *Oncogene* 1996; **12**: 813-818

Folkman J. Tumor angiogenesis: therapeutic implications. *N Engl J Med* 1971; **285**(21): 1182-1186

Foulkes NS, Sassone-Corso P. More is Better: Activators and Repressors from the Same Gene. *Cell* 1992; **68**: 411-414

Franz WM, Berger P, Wang JYJ. Deletion of an N-terminal regulatory domain of the c-*abl* tyrosine kinase activates its oncogenic potential. *EMBO J* 1989; **8**(1): 137-147

Gaffney EF, O'Neill AJ, Staunton MJ. In situ end-labelling, light microscopic assesment and ultrastructure of apoptosis in lung carcinoma. *J Clin Pathol* 1995; **48**(11): 1017-1021

Gaffney EF. The extent of apoptosis in different types of high grade prostatic carcinoma. *Histopathology* 1994; **25**: 269-273

Gale RP, Grosveld G, Canaani E, Goldman JM. Chonic Myelogenous Leukemia: Biology and Therapy. *Leukemia* 1993; **7**: 653-658

Gazzeri S, Brambilla E, Caron de Fromentel C, Gouyer V, Moro D, Perron P, Berger F, Brambilla C. p53 Genetic abnormalities and *myc* activation in human lung carcinoma. *Int J Cancer* 1994; **58**: 24-32

Gelmini S, Orlando C, Sestini R, Vona G, Pinzani P, Ruocco L, Pazzagli M. Quantitative polymerase chain reaction-based homogeneous assay with fluorogenic probes to measure c-*erb*B-2 oncogene amplification. *Clin Chem* 1997; **43**(5): 752-758

George D. Platelet-derived growth factor receptors: a therapeutic target in solid tumours. *Semin Oncol* 2001; **28**(5): 27-33

Gerard CJ, Andrejka LM, Macina RA. Mitochondrial ATP synthase 6 as an Endogenous Control in the Quantitative RT-PCR Analysis of Clinical Cancer Samples. *Mol Diagn* 2000; **5**(1): 39-46

Gibson UEM, Heid CA, Williams PM. A Novel Method for Real Time Quantitative RT-PCR. *Genome Research* 1996; **6**: 995-1001

Gimbrone MA, Leapman SB, Cotran RS, Folkman J. Tumour dormancy *in vivo* by prevention of neovascularisation. *J Exp Med* 1972; **3**: 77-85

Goelz SE, Hamilton SR, Vogelstein B. Purification of DNA from formaldehyde fixed and paraffin embedded human tissues. *Biochem Biophys Res Commun* 1985; **130**(1): 118-126

Goga A, McLaughlin J, Afar DE, Saffran DC, Witte ON. Alternative signals to RAS for hematopoietic transformation by the BCR-ABL oncogene. *Cell* 1995; **82**(6): 981-988

Going JJ, Lamb RF. Practical histological microdissection for PCR Analysis. *J Pathol* 1996; **179**: 121-124

Goldstein SR, McQueen PG, Bonner RF. Thermal modeling of laser capture microdissection. *Appl Opt* 1998; **37**: 7378-7391

Gong J, Costanzo A, Yang HQ, Melino G, Kaelin WG Jr., Levrero M, Wang JYJ. The tyrosine kinase c-Abl regulates p73 in apoptotic response to cisplatin-induced DNA damage. *Nature* 1999; **399**: 806-809

Gotoh A, Broxmeyer HE. The function of BCR/ABL and related proto-oncogenes. *Curr Opinion Hematology* 1997; **4**: 3-11

Gotoh A, Miyazawa K, Ohyashiki K, Toyama K. Potential molecules implicated in downstream signalling pathways of p185$^{BCR-ABL}$ in Ph$^+$ ALL involve GTPase activating protein, phopholipase C-$_{\gamma 1}$, and phosphatidylinositol 3'-kinase. *Leukemia* 1994; **8**: 115-120

Greer CE, Lund JK, Manos MM. PCR Amplification from Paraffin-embedded Tissues: Recommendations on Fixatives for Long-Term Storage and Prospective Studies. *In PCR Methods and Applications* 1991; 46-49

Greer CE, Peterson SL, Kiviat NB, Manos MM. PCR Amplification from Paraffin-embedded tissues – Effects of Fixative and Fixation Time. *Am J Clin Pathol* 1991; **95**(2): 117-124

Groffen J, Stephenson JR, Heisterkamp N, deKlein A, Bartram CR, Grosveld G. Philadelphia chromosomal breakpoints are clustered with a limited region, bcr, on chromosome 22. *Cell* 1984; **36**: 93-99

Guinee DG, Holden JA, Benfield JR, Woodward ML, Przygodzki RM, Fishback NF, Koss MN, Travis WD. Comparison of DNA Topoisomerase IIα Expression in Small Cell and Nonsmall Cell Carcinoma of the lung. In Search of a Mechanism of Chemotherapeutic Response. *Cancer* 1996; **78**(4): 729-735

Gupta S. Molecular steps of cell suicide: an insight into immune senescence. *J Clin Immunol* 2000; **20**: 229-239

Gupta S. Molecular steps to death receptor and mitochondrial pathways of apoptosis. *Life Sciences* 2001; **69**: 2957-2964

Haake AR, Polakowska RR. Cell Death by Apoptosis in Epidermal Biology. *Journal of Investigative Dermatology* 1993; **101**(2): 107-112

Haase AT, Retzel EF, Staskus KA. Amplification and detection of lentiviral DNA inside cells. *Proc Natl Acad Sci USA* 1990; **87**(13): 4971-4975

Hall PA, Meek D, Lane DP. p53-Integrating the Complexity. *J Pathol* 1996; **180**: 1-5

Hamdane M, David-Cordonnier MH, D'Halluin JC. Activation of p65 NF-kappa B protein by p210BCR-ABL in a myeloid cell line. *Oncogene* 1997; **15**(19): 2267-2275

Hanahan D, Folkman J. Patterns and emerging mechanisms of the angiogenic switch during tumourigenesis. *Cell* 1996; **86**: 353-364

Hanahan D, Weinberg RA. The Hallmarks of Cancer. *Cell* 2000; **100**: 57-70

Handel ML, McMorrow LB, Gravallese EM. Nuclear factor kB in rheumatoid synovium. *Arthritis & Rheumatism* 1995; **38**: 1762-1770

Hanks S, Hunter T. The eukaryotic protein kinase superfamily: Kinase catalytic domain structure and classification. *FASEB J* 1995; **9**: 576-596

Harrison TJ. The polymerase chain reaction – a time of transition from research to routine. *J Clin Pathol* 1998; **51**(7): 491-492

Hasegawa T, Seki K, Yang P. Differentiation and proliferative activity in benign and malignant cartilaginous tumours of bone. *Hum Pathol* 1995; **26**: 838-845

Heid CA, Stevens J, Livak KJ, Williams PM. Real Time Quantitative PCR. *Genome Research* 1996; **6**: 986-994

Hengartner MO. The biochemistry of apoptosis. *Nature* 2000; **407**: 770-775

Heriche JK, Chambaz EM. Protein kinase CK2α is a target for the Abl and Bcr-Abl tyrosine kinases. *Oncogene* 1998; **17**: 13-18

Herrington CS. Demystified…In situ hybridisation. *J Clin Pathol: Mol Pathol* 1998; **51**: 8-13

Herstens HMJ, Poddighe PJ, Haselaar GJM. A Novel In Situ Hybridization Signal Amplification Method Based on the Deposition of Biotinylated Tyramine. *J Histochem Cytochem* 1995; **43**(4): 347-352

Heuttner CS, Zhang P, Van Etten RA, Tenen DG. Reversibility of acute B-cell leukaemia induced by *BCR-ABL1*. *Nat Genet* 2000; **24**: 57-60

Hickman JA. Apoptosis and tumourigenesis. *Current Opinion in Genetics & Development* 2002; **12**: 67-72

Higuchi R, Dollinger G, Walsh PS, Griffith R. Simultaneous amplification and detection of specific DNA sequences. *Biotechnology* 1992; **10**(4): 413-417

Higuchi R, Fockler C, Dollinger G, Watson R. Kinetic PCR Analysis: Real-time Monitoring of DNA Amplification Reactions. *Biotechnology* 1993; **11**: 1026-1030

Hobson B, Denekamp J. Endothelial proliferation in tumours and nomal tissues: continuous labelling studies. *Br J Cancer* 1984; **49**(4): 405-413

Holden JA, Snow GW, Perkins SL, Jolles CJ, Kjeldsberg CR. Immunohistochemical Staining for DNA Topoisomerase II in Frozen and Formalin-Fixed Paraffin-Embedded Human Tissues. *Mod Pathol* 1994; **7**(8): 829-834

Holgate CS, Jackson P, Pollard K, Lunny K, Bird CC. Effect fixation on T and B Lymphocyte Surface Membrane Antigen demonstration in paraffin processed tissue. *J Pathol* 1986; **149**: 293-300

Holland PM, Abramson RD, Watson R, Gelfand DH. Detection of specific polymerase chain reaction product by utilizing the 5' to 3' exonuclease activity of *Thermus aquaticus* DNA polymerase. *Proc Natl Acad Sci USA* 1991; **88**: 7276-7280

Hoof T, Riordan JR, Tummler B. Quantitation of mRNA by the kinetic polymerase chain reaction assay: a tool for monitoring P-glycoprotein gene expression. *Anal Biochem* 1991; **1996**(1): 161-169

Huang Y, Yuan ZM, Ishiko T, Nakada S, Utsuqisawa T, Kato T, Kharbanda S, Kufe DW. Pro-apoptotic effect of the c-Abl tyrosine kinase in the cellular response to 1-β-D-arabinofuranosylcytosine. *Oncogene* 1997; **15**: 1947-1952

Hudson L, Hay FC (eds). Practical Immunology, 1st edition; 1976. Blackwell Scientific Publications, Oxford.

Hunter T. Signalling – 2000 and beyond. *Cell* 2000; **100**:113-127

Hussong JW, Rodgers GM, Shami PJ. Evidence of increased angiogenesis in patients with acute myeloid leukemia. *Blood* 2000; **95**: 309-315

Ibrahim MS, Lofts RS, Jahrling PB, Henchal PB, Weedn VW, Northrup MA, Belgrader P. Real-Time Microchip PCR for detecting Single-Base Differences in Viral and Human DNA. *Anal Chem* 1998; **70**: 2013-2017

Ito Y, Pandey P, Mishra N, Kumar S, Narula N, Kharbanda S, Saxena S, Kufe D. Targeting of the c-Abl tyrosine kinase to mitochondria in endoplasmic reticulum stress induced apoptosis. *Mol Cell Biol* 2001; **21**(8): 6233-6242

Jackson DP, Lewis FA, Taylor GR, Boylston AW, Quirke P. Tissue extraction of DNA and RNA and analysis by the polymerase chain reaction. *J Clin Pathol* 1990; **43**(6): 499-504

Jain SK, Susa M, Keeler ML, Carlesso N, Druker B, Varticovski L. PI3-kinase activation in BCR-abl-transformed hematopoietic cells does not require interaction of p85 SH2 domains with p210 BCR/abl. *Blood* 1996; **88**(5): 1542-1550

Jarpe MB, Widmann C, Knall C, Schlesinger TK, Gibson S, Yujiri T, Fanger GR, Gelfan EW, Johnson GL. Anti-apoptotic *versus* pro-apoptotic signal transduction: Checkpoints and stop-signs along the road to death. *Oncogene* 1998; **17**: 1475-1482

Jena N, Deng M, Sicinska E, Sicinska P, Daley CQ. Critical role for cyclin D2 in BCR/ABL-induced proliferation of hematopoietic cells. *Cancer Res* 2002; **62**(2): 535-541

Jing Y, Nakajo S, Xia L, Nakaya K, Fang Q, Waxman S, Han R. Boswellic acid acetate induces differentiation and apoptosis in leukemia cell lines. *Leukemia Research* 1999; **23**: 43-50

Kaghad M, Bonnet H, Yang A, Creancier L, Biscan JC, Valent A, Minty A, Chalon P, Lelias JM, Dumont X, Ferrara P, McKeon F, Caput D. Monoallelically Expressed Gene Related to p53 at 1p36, a Region Frequently Deleted in Neuroblastoma and Other Human Cancers. *Cell* 1997; **90**: 809-819

Kaklamanis L, Savage A, Mortensen N, Tsiotos P, Doussis-Anagnostopoulou I, Biddolph S, Whitehouse R, Harris AL, Gatter KC. Early expression of bcl-2 protein in the adenocarcinoma sequence of colorectal neoplasia. *J Pathol* 1996; **179**: 10-14

Kantarjian HM, Deisseroth A, Kurzrock R, Estrov Z, Talpaz M. Chronic Myelogenous Leukemia: A Concise Update. *Blood* 1993; **82**: 691-703

Kawano S, Miller CW, Gombart AF, Bartram CR, Matsuo Y, Asou H, Sakashita A, Said J, Tatsumi E, Koeffler HP. Loss of *p73* Gene Expression in Leukemias/ Lymphomas Due to Hypermethylation. *Blood* 1999; **94**(3): 1113-1120

Kennedy MM, Cooper K, Howells DD, Picton S, Biddolph S, Lucas SB, McGee JO'D, O'Leary JJ. Identification of HHV8 in early Kaposi's sarcoma: implications for Kaposi's sarcoma pathogenesis. *J Clin Pathol: Mol Pathol* 1998; **51**: 14-20

Kennedy MM, Lucas SB, Jones RR, Howells DD, Picton SJ, Bardon A, Comley IL, McGee JO'D, O'Leary JJ. HHV8 and Female Kaposi's sarcoma. *J Pathol* 1997a; **183**: 447-452

Kennedy MM, Lucas SB, Jones RR, Howells DD, Picton SJ, Hanks EE, McGee JO'D, O'Leary JJ. HHV8 and Kaposi's sarcoma: a time cohort study. *J Clin Pathol* 1997b; **50**: 96-100

Kernohan NM, Cox LS. Regulation of apoptosis by Bcl-2 and its regulated proteins: Immunochemical challenges and therapeutic implications. *J Pathol* 1996; **179**: 1-3

Kerr JFR, Wyllie AH, Currie AR. Apoptosis: A basic biological phenomenon with wide ranging implications in tissue kinetics. *Br J Cancer* 1972; **26**: 239-257

Kerstens HMJ, Poddighe PJ, Hanselaar AGJM. A Novel In Situ Hybridization Signal Amplification Method Based on the Deposition of Biotinylated Tyramine. *J Histochem Cytochem* 1995; **43**(4): 347-352

Kharbanda S, Yuan ZM, Weichselbaum R, Kufe D. Determination of cell fate by c-Abl activation in the response to DNA damage. *Oncogene* 1998; **17**(25): 3309-3318

Kharbanda S, Bharti A, Pei D, Wang J, Pandey P, Ren R, Weichselbaum R, Walsh CT, Kufe D. The stress response to ionizing radiation involves c-Abl dependent phosphorylation of SHPTP1. *Proc Natl Acad Sci USA* 1996; **93**(14): 6898-6901

Kharbanda S, Pandey P, Ren R, Mayer B, Zon L, Kufe D. c-Abl Activation Regulates Induction of the SEK1/Stress-activated Protein Kinase Pathway in the Cellular Response to 1-β-D-Arabinofuranosylcytosine. *J Biol Chem* 1995a; **270**(51): 30278-30281

Kharbanda S, Ren R, Pandey P, Shafman TD, Feller SM, Weichselbaum RR, Kufe DW. Activation of the c-Abl tyrosine kinase in the stress response to DNA damaging agents. *Nature* 1995b; **376**: 785-788

Kharbanda S, Yuan ZM, Weichselbaum R, Kufe D. Functional role for the c-Abl protein tyrosine kinase in the cellular response to genotoxic stress. *Biochimica et Biophysica Acta* 1997; **1333**: O1-O7

Kidd V, Lion T. Debate round-table. Approptiate controls for RT-PCR. *Leukaemia* 1996; **11**(6): 871-881

Kilpatrick SE, Doyon J, Choong PFM, Slim FH, Nascimento AG. The Clinicopathologic Spectrum of Myxoid and Round Cell Liposarcoma. A study of 95 Cases. *Cancer* 1996; **36**: 785-788

Kim JW, Kim SJ, Han SM, Paik SY, Hur SY, Kim YW, Lee JM, Namkoong SE. Increased glyceraldehyde-3-phosphate dehydrogenase expression in human cervical cancers. *Heart Vessels* 1998; **13**(1): 1-8

King G, Payne S, Walker F, Murray GI. A highly sensitive detection method for immunohistochemistry using biotinylated tyramine. *J Pathol* 1997; **183**: 237-241

Kipreos ET, Wang JYJ. Differential phosphorylation of c-*abl* in cell cycle determined by cdc2 kinase and phosphatase activity. *Science* 1990; **248**: 217-220

Kipreos ET, Wang JYJ. Cell cycle-regulated binding of c-*abl* tyrosine kinase to DNA. *Science* 1992; **256**: 382-385

Kissil JL, Kimchi A. Death-associated proteins: from gene identification to the analysis of their apoptotic and tumour suppressive functions. *Mol Med Today* 1998; **4**: 268-274

Kneba M, Eick S, Herbst H, Pott C, Bolz I, Dallenbach F, Hiddemann W, Stein H. Low Incidence of mbr *bcl*-2/J_H Fusion Genes in Hodgkin's Disease. *J Pathol* 1995; **175**: 381-389

Knudson CM, Korsmeyer SJ. *Bcl-2* and *Bax* function independently to regulate cell death. *Nat Genetics* 1997; **16**: 358-363

Kohn KW. Molecular interaction map of the mammalian cell cycle control and DNA repair. *Mol Cell Biol* 1999; **10**: 2703-2734

Koleske AJ, Gilford AM, Scott ML, Nee M, Bronson RT, Miczek KA, Baltimore D. Essential roles for the Abl and Arg tyrosine kinases in neurulation. *Neuron* 1998; **21**(6): 1259-1272

Kolibaba KS, Druker BJ. Protein tyrosine kinases and cancer. *Biochimica et Biophysica Acta* 1997; **1333**: F217-F248

Komminoth P, Long AA, Ray R, Wolfe HJ. In situ polymerase chain reaction detection of viral DNA, single-copy genes, and gene rearrangements in cell suspensions and cytospins. *Diagn Mol Pathol* 1992b; **1**(2): 85-97

Komminoth P, Long AA. In-situ polymerase chain reaction. [Review] *Virchows Archiv B Cell Pathol* 1993; **64**: 67-73

Komminoth P. Digoxigenin as an alternative probe labeling for in situ hybridisation. *Diagn Mol Pathol* 1992a; **1**(12): 142-150

Konopka JB, Watanbe SM, Witte ON. An alteration of the human c-Abl protein in K562 leukemia cells unmasks associated tyrosine kinase activity. *Cell* 1984; **37**: 1035-1042

Koreth J, O'Leary JJ, McGee JO'D. Microsatellites and PCR Genomic Analysis. *J Pathol* 1996; **178**: 239-248

Korsmeyer SJ. Bcl-2: An Antidote to Programmed Cell Death. *In* Cancer Surveys, Volume 15: Oncogenes in the Development of Leukaemia, pg 105-118

Kroemer G, Dallaporta B, Resche-Rigon M. The mitochondrial death/life regulator in apoptosis and necrosis. *Annu Rev Physiol* 1998; **16**: 1055-1064

Kroemer G, Zamzami N, Susin SA. Mitochondrial control of apoptosis [Review]. *Immunol Today* 1997; **18**(1): 44-51

Kroemer G. The proto-oncogene Bcl-2 and its role in regulating apoptosis. *Nat Medicine* 1997; **3**(6): 614-620

Kubbutat MHG, Voudsen KH. Keeping an old friend under control: regulation of p53 stability. *Mol Med Today* 1998; **4**: 250-256

Kumar S, Bharti A, Mishra NC, Raina D, Kharbnda S, Saxena S, Kufe D. Targeting of the c-Abl tyrosine kinase to mitochondira in the necrotic cell death to oxidative stress. *J Biol Chem* 2001; **276**(20): 17281-17285

Kumar S, Mshra N, Raina D, Saxena S, Kufe D. Abrogation of the cell death response to oxidative stress by the c-Abl tyrosine kinase inhibitor STI571. *Mol Pharmacol* 2003; **63**(2): 276-282

Kurian KM, Watson CJ, Wyllie AH. DNA Chip Technology. *J Pathol* 1999; **187**: 267-271

Kuwano K, Hagimoto N, Nomoto Y, Kawasaki M, Kunitake R, Fujita M, Miyazaki H, Hara N. p53 and p21 (Waf1/Cip1) mRNA Expression Associated with DNA Damage and Repair in Acute Immune Complex Alveolitis in Mice. *Laboratory Investigation* 1997; **76**(2): 161-169

Landers RJ, O'Leary JJ, Crowley M, Healy I, Annis P, Burke L, O'Brien D, Hogan J, Kealy WF, Lewis FA, Doyle CT. Epstein-Barr virus in normal, pre-malignant, and malignant lesions of the uterine cervix. *J Clin Pathol* 1993; **46**: 931-935

Leavitt J, Gunning P, Porreca P. Ng SY, Lin CS, Kedes L. Molecular cloning and characterisation of mutant and wild-type human beta-actin genes. *Clinical Chemistry* 1984; **4**(10): 1961-1969

Leoncini L, Del Vecchio MT, Megha T, Barbini P, Galieni P, Pileri S, Sabattini E, Gherlinzoni F, Tosi P, Kraft R, Cottier H. Correlations between Apoptotic and Proliferative Indices in Malignant Non-Hodgkin's Lymphomas. *Am J Pathol* 1993; **142**: 755-763

Leong AS-Y, Milios J. Accelerated Immunohistochemical Staining by Microwaves. *J Pathol* 1990; **161**: 327-334

Lewis FA. *In situ* PCR - myth or magic? *J Cell Pathol* 1996; **1**: 13-23

Lewis JM, Baskaran R, Taagepera S, Schwartz MA, Wang JYJ. Integrin regulation of c-Abl tyrosine kinase activity and cytoplasmic-nuclear transport. *Proc Natl Acad Sci, USA* 1996: **93**: 15174-15179

Li B, Cong F, Tan CP, Wan SX, Goff SP. Aph2, a protein with a zf-DHHC motif, interacts with c-Abl and has Pro-Apoptotic activity. *J Biol Chem* May 20 [e-pub, ahead of print]; 2002

Li X, Cai M. Recovery of the yeast cell cycle from heat shock-induced G(1) arrest involves a positive regulation of G(1) cyclin expression by the S phase cyclin Clb5. *J Biol Chem* 1999; **274**: 24220-24231

Lie YS, Petropoulos CJ. Advances in quantitative PCR technology: 5' nuclease assays. *Current Opinion in Biotechnology* 1998; **9**: 43-48

Litwin C, Leong KG, Zapf R, Sutherland H, Narman SC, Karsan A. Role of the microenvironment in acute myeloid leukemia. *Am J Pathol* 2002; **70**(1): 22-30

Liu J, Wu Y, Arlinghaus RB. Sequences within the first exon of BCR inhibit the activated tyrosine kinase of c-Abl and the Bcr-Abl oncoprotein. *Cancer Res* 1996; **56**: 5120-5124

Livak KJ, Flood SJA, Marmaro J, Giusti W, Deetz K. Oligonucleotides with Fluorescent Dyes at Opposite Ends Provide a Quenched Probe System Useful for Detecting PCR Product and Nucleic Acid Hybridization. *PCR Methods and Applications* 1995; **4**: 357-362

Livak KJ. Allelic Discrimination using fluorogenic probes and the 5' nuclease assay. *Genetic Analysis: Biomolecular Engineering* 1999; **14**:143-149

Long AA, Komminoth P, Lee E, Wolfe HJ. Comparison of indirect and direct in-situ polymerase chain reaction in cell preparations and tissue sections. Detection of viral DNA, gene rearrangements and chromosomal translocations. *Histochemistry* 1993; **99**: 151-162

Luthra R, McBride JA, Cabanillas F, Sarris A. Novel 5' Exonuclease-Based Real-Time PCR Assay for the Detection of t(14;18)(q32;q21) in Patients with follicular Lymphoma. *Am J Pathol* 1998; **153**(1): 63-68

Mader SS. Biology, 3rd Edition. Wm C. Brown Publishers 1990, pg248

Malkowicz SB, Tomaszewski JE, Linnenbach AJ, Cangiano TA, Maruta Y, McGarvey TW. Novel p21$^{WAF1/CP1}$ mutations in superficial and invasive transitional cell carcinomas. *Oncogene* 1996; **13**: 1831-1837

Manna SK, Aggarwal BB. Wortmannin inhibits activation of nuclear transcription factors NF-kappa B and activated protein-1 induced by lipopolysaccharide and phorbol ester. *FEBS Letts* 2000; **473**(1): 113-118

Mannhalter C, Koizar D, Mitterbauer. Evaluation of RNA Isolation Methods and Reference Genes for RT-PCR Analyses of Rare Target RNA. *Clin Chem Lab Med* 2000; **38**(2): 171-177

Marchetti A, Buttitta F, Merlo G, Diella F, Pellegrini S, Pepe S, Macchiarini P, Chella A, Angeletti CA, Callahan R, Bistocchi M, Squartini F. p53 Alterations in Non-Small Cell Lung Cancers Correlate with Metastatic Involvement of Hilar and Mediastinal Lymph Nodes. *Cancer* 1993; **53**: 2846-2851

Mathiasen IS, Jaattela M. Review: Triggering caspase independent cell death to combat cancer. *Trends in Mol Med* 2002; **8**(5): 212-220

Mayer BJ, Baltimore D. Mutagenic analysis of the roles of SH2 and SH3 domains in regulation of the Abl tyrosine kinase. *Mol Cell Biol* 1994; **14**(5): 2883-2894

McGahon A, Bissonnette R, Schmitt M, Cotter KM, Green DR, Cotter TG. BCR-ABL maintains resistance of chronic myelogenous leukemia cells to apoptotic cell death. *Blood* 1994; **83**(5): 1179-1187

McGahon AJ, Cotter TG, Green DR. The abl oncogene family and apoptosis. *Cell Death and Differentiation* 1994; **1**: 77-83

McKay JA, Murray GI, Keith WN, McLeod HL. Amplification of fluorescent in situ hybridisation signals in formalin fixed paraffin wax embedded sections of colon tumour using biotinylated tyramide. *J Clin Pathol: Mol Pathol* 1997; **50**: 322-325

McWhirter JR, Wang JY. An actin-binding function contributes to transformation by the Bcr-Abl oncoprotein of Philadelphia chromosome-positive human leukemias. *EMBO J* 1993; **12**:1533-1546

McWhirter JR, Wang JYJ. Activation of Tyrosine Kinase and Microfilament-Binding Functions of c-*abl* by *bcr* Sequences in *bcr/abl* Fusion Proteins. *Mol Cell Biol* 1991; **11**(3): 1553-1565

McWhirter JR, Wang JYJ. An actin-binding function contributes to transformation by the Bcr-Abl oncoprotein of Philadelphia chromosome positive leukemias. *EMBO J* 1993; **4**: 1533-1546

Mee AP, Denton J, Hoyland JA, Davies M, Mawer EB. Quantification of Vitamin D receptor mRNA in sections demonstrates the relative limitations of *in situ*-reverse transcriptase-polymerase chain reaction. *J Pathol* 1997; **182**: 22-28

Meier P, Finch A, Evan G. Apoptosis in development. *Nature* 2000; **407**: 796-801

Melo JV. BCR-ABL gene variants. In Bailliere's Clinical Haematology 1997; **10**: Bailliere Tindall, London, p203-222

Melo JV. The diversity of BCR-ABL fusion proteins and their relationship to leukaemia phenotype. *Blood* 1996; **88**: 2375-2384

Mentzel T, Fletcher CDM. Dedifferentiated myxoid liposarcoma: a clinicopathological study suggesting a closer relationship between myxoid and well-differentiated liposarcoma. *Histopathology* 1997; **30**: 457-463

Miao YJ, Wang JY. Binding of A/T-rich DNA by three high mobility group-like domains in c-Abl tyrosine kinase. *J Biol Chem* 1996; **271**(37): 22823-22830

Mies C. A Simple, Rapid Method for Isolating RNA from Paraffin-embedded Tissues for Reverse Transcription-Polymerase Chain Reaction (RT-PCR). *J Histochem Cytochem* 1994; **42**(6): 811-813

Moreno S, Nurse P, Russell P. Regulation of mitosis by cyclic accumulation of p80cdc25 mitotic inducer in fission yeast. *Nature* 1990; **344**(6266): 549-552

Mrozek K, Szumigala J, Brooks JSJ, Crossland DM, Karakousis CP, Bloomfield CD. Round Cell Liposarcoma With the Insertion (12;16)(q13;p11.2p13). *Am J Clin Pathol* 1997; **108**(1): 35-39

Mulcahy LS, Smith MR, Stacey DW. Requirement for ras proto-oncogene function during serum-stimulated growth of NIH 3T3 cells. *Nature* 1985; **313**(5999): 241-243

Muller AJ, Young JC, Pendergast AM, Pondel M, Landau NR, Lithman DR, Witte ON. Bcr first exon sequence specifically activates the BCR/ABL tyrosine kinase oncogene of Philadelphia-chromosome positive human leukaemias. *Mol Cell Biol* 1991; **11**: 1785-1792

Mullis KB, Faloona FA. Specific synthesis of DNA in vitro via polymerase-catalyzed chain reaction. *Methods in Enzymology* 1987; **155**: 335-350

Mustonen T, Alitalo K. Endothelial receptor tyrosine kinases involved in angiogenesis. *J Cell Biol* 1995; **129**: 895-898

Nagel S, Schmidt M, Thiede C, Huhn D, Neubauer A. Quantification of Bcr-Abl transcripts in chronic myelogenous leukemia (CML) using standardized, internally controlled, competitive differential PCR (CD-PCR). *Nucl Acids Res* 1996; **24**(20): 4102-4103

Neet K, Hunter T. Vertebrate non-receptor protein-tyrosine kinase families. *Genes to Cells* 1996; **1**: 147-169

Nehme A, Baskaran R, Nebel S, Fink D, Howell SB, Wang JYJ, Christen RD. Induction of JNK and c-Abl signalling by cisplatin and oxaliplatin in mismatch repair-proficient and –deficient cells. *Br J Cancer* 1999; **79**(7/8): 1104-1110

Nguyen PL, Zuckerberg LR, Benedict WF, Harris NL. Immunohistochemical Detection of p53, *bcl*-2, and Retinoblastoma Proteins in Follicular Lymphoma. *Am J Clin Pathol* 1996; **105**(5): 538-543

Nguyen TT, Mohrbacher AF, Tsai YC, Groffen J, Heisterkamp N, Nichols PW, Yu MC, Lubbert M, Jones PA. Quantitative measurement of *c-abl* and *p15* methylation in chronic myelogenous leukaemia: biological implications. *Blood* 2000, **95**(9): 2990-2993

Nielsen PE. Sequence-selective DNA recognition by synthetic ligands. *Bioconjug Chem* 1991; **2**(1): 1-12

Nitta M, Okamura H, Aizawa S, Yamaizumi M. Heat shock induces transient p53-dependent cell cycle arrest at G1/S. *Oncogene* 1997; **15**: 561-568

Nowell PC, Croce CM. Chromosomes, Genes, and Cancer. *Am J Pathol* 1986; **125**(1): 8-15

Nowell PC, HungerfordDA. Chromosome studies on normal and leukemic human leukocytes. *J Natl Cancer Inst* 1960; **25**: 85-109

Nuovo GJ, Gallery F, MacConnell P, Becker J, Bloch W. An Improved Technique for the *In Situ* Detection of DNA after Polymerase Chain Reaction Amplification. *Am J Pathol* 1991a; **139**(6): 1239-1244

Nuovo GJ, Hochman HA, Eliezri YD, astarria D, Comite SL, Silvers DN. Detection of human papillomavirus DNA in penile lesions histologically negative for condylomata. Analysis by in situ hybridisation and the polymerase chain reaction. *Am J Surg Pathol* 1990; **14**(9): 829-836

Nuovo GJ, MacConnell P, Forde A, Delvenne P. Detection of Human Papilloma Virus DNA in Formalin-fixed Tissues by *In Situ* Hybridization After Amplification by Polymerase Chain Reaction. *Am J Pathol* 1991b; **39**: 847-854

Nuovo GJ, Simsir A, Steigbiegel RT, Kuschner M. Analysis of fatal pulmonary hantaviral infection in New York by reverse transcriptase in situ polymerase chain reaction. *Am J Pathol* 1996; **148**(3): 685-692

O'Donovan M, Russell JM, O'Leary JJ, Gillan J, Lawler MP, Gaffney EF. Abl expression, tumour grade and apoptosis in chondrosarcoma. *J Clin Pathol: Mol Pathol* 1999; **52**: 341-344

O'Driscoll L, Kennedy S, McDermott E, Kelehan P, Clynes M. Multiple Drug Resistance-related Messenger RNA Expression in Archival Formalin-fixed Paraffin-embedded Human Breast Tumour Tissue. *Eur J Cancer* 1996; **32A**(1): 128-133

O'Leary JJ, Browne G, Johnson MI, Landers RJ, Crowley M, Healy I, Street JT, Pollock AM, Lewis FA, Andrew A, Cullinane C, Mohamdee O, Kealy WF, Hogan J, Doyle CT. PCR in situ hybridisation detection of HPV 16 in fixed CaSki and fixed SiHa cell lines. *J Clin Pathol* 1994; **47**:933-938

O'Leary JJ, Chetty R, Graham AK, McGee JO'D. *In Situ* PCR: Pathologist's Dream or Nightmare? *J Pathol* 1996; **178**: 11-20

O'Leary JJ, Engels K, Dada MA. *Origins of...* The polymerase chain reaction in pathology. *J Clin Pathol* 1997a; **50**: 805-810

O'Leary JJ, Kennedy M, Luttich K,Uhlmann V, Silva I, Russell J, Sheils O, Ring M, Sweeney M, Kenny C, Bermingham N, Martin C, O'Donovan M, Howells D, Picton S, Lucas SB. Localisation of HHV-8 in AIDS related lymphadenopathy. *Mol Pathol* 2000; **53**(1): 43-47

O'Leary JJ, Kennedy MM, McGee JO'D. Kaposi's sarcoma associated herpes virus (KSHV/HHV 8): epidemiology, molecular biology and tissue distribution. *J Clin Pathol* 1997b; **50**: 4-8

O'Leary JJ. Seeking the cause of Kaposi's sarcoma. *Nat Med* 1996; **2**(8): 862-863

O'Neill AJ, Cotter TG, Russell JM, Gaffney EG. Abl expression in human fetal and adult tissues, tumours and tumour microvessels. *J Pathol* 1997; **183**: 325-329

O'Neill AJ, Staunton MJ, Gaffney EF. Apoptosis occurs independently of bcl-2 and p53 over-expression in Non-Small Cell Lung Carcinoma. *Histopathology* 1996; **29**: 45-50

Okuda K, D'Andrea A, Van Etten RA, Griffin JD. The C-Terminus of c-Abl Is Required for Proliferation and Viability Signalling in a c-Abl/Erythropoietin Receptor Fusion Protein. *Blood* 1998; **92**(10): 3848-3856

Orlando C, Pinzani P, Pazzagli M. Developments in Quantitative PCR. *Clin Chem Lab Med* 1998; **36**(5): 255-269

Owen-Lynch PJ, Wong AKY, Whetton AD. V-Abl mediated Apoptotic Suppression Is Associated with SHC Phosphorylation without Concomitant Mitogen-activated Protein Kinase Activation. *J Biol Chem* 1995; **270**(11): 5956-5962

Panchalingam S, Reynolds GM, Lammas DA, Rowlands DC, Kumararatne DS. Simple method for pretreatment of tissue sections for the detection of apoptosis by in situ end-labelling and in situ nick translation. *J Clin Pathol* 1996; **49**: M273-M277

Pandey P, Raingeaud J, Kaneki M, Weichselbaum R, Davis RJ, Kufe D, Kharbanda S. Activation of p38 mitogen-activated protein kinase by c-Abl dependent and independent mechanisms. *J Biol Chem* 1996; **271**(39): 23775-23779

Pane F, Frigeri F, Sindona M, Luciano L, Ferrara F, Climino R, Meloni G, Saglio G, Salvatore F, Rotoli B. Neutrophilic-Chronic Myeloid Leukemia: a distinct disease with a specific molecular marker (BCR/ABL with c3/a2 junction). *Blood* 1996; **88**: 2410-2414

Partanen J, Makela TP, Alitalo R, Lehvaslaiho H, Alitalo K. Putative tyrosine kinases expressed in k-562 human leukemia cells. *Proc Natl Acad Sci USA* 1990; **87**: 8913-8917

Pendergast AM, Muller AJ, Havlik MH, Clark R, McCormick F, Witte ON. Evidence for regulation of the human ABL tyrosine kinase by a cellular inhibitor. *Proc Natl Acad Sci, USA* 1991; **88**: 5927-5931

Pendergast AM, Quilliam L, Cripe LD, Bassing C, Dai Z, Li N, Batzer A, Rabun K, Channing J, Schlessinger J, Gishizky L. BCR-ABL-induced oncogenesis is mediated by direct interaction with the SH2 domain of the GRB-2 adaptor protein. *Cell* 1993; **75**: 175-185

Perez-Atayde A, Sallan S, Tedrow U, Connors S, Allred E, Folkman J. Spectrum of tumour angiogenesis in the bone marrow of children with acute lymphoblastic leukemia. *Am J Pathol* 1997; **150**: 815-821

Perlman H, Pagliari LJ, Volin MV. Regulation of apoptosis and cell cycle activity in rheumatoid arthritis. *Curr Mol Med* 2001; **1**(5): 597-608

Pezzella F, Harris AL, Gatter KC. Ways of escape: are all tumours angiogenic? *Hitopathology* 2001; **39**(6): 551-553

Pilling A. Increased Sensitivity of In Situ Hybridisation: Implications for In Situ Amplification. *Diagn Mol Pathol* 1997; **6**(3): 174-176

Pocock CFE, Malone M, Booth M, Evans M, Morgan G, Greil J, Cotter FE. BCL-2 expression by leukaemic blasts in a SCID mouse model of biophenotypic leukaemia associated with the t(4;11)(q21;q23) translocation. *Br J Haematol* 1995; **90**: 855-867

Potten CS. What is an apoptotic index measuring? A commentary. *Br J Cancer* 1996; **74**: 1743-1748

Preudhomme C, Henic N, Cazin B, Lai JL, Bertheas MF, Vanrumbeke M, Lemoine F, Jouet JP, Deconninck E, Nelken B, Cosson A, Fenaux P. Good correlation between RT-PCR analysis and relapse in Philadelphia (Ph1)-positive acute lymhoblastic leukemia (ALL). *Leukemia* 1997; **11**:294-294

Prosperi MT, Ferbus D, Rouillard D, Goubin G. The *pag* gene product, a physiological inhibitor of c-*abl* tyrosine kinase, is overexpressed in cells entering S phase and by contact with agents inducing oxidative stress. *FEBS Letters* 1998; **423**: 39-44

Raitano AB, Whang YE, Sawyers CL. Signal transduction by wild-type and leukemogenic Abl proteins. *Biochimica et Biophysica Acta* 1997; **1333**: F201-F216

Randhawa JS, Easton AJ. *Demystified...* DNA nucleotide sequencing. *J Clin Pathol: Mol Pathol* 1999; **52**: 117-124

Ray R, Cooper PJ, Sim R, Chadwick N, Earle P, Dhillon AP, Pounder RE, Wakefield AJ. Direct in situ reverse transcriptase polymerase chain reaction for the detection of measles virus. *J Virol Methods* 1996; **60**: 1-17

Reddy EP, Smith MJ, Srinivasan A. Nucleotide sequence of Abelson murine leukemia virus genome: structural similarity of its transforming gene product to other onc gene products with tyrosine-specific kinase activity. *Proc Natl Acad Sci USA* 1983; **80**(12): 3623-3627

Redline RW, Genest DR, Tycko B. Detection of Enteroviral Infection in Paraffin-Embedded Tissue by the RNA Polymerase Chain Reaction Technique. *Am J Clin Pathol* 1991; **96**(5): 568-571

Reid AH, Cunningham RE, Frizzera G, O'Leary TJ. Bcl-2 rearrangement in Hodgkin's Disease. Results of Polymerase Chain Reaction, Flow Cytometry, and Sequencing on Formalin-Fixed Paraffin-Embedded Tissue. *Am J Pathol* 1993; **142**(2): 395-402

Remmelink M, Salmon I, Petein M. Determination of DNA ploidy, nuclear size, and proliferative activity by means of computer-assisted image analysis of Feulgen-stained nuclei in 68 soft tissue tumours of adults. *Hum Pathol* 1994; **25**: 694-701

Renshaw MW, Capozza MA, Wang JYJ. Differential expression of type-specific c-abl mRNA in mouse tissues and cell lines. *Mol Cell Biol* 1988; **9**: 4547-4551

Revillion F, Pawlowski V, Hornez L, Peyrat JP. Glyceraldehyde-3-phosphate dehydrogenase gene expression in human breast cancer. *Eur J Cancer* 2000; **36**(8): 1038-1042

Rich T, Allen RL, Wyllie AH. Defying death after DNA damage. *Nature* 2000; **407**: 777-783

Roach HI, Erenpreisa J, Aigner T. Osteogenic Differentiation of Hypertrophic Chondrocytes Involves Asymmetric Cell Divisions and Apoptosis. *J Cell Biol* 1995; **131**(2): 483-494

Rosen LS. Clinical experience with angiogenesis signalling inhibitors: focus on vascular endothelial growth factor (VEGF) blockers [Review]. *Cancer Control* 2002; **9**(2): 36-44

Roth MS, Antin JH, Ash R, Terry VH, Gotlieb M, Silver SM, Ginsburg V. Prognostic Significance of Philadelphia Chromosome-Positive Cells Detected by the Polymerase Chain Reaction After Allogenic Bone Marrow Transplant for Chronic Myelogenous Leukemia. *Blood* 1992; **79**(1): 276-282

Roth MS, Antin JH, Bingham EL, Ginsburg D. Detection of Philadelphia Chromosome-Positive Cells by the Polymerase Chain Reaction Following Bone Marrow Transplant for Chronic Myelogenous Leukemia. *Blood* 1989; **74**(2): 882-885

Rowan S, Fisher DE. Mechanisms of apoptotic cell death. *Leukemia* 1997; **11**: 457-465

Rowley JD. A new consistent abnormality in chronic myelogenous leukaemia identified by quinacrine fluorescence and giemsa staining. *Nature* 1973; **243**: 290-293

Rubin E, Farber JL. *In* Essential Pathology, Chapter 26, Bones and Joints, pg. 700-736. J.B.Lippincott Company. **(Year!)**

Rupp GM, Locker J. Purification and Analysis of RNA from Paraffin-Embedded Tissues. *BioTechniques* 1988; **6**(1): 56-60

Sanchez-Beato M, Martinez-Montero JC, Doussos-Anagnostopoulou TA, Gatter KC, Garcia J, Garcia JF, LLoret E, Piris MA. Anomalous retinoblastoma protein expression in Sternberg-Reed cells in Hodgkin's disease: a comparative study with p53 expression and Ki67 expression. *B J Cancer* 1996; **74**: 1056-1062

Sanger F, Nicklen S, Coulson AR. DNA sequencing with chain-terminating inhibitors. *Proc Natl Acad Science USA* 1977; **74**(12): 5463-5467

Sartorius U, Schmitz I, Krammer PH. Molecular mechanisms of death-receptor-mediated apoptosis [Review]. *Chembiochem* 2001; **2**(1): 20-29

Sauerbrey A, Stammler G, Zintl F, Volm M. Expression and prognostic value of the retinoblastoma tumour suppressor (RB-1) in childhood acute lymphoblastic leukaemia. *Br J Haematology* 1996; **94**: 99-104

Sawyers CL, Callahan W, Witte ON. Dominant negative MYC blocks transformation by ABL oncogenes. *Cell* 1992; **70**(6): 901-910

Sawyers CL, McLaughlin J, Goga A, Havlik M, Witte O. The nuclear tyrosine kinase c-Abl negatively regulates cell growth. *Cell* 1994; **77**(1): 121-131

Sawyers CL. Signal transduction pathways involved in BCR-ABL transformation. *Baill Clin Haematol* 1997; **10**(2): 223-231

Schek N, Hall BL, Finn OJ. Increased glyceraldehyde-3-phosphate dehydrogenase gene in human pancreatic adenocarcinoma. *Cancer Res* 1988; **48**: 6354-6359

Schlessinger J, Ullrich A. Growth factor signaling by receptor tyrosine kinases. *Neuron* 1992; **9**(3): 383-391

Schmittgen TD, Zakrajsek BA. Effect of experimental treatment on house keeping gene expression: validation by real-time, quantitative RT-PCR. *J Biochem Biophys Methods* 2000; **46**: 69-81

Searle MS, Embrey KJ. Sequence-specific interaction of Hoescht 33258 with the minor groove of an adenine-tract DNA duplex studied in solution by 1H NMR spectroscopy. *Nucleic Acids Res* 1990; **18**(13): 3753-3762

Sestini R, Orlando C, Peri A, Tricarico C, Pazzagli M, Serio M, Pagani A, Bussolati G, Granchi S, Maggi M. Quantitation of somostatin receptor type 2 gene expression in neuroblastoma cell lines and primary tumors using competitive reverse transcription-polymerase chain reaction. *Clinical Cancer Res* 1996; **2**(10): 1757-1765

Shafman T, Khanna KK, Kedar P Spring K, Kozlov S, Yen T, Hobson K, Gatei M, Zhang N, Watters D, Egerton M, Shiloh Y, Kharbanda S, Kufe D, Lavin MF. Interaction between ATM protein and c-Abl in response to DNA damage. *Nature* 1997; **387**: 520-523

Shaul Y. c-Abl: activation and nuclear targets. *Cell Death and Differentiation* 2000; **7**: 10-16

Shi SR, Cote RJ, Yang C, Chen C, Xu HJ, Benedict WF, Taylor CR. Development of an optimal protocol for antigen retrieval: a 'test battery' approach exemplified with reference to the staining of retinoblastoma protein (pRB) in formalin-fixed paraffin sections. *J Pathol* 1996; **179**: 347-352

Shi Y, Alin K, Goff SP. Abl-interactor-1, a novel SH3 protein binding to the carboxy-terminal portion of the Abl protein, suppresses *v*-abl transforming activity. *Genes Dev.* 1995; **9**: 2583-2597

Shibata D, Martin WJ, Appleman MD, Causey DM, Leedom JM, Arnheim N. Detection of cytomegalovirus DNA in peripheral blood of patients infected with human immunodeficiency virus. *Journal of Infectious Diseases* 1988; **158**(6): 1185-1192

Shtivelman E, Lifshitz B, Gale RP, Canaani E. Fused transcripts of abl and bcr genes in chronic myelocytic leukaemia. *Nature* 1985; **315**: 550-554

Shtivelman E, Lifshitz B, Gale RP, Roe BA, Canaani E. Alternative splicing of RNAs Transcribed from the Human *abl* Gene and from the *bcr-abl* Fused Gene. *Cell* 1986; **47**: 277-284

Sibony M, Commo F, Callard P, Gasc JM. Enhancement of mRNA *in Situ* Hybridization Signal by Microwave Heating. *Lab Invest* 1995; **73**(4): 586-591

Sirivatanauksorn Y, Drury R, Crnogorac-Jurcevic T, Sirivatanauksorn V, Lemoine NR. Laser-assisted microdissection: Applications in molecular pathology. *J Pathol* 1999; **189**: 150-154

Sirover MA. Role of the Glycolytic Protein, Glyceraldehyde-3-Phosphate Dehydrogenase in Normal Cell Function and in Cell Pathology. *J Cellular Biochemistry* 1997; **66**: 133-140

Skorski T, Bellacosa A, Nieborowska-Skorska M, Majewski M, Martinez R, Choi JK, Trotta R, Wlodarski P, Perrotti D, Chan TO, Wasik MA, Tsichlis PN, Calabretta B. Transformation of hematopoietic cells by BCR/ABL requires activation of a PI-3K/Akt-dependent pathway. *EMBO J* 1997; **16**: 6151-6161

Skorski T, Kanakaraj P, Nieborowska-Skorska M, Ratajczak MZ, Wen S-C, Zon G, Gewitz AM, Perussia B, Calabretta B. Phosphatidylinositol-3 kinase activity is regulated by BCR/ABL and is required for the growth of Philadelphia chromosome positive cells. *Blood* 1995; **86**: 726-736

Smith MD, Triantafillou S, Parker A, Wikaningrum R, Coleman M. A Nonradioactive Method of In Situ Hybridization That Uses Riboprobes and Paraffin-embedded Tissue and Its Combination with Immunohistochemistry. *Diagn Mol Pathol* 1997; **6**(1): 34-41

Solary E, Dubrez L, Eymin B. The role of apoptosis in the pathogenesis and treatment of diseases. *Eur J Respir* 1996; **9**: 1293-1305

Solomon E, Borrow J, Goddard AD. Chromosome Aberrations and Cancer. *Science* 1991; **254**: 1153-1159

Spencer A, Yan XH, Chase A, Goldman JM, Melo JV. BCR-ABL-positive lymphoblastoid cells display limited proliferative capacity under *in vitro* culture conditions. *Br J Haematology* 1996; **94**: 654-658

Sperry A, Jin L, Lloyd RV. Microwave Treatment enhances Detection of RNA and DNA by In Situ Hybridization. *Diagn Mol Pathol* 1996; **5**(4): 291-296

Stacey DW, Roudebush M, Day R, Mosser SD, Gibs JB. Dominant inhibitory Ras mutants demonstrate the requirement for Ras activity in the action of tyrosine kinase oncogenes. *Oncogene* 1991; **6**(12): 2297-2304

Stanta G, Schneider C. RNA extracted from Paraffin-Embedded Human Tissues is Amenable to Analysis by PCR Amplification. *BioTechniques* 1991; **11**(3): 304-308

Staskus A, Couch L, Bitterman P, Retzel EF, Zupancic M, List J, Hasse AT. In situ amplification of visna virus DNA in tissue sections reveals a resevoir of latently infected cells. *Microb Pathol* 1991; **11**(1): 67-76

Staunton MJ, Gaffney EF. Apoptosis – Basic Concepts and Potential Significance in Human Cancer. *Arch Pathol Lab Med* 1998; **122**: 310-319

Staunton MJ, Gaffney EF. Tumor Type is a Determinant of Susceptibility to Apoptosis. *Am J Clin Pathol* 1995; **103**: 300-307

Steel JH, Poulsom R. Making sense out of *In Situ* PCR. *J Pathol* 1997; **182**: 11-12

Suarez-Quian CA, Goldstein SR, Pohida T, Smith PD, Peterson JI, Wellner E, Ghany M, Bonner RF. Laser Capture Microdissection of Single Cells from Complex Tissues. *Biotechniques* 1999; **26**: 328-335

Sun X, Majumder P, Shioya H, Wu F, Kumar S, Weichselbaum R, Kharbanda S, Kufe D. Activation of the Cytoplasmic c-Abl tyrosine Kinase by Reactive Oxygen Species. *J Biol Chem* 2000; **275**(23): 17237-17240

Superta-Fuga G, Courtneidge SA. Structure-function relationships in Src family and related protein tyrosine kinases. *Bioessays* 1995; **17**: 321-330

Susin SA, Zamzami N, Kroemer G. Mitochondria as regulators of apoptosis: doubt no more. *Biochim Biophys Acta* 1998; **1366**: 151-165

Taagepera S, McDonald D, Loeb JE, Whitaker LL, McElroy AK, Wang JY, Hope TJ. Nuclear-cytoplasmic shuttling of c-ABL tyrosine kinase. *Proc Natl Acad Sci USA* 1998; **95**(13): 7457-7462

Taagepera S, McDonald D, Loeb JE, Whitaker LL, McElroy AK, Wang JYJ, Hope TJ. Nuclear-cytoplasmic shuttling of c-ABL tyrosine kinase. *Proc Natl Acad Sci, USA* 1998; **95**: 7457-7462

Takahashi A, Earnshaw WC. ICE-related proteases in apoptosis. *Curr Opin Genet Devel* 1996; **6**: 50-55

Takeyama N, Miki S, Hirakawa A, Tanaka T. Role of the mitochondrial permeability transition and cytochrome C release in hydrogen peroxide-induced apoptosis. *Exp Cell Res* 2002; **274**(1): 16-24

Taoufik Y, Froger D, Benoliel S, Wallon C, Dussaix E, Delfraissy JF, Lantz O. Quantitative ELISA-polymerase chain reaction at saturation using homologous internal standards and chemiluminescence revelation. *Eur Cytokine Netw* 1998; **9**(2): 197-204

Taylor JJ, Heasman PA. Control Genes for Reverse Transcription. *Br J Haematology* 1994; **86**: 444-447

Templeton NS. The Polymerase Chain Reaction. History, Methods, and Applications. *Diagn Mol Pathol* 1992; **1**(1): 58-72

Testoni N, Martinelli G, Farabegoli P, Zaccaria A, Amabile M, Donatella R, Pelliconi S, Zuffa E, Carboni C, Tura S. A New Method of "In-Cell Reverse Transcriptase-Polymerase Chain Reaction" for the Detection of BCR/ABL Transcripts in Chronic Myeloid Leukemia Patients. *Blood* 1996; **87**(9): 3822-3827

Theis S, Roemer K. c-Abl tyrosine kinase can mediate tumor cell apoptosis independently of the RB and p53 tumor suppressors. *Oncogene* 1998; **17**: 557-564

Thijsen SFT, Schuurhuis GJ, van Oostveen JW, Theijsmeijer A, Langenhuijsen MMAC, Ossenkoppele GJ. Molecular analysis of hematopoietic colonies derived from chronic myeloid leukemia patients: interphase fluorescence *in situ* hybridization compared with RT-PCR. *Leukemia* 1997; **11**: 301-305

Thornberry NA, Lazebnik Y. Caspases: Enemies Within. *Science* 1998; **281**(5381): 1312-1316

Till JH, Chan PM, Miller WT. Engineering the Substrate Specificty of the Abl Tyrosine Kinase. *J Biol Chem* 1999; **274**(8): 4995-5003

To MD, Done SJ, Redston M, Andrulis IL. Analysis of mRNA from Microdissected Frozen Tissue Sections without RNA Isolation. *Am J Pathol* 1998; **153**(1): 47-51

Tormanen U, Eerola A, Rainio P. Enhanced apoptosis predicts shortened survival in non-small cell lung carcinoma. *Cancer Res* 1995; **55**: 5595-5602

Uhlmann V, Prasad M, Silva I, Luettich K, Grande L, Alonso L, Thisted M, Pluzek K, Ring M, Sweeney M, Kenny C, Martin C, Russell J, Bermingham N, O'Donovan M, O'Leary JJ. Improved in situ detection method for telomeric tandem repeats in metaphase spreads and interphase nuclei. *Mol Pathol* 2000; **53**(1): 48-50

Uhlmann V, Rofts A, Mix E, Silva I, Hully J, Lu L, Lohman K, Howells D, Picton S, O'Leary JJ. A novel, rapid in cell RNA amplification technique for the detection of copy mRNA transcripts. *J Clin Pathol: Mol Pathol* 1998b; **51**: 160-167

Uhlmann V, Silva I, Luttich K, Picton S, O'Leary JJ. *Demystified...*In cell amplification. *J Clin Pathol: Mol Pathol* 1998a; **51**: 119-130

Ullrich A, Schlessinger J. Signal transduction by receptors with tyrosine kinase activity. *Cell* 1990; **61**(2): 203-212

Van der Geer P, Hunter T, Lindberg RA. Receptor protein-tyrosine kinases and their signal transduction pathways. *Ann Rev Cell Biol* 1994; **10**: 251-337

Van Etten RA, Jackson P, Baltimore D. The Mouse Type IV c-*abl* Gene Product Is a Nuclear Protein, and Activation of Transforming Ability Is Associated with Cytoplasmic Localization. *Cell* 1989; **58**: 669-678

Van Etten RA, Jackson PK, Baltiomer D, Sanders MS, atsudaira PT, Janmey PA. The COOH terminus of the c-Abl tyrosine kinase contains distinct F- and G-actin binding domains with bundling activity. *J Cell Biol* 1994; **124**:325-340

Van Etten RA. Cycling, stressed-out and nervous: cellular functions of c-Abl. *Trends in Cell Biology* 1999; **9**: 179-186

Van Roggen, JFG, Bovee JVMG, Morreau J, Hogendoorn PCW. Diagnostic and prognostic implications of the unfolding molecular biology of bone and soft tissue tumours. *J Clin Pathol* 1999; **52**: 481-489

Varticovski L, Daley GO, Jackson P, Baltimore D, Cantley L. Activation of phosphatidylinositol-3-kinase in cells expressing Abl oncogene variants. *Mol Cel Biol* 1991; **11**: 1107-1113

Venetianer A, Dubois MF, Nguyen VT, Bellier S, Seo SJ, Bensaude O. Phosphorylation state of the RNA polymerase II C-terminal domain (CTD) in heat-shocked cells. Possible involvement of the stress-activated mitogen-activated protein (MAP) kinases. *Eur J Biochem* 1995; **233**: 83-92

Wallace DM. Large- and Small-Scale Phenol Extractions. *In Methods in Enzymology* 1987; **152** (Chapter 4): 33-41

Wallace DM. Precipitation of Nucleic Acids. *In Methods in Enzymology* 1987; **152**(Chapter 5): 41-48

Wang J, Medeiros LJ, Longo DL, Mansoor A, Raffeld M, Duffey PL, Jaffe ES, Stetler-Stevenson M. Use of the Polymerase Chain Reaction Technique to determine c-myc expression in Follicular Center Cell Lymphoma. *Diagn Mol Pathol* 1996; **5**(1): 20-25

Wang JYJ. Abl tyrosine kinase in signal transduction and cell-cycle regulation. *Curr Opin Genet Devel* 1993; **3**: 35-43

Wang JYJ. Integrative Signaling Through c-Abl: A Tyrosine Kinase with Nuclear and Cytoplasmic Functions. *In Signalling Networks and Cell Cycle Control: The Molecular Basis of Cancer and Other Diseases.* Edited by J.S. Gutkind © Humana Press Inc., Totowa, NJ.

Wang T, Brown MJ. mRNA Quantification by Real Time TaqMan Polymerase Chain Reaction: Validation and Comparison with RNase Protection. *Analytical Biochem* 1999; **269**: 198-201

Warford A, Pringle JH, Hay J, Henderson SD, Lauder I. Southern blot analysis of DNA extracted from formal-saline fixed and paraffin wax embedded tissue. *J Pathol* 1988; **154**(4): 313-320

Weiss MM, Hermsen MAJA, Meijer GA, Van Grieken NCT, Baak JPA, Kuipers EJ, Van Diest PJ. *Demystified...* Comparative genomic hybridisation. *J Clin Pathol: Mol Pathol* 1999; **52**: 243-251

Weiss RA, Marshall CJ. DNA in Medicine: Oncogenes. *The Lancet* 1987: 1138-1142

Welch PJ, Wang JY. A C-terminal protein-binding domain in the retinoblastoma protein regulates tyrosine kinase in the cell. *Cell* 1993; **75**(4): 779-790

Welch PJ, Wang JYJ. Abrogation of retinoblastoma protein function by c-Abl tyrosine kinase-dependent and –independent mechanisms. *Mol Cell Biol* 1995; **15**: 5542-5551

Wells SJ, Phillips CN, Winton EF, Farhi DC. Reverse Transcriptase-Polymerase Chain Reaction for *bcr/abl* Fusion in Chronic Myelogenous Leukemia. *Am J Clin Pathol* 1996; **105**(6): 756-760

Wen ST, Jackson PK Van Etten RA. The cytostatic function of c-Abl is controlled by multiple nuclear localisation signals and requires *p53* and *Rb* tumor suppressor gene products. *EMBO J* 1996; **15**(7): 1583-1595

Wetzler M, Talpaz M, Van Etten RA, Hirsh-Ginsberg C, Beran M, Kurzrock. Subcellular Localization of Bcr, Abl, and Bcr-Abl Proteins in Normal and Leukemic Cells and Correlation of Expression with Myeloid Differentiation. *J Clin Invest* 1993; **92**: 1925-1939

Whitcombe D, Brownie J, Gillard HL, McKechnie D, Theaker J, Newton CR, Little S. A homogeneous fluorescence assay for PCR amplicons: its application to real-time, single-tube genotyping. *Clin Chem* 1998; **44**(5): 918-928

Wijsman JH, Jonker RR, Keijzer R, Van de Velde CJH, Cornelisse CJ, Van Dierendonck JH. A New Method to Detect Apoptosis in Paraffin Sections: In Situ End-labeling of Fragmented DNA. *J Histochem Cytochem* 1993; **41**(1): 7-12

Wong KK, Hardin JD, Boast S, Cooper CL, Merrell KT, Doyle TG, Goff SP, Calame KL. A role for c-Abl in c-myc regulation. *Oncogene* 1995; **10**(4): 705-711

Woscholski R, Kodaki T, McKinnion M, Waterfield MD, Parker PJ. A comparison of demothoxyviridin and wortmannin as inhibitors of phosphatidylinositol 3-kinase. *FEBS Lett* 1994; **42**: 109-114

Wu JJ, Phan H, Lam KS. Comparison of the intrinsic kinase activity and substrate specificity of c-Abl and BCR-Abl. *Bioorganic & Medicinal Chemistry Letters* 1998; **8**: 2279-2284

Wyllie AH, Morris RG, Smith AL, Dunlop D. Chromatin cleavage in apoptosis: Association with condensed chromatin morphology and dependence on macromolecular synthesis. *J Pathol* 1984; **142**: 67-77

Wyllie AH. Apoptosis and Carcinogenesis. *Euro J Cell Biol* 1997; **73**: 189-197

Wyllie AH. Apoptosis and the regulation of cell numbers in normal and neoplastic tissues: an overview. *Cancer and Metastasis Reviews* 1992; **11**: 95-103

Wyndford-Thomas, D. Cellular Senescence and Cancer. *J Pathol* 1999; **187**: 100-111

Yoshida K, Komatsu K, Wang HG, Kufe D. c-Abl tyrosine kinase regulates the human Rad9 checkpoint in response to DNA damage. *Mol Cell Biol* 2002; **22**(10): 3292-3300

Yuan ZM, Huang Y, Ishiko T, Kharbanda S, Weichselbaum R, Kufe D. Regulation of DNA damage-induced apoptosis by the c-Abl tyrosine kinase. *Proc Natl Acad Sci USA* 1997; **94**: 1437-1440

Yuan ZM, Shioya H, Ishiko T, Sun X, Gu J, Huang Y, Lu H, Kharbanda S, Weichselbaum R, Kufe D. P73 is regulated by tyrosine kinase c-Abl in the apoptotic response to DNA damage. *Nature* 1999; **399**: 814-817

Yuan ZM, Utsugisawa T, Ishiko T, Nakaa S, Huang Y, Kharbanda S, Weichselbaum R, Kufe Y. Activation of protein kinase C delta by the c-Abl tyrosine kinase in response to ionizing radiation. *Oncogene* 1998; **16**(13): 1643-1648

Yuan ZM, utsugisawa T, Ishiko T, Nakada S, Kharbanda S, Weichselbaum R, Kufe D. Inhibition of Phosphatidylinositol 3-Kinase by c-Abl in the Genotoxic Stress Response. *J Biol Chem* 1997; **272**(38): 23485-23488

Zamzami N, Hirsch T, Dallaporta B, Petit PX, Kroemer G. Mitochondrial implication in accidental and programmed cell death: apoptosis and necrosis. *J Bioenerg Biomembranes* 1997; **29**: 185-193

Zamzami N, Marzo I, Larochette N, Brenner C, Hirsch T, Susin SA, Merchetti P, Reed J, Kofler R, Kroemer G. The thiol crosslinking agent diamide overcomes the apoptosis inhibitory effect of Bcl-2 by enforcing mitochondrial permeability transition. *Oncogene* 1998; **16**: 1055-1064

Zenmyo M, Komiya S, Kawabata R, Sasaguri Y, Inoue A, Morimatsu M. Morphological and Biochemical evidence for Apoptosis in the terminal hypertrophic chondrocytes of the growth plate. *J Pathol* 1996; **180**: 430-433

Zhu J, Shore SK. c-Abl tyrosine kinase is regulated by association with a novel SH3-domain-binding protein. *Mol Cell Biol* 1996; **16**: 7054-7062

Zou X, Calame K. Signaling Pathways Activated by Oncogenic Forms of Abl Tyrosine Kinase. *J Biol Chem* 1999; **274**(26): 18141-18144